Rh(II)-catalyzed cyclopropanation-ring expansion of 7-azaindoles with halodiazoacetates and indoles with halodiazophosphonates

Reactions directed towards the synthesis of quinolone antibacterial agents

Linn Neerbye Berntsen

Thesis submitted for the degree of
Master in Chemistry
60 credits

Department of Chemistry
Faculty of mathematics and natural sciences

UNIVERSITY OF OSLO

15.05.2018

Rh(II)-catalyzed cyclopropanation-ring expansion of 7-azaindoles with halodiazoacetates and indoles with halodiazophosphonates

Reactions directed towards the synthesis of quinolone antibacterial agents

Linn Neerbye Berntsen

Rh(II)-catalyzed cyclopropanation-ring expansion of 7-azaindoles with halodiazoacetates and indoles with halodiazophosphonates

http://www.duo.uio.no/

Printed: Reprosentralen, University of Oslo

Acknowledgments

The work presented in this master thesis was carried out in the Department of Chemistry at the University of Oslo under the supervision of Associate Professor Tore Bonge-Hansen and Pål Rongved.

First and foremost, I would like to thank my supervisor Tore Bonge-Hansen. Your support and encouragement have truly been important to me, as have your never ending patience, enthusiasm and positivity (how does one get *this* patient?). Thank you for giving me a exciting project and for teaching me a great amount of chemistry. I have really enjoyed our conversations, being about chemistry or anything else entirely. They have been a lot of fun!

My thanks are extended to my co-supervisor - Pål Rongved - and the SYNFAS group. I have enjoyed the interesting conversations and presentations during our group meetings. You have extended my knowledge about chemistry and antibiotic resistance, which is truly appreciated.

Thank you, Frode Rise and Dirk Pedersen, for your constant work on maintaining and improving the NMR facilities, and for helping me out whenever I needed. Carl Henrik Görbitz, thank you for the general introduction to X-ray analysis and for the analysis and characterization of one of my samples. Thanks a lot, David Wragg, for doing the X-ray analysis and characterization of the rest of my samples. Osamu Sekiguchi, thank you for providing me with MS-data.

My gratitude is extended to Simen Gjelseth Antonsen for reading through my thesis and giving me constructive feedback. It was much-needed!

I am very grateful for all the new friendships established over the last five years. A thanks to all of you for fun times we have had! A special thanks goes to Sara Peeters, Sunniva Furre Amundsen and Ramneet Kaur Kular. I truly appreciate our friendship. Time spent with you is invaluable and I will always be grateful to call you my friends.

Lastly, my sincerest gratitude goes to my family and Emir. For always letting me know how proud you are of me, supporting me no matter what and for your endless love. I could not have done this without you.

Abstract

Up until now, the antibacterial 8-azaquinolones have been prepared using various ring-closing reactions.

This work demonstrates the attempted synthesis of 8-azaquinolone antibacterial agents using a synthetic route that involves a reaction recently developed in our group. The reaction is considered the key step of the synthesis and allows for the transformation of 7-azaindoles to 8-azaquinoline-3-carboxylates via a Rh(II)-catalyzed cyclopropanation-ring expansion reaction with ethyl halodiazoacetates. No 8-azaquinolone antibacterial agent was successfully synthesized from 7-azaindoles using this reaction due to decomposition of an intermediate product. The majority of the time was spent on optimization of the reaction conditions as the major product turned out to be the undesired N-H-insertion product. With the new, optimized conditions, reproducibility was seemingly an issue. Even so, some already reported and some novel 8-azaquinolines were successfully synthesized in modest to good yields.

The chemistry and transformations of halodiazophosphonates have not been extensively investigated. For that reason, it was of large interest to investigate if they could participate in the same cyclopropanation-ring expansion reactions as the halodiazoacetates, and further be used in synthesis towards a bioisoster of a (fluoro)quinolone antibacterial agent.

In this part of the work, the successful generation and isolation of diethyl halodiazophosphonates, and the generation of quinolinyl-3-phosphonates from indoles and diethyl halodiazophosphonates is described. The reaction was investigated for a series of indole derivatives with substituents in selected positions. The majority of the reactions afforded the desired product in modest to good yields. Except for one product, the 3-quinolinyl-phosphonates described are synthesized and isolated here for the first time. Purification and isolation of these compounds on silica gel proved to be troublesome due to tailing of the products and traces of several byproducts. No bioisoster of a (fluoro)quinolone was successfully synthesized as the investigation of the indole series revealed that the reaction was not compatible with the required substitution pattern.

Both diazo compounds used throughout this work were halogenated according to a procedure developed in our group. The successful quantification of the halogenated ethyl halodiazoacetates where excellent yields were afforded is also described in this work. The same success was not obtained in the quantitative analysis of the halogenated diazophosphonates due to a large degree of varying yields.

Graphical abstract

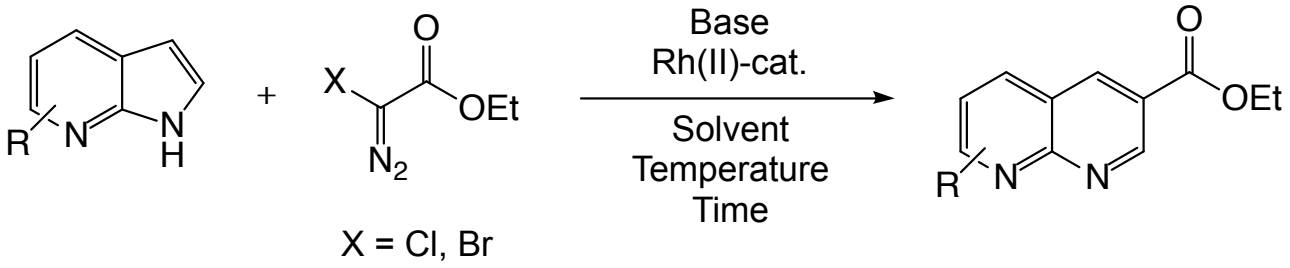

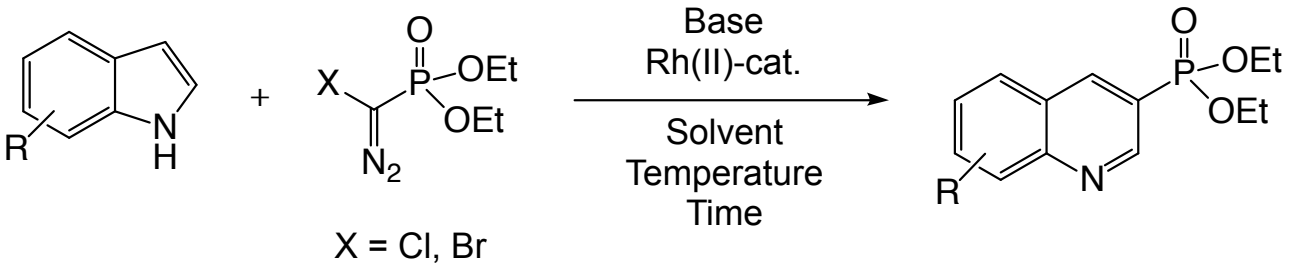

Abbreviations

18c6	18-crown-6
4VBA	4-vinylbenzoic acid
Boc	*t*-butyloxycarbonyl
n-BuLi	*n*-butyllithium
Cbz	carboxybenzyl
Δ	heat
DBU	1,8-Diazabicyclo[5.4.0]undec-7-ene
DCM	dichloromethane
DEEMM	diethyl ethoxymethylenemalonate
DMF	*N,N*-dimethylformamide
EDA	ethyl diazoacetate
EDG	electron donating group
EDP	diethyl diazophosphonate
esp	α,α,α',α'-tetramethyl-1,3-benzenedipropionic acid
EtOAc	ethyl acetate
EtOH	ethanol
EWG	electron withdrawing group
IS	internal standard
KHMDS	potassium hexamethyldisilazide
MCES	mono-2-(methacryloyloxy) ethyl succinate
MeCN	acetonitrile
MeOH	methanol
NaHMDS	sodium hexamethyldisilazide
NBS	*N*-bromosuccinimide
NCS	*N*-chlorosuccinimide
NXS	*N*-halosuccinimide
OTf	triflate
$PhCF_3$	α,α,α-trifluorotoluene
Pol(II)	immobilized rhodium(II)-carboxylate, generation (II)
PTSA	para-toluenesulfonic acid
SAR	structure-activity relationship
t-BuOLi	lithium tert-butoxide
TFA	trifluoroacetic acid
THF	tetrahydrofuran
TMB	1,3,5-trimethoxybenzene
TsN_3	para-toluenesulfonyl azide
UTI	Urinary tract infection
WHO	World Health Organization

Description and aim of the project

In the Bonge-Hansen group, a great amount of work regarding the synthesis and reactions of halodiazocompounds have been performed. Halogenation of diazo compounds and further transformation with or without appropriate transition metals have been a major focus over the last few years [1–6].

During his masters, Magnus Mortén discovered, somewhat surprisingly, that the Rh(II)-catalyzed reaction between a halodiazoacetate and an indole afforded the cyclopropanated-ring expanded quinoline-3-carboxylate (Scheme 1) [7]. This route has proven very useful as it compatible with a range of substituted indoles, making it an efficient and lucrative route to synthesize various quinolines.

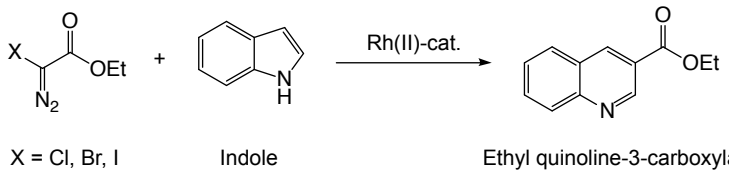

Scheme 1: Rh(II)-cat. cyclopropanation-ring expansion reaction between indoles and halodiazoacetates [3].

With a chlorine atom in the proper position, the quinol*ine* can be converted to the corresponding quinol*one* in one step [8]. Quinolones are a group of synthetic, broad-spectrum antibacterial agents used to treat bacterial infections in both human and animal, and are therefore of great importance. The development of halodiazo compounds in combination with possibly new, synthetic routes to antibacterial agents are indeed highly useful as well as intriguing.

This project consists of two parts where both focuses on the utilization and further development of the cyclopropanation-ring expansion reaction.

In the first part, the initial goal was to investigate the reaction between halodiazoacetates and 7-azaindoles. Further, the main goal was to use this reaction as a key step in the synthesis of 8-azaquinolone antibacterial agents. Two 8-azaquinolones, one of which was the first 8-azaquinolone antibacterial agent, nalidixic acid, and a non-fluorinated enoxacin analogue were to be synthesized in order to demonstrate the cyclopropanation-ring expansion reactions' usefulness (Scheme 2).

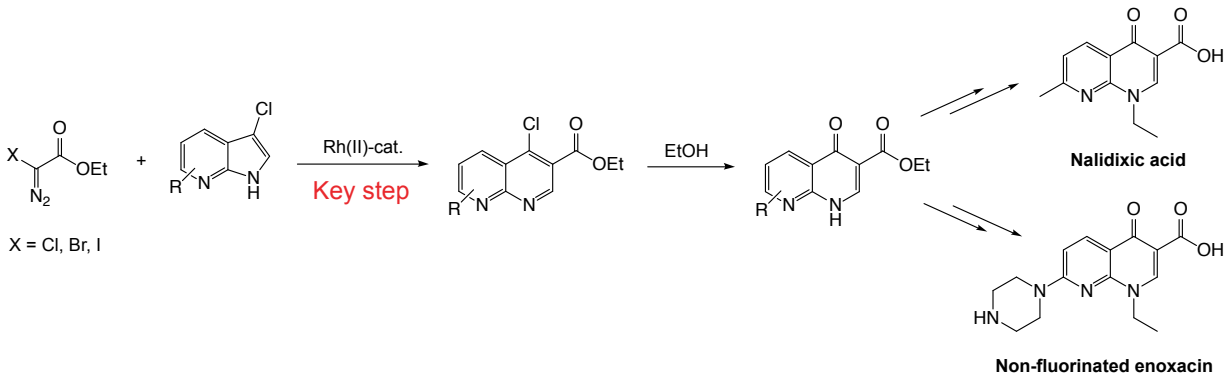

Scheme 2: Rh(II)-cat. cyclopropanation-ring expansion reaction between 7-azaindoles and halodiazoacetates as a key step in the synthesis of 8-azaquinolone antibacterial agents.

In the second part, the initial goal was to investigate the reaction between halodiazophosphonates and indoles. Further, the main goal was to demonstrate the reactions' usefulness as a key step in the synthesis of a phosphonic acid bioisoster of norfloxacin (Scheme 3). Norfloxacin is a quinolone antibacterial agent currently on the market.

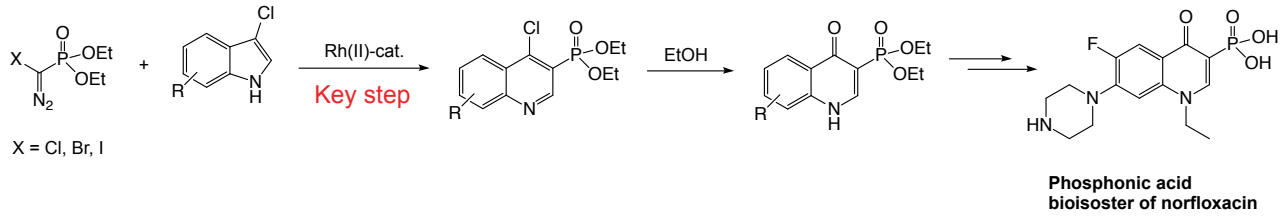

Scheme 3: Rh(II)-cat. cyclopropanation-ring expansion reaction between 7-azaindoles and halodiazoacetates as a key step in the synthesis of phosphonic acid bioisoster of norfloxacin.

Table of Contents

Chapter 1

Introduction

1.1 Biological background

This section will first give a short overview of antibiotics/antibacterial agents and the development of resistance towards antibiotics. Then, an overview over quinolone antibacterial agents, including a short description of their discovery, structure, cellular targets, mechanism of action, binding mechanism, resistance and structure-activity relationship (SAR) and bioisosterism will be described. Lastly, examples of synthetic routes to 8-azaquinolone antibacterial agents will be presented.

1.1.1 Antibacterial resistance

Antibiotics and antibacterial agents are medicine used to treat or prevent bacterial infections. They are either bacteriostatic; inhibits bacteria from reproducing, or bactericidal; kills the bacteria. The discovery of antibiotics revolutionized medicine in the 20th century. Antibiotics are among the medicinal discoveries that have contributed to better public health and an increase in life expectancy more so than any other medicine [9]. Since the introduction of penicillin in the 1940's [10], illness and death from infectious diseases have been considerably reduced by antibiotics [11]. Together with vaccination they have almost eradicated infectious diseases such as tuberculosis, especially in western countries [12]. However, the reckless and excessive use of antibiotics have caused bacteria to become drug-resistant. Resistance occurs naturally as bacteria adapts over time, but overuse and misuse are accelerating the process [13].

Resistance towards penicillin was detected in the Gram-positive bacteria *Staphylococcus aureus* already in the 1940's [14]. In the early 1960's strains resistant to methicillin was detected [14] With this, the well known Methicillin-resistant *Staphylococcus aureus* (MRSA) was "born". Over the years, both MRSA and several other harmful bacterial pathogens have evolved into multidrug-resistant forms [15]. Some Carbapenem-resistant[1] Gram-negative bacteria such as *Acinetobacter baumannii*, *Pseudomonas aeruginosa* and various *Enterobacteriaceae* are even classified as pandrug-resistant, *i.e.* non-susceptible to *all* antibacterial agents [16–18]. These bacterial pathogens are currently on top of the World Health Organization (WHO) list over the most critical bacteria where new antibiotics are urgently needed [19].

In 2014, a report concerning the global antimicrobial resistance[2] was published by WHO [20]. The report examines the current status of surveillance and information on worldwide antimicrobial resistance, and particularly antibacterial resistance. A "post-antibiotic era", where diseases that have been treatable over the last decades are getting impossible to treat and where a minor

[1] Carbapenems are often used as last-resort drugs.
[2] The term "antimicrobial resistance" includes resistance in parasites, fungi and virus as well as bacteria.

infection can kill, are becoming a real possibility and consequently one of the biggest threats to the global public health [20]. Today, the resistance is responsible for about 6 million infections and 60 000 deaths per year in Europe and the U.S alone [11, 21] and far greater numbers world wide [13].

1.1.2 Quinolones and 8-azaquinolones as antibacterial agents

As quinolones and 8-azaquinolones are structurally related (explained in the following section), their biological features and properties are considered highly similar. When discussing topics concerning these features, the 8-azaquinolones will, for simplicity sake, be referred to as just quinolones. In the section concerning synthetic routes, however, only those of 8-azaquinolones will be included.

1.1.2.1 General structure

Quinolones are a class of nitrogen containing aromatic heterocycles with a fused bicyclic core, derived from quinolines. The simple term "quinolone" can refer to either 2-quinolone (1.1a) or 4-quinolone (1.1b) where the latter is the one represented in a large, important class of antibacterial agents.

(a) 2-quinolone **(b)** 4-quinolone

Figure 1.1: General structure and numbering of 2- and 4-quinolones.

They both exist as the major tautomer in equilibrium with their respective 2- and 4-hydroxyquinolines (Figure 1.2) [22].

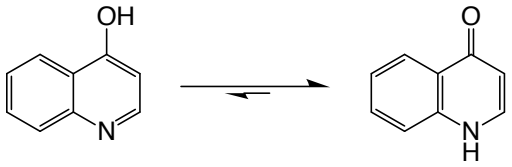

Figure 1.2: 4-hydroxyquinoline-4-quinolone equilibrium.

An aza-quinolone is a quinolone analogue where a carbon is replaced by a nitrogen.
In 8-azaquinolone, the pyridyl nitrogen is located in the 8th position of the bicycle (Figure 1.3).

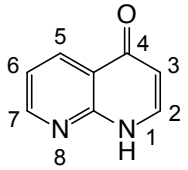

Figure 1.3: General structure and numbering of 8-azaquinolone.

In quinolone antibacterials, a carboxylic acid is present in the 3-position as well as substituted N-1 and various substituents in positions 5-8 (Figure 1.4). This is considered to be the pharmacophore, i.e the part of the molecule that is necessary to ensure antibacterial activity [23]. More details of the pharmacophore will be discussed in 1.1.2.3.

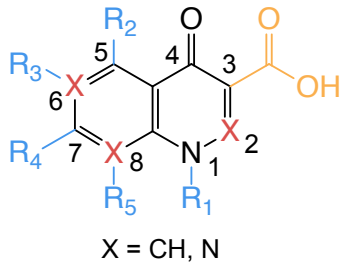

Figure 1.4: The pharmacophore of a quinolone antibacterial agent.

1.1.2.2 Discovery and development

Quinolones are a family of synthetic antibacterial agents used world wide over the last 40 years to treat various bacterial infections. Their widespread use is due to the fact that they have a broad antimicrobial spectrum, are orally and parentally active, have excellent bioavailability and, with a few exceptions, are safe [24, 25].

The discovery and developement of quinolones started in the early 1960s when Lesher *et al.* discovered 7-chloroquinolone (Scheme 1.1) as a by-product in a synthesis for an antimalaria agent, chloroquine (Scheme 1.1) [26]. The 7-chloroquinolone showed some anti Gram-negative bacteria potency, but had limited usefulness as a drug [27]. It was therefore optimized to nalidixic acid (Scheme 1.1), but was not introduced for clinical use until 1967 [28] due to its narrow antimicrobial spectrum and poor pharmacokinetics. The narrow antimicrobial spectrum and poor pharmacokinetics limited their used primarily to treatment of urinary tract infections (UTIs) [29].

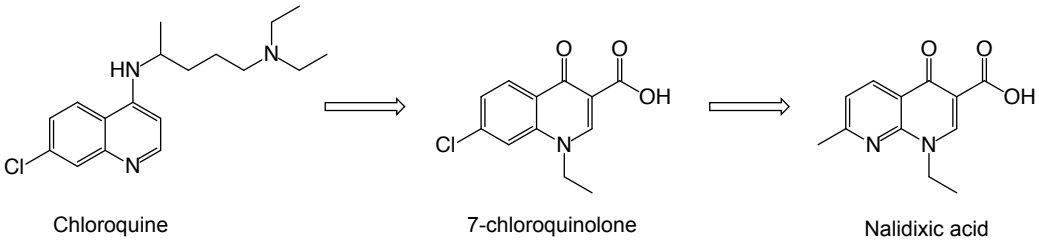

Scheme 1.1: Discovery of nalidixic acid [26]. As the first quinolone antibacterial, it is a part of the first generation of quinolones.

Introduction of a fluorine atom in the 6th position of the quinolone core was found to significantly increase the antimicrobial spectrum, pharmacokinetics and tissue penetration of new quinolones. Some of them were up to 60 times more active than nalidixic acid and could be used to treat a wider range of infections [27–30]. The first fluorinated quinolones, referred to as fluoroquinolones (FQ), are the second generation of quinolones. Today, there are four generations (Figure 1.5) based on their microbiologic activity and indications [27, 31].

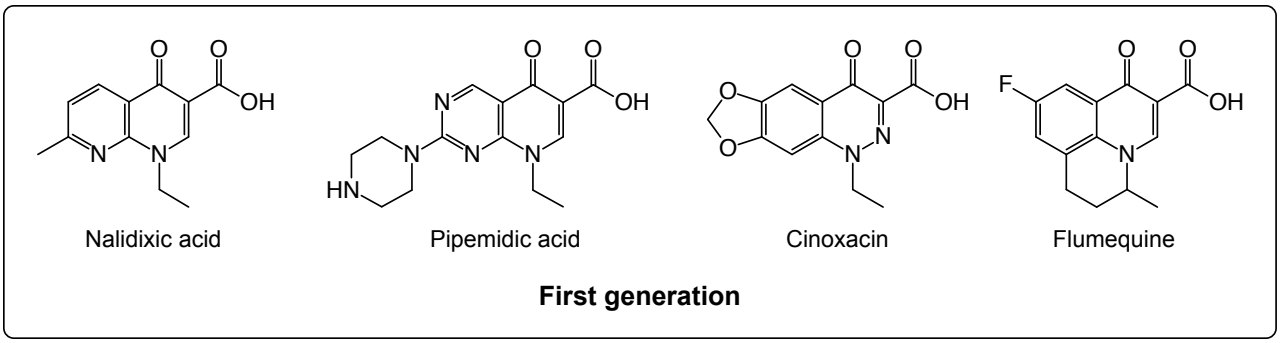

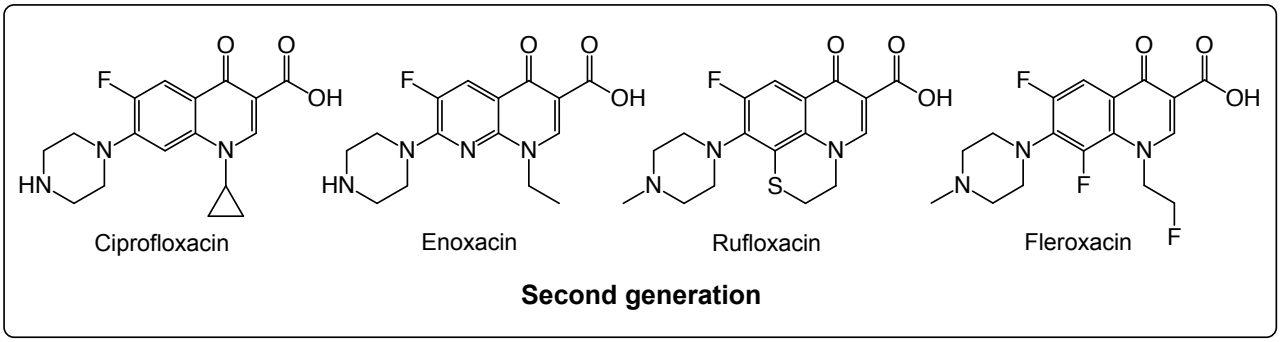

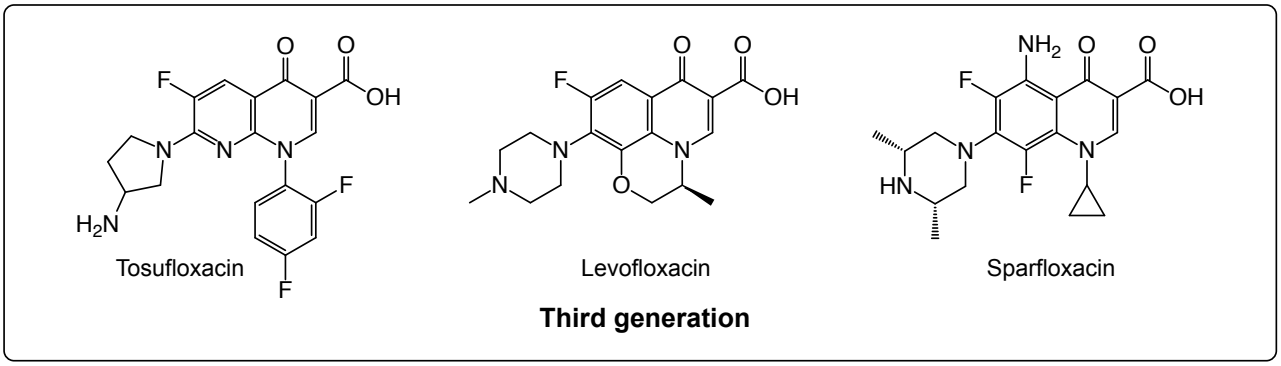

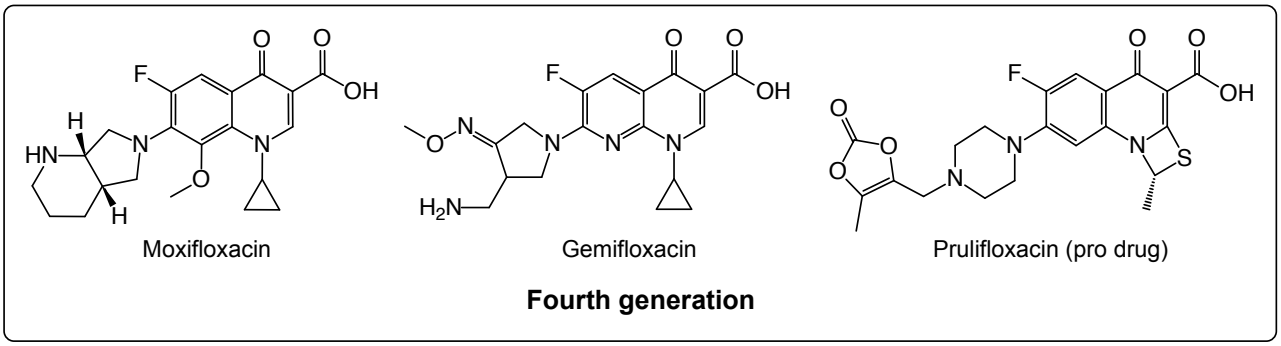

Figure 1.5: Generations of some selected quinolones. Ciprofloxacin (second generation) is the most consumed antibacterial agent worldwide [32, 33]

1.1.2.3 Cellular targets, mechanism of action, binding mechanism, resistance and structure-activity relationship (SAR)

It's essential for an antibiotic to target the prokaryotic bacterial cells rather than the eukaryotic human cells. Because of differences in some enzymes present in human and bacteria, quinolones are able to attack the bacterial cell rather than the human cell. The cellular target of the quinolones are the two bacterial topoisomerase II enzymes; DNA gyrase and topoisomerase IV [29, 34–36]. Both topoisomerases are essential to the bacteria as they catalyze DNA synthesis, and by interfering with these enzymes, DNA replication is disrupted and thus cell divison [36].

During bacterial DNA replication, a temporary double-stranded break in the double helix is created by the topoisomerases in order to prevent supercoiling (tangling) of the helix. [29, 34]. The ligation (rejoining) of the temporary cleaved DNA is dependent of, amongst other things, a divalent cation, preferably Mg^{2+} [29, 34]. Quinolones bind at this cleavage-ligation site and stabilizes the cleavage (Figure 1.6), preventing ligation and causing cell death.

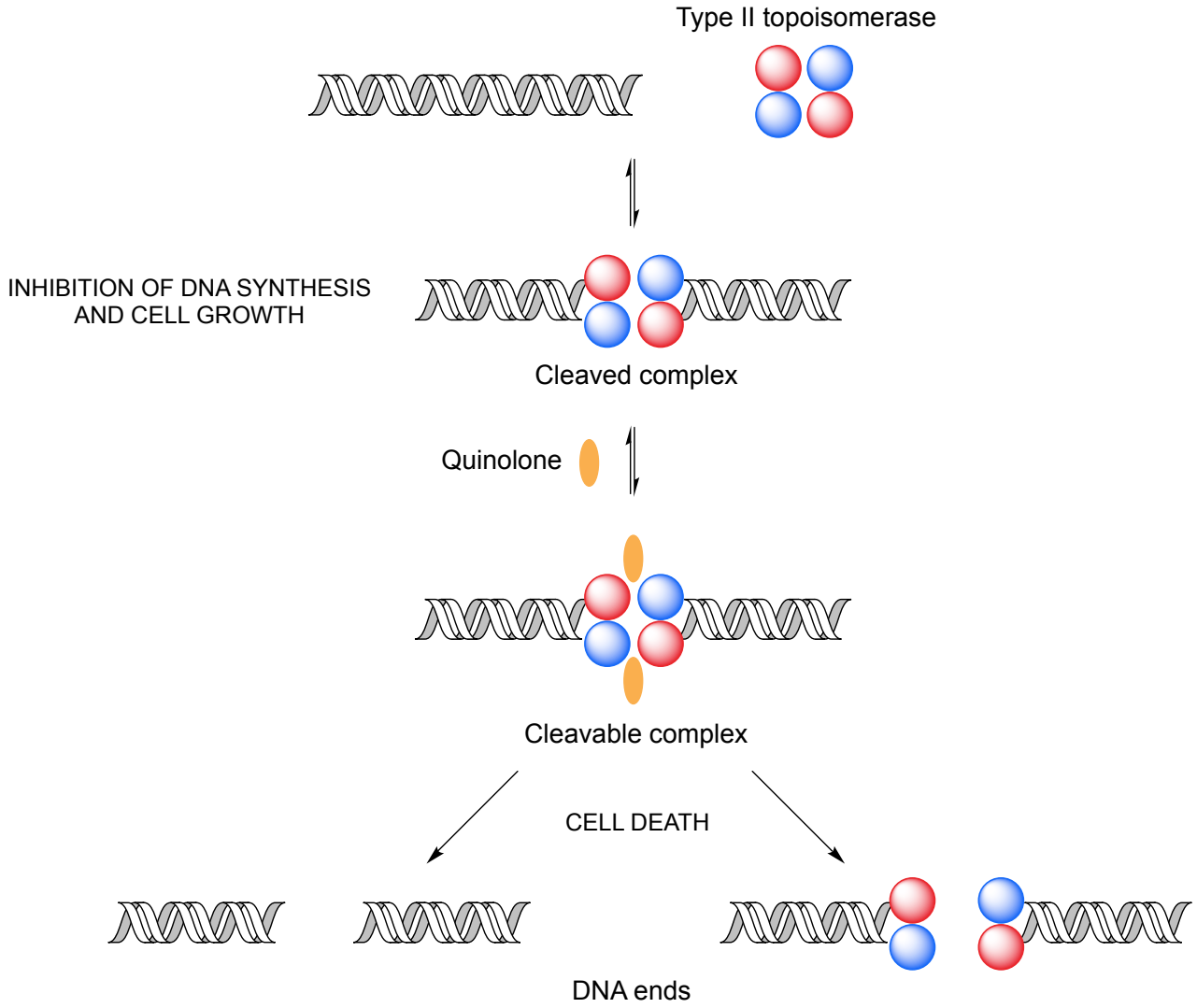

Figure 1.6: Quinolone mechanism of action: formation of a cleaved complex stabilized by quinolones leading to cell death [36]

The binding mechanism of quinolones to the topoisomerases has not been known until recently [37, 38]. A series of structural studies of the cleavage complex formed with topoisomerase II in the presence of quinolones have shown that the quinolones are located near the the serine and acidic resides (Figure 1.7). However, not in close enough proximity to mediate a direct drug binding [39–42]. Instead, it has been shown that the C3/C4 keto acid in the quinolone chelates a non-catalytic Mg^{2+} which is coordinated to four water molecules. Two of these water molecules are situated close enough to the serine and acidic resides to form hydrogen bonds, and two of them form hydrogen bonds with the DNA (Figure 1.7) [40, 43–45]. The primary reason for quinolone resistance is mutations in the amino acid residues (Figure 1.7) that anchor the water-metal-ion bridge [40, 46, 47]. Mutations in these cause disruption of the bridge and hence no bond formation between quinolone and topoisomerases, which in turn can lead to resistance.

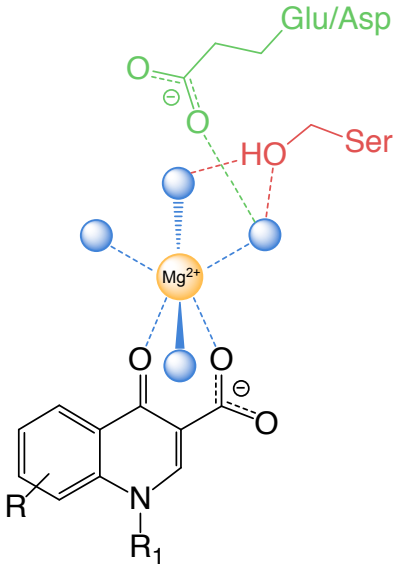

(a) The water-metal ion bridge that mediates interactions between quinolones and topoisomerase. DNA is omitted from this figure for simplicity. Residue numbering is also left out. The quinolone is depicted in black, water molecules in blue, Mg^{2+} in orange, serine in red and the acidic residue in green. The blue dashed lines represent octahedral coordination of four water molecules and C3/C4 keto acid to Mg^{2+}. The red dashed lines represent hydrogen bonding between water and the serine residue. The green dashed line represents hydrogen bond between water and the carboxylate of glutamic/aspartic acid [40].

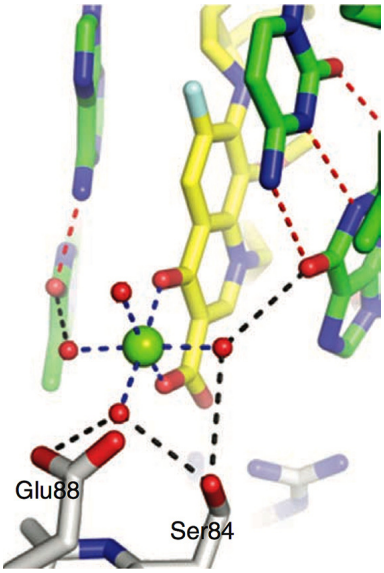

(b) The water-metal ion bridge between moxifloxacin and topoisomerase IV from the bacteria *A.Baumanii*. DNA is depicted in green, numbered serine and glutamic acid in gray, moxifloxacin in yellow, Mg^{2+} as a green sphere and the water molecules as red spheres. The blue dashed lines represent octahedral coordination of four water molecules and C3/C4 keto acid to Mg^{2+}. The black dashed lines represent hydrogen bonding between enzymes residues and water and DNA and water [43].

Figure 1.7: Quinolone binding mechanism.

What could be understood from the binding mechanism is that there are certain structural features in the quinolone that are necessary to ensure the appropriate action/biological activity. This relationship is referred to as a structure-activity relationship (SAR). There are also structural features that is not crucial for biologic activity, but that increases other effects such as efficacy, potency and that reduces undesired side-effects. Domagala *et al.* published an extensive review on the SAR of quinolones in 1994 which is summed up in Figure 1.8 [48].

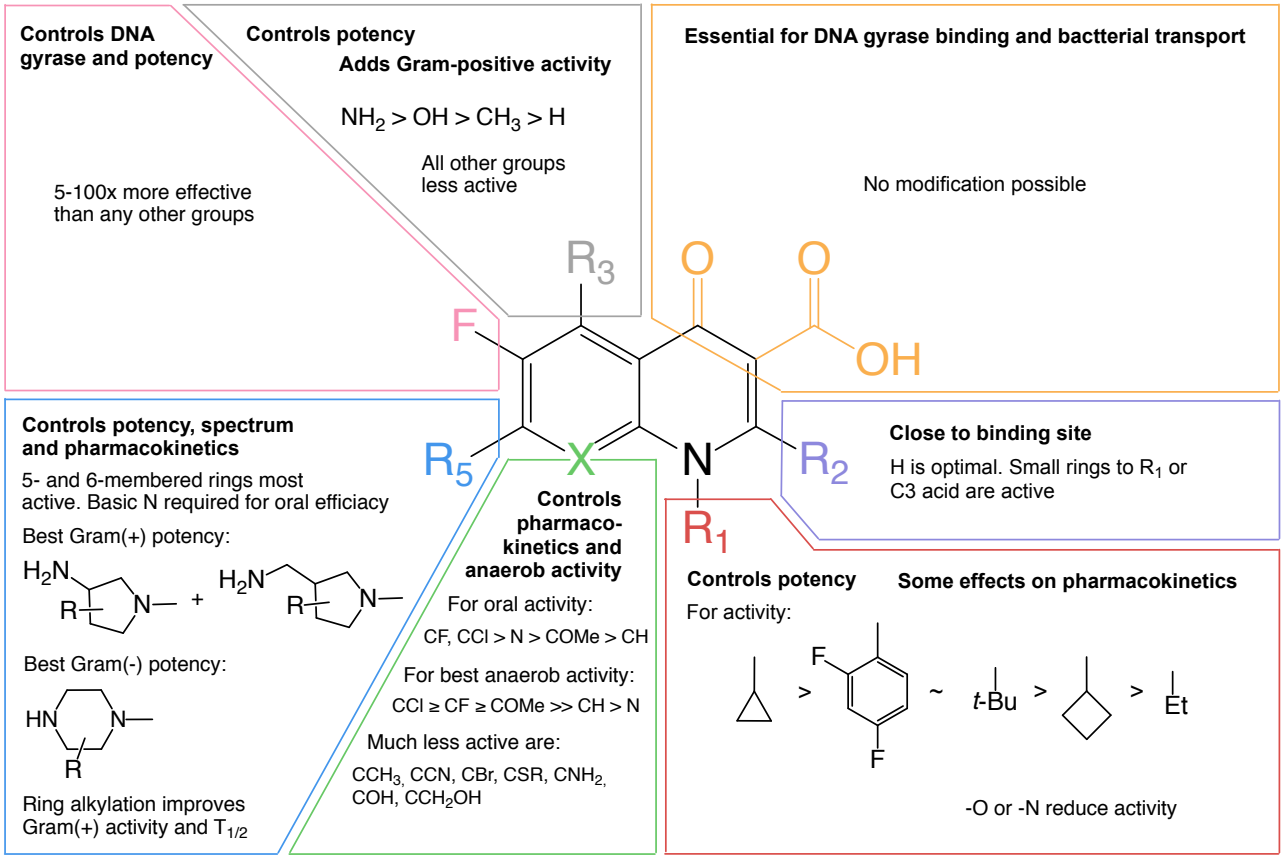

Figure 1.8: Structure-activity relationship (SAR) of quinolones [48]

The substituent in position 1 is a part of the enzyme-DNA binding complex (depicted in Figure 1.7), and has a hydrophobic interaction with the DNA [47, 49]. It also controls potency and has some effect on pharmacokinetic. A cyclopropyl group is considered the most optimal group in this position [47, 48]. In position 2, the substituent is in close proximity to the binding site and a hydrogen is optimal to avoid steric hindrance [47, 48].

Modification of the 3-carboxylic acid and/or 4-carbonyl in position 3 and 4 will lead to significant loss of biological/antibacterial activity [47, 48]. The keto acid is directly involved in the binding mechanism and considered essential for biological activity [40, 43, 44].

The substituent in position 5 controls potency. The optimal groups are considerd to be NH_2 and OH followed by CH_3, then H. These groups show increased activity against Gram-positive bacteria [48]. An introduction of fluorine in this position 6 has shown a considerable increase of potency and modifications at this site will reduce antibacterial efficacy [48].

The substituent in this position 7 influences potency, spectrum and pharmacokinetics [48]. The optimal groups for this position have been 5- or 6-membered nitrogen heterocycles. The most common ones are aminopyrrolidines and piperazines. The basic nitrogen is required for oral efficacy [48]. Position 8 primarily controls *in-vivo* efficacy with CF, CCl or N being the optimal groups [48].

Both older and more recent studies on quinolones or hybrid-quinolones have revealed that certain molecular features can be modified in other ways than illustrated in Figure 1.8, preserving or enhancing antibacterial activity, potency and/or other aspects of biological activity [50–65]. However, none of these are or have been actual antibacterial agents on the market.

1.1.2.4 Other biological effects of quinolones

Besides their typical antibacterial activity, quinolones display other biological effects such as anti-cancer, anti-viral and anti-tuberculosis [66–74]. Vosaroxin (Figure 1.9), a 8-azaquinolone, was the first-in-class anticancer quinolone derivative to be used in treatment for acute myelogenous leukemia (AML) and ovarian cancer, but recently failed phase III of the clinical trials [75–77].

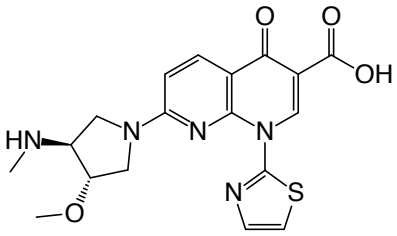

Figure 1.9: Vosaroxin

1.1.3 Bioisosterism

In drug design, bioisosterism is a strategy used for molecular modification [78]. Bioisosters are atoms, groups or molecules with similar chemical and physical properties which produce broadly similar biological properties [78]. The purpose of exchange one bioisoster for another is, amongst other tings, to maximize a drugs' desired activity and simultaneously reduce side-effects [79]. A few examples to illustrate bioisosteric groups are presented in figure Figure 1.10.

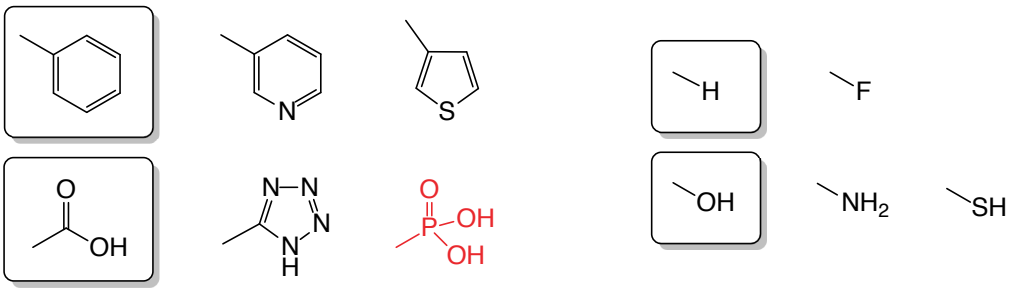

Figure 1.10: Examples of bioisosters [80]. The red colored structure is phosphonic acid.

The structure represented in red in Figure 1.10 is a phosphonic acid, which is a bioisoster of carboxylic acid. Synthesis of phosphonic acid bioisosters of a chosen quinolone was one of the goals in the second part of this project.

1.2 Examples of synthetic routes to 8-azaquinolone antibacterial agents

This section will only focus on reported synthetic routes to *8-azaquinolones*. Examples of routes to two different 8-azaquinolones; nalidixic acid and enoxacin, will be given as they were the focus of the work that will be presented later in this report.

1.2.1 Nalidixic acid

Lesher *et al.* reported the first synthesis of nalidixic acid as depicted in Scheme 1.2 [26]. The bicyclic ring was formed in a Gould-Jacobs type reaction [81]. Condensation of **I** with diethyl ethoxymethylenemalonate (DEEMM) gave **II** which was cyclized to **III**. Nalidixic acid was afforded after alkylation and hydrolysis. Reagents used in the last two steps were not included in the paper. Nor were any yields.

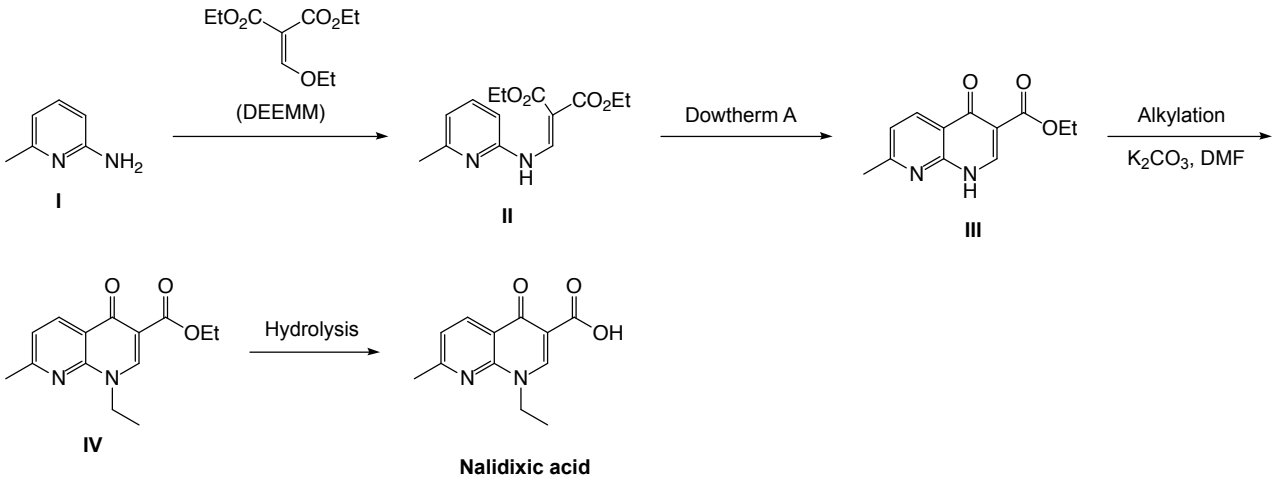

Scheme 1.2: Synthesis of nalidixic acid by Lesher *et al.* [26].

Another route to nalidixic acid was reported by Santilli *et al.* and are displayed in Scheme 1.3 [82]. Dechloroamination of **V** gave compound **VI**. Cyclized compound **VII** was obtained after a Dieckmann condensation. Nalidixic acid was afforded after hydrolysis at elevated temperatures and treatment with acid. Introduction of the 2,3-double bond was done by oxidation during the last step. The yield of the last step was not included in the paper.

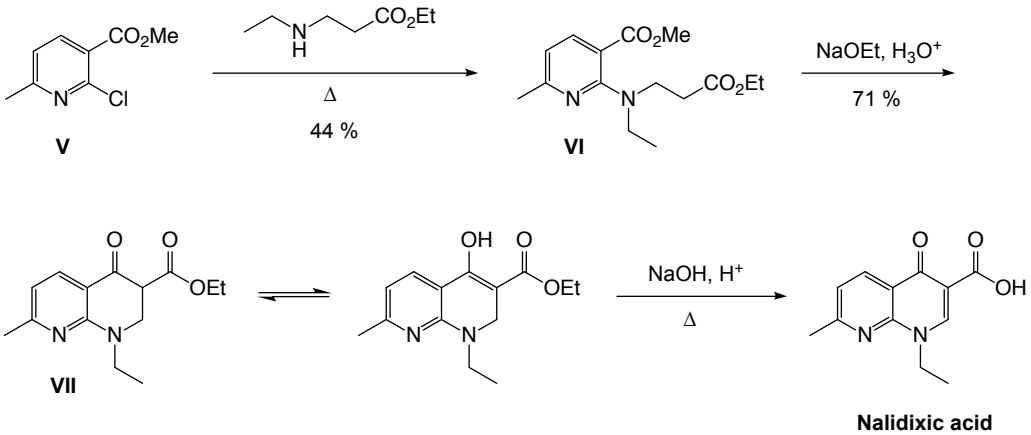

Scheme 1.3: Synthesis of nalidixic acid by Santilli *et al.* [82].

1.2.2 Enoxacin

The synthesis of enoxacin depicted in Scheme 1.4 was reported by Matsumoto *et al.* [83, 84] as an improvement of the first synthetic route they developed [85].

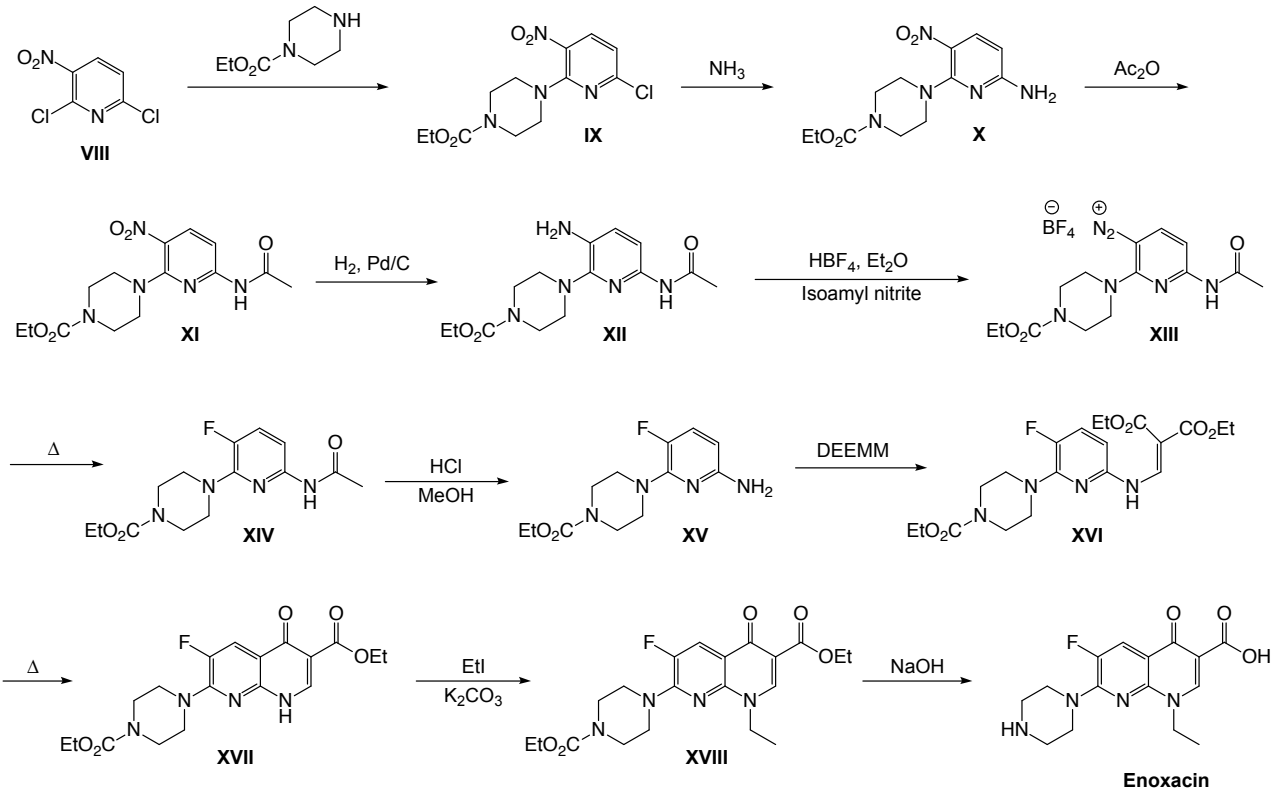

Scheme 1.4: Synthesis of enoxacin by Matsumoto *et al.* [83, 84, 86].

In the first two steps of the synthesis, two chlorine atoms were displaced with carboethoxypiperazine and ammonia, respectively, which gave compound **X**. The amine was acylated with acetic anhydride and the nitro group was reduced by hydrogenation with palladium on carbon, which afforded **XII**. Further, a Sandmeyer reaction was carried out in order to generate **XIII**. Heating of **XIII** afforded the fluorinated compound **XIV**. After deacylation of the amide, the same cyclization approach as previously mentioned; Gould-Jacobs cyclization, gave the quinolone **XVII**. Enoxacin was afforded after alkylation and hydrolysis.

1.3 Chemical background

This section will provide an overview over diazo compounds as they are a vital part of the work presented in this report. First, the properties of diazo compounds in general will be discussed, followed by carbenes and carbenoids (metal-carbenes). The reaction modes of diazo compounds along with examples of reactions employing them will also be given. The background for this project will be presented in the last section.

1.3.1 Introduction to diazo compounds

A diazo compound is a compound bearing N_2 as a terminal functional group (general formula $R_2C{=}N_2$). The first diazo compound was discovered in 1883 when Theodor Curtius synthesized ethyl diazoacetate (EDA) from the ethyl ester of glycine [87]. The simplest diazo compound, diazomethane, was not synthesized until a few years later (1894) by Hans von Pechmann [88]. Since their discovery, diazo compounds have been widely used in organic synthesis. Their ability to generate carbenoids in combination with appropriate transition-metal catalysts allow them to participate in a number of both intra- and intermolecular reactions [89, 90]. Such reactions are for instance cyclopropanations [91], C-H insertions [92], heteroatom-H (O-H, N-H, S-H, Si-H) insertions [93] and ylide transformations [94]. The chemo- and stereoselective properties of carbenoids generated from diazo compounds make them useful in synthesis of natural products and drugs [95, 96].

1.3.2 Properties of diazo compounds

In the early years after its discovery, it was unclear whether the structure of the diazo group was linear **1** or cyclic **2** (Figure 1.11). The molecular structure of diazomethane was solved by Boersch in 1935 as an open, linear structure [97]. Later, in 1957, Clusius resolved the structure of EDA, proving its linearity as well [98].

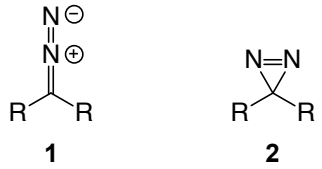

Figure 1.11: Proposed structure of the diazo group; linear (left) and cyclic (right). Compounds bearing the cyclic structure to the right are known as diazirines.

The linear structure of the diazo group is generally described with resonance forms **3a-d** (Figure 1.12), where **3a** and **3b** are the main contributors to the overall structure [99].

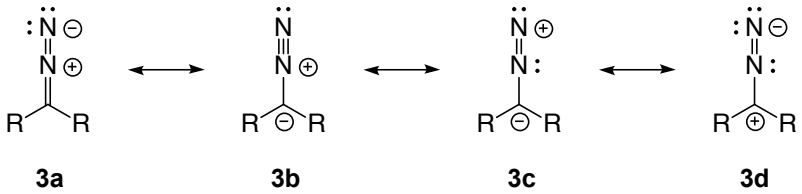

Figure 1.12: Resonance structure of general diazo compound.

Diazo compounds can be highly reactive due to favorable loss of nitrogen gas (Scheme 1.5). As a result, explosions are a hazard when working with these compounds. Diazomethane may

be the prime example, well known for being a very explosive and highly toxic yellow gas at room temperature [100]. Diazomethane can explode at room temperature upon contant with impurites, alkali metals, rough glass or solid surfaces, and can even explode in storage if the solution is higly concentrated [101]. EDA, a yellow oil at room temperature, is also a highly reactive compound, but much less explosive and is much easier to handle.

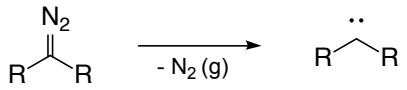

Scheme 1.5: Loss of nitrogen gas in order to generate the corresponding carbene. R=H gives diazomethane.

The thermal stability of diazo compounds is dependent on the R-groups in the α-position to the diazo carbon. Electron withdrawing groups (EWGs) will help increase the stability. The additional stabilization might be explained by resonance effects as illustrated with resonance forms **4a-c** in Figure 1.13. The delocalization of the negative charge in **4b** onto the carbonyl in **4c** is not possible in alkylated diazo compounds where the carbonyl (or other EWGs) are absent, which rationalizes the added stability [101]. The degree of electron withdrawal from the EWG is also significant for the thermal stability. Generally, the *more* electron withdrawing, the *less* stable [99].

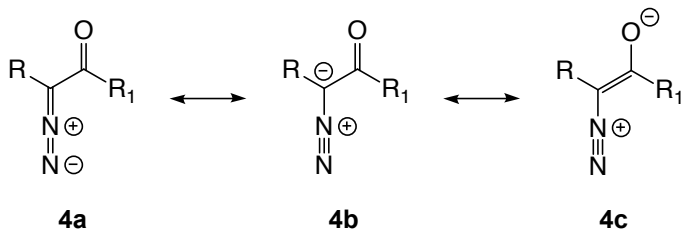

Figure 1.13: Resonance stabilizaed α-diazocarbonyl. R=H and R_1=OEt gives EDA.

Resonance structure **4b** has importance in explaining the nucleophilic and basic character of the diazo carbon. Bug *et al.* investigated the nucleophilicity of diazo compounds with different α-substituents in reactions against benzyhydryl cations [102]. They showed that the substituents on the diazo carbon largely influences the nucleophilicity and that the more electron withdrawing substituents gave the less nucleophilic diazo carbon.

There has also been an attempt to find a relationship between thermal stability and basicity of diazo compounds. Diazo compounds are known to decompose in acid [103–106]. Early studies by Staudinger *et al.* from 1916 investigating the thermal and acidic stability of diazo compounds revealed that there was not always a correlation between the two [107]. Later, in 1960s, thermal decomposition and acid catalyzed hydrolysis of series of diazocarbonyl compounds and analogous diazophosphonates was investigated by Jugelt *et al.* [108–112]. It was observed that diazocarbonyls show 2-6 times slower acidic hydrolysis than the phosphonate analogues which was due to increased mesomeric effect of the carbonyl group compared to the phosphonate group [112]. The increased delocalization of the electron pair of the diazo carbon on to the ester group (resonance structure **4c**) was responsible for a slower protonation [112]. Thermal decomposition of the diazoesters and diazophoshponates showed that the phosphonates were more thermally stable than the esters. This was explained by the larger contribution of resonance structure **4a** (Figure 1.13) for the phosphonates compared to structure **4c** (Figure 1.13) for the esters. This suggest an increase in double bond character of the C-N bond of the phosphonates which do not favor release of N_2 in the same way as the esters. The relationship between thermal stability and basicity is summed up in Figure 1.14.

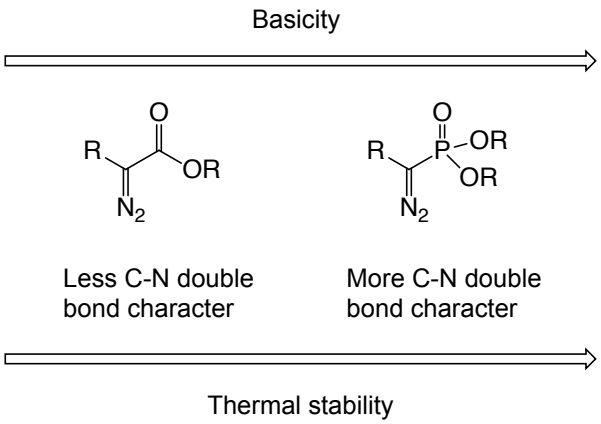

Figure 1.14: The relationship between thermal stability and basicity of diazoesters and diazophosphonates [112].

1.3.3 Carbenes

Diazo compounds decompose thermally or photochemically by release of N_2 in order to generate the corresponding carbene. Carbenes are neutral, divalent species with six valence electrons where two of them exist in non-bonding orbitals. They are divided into two classes, singlet or triplet (Figure 1.15), based on the spin state of the system, which also dictates their reactivity [113, 114]

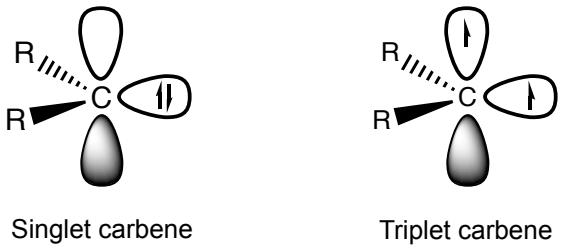

Figure 1.15: Singlet and triplet carbene.

Singlet carbenes feature an empty p-orbital and a paired electron pair in a non-bonding sp^2 orbital and possess an ambiphilic character [113]. Triplet carbenes have two singly occupied orbitals, one sp^2 and one p, and are regarded as diradicals [113]. The spin state and stability of carbenes are highly influenced by its substituents. It is etablished that σ-electron withdrawing substituents favor the singlet carbene over the triplet [113], and π-donating substituents such as N, O and halogens stabilize the singlet state by donating lone-pairs into the empty p-orbital [114].

Over the years extensive work has been performed in order to correlate the structure and reactivity of carbenes [115–118]. By studying a series of different substituted carbenes towards cyclopropanation with olefins, Moss *et al.* demonstrated the substituents effect on philicity [119–121]. An "intrinsic reactivity index" has been established, ranking the nucleophilicity and electrophilicity of singlet carbenes [122].

1.3.4 Reactivities and decomposition modes of diazo compounds

Diazo compounds are able to generate carbenes by N_2-extrusion and carbenoids with appropriate transition-metals. There are also other reaction modes of diazo compounds. All together they can be categorized into four modes: reactions without loss of the diazo group, reactions with loss of N_2 without carbene or carbenoid intermediates, reactions with loss of N_2 and generation of free carbenes and reactions with loss of N_2 and catalytic generation of transition-metal carbenoids. The reactions presented in this report are mainly based on transition-metal carbenoids and will be discussed in more detail from 1.3.4.2. The remaining three modes are briefly exemplified below.

1.3.4.1 Examples of non-carbenoid reactions

In Scheme 1.6 are selected examples of reactions of diazo compounds with no carbenoid formation. Preparation of heterocycles such as pyrazoles or pyrazolines can be accomplished by a 1,3-dipolar cycloaddition (Huisgen reaction) between a diazo compound and an dipolarophile as in route **A** (Scheme 1.6). In these reactions, the diazo is the 1,3-dipolar component and N_2-group is preserved [123]. Diazo compounds can serve as nucleophiles in homologation reactions adding to carbonyls and extending chains as in route **B** (Scheme 1.6) (Büchner–Curtius–Schlotterbeck reaction)[124–126] or expanding rings as in route **C** (Scheme 1.6) [127–129]. Reactions of diazo compounds as free carbenes can be found in homologation of carboxylic acids (Arndt-Eistert reaction) as in reaction (and rearrangement) route **D** (Scheme 1.6) [128, 130].

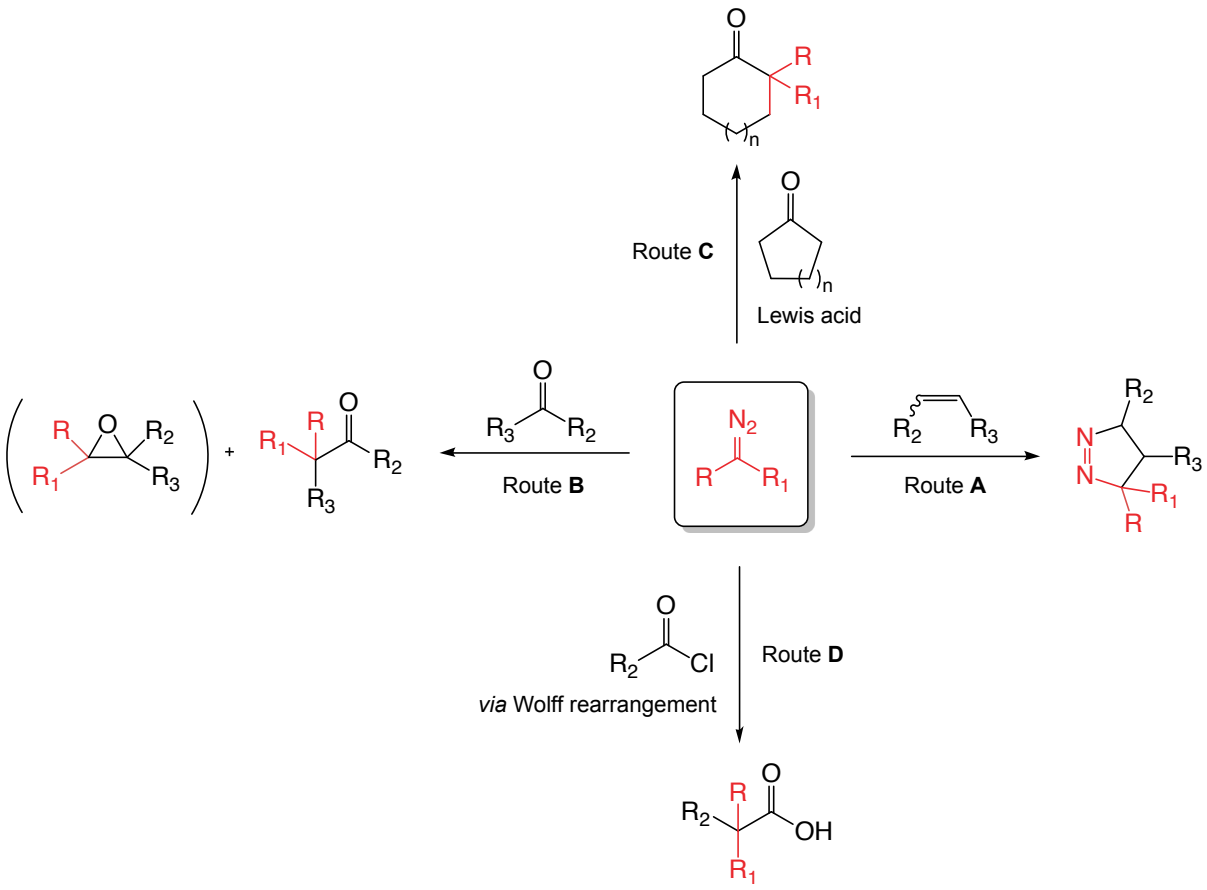

Scheme 1.6: Reactions of diazo compounds without carbenoid formation [123–130].

1.3.4.2 Catalytic decomposition of diazo compounds with transition-metals

In presence of appropriate transition-metals catalyst, diazo compounds decompose to generate the corresponding metal-carbenoid. The first metal-carbenoid was proposed by Yates in 1952 who investigated the decomposition of α-diazoketones in the presence of copper and suggested that an intermediate copper-carbenoid was formed [131]. Compared to free carbenes, metal-carbenoids are generally less reactive allowing more selective reactions. As in the free carbenes described in 1.3.3, the carbenoids' α-substituents is one of the main parameters affecting their reactivity [132]. The other being the ligands of the metal catalyst [133]. The metal-carbenoids can categorized into three different classes defined by their substituents; acceptor, acceptor/acceptor and donor/acceptor (Figure 1.16) [134, 135].

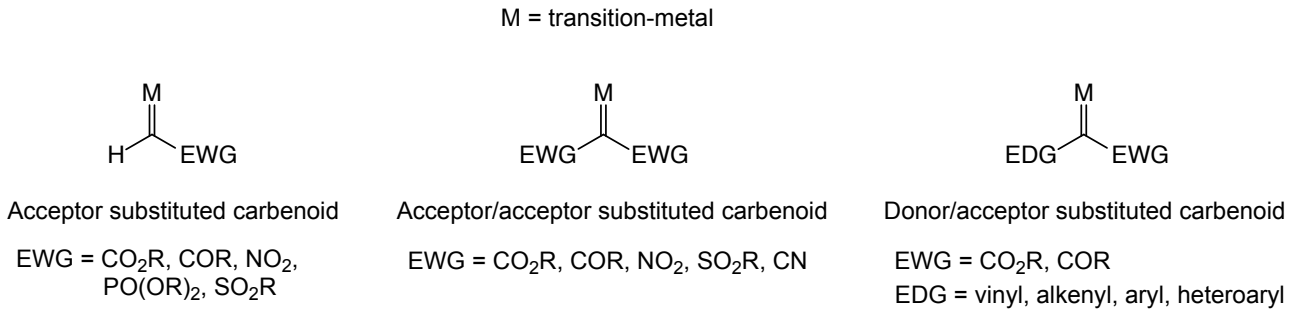

Figure 1.16: Classification of carbenoid intermediates by Davies [134, 135].

Acceptor groups (EWGs) increase the electrophilicty and thus the reactivity of the carbenoids [134, 135]. The donor groups (EDGs) has a stabilizing effect by lowering the electrophilicity of the carbenoids, and thus its reactivity making them highly selective in a number of both intra- and intermolecular reactions [136, 137].

1.3.4.3 Dirhodium(II)-catalysts

A number of transition-metals have been investigated for their effectiveness as catalysts for decomposition of diazo compounds [138]. Several transition-metals *can* be utilized [139], but since the introduction of dirhodium(II) tetraacetate, $Rh_2(OAc)_4$ (**5a**) (1.17a in Figure 1.17), by Teyssié *et al.* [140], Rh(II)-based catalysts have been the most frequently applied catalysts in the decomposition of diazo compounds [138]. Rh(II) catalysts have proven useful in a number of reactions being highly regio-, chemo- and stereoselective as well as affording high yields [135]. Examples of some Rh(II)-carbenoid reactions will be presented in 1.3.4.4.

Since the discovery of the catalytic properties of **5a**, one of the most frequently employed classes of Rh(II)-catalysts are the carboxylates. In a one-step ligand-exchange, **5a** can be converted to, amongst other, another popular Rh(II)-catalyst, namely the $Rh_2(esp)_2$ (**6**) (1.17c in Figure 1.17) [141]. As other Rh(II)-catalysts, **5a** and **6** are bimetallic paddlewheel complexes stable to heat, moisture and ambient atomsphere [142]. They are neutral 16-electron complexes with two axial coordination centers, one on each rhodium [143]. They behave as Lewis acids and the degree of electrophilicity is determined by the ligands. Electrophilicity and reactivity towards diazo compound decomposition are increased by electron withdrawing ligands. The aforementioned regio-, chemo- and stereoselectivity of Rh(II)-carbenoid reactions are highly dependent on the ligands [142, 144–146].

Rh(II)-complexes are inclined to coordinate to a number of different molecules in axial positions (**5b**) (1.17b in Figure 1.17). The coordination is due to σ-lone pair donation from the coordinating molecule and π-back donation from rhodium. The axial positions are often occupied

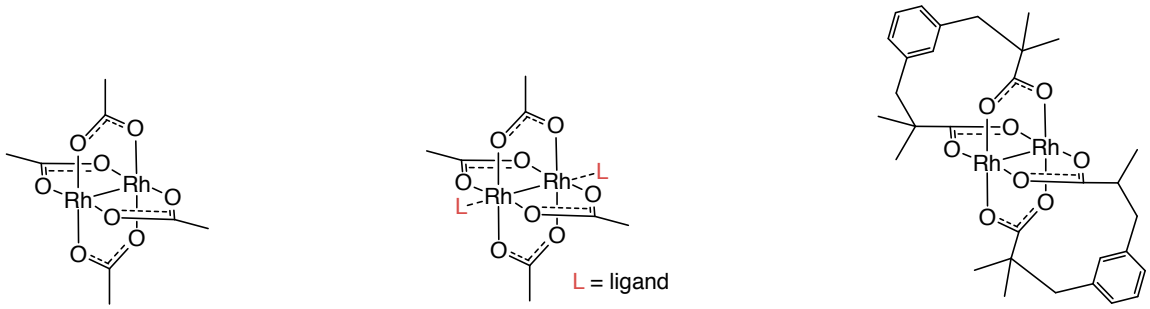

5a

(a) $Rh_2(OAc)_4$

5b

(b) $Rh_2(OAc)_4$ with axially bonded ligands

6

(c) $Rh_2(esp)_2$

Figure 1.17: Dirhodium(II)-complexes with carboxylate ligands.

by coordinating solvent molecules which can easily be displaced by other coordinating N-, O-, C-, P- and S-ligands [147]. Earlier, researchers have only used the bridging ligands to tune the catalytic properties of the Rh(II)-complexes since the axial ligands were considered less important. Over the last few years, strategies to axially modify the complexes have appeared and are of greater importance than first believed as it affects catalytic properties, reactivity *etc.* [147, 148]

1.3.4.4 Examples of reactions employing Rh(II)-carbenoids

In Scheme 1.7 are some selected examples of Rh(II)-carbenoid reactions. Cyclopropanation of olefins in route **A** (Scheme 1.7) is one of the most studied reactions of transition-metals carbenoids [149]. It has become one of the "standard" reactions for testing new catalysts and diazo compounds [149]. Cyclopropanes are versatile molecules with several potential applications in organic chemistry. They are an entity frequently found in natural products [150] and important in synthetic design as they, amongst other, undergo ring openings and rearrangements [151].

Another important reaction is the C-H-insertion (route **B**, Scheme 1.7). The superior selectivity of Rh(II)-carbenoids, as apposed to free carbenes, allows for synthetic useful transformations as they can selectively insert into either sp^3 or sp^2 hybridized C-H bonds [92, 152–155].

Rh(II)-carbenoids are also employed in heteroatom-H bond reactions as seen in route **C**, (Scheme 1.7). O-H-, N-H-, S-H- and Si-H insertions have been reported [93]. In the total synthesis of (±)-Maoecrystal V, Yang *et al.*, exploited a Rh(II)-catalyzed O-H-insertion reaction [156], and Merck an N-H-insertion in their synthesis of (+)-Thienamycin [157]. Rh(II)-carbenoids in reaction with basic heteroatoms can lead to ylide formation (route **D**, Scheme 1.7) [158]. Ylides are of synthetic interest as they can undergo carbenoid cyclization/cycloaddition [159] or rearrangements [158, 160].

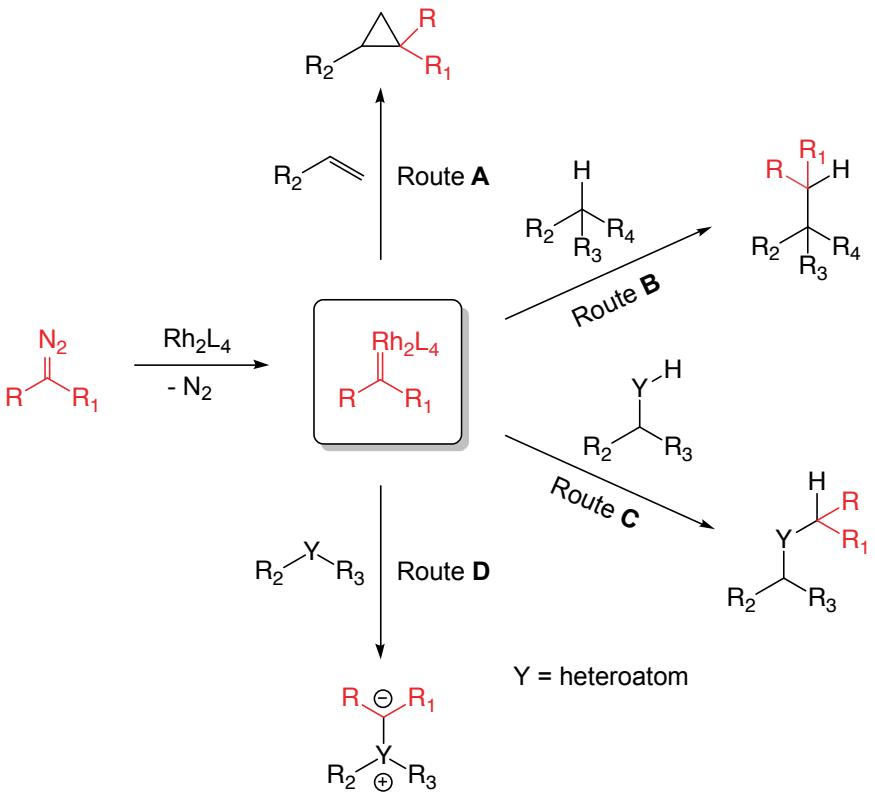

Scheme 1.7: Rh(II)-carbenoid reactions [92, 93, 149, 152–155, 158].

1.3.5 Halodiazoacetates and halodiazophoshponates

The work discussed later in this report is based on the employment of halodiazo compounds, more specifically ethyl halodiazoacetates (X-EDA) and diethyl halodiazophoshponates (X-EDP). Therefore, a separate section is devoted to the properties, synthesis and reactions of these compounds.

1.3.5.1 Properties of ethyl halodiazoacetates

The first synthesis of ethyl halodiazoacetates was reported in the late 1960s by Schöllkopf *et al.* when they synthesized ethyl chlorodiazoacetate (Cl-EDA), ethyl bromodiazoacetate (Br-EDA) and ethyl iododiazoacetate (I-EDA) [161–164]. Observations that these compounds readily decompose at room temperature was reported, but tangible data on the thermal stability were not reported until a systematic study was perfomed by Mortén *et al.* in 2016 [165]. Prior to this work, observations of carbene dimerization by decomposition of the X-EDAs had been reported (Scheme 1.8) [1].

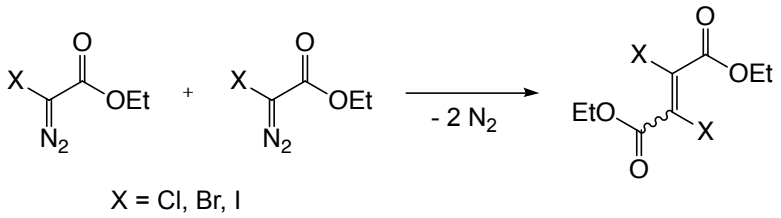

Scheme 1.8: Dimerization of X-EDA [1].

In the thermal stability study, it was discovered that the thermal stability of ethyl halodiazo compounds was in the same category as the non-stabilized alkyl diazo compounds even with an ester as α-substituent [165]. The thermal lability can be explained by the relatively high stability of the corresponding carbenes due to π-donation from the halogens into the empty p-orbitals of the carbenes [165]. It was also discovered that the nucleophilicity of X-EDA was much lower than EDA [165]. Thermal stability vs. carbene stability of the X-EDAs and EDA is summed up in Figure 1.18 while the relative thermal stability and nucleophilicity of X-EDAs against other diazo compounds are summed up in Figure 1.19.

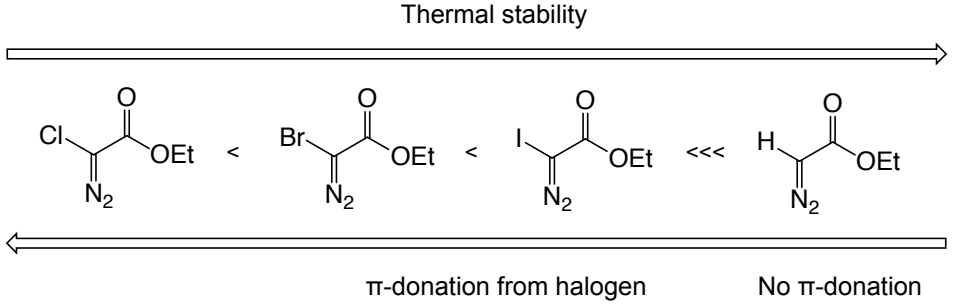

Figure 1.18: Thermal stability and halogen substituent contribution to π-donation [165].

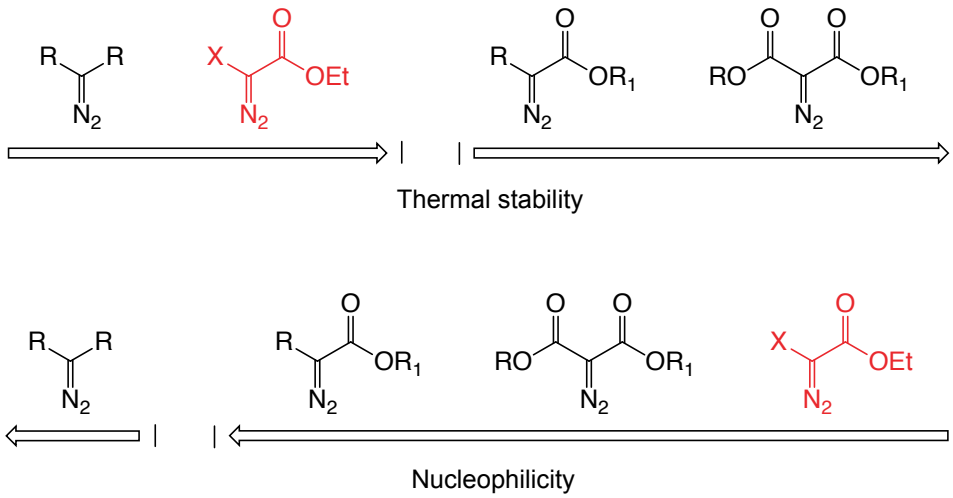

Figure 1.19: Relative thermal stability and nucleophilicity of X-EDA (red) [165]. R and R_1 are alkyl and/or aryl groups.

1.3.5.2 Synthesis and reactions of ethyl halodiazoacetates

Diazo compounds can undergo numerous transformations. By halogenation of diazo compounds prior to these transformations, halogens can be introduced in the target molecule. Introduction of halogens are of synthetic interest as several natural products and biologically active molecules contains them [166, 167]. With the introduction of halogens comes multiple ways of further functionalization/manipulation if desired.

Halogenation is one of several ways diazo compounds can be functionalized with retention of the diazo group [168, 169]. The first halogenations of EDA was, as mentioned, demonstrated by Schöllkopf *et al.* They synthesized X-EDA from EDA via metalation with HgO, then electrophilic halogenation by metal-halogen exchange with SO_2Cl_2, Br_2 and I_2 as halogenation sources (Scheme 1.9) [163].

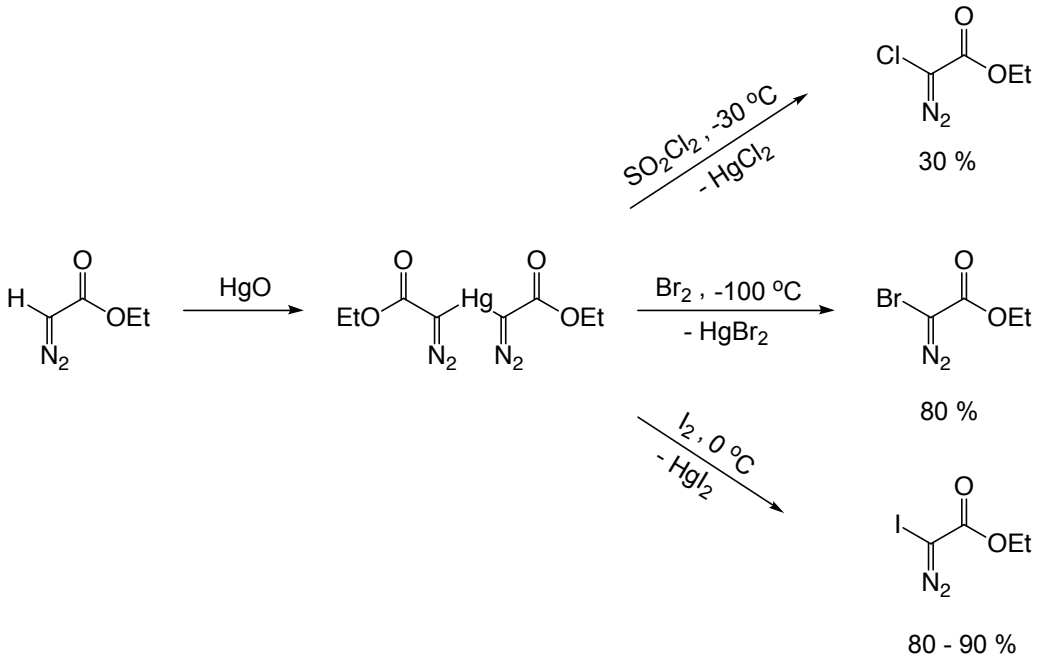

Scheme 1.9: Formation of halogenated EDA analogues by Schöllkopf *et al.* [163].

The apparent disadvantage of these reactions is the use and formation of mercury containing compounds. The toxicity and environmental hazards associated with mercury make them very little desirable to work with. Schöllkopf *et al.* did also report a synthetic route using silver [164], but the explosive nature of Ag-EDAs does not render this route any more favorable. A new, less toxic route for halogenation of EDA was reported by Bonge *et al.* in 2008 (Scheme 1.10) [1].

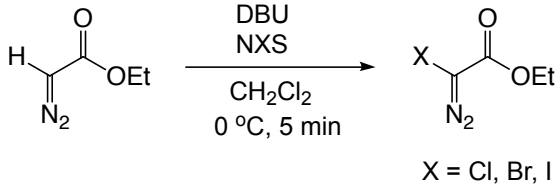

Scheme 1.10: Formation of halogenated EDA analogues by Bonge *et al.*[1].

The reaction employs an organic base (DBU) for deprotonation, then an electrophilic halogenation agent, *N*-halosuccinimide (NXS, where X = Cl, Br or I), and yields almost quantitatively conversion of EDA in 5 minutes. After a cold silica plug filtration, the obtained X-EDA can be employed in several Rh(II)-catalyzed reactions, summarized in Scheme 1.11.

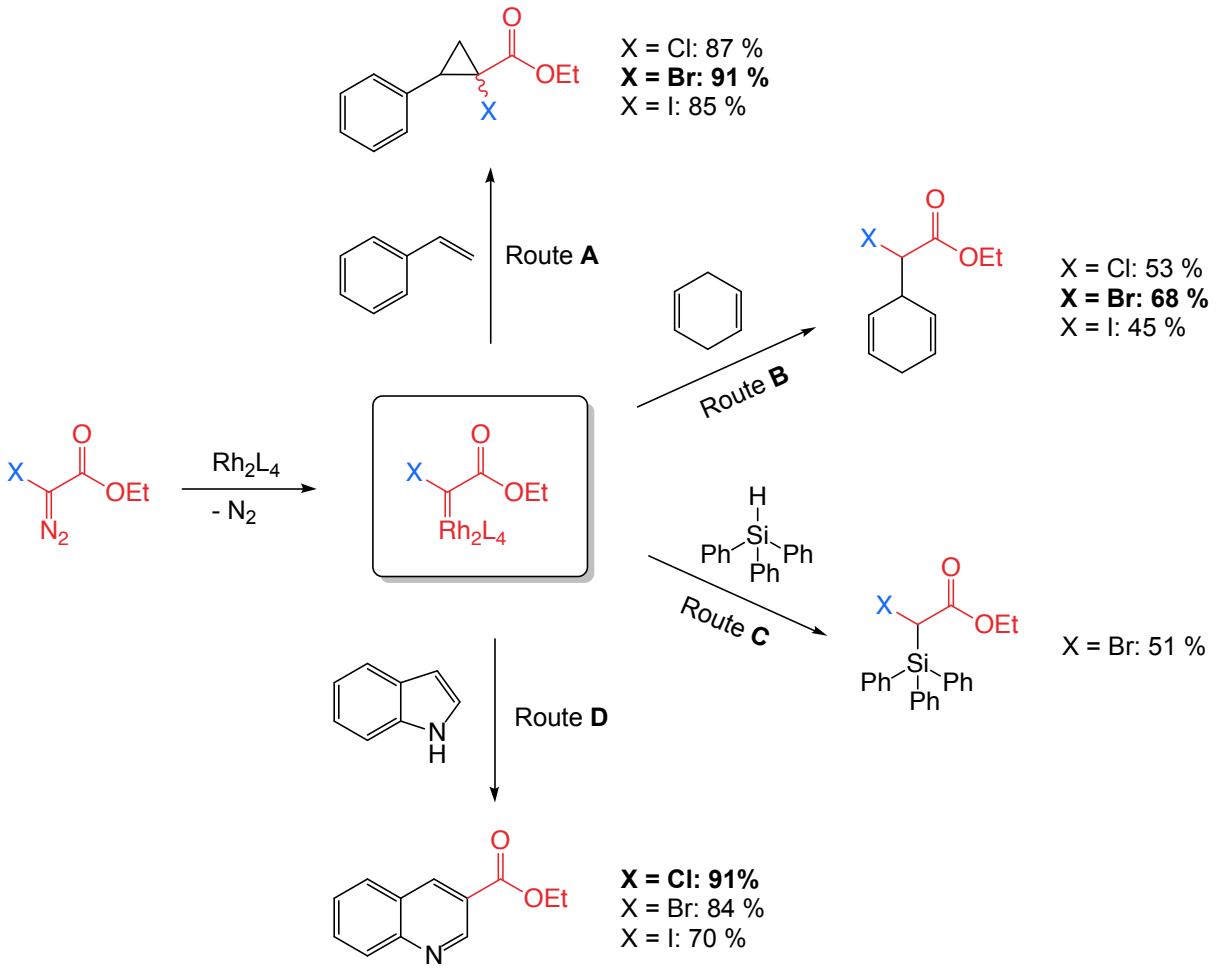

Scheme 1.11: Reactions and yields of various substrates with ethyl halodiazoacetates [1–3].

As can be seen from Scheme 1.11, halodiazoacetates can undergo many of the same Rh(II)-catalyzed transformations as the non-halogenated analogues: cyclopropanation route (**A**, Scheme 1.11) [1], C-H insertion (route **B**, Scheme 1.11) [2] and Si-H insertion (route **C**, Scheme 1.11) [2]. The reaction between X-EDA and indole in route **D** (Scheme 1.11), yielding a quinoline-3-carboxylate, is some of the work Magnus Mortén did during his master thesis, and the background for this very thesis. This reaction will therefore be discussed in more details in 1.3.6.

1.3.5.3 Properties of halodiazophosphonates

Very little is known about the properties of halodiazophosphonates as no systematic studies have been reported.

1.3.5.4 Synthesis and reactions of halodiazophosphonates

The phosphonate group is employed in several important reactions such as Horner-Wadsworth-Emmons olefination [170–172], Seyferth-Gilbert homologation [173] and Ohira-Bestmann modification [174, 175]. The phosphonate group is of interest as several natural and synthetic phosphonates have found widespread use medicine [176]. Their biological activity stems from their ability to function as, amongst others, bioisosters of carboxylic acids and phosphates/phosphate esters [176, 177]. More recently, the interest of α-brominated phosphonates have increased as they have begun to emerge as inhibitors of phosphate-recognizing proteins, which have potential as medicinal agents [178]. Development of methods allowing direct introduction of halogens (whose importance was emphasized in 1.3.5.2) and phosphonates are therefore of great interest, and transformations halodiazophosphonates can potentially do that.

The first halogenations of diazophosphonates was reported by Regitz *et al.* in 1979 [179]. They synthesized Br- and I-diazophosphonates via metalation with Ag_2O, then electrophilic halogenation by metal-halogen exchange with BrCN or I_2 (Scheme 1.12). Due to their low thermal stability, the halogenated diazophosphoantes were trapped with vinyl ketone in a [3+2] cycloaddition (step **A**, Scheme 1.12) to generate the substituted pyrazole or with triphenylphosphine (PPh_3) in step **B** (Scheme 1.12) to generate the azine.

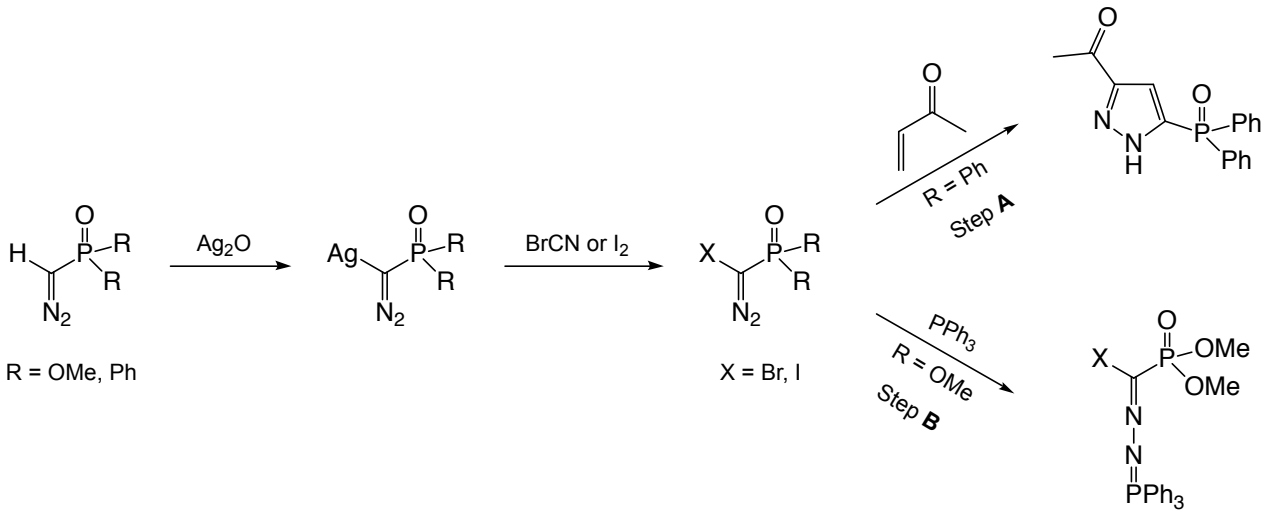

Scheme 1.12: Formation and trapping of halogenated diazophosphonates and -phosphinoxides [179].

For the same reasons mentioned in 1.3.5.2 and the synthetic and biologic relevance, new, less explosive and toxic routes to halogenated diethyl diazomethylphosphonate were developed by Schnaars *et al.* in 2012 and 2013 [4, 5]. Three different methods were used in the nucleophilic halogenation of α-aryliodonio diazophosphonate triflate salts in Scheme 1.13. The afforded halogenated diazophosphonate was then employed in Rh(II)-catalyzed cyclopropanation with styrene affording halocyclopropylphosphonates in various yields dependent on method and halogen.

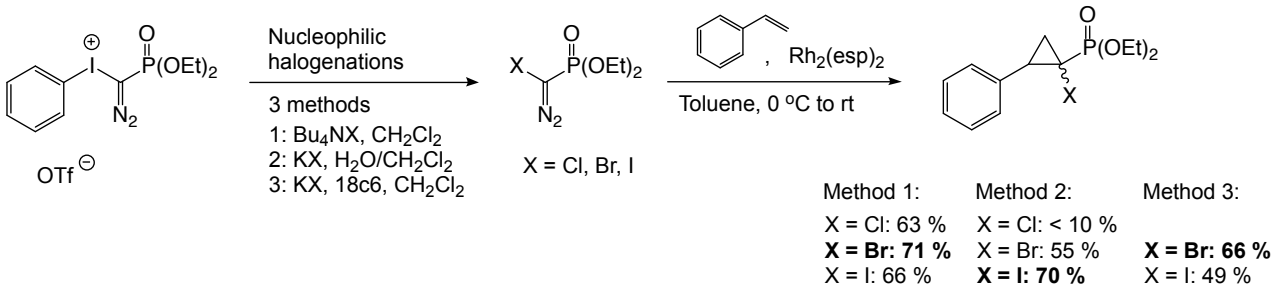

Scheme 1.13: Formation of X-EDP *via* nucleophilic halogenation of α-aryliodonio diazophosphonate triflate salts and subsequent Rh(II)-catalyzed cyclopropanation with styrene [5].

In the other route, NaH was employed as base for deprotonation, followed by electrophilic halogenation with *N*-halosuccinimide (NXS, where X = Cl, Br or I) and subsequent Rh(II)-catalyzed cyclopropanation reaction with styrene affording halocyclopropylphosphonates (Scheme 1.14).

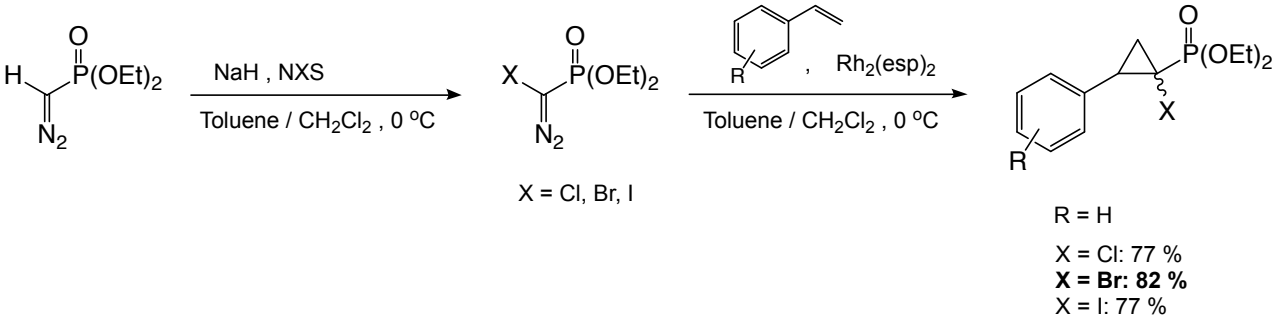

Scheme 1.14: Formation of X-EDP *via* electrophilic halogenation of EDP and subsequent Rh(II)-catalyzed cyclopropanation with styrene and substituted styrenes [4].

The substrate scope showed that the reaction was compatible with both electron withdrawing- and donating groups on styrene, as well 2-vinylnapthalene, *N*-vinylphthalimide and 1,1-diphenylethylene. The reactions gave good yields, ranging from 47% (1,1-diphenylethylene) to 82% (styrene), and good diastereoselectivity. Dimerization was observed for the halogenated EDP analogous to the dimerization in Scheme 1.8.

No other rhodium-catalyzed reactions with EDP or other halodiazophosphonates have been found in the literature.

1.3.6 Cyclopropanation-ring expansion reaction of indoles with X-EDA

As mentioned in the last part of 1.3.5.2, the reaction route **D** in Scheme 1.11 would be further discussed as it is the background for project presented in this report.

Prior to the reaction between halodiazoacetates and indole, the anticipated product, based on literature, was C-H insertion in position 3 of the indole. Instead, the cyclopropanation-ring expansion product was afforded [3]. The reaction conditions and proposed ring expansion mechanism is displayed in Scheme 1.15 [3].

Ring-expansions of indoles date back to (at least) 1887 [180–183]. Ring-expansions of various heterocycles with dihalogenated carbenes are fairly well known, *i.e.* the "abnormal" Reimer-Tiemann reaction with pyrrole and dichlorocarbene to form 3-chloropyridine [183]. However,

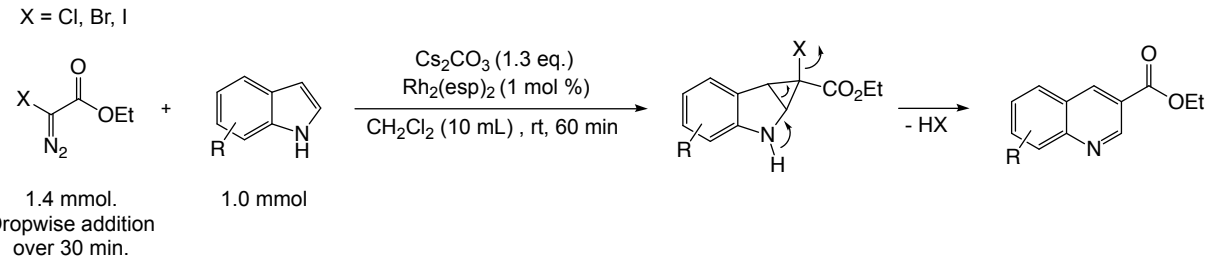

Scheme 1.15: Standard conditions and proposed mechanism for the $Rh_2(esp)_2$-catalyzed cyclopropanation-ring expansion between X-EDA and indoles [3]

none of these reactions involved Rh(II)-catalyed decomposition of a halodiazo compound and formation of the corresponding carbenoid to undergo cyclopropanation.

The substrate scope of the reaction in Scheme 1.15 showed compatibility with both electron withdrawing- and donating groups on the indole. With substiutents in position 3, 4, 5 and 6, yields ranging from 69-98% was obtained when X = Br. EDGs gave higher yield than EWGs. Substituents in position 7 gave much lower yield, 40%, and with substituents in position 2, no starting material was converted. *N*-Boc indole or *N*-methylindole did not give the cyclopropanated-ring expanded product, suggesting that a covalent bond to the nitrogen is detrimental [3]. The position of the substituents and their influence on the reaction is summarized in Figure 1.20.

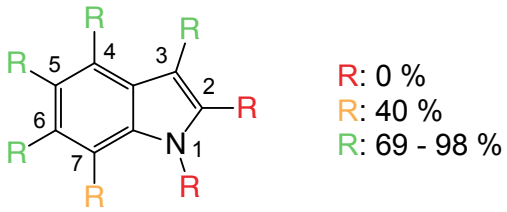

Figure 1.20: Graphical representation of the positional influence on the reaction. Green = positions that give excellent yields. Yellow = position that give decent yields. Red = positions that do not give the cyclopropanated-ring expanded product [3].

Chapter 2

Results and discussion - 7-Azaindoles and halodiazoacetates

In this chapter, the results of the Rh(II)-catalyzed cyclopropanation-ring expansion reaction between halodiazoacetates and 7-azaindoles will be presented. In addition, the yields of halodiazoacetates afforded from EDA and chlorination of 7-azaindoles will be presented. The results obtained will be discussed and explained.

2.1 Introduction

The substrate scope of the Rh(II)-catalyzed cyclopropanation-ring expansion reaction between halodiazoacetates and indoles have until now been limited to regular indoles with various substituents [3]

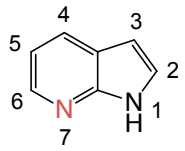

Figure 2.1: Numbering of 7-azaindole

In this study it was of interest to expand the substrate scope to include 7-azaindoles (Figure 2.1) and investigate whether these substrates behave similar to indoles, *i.e.* if the same cyclopropanated-ring expanded product is obtained and if the yields are as good as for the regular indoles (Scheme 2.1).

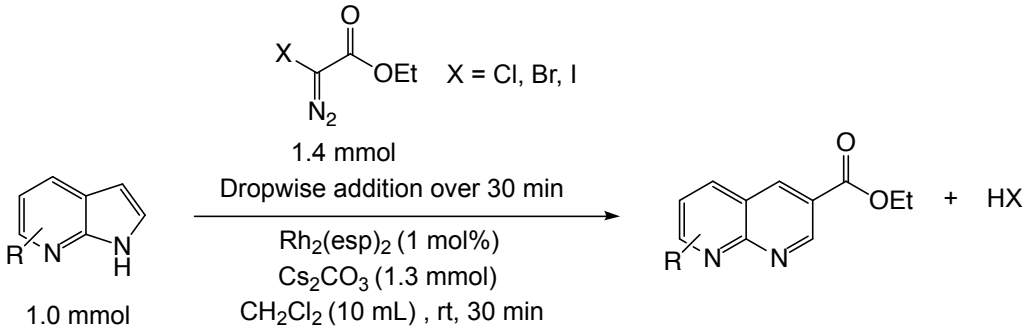

Scheme 2.1: Cyclpropanation of 7-azaindole and subsequent ring expansion/elimination to ethyl 8-azaquinolone-3-carboxylate under standard conditions. Anticipated reaction pathway and product formation based on literature [1, 3].

Further, it was of great interest to demonstrate the reactions' usefulness as a key step in the synthesis of the 8-azaquinolone antibacterial nalidixic acid and a non-fluorinated enoxacin analogue (Scheme 2.2). Synthetic routes towards both nalidixic acid and enoxacin were discussed in 1.2, but neither of these nor other reported synthetic routes to 8-azaquinolones employs the Rh(II)-catalyzed cyclopropanation-ring expansion reaction between halodiazoacetates and 7-azaindoles.

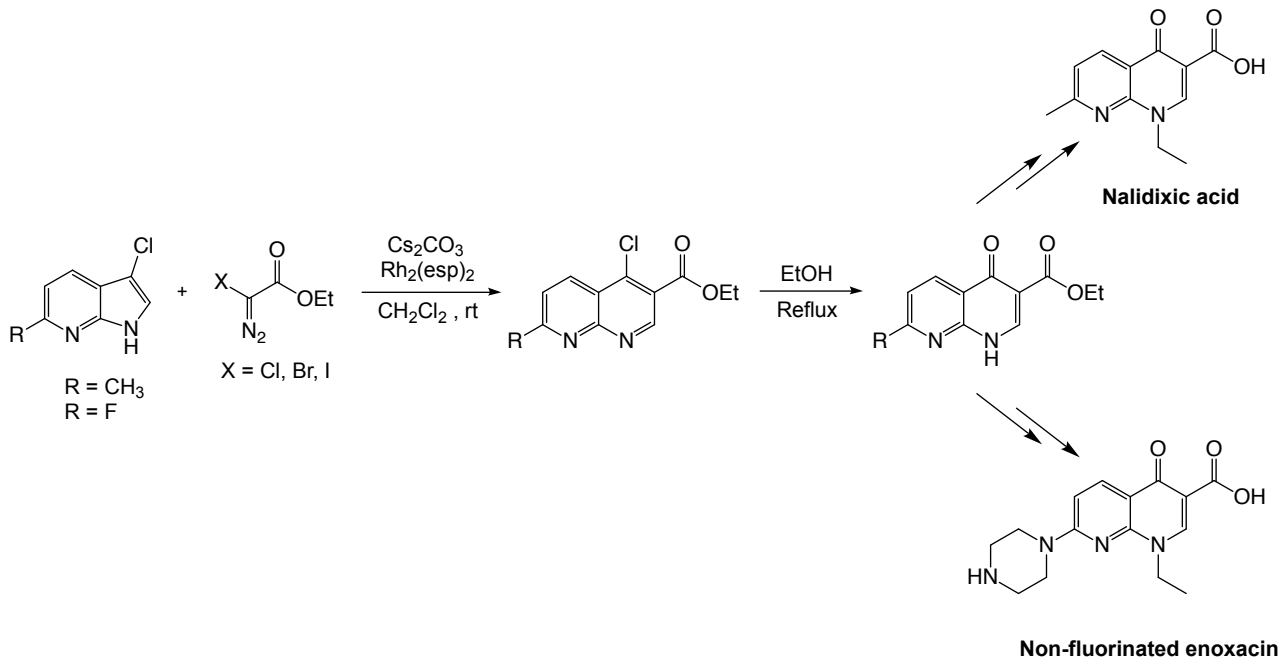

Scheme 2.2: Rh(II)-catalyzed cyclopropanation-ring expansion between C-3 chlorinated 7-azaindoles and halodiazoacetates as a key step in the synthesis of nalidixic acid and non-fluorinated enoxacin.

2.2 Halogenation of EDA

It was demonstrated by Mortén that both Cl-, Br and I-EDA could be employed in the cyclopropanation-ring expansion reaction of indole and form the same product [3]. However, since the yield was 14-20% lower when I-EDA was used (Scheme 1.11) it was decided to exclude it and focus on Cl- and Br-EDA throughout this work.

The EDA used in all reactions where X-EDA was employed, was provided by Sigma Aldrich. according to the supplier, the EDA contains $\geq$ 13 wt % DCM [184]. The exact amount of DCM was calculated prior to the yield measurements discussed below (2.2.1). The DCM content in EDA was determined by ^{1}H NMR analysis to be 12 %. The ^{1}H NMR spectrum of EDA and details concerning the calculations can be found in 6.1. The calculated amount was accounted for in every halogentation of EDA throughout this work.

2.2.1 Quantitative analysis of Br- and Cl-EDA

The halogenation method of choice was the one reported by Bonge *et al.* Quantitative conversion of EDA (**7**) to Br-EDA (**8**) and Cl-EDA (**9**) have been reported [1], but the yields obtained from these reactions have not been quantified. Thus, it was considered important to calculate the yields of Br- and Cl-EDA prior to the cyclopropanation-ring expansion reactions.

Because of the unstable (and possible explosive) nature of the X-EDAs, it was decided to keep them in solution and measure the yields by an internal standard using ^{1}H NMR spectroscopy. The internal standard of choice was 1,3,5-trimethoxybenzene (henceforward abbreviated as TMB) as it does not react nor overlap with any of product peaks in the ^{1}H NMR spectra. Br- and Cl-EDA was prepared according to procedure 5.2.1.1. DCM was partly removed *in vacuo* at 0 °C, and a deuterated solvent was added. The solution of X-EDA was kept cold until ^{1}H NMR analysis, which was performed directly after preparation.

$CDCl_3$ was chosen as deuterated solvent for the ^{1}H NMR analysis in the initial experiment of Br-EDA. From the spectra obtained it was clear that the chloroform was not suitable for the measurements due to decomposition of the Br-EDA. The thermal stability of Br-EDA have been reported to be lower in $CDCl_3$ than *i.e.* toluene-d_8, acetonitrile-d_3 and THF-d_8 [165]. This might be explained by trace amounts of acid in the $CDCl_3$, known to decompose diazo compounds [103–106]. Also, since several transition-metals can be used to decompose diazo compounds, the presence of silver foil (used for stabilization in $CDCl_3$) might also explain the unfavorable outcome. Therefore, it was decided to use benzene-d_6 as deuterated solvent instead. Results from the ^{1}H NMR yield analysis of Cl- and Br-EDA are displayed in Table 2.1.

Table 2.1: Results of the quantitative analysis of Br- and Cl-EDA in benzene-d_6 at 25 °C

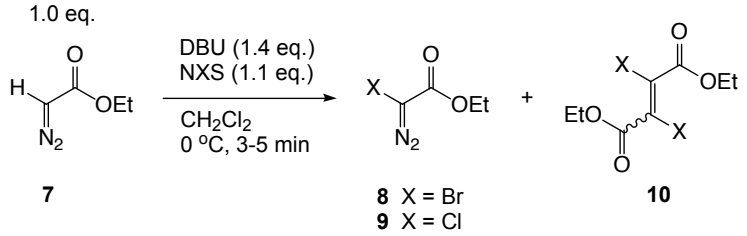

Entry	X	Yield of 8,9[a] [%]	Dimerization (10) [%]
1	Cl	93	trace
2	Cl	93	trace
3	Br	96	trace
4	Br	94	trace
5	Cl	93[b]	
6	Br	95[b]	

[a] Yield measured by ^{1}H NMR analysis of the crude product using TMB as internal standard.
[b] Average yield of two measurements.

Quantitative conversion of both Cl- and Br-EDA was observed in all experiments, along with only trace amounts of dimer **10**. Cl-EDA **9** was afforded in 93 % in both experiments as shown in entry 1 and 2 in Table 2.1. Displayed in entry 3 and 4 Table 2.1 are the yields of Br-EDA, which was calculated to 96 % and 94 %, respectively. The average yield from both chlorinations and brominations were calculated and are shown in entry 5 and 6 (Table 2.1). The average yield of Cl-EDA was 93 %, while 95 % was the average for Br-EDA.

2.3 Initial attempt to synthesize ethyl 8-azaquinoline-3-carboxylate (12) from Br-EDA and 7-azaindole

A natural starting point would be to perform the reactions between 7-azaindole (**11**) and a halodiazoacetate using the conditions shown in Table 2.2, hereby referred to as the standard conditions. Br-EDA (**9**) was the halodiazoacetate of choice due to slightly higher thermal stability than Cl-EDA, and the first synthesis was performed according to procedure 5.2.2.1. Analogous to the cyclopropanation-ring expansion reactions of indoles, the expected outcome of this reaction was the ring-expanded 8-azaquinoline-3-carboxylate **12**. Surprisingly, the results from the initial reactions was not quite as expected as only small amounts of **12** had been formed, according to ^{1}H NMR analysis of the crude product. From the same ^{1}H NMR spectrum, 88 % conversion of the starting material **11** was observed together with additional peaks in both the aromatic region and ester region. It was evident that another product had been formed in 2.7-3:1 ratio to the desired product **12**.

As discussed in 1.3.4.4, Rh(II)-carbenoids can undergo, amongst others, C-H- and N-H insertions reactions. It was believed that one of these was a competing reaction pathway in the reaction. Based on ^{1}H NMR analysis of the crude product it was assumed that the major product was the N-H insertion product **13** (Table 2.2). Therefore, **13** was isolated after column chromatography and analyzed by NMR spectroscopy and MS, which suggested that the suspected product was **13**. Compound **13** has not been reported in the literature and for that reason no comparison of spectroscopic data could be performed.

Table 2.2: Results from the initial reactions between 7-azaindole **11** and Br-EDA **9** using standard conditions.

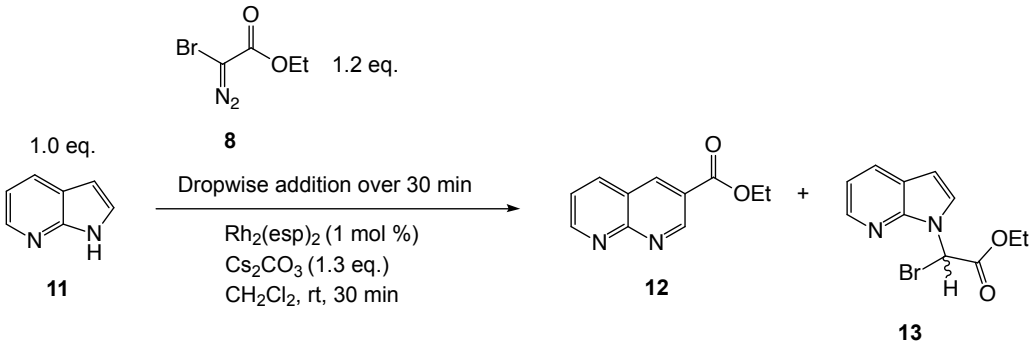

Entry	Conversion of 11 [%]	Products	Product ratio[a] (12 : 13)	Yield 12 [%]	Yield 13 [%]
1	88	**12** + **13**	1 : 2.7	9[b]	24[b]
2	83	**12** + **13**	1 : 3.0	22[c]	42[c]

[a] Ratio between **12** and **13** was measured from the crude mixture using ^{1}H NMR spectroscopy.
[b] Isolated yield.
[c] Yield measured by ^{1}H NMR analysis of the crude product using TMB as internal standard.

As displayed in Table 2.2, only 9 % of desired product **12** (entry 1) was isolated. This was by no means considered satisfactory. A somewhat higher yield, 24 %, was afforded of undesired product **13** (entry 1). Considering conversion of the starting material **11**, and the fact that there were no other notable byproducts the yields of both **12** and **13** combined were notably low. What is believed to be dimerization or polymerization of Br-EDA was, of course, present, but does not explain the combination of high conversion and low yields.

A new experiment was performed with addition of an internal standard prior to ^{1}H NMR analysis of the crude mixture. The results are displayed in entry 2 in Table 2.2. Loss of product during work-up might explain why only 9 % of the 22 % of **12** was isolated, and might also be some of the reason for lower isolated yield of **13**. It was, however, discovered that **13** was highly unstable and decomposed within hours.

2.4 Exploration of new conditions in the cyclopropanation ring expansion reaction of 7-azaindoles

The initial attempt to synthesize **12** from **9** and **11** using the standard conditions were deemed quite insufficient. Therefore, new conditions to suppress formation of **13** and increase yield of **12** was desirable.

2.4.1 Catalyst screening

In an attempt to increase the yield of **12** and decrease/eliminate formation of **13**, six different catalysts were tested. Four of which was prepared by Vladimir Levchenko during his masters in the Bonge-Hansen group. He prepared four novel Rh(II)-carboxylate based catalysts; two monomeric ($Rh_2(4\,VBA)_4$ and $Rh_2(MCES)_4$) and two polymeric (pol(II)$-Rh_2(4\,VBA)_4$ and pol(II)$-Rh_2(MCES)_4$) [185]. They gave good to excellent yields in cyclopropanation reactions with EDA and styrene [185], but have not been employed in cyclopropanation-ring expansion reactions with halodiazoacetates. For that reason, an investigation of their performance in such reactions was found interesting. A copper-catalyst, Cu_2O, was also chosen as copper have been widely used to decompose diazo compounds [131]. $Fe(ClO_4)_2$ was also included as high yields in C-H-insertion reactions with indoles have been reported [186]. The Cu- and Fe-catalysts are far less expensive than Rh-based catalysts, which would be an economical advantage if they should outperform Rh-catalysts. However, as can be seen in Table 2.3, Cu_2O did not convert the starting material (entry 5) and $Fe(ClO_4)_3$ barely gave any conversion (entry 6). The poor performance of the inorganic catalyst might partly be attributed to their poor solubility in DCM.

Table 2.3: Results from the catalyst screening for the synthesis of **12**[a,b]

Entry	Catalyst	Loading [mol %]	Conversion of 11 [%]	Product(s)	Product ratio[c] (12 : 13)
1	$Rh_2(4\,VBA)_4$	1	83	**12** + **13**	1 : 7
2	$Rh_2(MCES)_4$	1	49	**12** + **13**	1 : 2
3	Pol(II)-$Rh_2(4\,VBA)_4$	1	27	**12** + **13**	1 : 2
4	Pol(II)-$Rh_2(MCES)_4$	1	23	**12** + **13**	1 : 3
5	Cu_2O	17	0	-	-
6	$Fe(ClO_4)_3$	16	7	-	-

[a] Standard conditions.
[b] Yields were not included in this table due to the low formation of **12**.
[c] Ratio between **12** and **13** was measured from the crude mixture using ^{1}H NMR spectroscopy.

Of all the Rh-based catalysts, highest conversion of **11** was obtained by monomeric $Rh_2(4\,VBA)_4$ (entry 1, Table 2.3), highly similar to $Rh_2(esp)_2$ (88 %). However, the formation of **13** was 7 times higher than the formation of **12**, which was 2-3 times higher than for $Rh_2(esp)_2$ (ratio

1:2.7-3). Even though the ratio of **12**:**13** was slightly improved (1:2) by the other monomeric Rh-catalyst (entry 2, Table 2.3) compared to $Rh_2(esp)_2$, the conversion was low. The performance of the polymeric analogues (entry 3 and 4, Table 2.3) were not deemed sufficient at all. To summarize the short catalyst screening, none of the chosen catalysts could suppress formation of **13** or outperform $Rh_2(esp)_2$ in terms of conversion and product ratio (combined). Thus, none of the screened catalyst were engaged in any further reactions.

2.4.1.1 Rh(II)-catalysts, coordination and product distribution

Other attempts to find new reactions conditions will be further discussed. Prior to these discussions, a short analysis and explanation of why the reaction between 7-azaindoles and halodiazoacetates did not seem to work in the same manner as for the regular indoles will be addressed. The discussion is based on experimental observations and as far as possible, backed up by literature data. This is considered important as it rationalizes the choices that were made in optimizing the reaction conditions further.

What was immediately noticed in the first attempt of synthesizing **12** was how the very green catalyst, that stays green in a solution containing indole, (2.2a in Figure 2.2), turned pink onces added to a solution containing 7-azaindole (2.2b in Figure 2.2).

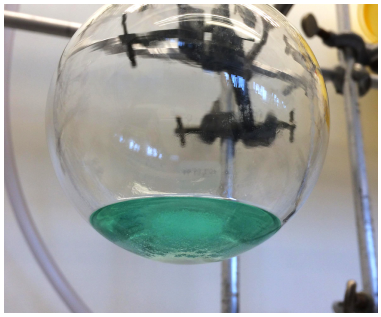

(a) A solution of indole, Cs_2CO_3, $Rh_2(esp)_2$ in DCM

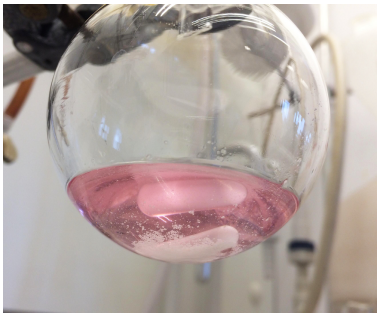

(b) A solution of 7-azaindole, Cs_2CO_3, $Rh_2(esp)_2$ in DCM

Figure 2.2: $Rh_2(esp)_2$ in a solution with indole (green) and 7-azaindole (pink).

As stated in crystal field theory, the color of a metal complex is highly dependent on its ligands [187]. With the drastic color change, suspicion about coordination of 7-azaindole **11** to the catalyst arose. The axial positions in Rh(II) complexes are electrophilic and can be occupied by various ligands as discussed in 1.3.4.3 and depicted in 1.17b. 7-Azaindoles are, in fact, known for their rich coordination chemistry, coordinating to a variety of metals [188–192] including rhodium [193, 194]. The most common coordination modes of 7-azaindole have been reported and are depicted in Scheme 2.3.

The neutral 7-azaindole shows a heterochelate mode where the pyridyl nitrogen lone pair is coordinated to the axial position of the metal M in a MX fragment and the pyrrolic NH is engaged in hydrogen bond formation with X^- (left side in Scheme 2.3). For 7-azaindolate, a *exo*-bidentate (top right in Scheme 2.3) or a *endo*-bidentate (bottom right Scheme 2.3) are considered possible, but due to the bite angle between the two nitrogens, the *exo*-bidentate is seen in most metal complexes [194].

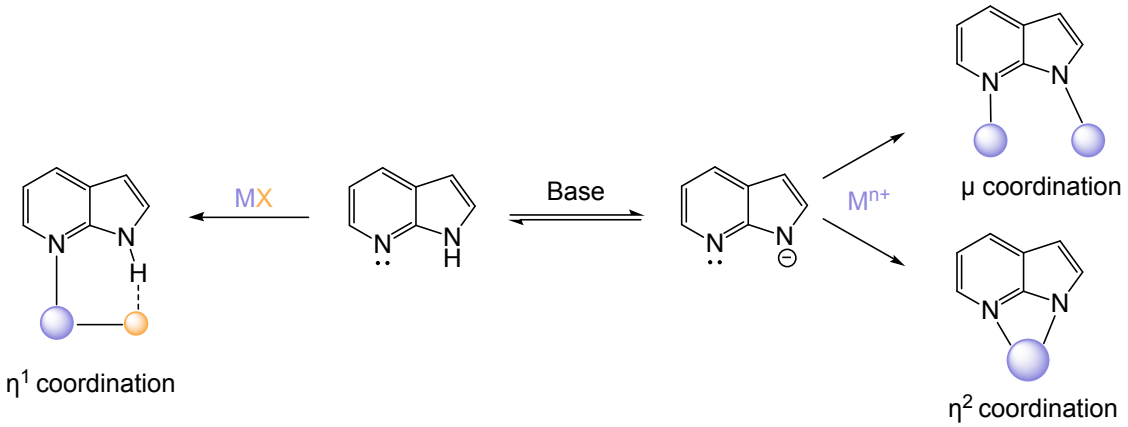

Scheme 2.3: Coordination modes of 7-azaindole (right) and its conjugate base, 7-azaindolate (left) [194].

Based on the various coordination modes of 7-azaindoles, the coordination mode of $Rh_2(OAc)_4$ and 7-azaindoles have been investigated and their paddlewheel complexes have been reported [194]. As displayed in Figure 2.3, the axial positions in both rhodium atoms can be occupied by the pyridyl nitrogen of 7-azaindole, and the each pyrrolic N-H have formed a hydrogen bond with an oxygen in the equatorial acetate group.

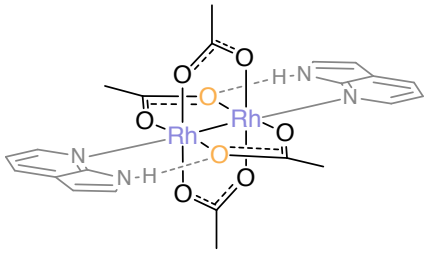

Figure 2.3: η^1 coordination of 7-azaindole to $Rh_2(OAc)_4$ [194].

No such, or any other coordination mode of $Rh_2(esp)_2$ have been found in literature. However, the similarity between $Rh_2(OAc)_4$ and $Rh_2(esp)_2$ might suggest that the heterochelate mode could be possible for the $Rh_2(esp)_2$ as well. Crystals of the $Rh_2(esp)_2$-7-azaindole complex suitable for X-ray analysis was attempted grown, but without success.

It has been demonstrated that only one of the two axial sites in Rh(II)-catalysts are catalytically active at any given time, and that lewis basic inhibitors (*i.e.* nitrogen lone pair) may occupy the second coordination site and that this interaction impedes the catalysts [195, 196]. Also, as discussed in 1.3.4.3, axial modifications can alter the properties of rhodium-catalysts and change their reactivity [147, 148]. Considering these factors, it might explain the formation of the N-H-insertion product **13** and the rather limited formation of cyclopropanated-ring expanded product **12**.

2.4.2 Attempts to avoid or inhibit catalyst coordination

The outcome of the reaction between 7-azaindole **11** and Br-EDA catalyzed by $Rh_2(esp)_2$ have been rationalized based on observations and literature reports. It was, naturally, still of interest to investigate ways to inhibit formation of **13**, but also examine the possibilities to prevent axial coordination of 7-azaindole to the catalyst.

2.4.2.1 Thermal reaction

Since the substrate-catalyst interaction seemed to be the main issue, the reaction was performed without the catalyst, *i.e.* thermally. During his masters in the Bonge-Hansen group, Magnus Mortén demonstrated that indoles do undergo thermal cyclopropanation-ring expansion reactions with halodiazoacetates [197]. Based on the reported mechanism of cyclopropanation of 2,3-dimethylindole with dichlorocarbene [198], it is believed that the thermal decomposition of X-EDA generate a free carbene that can undergo the analogous cyclopropanation and ring expansion. It was, however, demonstrated that the conversion of indole was lower and formation of byproducts was higher in the thermal reactions compared to the catalytic reactions. The same outcome was demonstrated in this work for the analogous reaction between 7-azaindole and Br-EDA. A 12 % conversion of **11** was afforded along with several byproducts, in addition to significant amounts of Br-EDA dimerization/polymerization. Hence, no further investigation of thermal reactions were performed during this work.

2.4.2.2 Coordination to zinc

Inspired by the many coordination modes of 7-azaindoles and the unique coordination chemistry of zinc [199], the possibility to coordinate the 7-azaindole to zinc rather than the rhodium catalyst was investigated. Zinc is known for its high affinity for nitrogen [199], and the idea was that 7-azaindole would prefer to coordinate to zinc rather than to the rhodium catalyst.

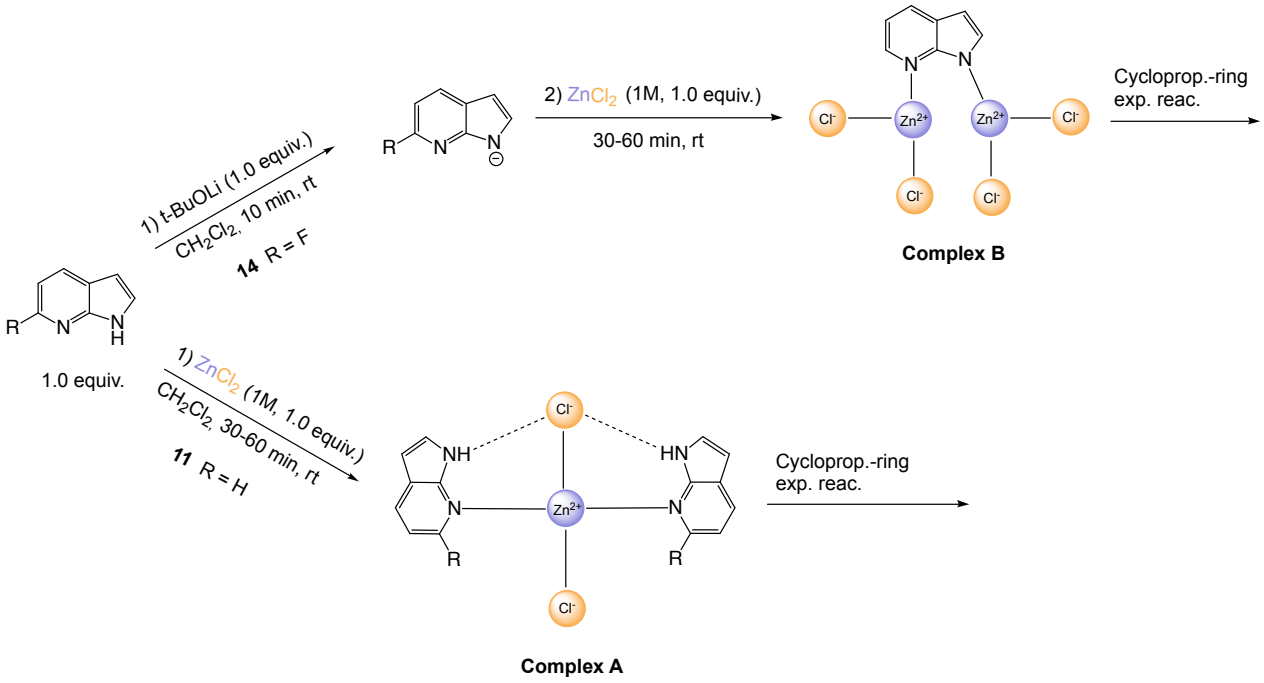

Scheme 2.4: Top: Suggested coordination of 7-azaindolate to $ZnCl_2$ based on the reported coordination mode in Scheme 2.3 [194]. Bottom: reported coordination mode of 7-azaindole to $ZnCl_2$ [200].

The chosen zinc source was $ZnCl_2$ due to easy accessibility and previously reported Zn(II) complexes with 7-azaindoles where $ZnCl_2$ was employed [200]. The first reaction was performed with the regular 7-azaindole in an attempt to generate the reported **Complex A** in Scheme 2.4 [200]. 1 equivalent of a 1.0 M diethylether solution of $ZnCl_2$ was added to **11** and stirred while Br-EDA was prepared (30-60 min). Then, catalyst and base was added, followed by dropwise addition of Br-EDA according to standard conditions. In the second reaction 6-

fluoro-7-azaindole[1] **14** was deprotonated with lithium *tert*-butoxide (*t*-BuOLi) and exposed to 1 equivalent of the same $ZnCl_2$ as in the former reaction. As it initially was believed that the *endo*-bidentate coordination mode (bottom right in Scheme 2.3) would prevail, only 1 equivalent was used. The rest of the reaction was perform using standard conditions. These rather exploratory attempts did not succeed as neither **11** nor **14** was converted. Solubility was an issue in these reactions as cloudy solutions of precipitates were formed. If **Complex A** and **Complex B** even were formed is not known as **Complex A** were reported formed under other conditions [200]. Due to the unsatisfactory outcome, no further investigations of these reactions were pursued.

2.4.2.3 Protonation of the pyridyl lone pair

As it is believed that the pyridyl lone pair of 7-azaindoles coordinate to rhodium. Experiments to remove this interaction by protonation was attempted as illustrated in Scheme 2.5. Two strong, organic acids, para-toluene sulfonic acid (PTSA) and trifluoroacetic acid (TFA) was employed in two different reactions. Equimolar amounts of strong acids were chosen to ensure an equilibrium shifted far towards the protonated 7-azaindole. In both reactions, the acid and **11** was allowed to stir while the X-EDA was prepared (45-60 min). Further, the protonated 7-azaindoles were exposed to $Rh_2(esp)_2$ prior to addition of excess Br-EDA or Cl-EDA. PTSA was used in combination with Br-EDA in DCM, while TFA was used with Cl-EDA in toluene. Both reactions were performed at room temperature. No starting material was converted in any of the reactions, much likely due to the acid labile nature of diazo compounds [103–106]. The acidic environment would, evidently, decompose the X-EDA.

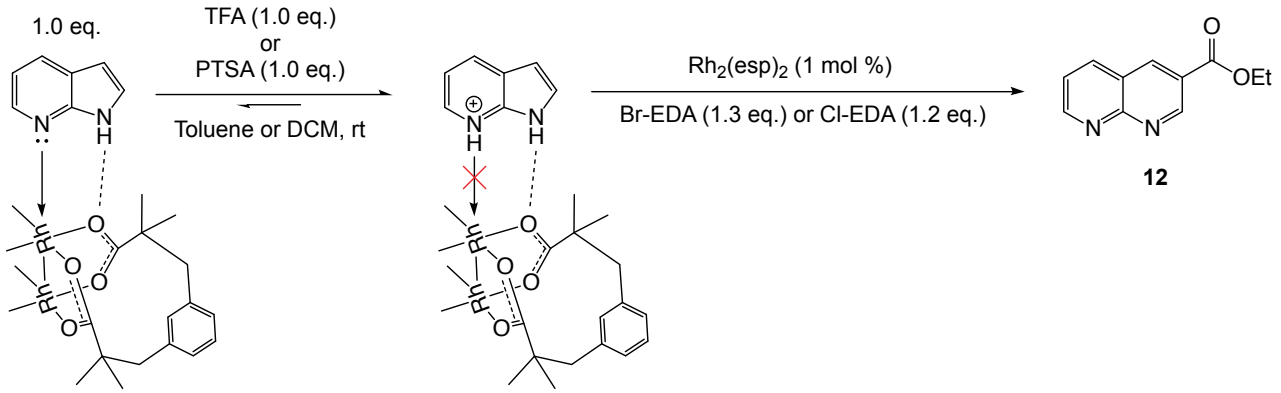

Scheme 2.5: Coordination of 7-azaindole to $Rh_2(esp)_2$ based on reported coordination of 7-azaindole to $Rh_2(OAc)_4$ (left) [194] and suggested inhibition of coordination by protonation of the pyridyl lone pair (middle).

[1] 7-azaindole was not available at the time.

2.5 Prevention of N-H insertion by deprotonation

With several failed attempts to block catalyst coordination, the focus was directed towards preventing formation of the N-H insertion product. A N-H insertion product generated from a Rh(II)-catalyst and a diazo compound is believed to proceed via an ylide intermediate (Scheme 2.6) [196, 201]. The highly unstable and reactive intermediate may undergo [1,2]-Stevens rearrangement, [2,3]-sigmatropic rearrangement or [1,2]-proton shifts [196, 201] to generate the N-H inserted product.

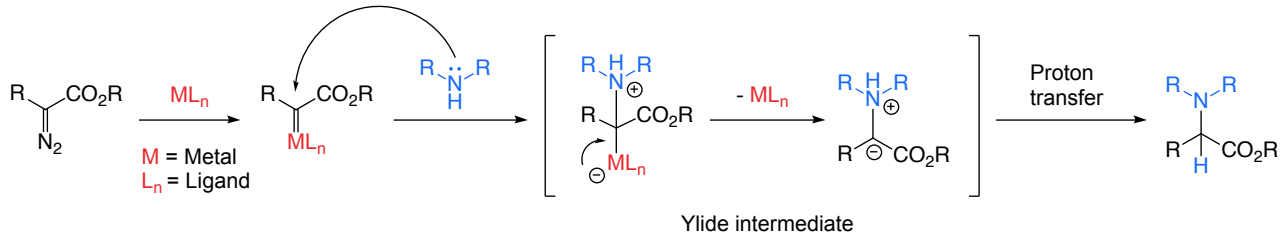

Scheme 2.6: General mechanism for metal-catalyzed carbenoid N–H insertion reactions via an ylide intermediate.

Primary and secondary amines as well as amides and Cbz-protected amines (carbamates) have been reported to undergo N-H insertion with diazo compounds under Rh(II)-catalysis [202, 203]. No examples of successful N-H insertion reactions employing deprotonated secondary amines have been found in literature. That can perhaps be rationalized by the mechanism; with a negatively charged secondary nitrogen, the ylide formation and proton transfer step (Scheme 2.7) can not occur.

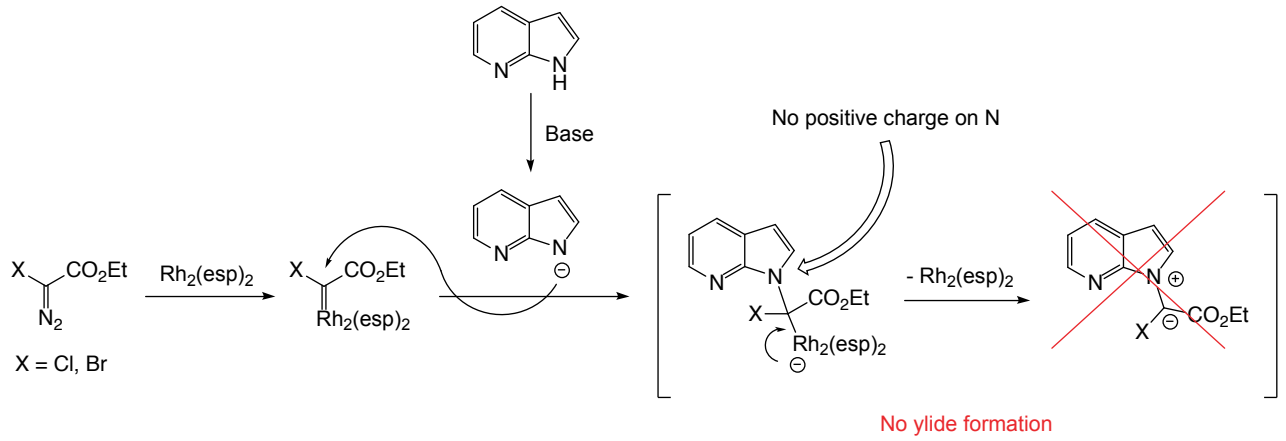

Scheme 2.7: Suggested mechanism for inhibition of ylide formation.

It was desirable to exploit this to prevent N-H insertion in the reactions between 7-azaindoles and halodiazoacetates. A suitable base to deprotonate 7-azaindole would form the corresponding 7-azaindolate which would exclude the N-H insertion reaction pathway and thus the formation of **13**. By using a base that generates a counterion like Li^+, Na^+ or K^+, could also, in a non-polar solvent, form a contact ion pair with N^- in 7-azaindole. This could might also help to "block" the N-1 as a reaction site.

2.5.1 Na- and KHMDS

Two metal silylamides, potassium hexamethyldisilazide (KHMDS) and sodium hexamethyldisilazide (NaHMDS) were chosen as they are fairly strong, lipophilic, non-nucleophilic bases with pk_a~30 in DMSO [204].

The reaction conditions were slightly changed relative to the standard conditions described previously. 7-Azaindole **11** was dissolved in DCM and equimolar amounts of HMDS base was added and stirred while Br-EDA was prepared (45-60 min). Then $Rh_2(esp)_2$ was added, followed by cold, dropwise addition of Br-EDA (excess) over 25-30 min, and subsequent stirring for 30 min. Both reactions were carried out in room temperature.

Table 2.4: Results from the deprotonation of 7-azaindole **11** with HMDS-bases and subsequent reaction with Br-EDA[a].

Entry	Base	Conversion of **11** [%]	Product(s)	Product ratio[b] (**12** : **13**)
1[c]	KHMDS	88	**12** + **13**	1 : 2.6
2	NaHMDS[d]	49	**12** + **13**	1 : 1.

[a] Conditions: 7-azaindole (1.0 eq.) (**11**) + HMDS base (1.0 eq.) stirred for 45-60 min at rt prior to addition of $Rh_2(esp)_2$ (1 mol%) then dropwise addition Br-EDA (1.2-1.4 eq.).
[b] Ratio between **12** and **13** were measured from the crude mixture using ^{1}H NMR spectroscopy.
[c] Cs_2CO_3 was added simultaneously with $Rh_2(esp)_2$.
[d] 1M in THF.

As displayed in Table 2.4 the results were somewhat dissimilar. Conversion of **11** was notably higher in the reaction employing KHMDS than NaHMDS. The ratio between desired **12** and undesired **13** was, however, more satisfactory when NaHMDS was used with a ratio of 1:1 (**12**:**13**) (entry 2, Table 2.2). As a reminder, in previous reactions N-H insertion product **13** have been favored (by 2-7 times). The reaction with KHMDS yielded similar results as the reaction performed under standard conditions (entry 1, Table 2.2). The goal of these reactions were to eliminate formation of **13**, but the fact that it was formed might be explained by the strength of the HMDS bases. With an equilibrium shifted towards 7-azaindolate, a small amount of 7-azaindole will still be present in solution. Considering substrate selectivity and chemoselectivity of Br-EDA towards the two unequal substrates, formation of both **12** and **13** might be justified. If the dissimilar outcome of the two reactions can be justified by the presence of Cs_2CO_3 in one reaction (entry 1, Table 2.4) or the presence of small amounts of THF (entry 2, Table 2.4) was not attempted resolved.

2.5.2 *t*-BuOLi

Inspired by results from the reaction with NaHMDS, other bases were tested to see if the results could be improved. As fairly strong (pk_a~29 in DMSO [204]) and non-nucleophilic, lithium *tert*-butoxide (*t*-BuOLi) in THF (1M) was tested. Because of low conversion with NaHMDS (entry 2, Table 2.4), catalyst loading of $Rh_2(esp)_2$ was increased to determine if a higher loading could help convert more starting material. Also, *t*-BuOLi was used in excess. 7-Azaindole and *t*-BuOLi in DCM was allowed to stir for 45-60 min prior to addition of the catalyst, then dropwise addition of excess Br-EDA.

Table 2.5: Results from the deprotonation of 7-azaindole **11** with *t*-BuOLi and subsequent reaction with Br-EDA [a]

Entry	Equiv. of *t*-BuOLi	Cat. load [%]	Conversion of 11 [%][b]	Product	Yield [%][c]
1	1.6 eq.	5	70	**12**	-
2	1.4 eq.	2	52	**12**	-
3	1.3 eq.	2	70	**12**	13

[a] Conditions: 7-azaindole (1.0 eq.) (**11**) in DCM + *t*-BuOLi (1M in THF) (1.x eq.) stirred for 45-60 min at rt prior to addition of $Rh_2(esp)_2$ (x mol%) then dropwise addition Br-EDA (1.3-1.4 eq.).
[b] Measured by ^{1}H NMR spectroscopy from crude mixture that where extracted once.
[c] Isolated yield.

Table 2.5 shows that no undesired N-H insertion product was formed in any of the three reactions. From entry 1 and entry 2 (Table 2.5) it may seem that higher catalyst loading gave higher conversion, but after the experiment was repeated with 2 mol % catalyst load (entry 3, Table 2.5), the conversion turned out to be similar to the reaction where 5 mol % catalyst load was used. The inconsistency might be due to the fact that the measurements where obtained after the crude mixtures had been extracted[2]. Even though the conversion was adequate and no N-H insertion product were formed in these reactions, the yield was not greatly improved (only by 4 %).

2.5.3 *n*-BuLi

The experiments with t-BuOLi demonstrated that formation of N-H insertion product **13** could be prevented. Because of the afforded low yields, we wanted to further explore other bases as well as the reaction conditions in general. It has been demonstrated that cyclopropanation-ring expansion between indoles and Cl-EDA gave slightly higher yield than with Br-EDA [3]. It has also been demonstrated that by switching from DCM to toluene in cyclopropanation reactions with halodiazoacetates higher yields can be obtained [1]. The base of choice in the following reactions was *n*-butyllithium (*n*-BuLi). Unlike the other bases it is nucleophilic and can undergo lithiation and lithium-halogen exchange [205]. It also stronger with pk_a~50 [204]. 7-Azaindole **11** was not available for further testing, therefore, the following reactions were performed with 6-fluoro-7-azaindole **14** and 6-methyl-7-azaindole **16**. Compound **14** and **16** were to be used further in the synthesis of 8-azaquinolone antibacterials and were therefore the chosen substrates. A further explanation of the substrate choices will be provided in section 2.6.

[2] Necessary to obtain readable ^{1}H NMR spectra

Equimolar amounts of *n*-BuLi was added to **14**, in anhydrous α,α,α-trifluorotoluene ($PhCF_3$)[3] under inert (nitrogen) atmosphere. After 10-15 min stirring, 2.5 mol % $Rh_2(esp)_2$ was added, followed by dropwise addition of excess Cl-EDA and 30 min additional stirring. The reaction yielded surprisingly good results with 43 % isolated yield of **15** (entry 1, Table 2.6).

Because of the high reactivity of *n*-BuLi, the temperature was kept at 0 °C and equimolar amounts was used. Further, the reaction was performed at lower temperatures, −78 °C with dry toluene (entry 2, Table 2.6). Toluene was used as $PhCF_3$ freezes at −29 °C. Comparing the yields measured with internal standard using ^{1}H NMR analysis, the former reaction at 0 °C (entry 1) gave somewhat higher yield.

Table 2.6: Results from the deprotonation of **14** and **16** with *n*-BuLi and subsequent reaction with Cl-EDA in various solvents and temperatures.

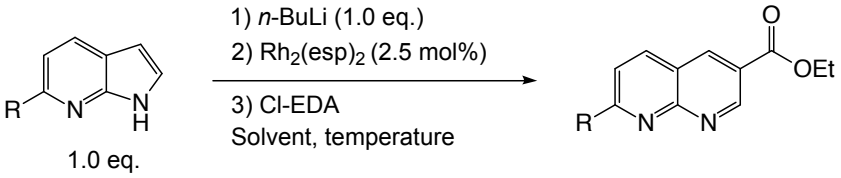

14 R = F
16 R = CH_3

15 R = F
17 R = CH_3

Entry	Solvent (dry)	Temperature [°C]	Conversion of 14/16 [%][a]	Product	Yield [%][e]
1[b]	$PhCF_3$	0	**14**, 96	**15**	53, 43[f]
2[b]	Toluene	-78	**14**, 67	**15**	42
3[b]	THF	-78	**14**, 20	**15**	4
4[c]	$PhCF_3$	0	**14**, 75	**15**	31
5[d]	$PhCF_3$	0	**14**, -	**15**	9
6[b]	$PhCF_3$	0	**16**, 77	**17**	36, 24[f]

[a] Conversion measured by ^{1}H NMR analysis of crude reaction mixture.
[b] Conditions: Nitrogen atmosphere, *n*-BuLi (1.0 eq.) added and stirred 10-15 min before $Rh_2(esp)_2$ was added, followed by dropwise addition of Cl-EDA (1.3-1.4 eq.).
[c] Conditions: Nitrogen atmosphere, *n*-BuLi (1.0 eq.) added and stirred 10-15 min before 12-crown-4 was added and stirred for 10 min. Cl-EDA (1.3-1.4 eq.) was added in one portion followed by, portionwise addition of $Rh_2(esp)_2$.
[d] Conditions: Nitrogen atmosphere, *n*-BuLi (1.0 eq.) added and stirred 10-15 min before 12-crown-4 was added and stirred for 10 min. Cl-EDA (0.3 eq.) was added in one portion followed by, portionwise addition of $Rh_2(esp)_2$.
[e] Yield measured by ^{1}H NMR analysis of the crude product using TMB as internal standard
[f] Isolated yield.

One reaction was performed using THF as solvent to briefly investigate the effect of a catalyst-coordinating solvent on the reaction. As displayed in entry 3, Table 2.6, the reaction afforded 4 % of **15** and THF was deemed unsuitable as solvent for these reactions.

In these reactions, as *n*-BuLi was added, a precipitate was formed (presumably Li-6-fluoro-7-azaindole salt). An attempt to increase solubility of the Li-salt with a crown ether, 12-crown-4, was attempted. Visually, the addition of crown ether did not seem to work as a heterogeneous solution still was observed. Also, in these reactions, it was attempted to add Cl-EDA in one portion and add $Rh_2(esp)_2$ portionwise.

[3] $PhCF_3$ was used as it was commercially available anhydrous

In one of the reactions (entry 4, Table 2.6) Cl-EDA was used in excess, and in the other (entry 5, Table 2.6) it was used as limiting reagent. The yield of **15** was higher in the reaction with excess Cl-EDA, but not as good as when Cl-EDA was added dropwise (entry 1, Table 2.6).

As the conditions in entry 1 were seemingly the most satisfactory, 6-methyl-7-azaindole **16** was exposed to the same conditions, and resulting compound **17** was successfully isolated. As can be seen in entry 6, Table 2.6, lower yields were afforded with only 24 % isolated **17**, compared to the analogous reaction of **14** to **15** which gave 43 % (entry 1). The difference in results might be attributed to the different substituents in position 6 of **14** (-F) and **16** (-CH_3). For comparison, the protons in the methyl group of the 2-methylpyridine are considered weakly acidic[4] due to resonance stabilization of the anion generated by deprotonation (Scheme 2.8) [22].

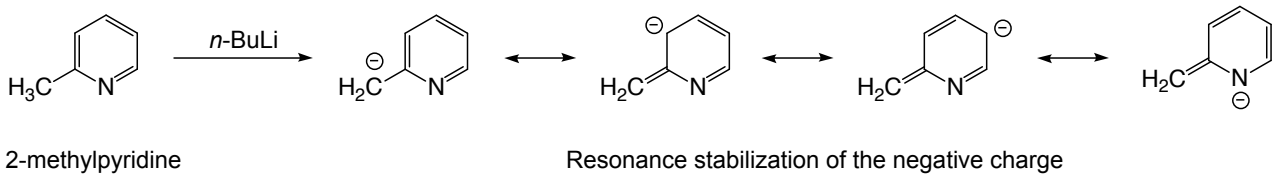

Scheme 2.8: Deprotonation of 2-methylpyridine and resonance stabilization of the resulting anion.

n-BuLi is one of several bases that are known to deprotonate this methyl group [22]. As the the methyl group in **16** resemble that of 2-methylpyridine, deprotonation *might* occur at this site. However, the N-H proton is considered to be more acidic, and hence only 1 equivalent of *n*-BuLi was used.

Considering that only 1 equivalent of *n*-BuLi was used, a more convincing explanation would be the enhanced nucleophilicity of **16**. The weakly electron donating nature of methyl groups in combination with a negative charge generated by deprotonation of N-H might be *too* nucleophilic causing other reaction pathways to predominate.

The results in Table 2.6 were considered promising as no N-H insertion products were observed in addition to increased formation of the desired cyclopropanated-ring expanded product. For that reason, it was decided to use the conditions in the most successful reaction discussed above further in the synthesis towards 8-azaquinolone antibiotics.

[4] pka of 4-methylpyridine~35 in DMSO [204]

2.6 C-3 chlorination of 7-azaindoles and synthesis of 4-chlorinated 8-azaquinoline-3-carboxylates from 3-chlorinated 7-azaindoles and halodiazoacetates

In order to generate 8-aza-4-quinolones from 8-azaquinolines, a chloride must be present in position 4 of the quinoline [8]. Thus, a 3-chlorinated 7-azaindole must undergo the cyclopropanation-ring expansion. Initially, the goal was to synthesize the second generation antibacterial enoxacin by starting from 3-chloro-5,6-difluoro-7-azaindole (Scheme 2.9). This starting material was not obtainable, so a possibility was to purchase 5,6-difluoro-7-azaindole and chlorinate it, but the high cost of the starting material made us reconsider. As the goal, first and foremost, was to demonstrate our approach in synthesizing quinolone antibacterials, it was decided to purchase 6-fluoro-7-azaindole **14** instead and aim for a synthesis of the non-fluorinated enoxacin analogue (bottom right in Scheme 2.9). Due to lack of time at the end of this work, it was decided to redirect the goal towards a quinolone antibacterial agents with a shorter synthetic route. Nalidixic acid was chosen and hence 6-methyl-7-azaindole **16** was purchased. For this reason, both **14** and **16** were subjected to chlorination.

The planned synthetic route towards nalidixic acid, enoxacin and non-fluorinated enoxacin analogue are displayed Scheme 2.9. Step **A** of the synthesis involves a chlorination in 3 position of the 7-azaindoles according to reported procedures [206]. The new, improved conditions reactions discussed in the last part of 2.5 will be used as the key step **B** (Scheme 2.9) to generate the 8-azaquinoline. Generation of the 8-azaquinolone (step **C**, Scheme 2.9) will be carried out according to reported literature procedures [8]. The quinolone can then be alkylated at N-1 with ethyl iodide (step **D**, Scheme 2.9) [86]. If R_1 = methyl, nalidixic acid can be obtained after a basic hydrolysis of the ester (step **E**, Scheme 2.9) [26, 86]. Enoxacin can be afforded after a nucleophilic aromatic substiution with piperazine (step **F**) [86] and a basic hydrolysis of the ester (step **G**) [86].

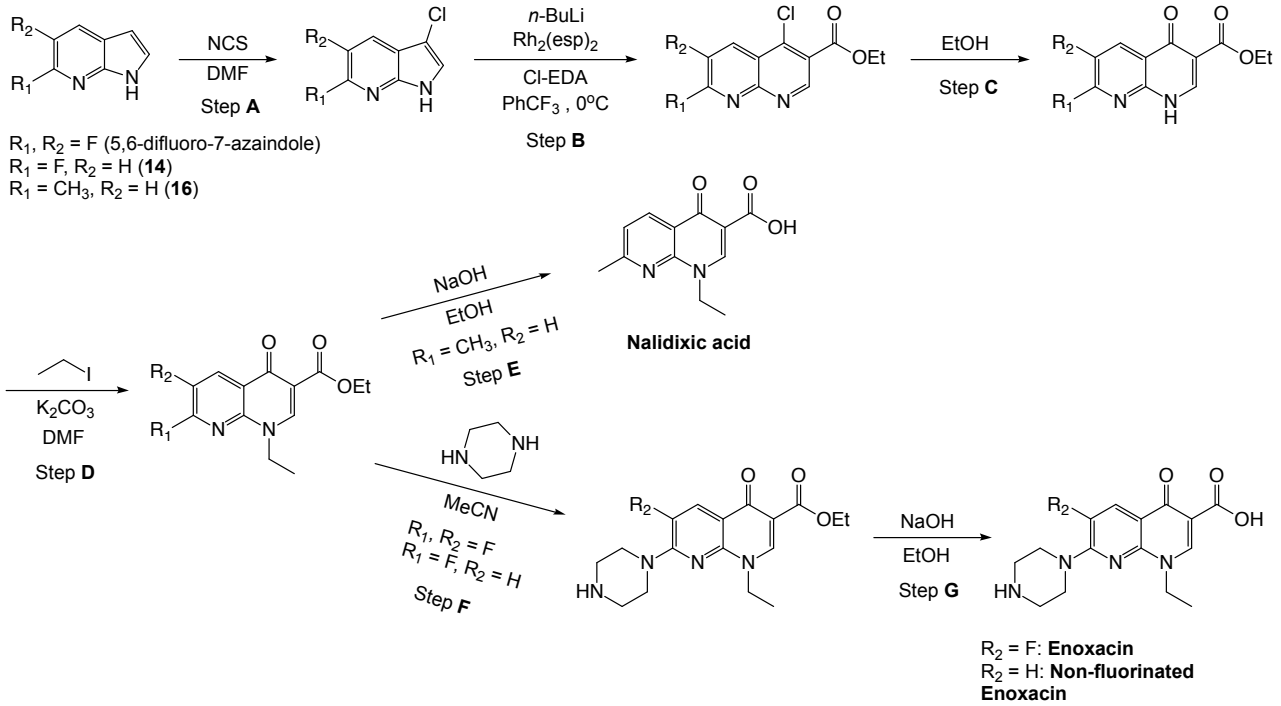

Scheme 2.9: Planned synthetic route to nalidixic acid, enoxacin and non-fluorinated enoxacin via Rh(II)-catalyzed cyclopropanation-ring expansion reaction between 3-chlorinated 7-azaindoles and halodiazoacetates.

2.6.1 C-3 chlorination of 7-azaindoles

With modifications, both **14** and **16** were subjected to electrophilic chlorination with NCS as reported for *indoles* in literature [206] (Scheme 2.10). No C-3 chlorination of 7-azaindoles were reported at the time the reactions took place. 7-Azaindoles reactivity towards electrophiles at C-3 are only slightly lower than that of indoles [22].

The reactions were tracked by TLC analysis and ^{1}H NMR analysis until the starting material was fully converted. As a consequence of excess (1.05 - 1.1 equivalents) NCS and stirring past full conversion, additional peaks in the crude ^{1}H NMR spectra was observed. As the 2 position of the 7-azaindole also is considered nucleophilic, formation of the 2,3-dichlorinated products (**19**/**21**) was suspected. To confirm the suspicion, a total of 2.2 equivalents NCS were added in a reaction of **14** in DMF an allowed to stir until full conversion. Some of **19** was isolated by a quick trituration with chloroform and filtration. The resulting fine powder was analyzed by NMR spectroscopy and MS which strongly indicated **19**. Compound **21** was also isolated and the structure was confirmed by NMR analysis and MS analysis. Neither **19** nor **21** were of any use further in this work, and therefore, no efforts were made to obtain high yields, nor where their yields calculated.

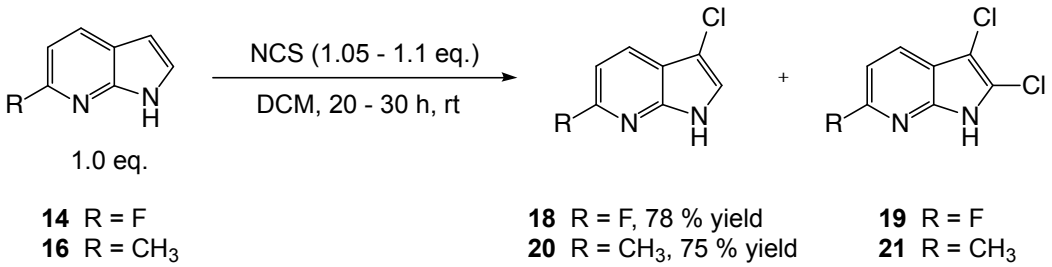

Scheme 2.10: Chlorination of 6-fluoro-7-azaindole **14** and 6-methyl-7-azaindole **16**.

It was discovered that **18** was insoluble in DCM, and as several chlorinations with NCS have been carried out in DCM [207–209], it was decided to switch from DMF (originally used) to DCM as an effort to ease the purification. As **18** would precipitate from solution, isolation by filtration would be both simple and time saving. However, the particles from the precipitate were very small and too much product was lost during filtration. Recrystallization from DCM was attempted in order to grow sufficiently large crystals that could easily be filtered. But with NCS still present in solution, the chlorination continued and peaks from the 2,3-dichlorinated analogue was observed in the ^{1}H NMR spectra from recrystallized **18**.

18 was obtained in 78 % yield using DCM as solvent and stirring at room temperature for 20-30 hours (Scheme 2.10). Because of the long reaction times, the chlorination of **16** was performed at higher temperature (approximately 4 °C) to briefly investigate if the reaction times could be shortened with no loss of yield. The reaction time could be shortened to 8.5 hours while keeping the good yield. 75 % of **20** was afforded using these conditions (Scheme 2.10).

It was also discovered that the excess of NCS should be kept to a minimum to prevent dichlorination. 1.005 equiv. did not fully convert the starting material, but 1.05 gave full conversion over 20-30 hours at room temperature. With 1.2 equiv, full conversion was reach in the same time frame as 1.05 equiv., but it was harder to control further chlorination. Full conversion was desirable as the starting material and mono-chlorinated product were practically inseparable on a silica gel column.

2.6.2 7-substituted ethyl 4-chloro-8-azaquinoline-3-carboxylates from 6-substituted 3-chloro-7-azaindoles and halodiazoacetates

According to the planned synthetic route to nalidixic acid and non-fluorinated enoxacin (Scheme 2.9), a 7-azaindole with Cl in 3 position is necessary to, in the next step, convert the 8-azaquinoline to its 8-azaquinolone analogue. Also, a substituent in position 6 of the 3-chloro-7-azaindole is necessary to obtain the correct substitution pattern in the final product(s). Formation of quinolines by cyclopropanation-ring expansion between indoles and haldodiazoacetates are compatible with both EWGs and EDGs in 3, 4, 5, and 6 position [3]. A 70 % yield was reported in a reaction with methyl 3-indolylacetate and Br-EDA. In the same reaction with 6-bromoindole, 94 % yield was reported [3]. In the same study, no reaction with 3,6-disubstituted indole was reported. No cyclopropanation-ring expansion of 7-azaindoles with various substituents have been found in literature.

3-Chloro-6-fluoro-7-azaindole **18** was subjected to the new and improved conditions. From the chlorination reactions discussed in 2.6.1, it was demonstrated that **18** was poorly soluble in DCM. Poor solubility was also observed once **18** was attempted to be dissolved in $PhCF_3$. The reaction was still carried out as a precipitate eventually would form by addition of *n*-BuLi. The desired cyclopropanated-ring expanded product **22** was successfully formed in 50 % yield (measured with internal standard from the crude ^{1}H NMR spectra) (entry 1, Table 2.7). As there were some difficulties with the purification and isolation, no isolated yield was calculated at this point.

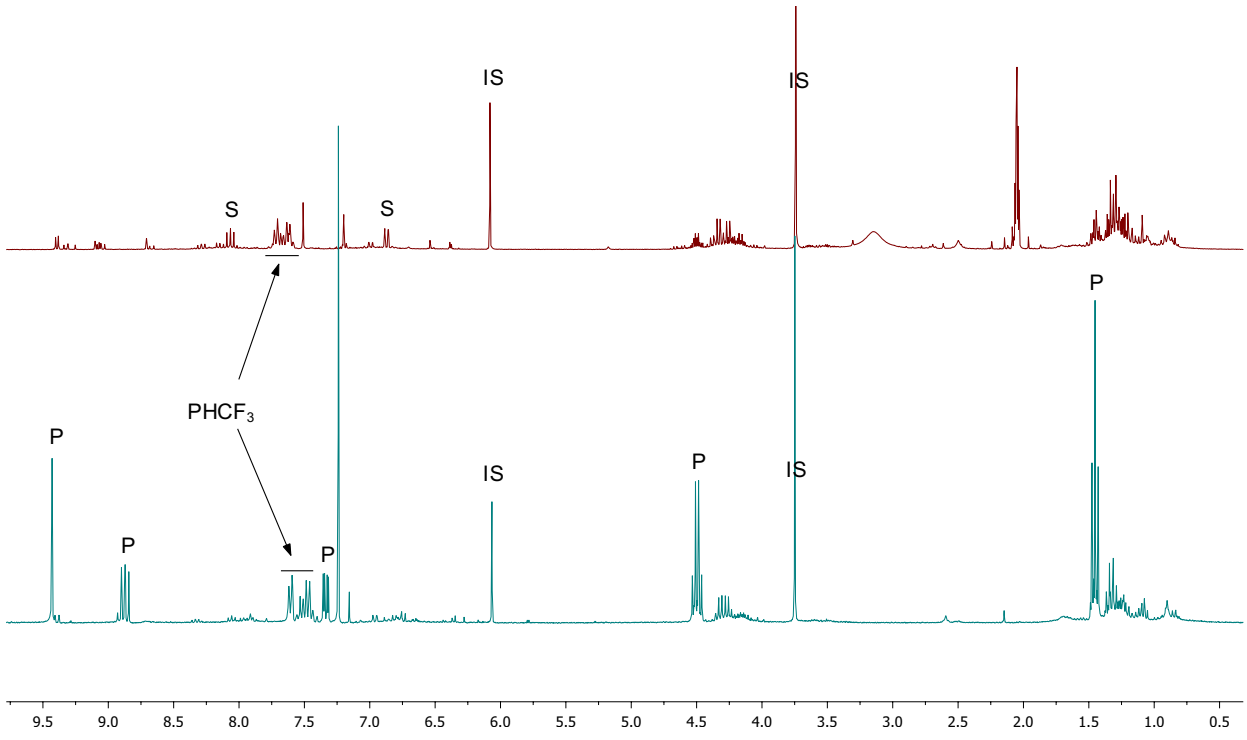

Figure 2.4: ^{1}H NMR (300 MHz, acetone-d_6) of the crude mixture from an unsuccessful reaction with **18** (top), and ^{1}H NMR (300 MHz, $CDCl_3$) of the successful reaction with **18** (bottom). P = product (**22**), S = starting material (**18**) and IS = internal standard (TMB). Dimerization/polymerization is present at 1.0 - 1.4 ppm and 4.0 - 4.4 ppm.

The reaction was repeated with an excess of **18** to see if the yield could be increased, but according to ^{1}H NMR analysis, no product was formed. With the failed attempt, the reaction with **18** as limiting agent was repeated. This time at a slightly larger scale; from 0.50 mmol

to 1.76 mmol of **18**), as an upscale (even larger) would be necessary to potentially reach the end products in Scheme 2.9. According to ^{1}H NMR analysis of the crude mixture, the reaction was unsuccessful. For comparison, a successful and an unsuccessful reaction crude mixture are displayed in Figure 2.4. The top (red) spectra shows a complex reaction mixture with a number of peaks in the aromatic region as well as two of the peaks belonging to unconverted starting material (S). The many peaks makes it hard to tell if any desired product (P) was formed at all. Also, diazo di/polymerization is present to a great extent at 4.0 - 4.4 ppm and 1.0 - 1.4 ppm. The crude mixture in the bottom spectra (green) is from the successful reaction and displays a rather neat crude product, dimerization/polymerization, and several microscopic peaks in the aromatic region.

What was noticed during both the unsuccessful reactions was that no precipitation occured once *n*-BuLi was added, as was the case for the non-chlorinated substrates and the first reaction of the chlorinated substrate. Compound **18** used in the first reaction came from one batch, while **18** in the next two reactions came from a second batch mixed with the first. Both batches were re-examined by NMR spectroscopy and MS to see if any impurities or water (which could quench *n*-BuLi) were present, but the level of purity was the same, and no water were present. As a precaution, they were both placed under high vacuum for 24 hours after the examination. Even though it did not seem like the substrate was the problem, 3-chloro-6-methyl-7-azaindole **20** was subjected to the same reaction conditions as the successful reaction. As the previous two reactions, this reaction was also unsuccessful with only 15 % yield of **23** (entry 2, Table 2.7 in the following page). Starting material **20** was soluble in $PhCF_3$, and no precipitation with *n*-BuLi was observed.

Many details concerning the reaction and its conditions were checked. The solvent, $PhCF_3$, was replaced by dry toluene with oven dried molecular sieves, in case water had been accumulated in the anhydrous $PhCF_3$ after being opened several times. No change was observed. Further, the solution containing the substrate and solvent was purged with nitrogen gas for an extensive period in case of improper degassing in the failed attempts. This attempt was also unsuccessful. As *n*-BuLi degrade upon aging [205], it was replaced with new, unopened *n*-BuLi, but yielded no success. Even the syringes and needles used for the *n*-BuLi were replaced with new ones, and the glassware was dried at (110 °C) for almost 24 hours. This did not seem to have any positive effect.

As briefly mentioned in 2.5.3, the reactivity of *n*-BuLi is diverse. Lithium-halogen exchange may occur on C-3, but requires Br or I as halogen, as well as *N*-substitution or at least 2 equivalents of *n*-BuLi (1 equiv. to deprotonate N-H first) [22, 210]. Direct C-2 lithiation could be a possible reaction pathway, but requires a N-substitution, preferably by a *ortho*-directing substituent [22, 210]. In the case of **20**, deprotonation of the methyl group is a possibility [22]. All the above reactions do undergo subsequent reaction with electrophiles. The conditions used in the reactions of **18** and **20** with *n*-BuLi, $Rh_2(esp)_2$ and Cl-EDA were carefully chosen to prevent the possibility for the above mentioned reactions to occur. If these or any other reaction pathway were predominating in the failed attempts are not known as it was too time consuming to investigate. Also, at this point, there was no obvious reason why the reaction worked the first time, but failed on the other attempts.

As sodium hydride (NaH) is regarded a convenient strong base (pka~35 [204]) to fully deprotonate indoles [22], several reactions with **20** was performed to, again, find new, suitable conditions. Compound **18** was disregarded in these experiments for two reasons. The first being directing the focus to complete the synthesis of (only) nalidixic acid. The second being the poor solubility of **18** in the appropriate solvents as the solubility of NaH is quite limited.

As considered safer and easier to handle than pure NaH, 60 NaH % in dispersion oil was used in the reactions discussed below (Table 2.7).

Table 2.7: Results from the deprotonation of **18** and **20** with a selection of bases and subsequent reaction with Cl-EDA under various conditions.

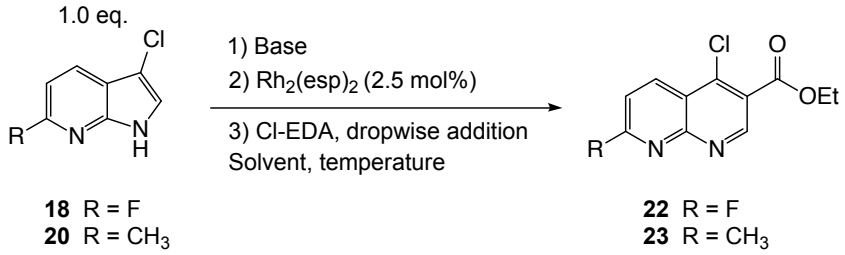

18 R = F
20 R = CH_3

22 R = F
23 R = CH_3

Entry	Base (equiv.)	Solvent (dry)	Temp. [°C]	Conversion of 18/20 [%][a]	Product	Yield[b] [%]
1[c]	*n*-BuLi (1.0)	$PhCF_3$	0	**18**, 85	**22**	50
2[c]	*n*-BuLi (1.0)	$PhCF_3$	0	**20**, 79	**23**	15
3[d]	NaH (1.0)	Toluene	0	**20**, 100	**23**	27
4[d]	NaH (1.5)	Toluene	rt	**20**, 67	**23**	41
5[e]	NaH (1.5)	Toluene	rt	**20**, 100	**23**	28
6[d]	NaH (3.0)	Toluene	rt	**20**, 100	**23**	63
7[d]	NaH (3.0)	Toluene	rt	**20**, 100	**23**	26
8[e]	NaH (3.0)	Toluene	rt	**20**, 100	**23**	28
9[d]	LiH (1.6)	Toluene	rt	**20**, 28	**23**	26
10[d]	*t*-BuOLi (1.5)	Toluene	rt	**20**, 71	**23**	24

[a] Conversion measured by ^{1}H NMR analysis of crude reaction mixture.
[b] Yield measured by ^{1}H NMR analysis of the crude product using TMB as internal standard.
[c] Conditions: Nitrogen atmosphere, *n*-BuLi (1.0 eq.) added and stirred 10-15 min before $Rh_2(esp)_2$ was added, followed by dropwise addition of Cl-EDA (1.3 eq.)
[d] Conditions: Base and **20** stirred for 60-70 min before $Rh_2(esp)_2$ was added, followed by dropwise addition of Cl-EDA (1.3 eq.)
[e] Conditions: Base and **20** stirred until gas evolution stopped (5-10 min) before $Rh_2(esp)_2$ was added, followed by dropwise addition of Cl-EDA (1.3 eq.)

A 60 % yield of **23** was obtained from reaction in entry 6, Table 2.7. This reaction was performed at a 0.12 mmol with 3.0 equivalents of NaH, and once scale up to 0.50 mmol using the same conditions and same amount of NaH (entry 7, Table 2.7), the yield dropped to 26 %. When 1.5 equivalents of NaH was used under the same conditions (entry 4, Table 2.7), the yield was measured to 38 %. In these reactions, a slight color change from pale yellow to pale green was observed while NaH and **20** was stirred for 60-70 minutes prior to addition of $Rh_2(esp)_2$ and Cl-EDA. If any reactions besides deprotonation occured was not investigated. If the color change had any impact on the subsequent reaction with the carbenoid was considered more important. Thus, two reactions were 1.5 and 3.0 equivalents of NaH (entry 5 and 8, Table 2.7, respectively) was only allowed to stir until gas evolution had stopped. As displayed in the table, the same results were obtained from the reactions with 28 % yield. These results did not seem to differ considerably from the reactions were NaH and **20** was stirred for 60-70 minutes (entry 3, 4 and 7, Table 2.7).

Two lithium based bases, LiH and *t*-BuOLi were also tested. Reactions with *t*-BuOLi using DCM as solvent were tested and was discussed in 2.5. A new attempt was made as toluene proved to be a better solvent. A small increase in yield, 24 %, (entry 10, Table 2.7) was observed. In the reaction with LiH the starting material was barely converted (entry 9, Table 2.7), but

the yield matched the conversion. Surprisingly, the reactions with LiH and NaH seemed to differ quite a lot in terms of conversion of **20**.

As **23** was to be employed in further reactions, isolation was necessary. Once isolated and purified, white crystals was obtained (left picture, Figure 2.5), but while removing the last traces of solvent, a dark purple oil emerged (right picture, Figure 2.5), which turned into a brown mixture after a while. The purple and brown mixtures were analyzed by ^{1}H NMR spectroscopy, which surely revealed decomposition of **23** (Figure 2.6).

Figure 2.5: 23 as white crystals (left) and decomposed **23** (right).

The instability of the product might be due to pressure, heat, light or air. The observed decomposition of **23** first occurred on the rotary evaporator with the heating bath set to 40 °C. Compound **23** was attempted purified from another reaction, keeping the heat low and shielding it from light as much as possible, but decomposition could not be prevented. Because of the limited stability of **23**, structure confirmation was only done by NMR spectroscopy.

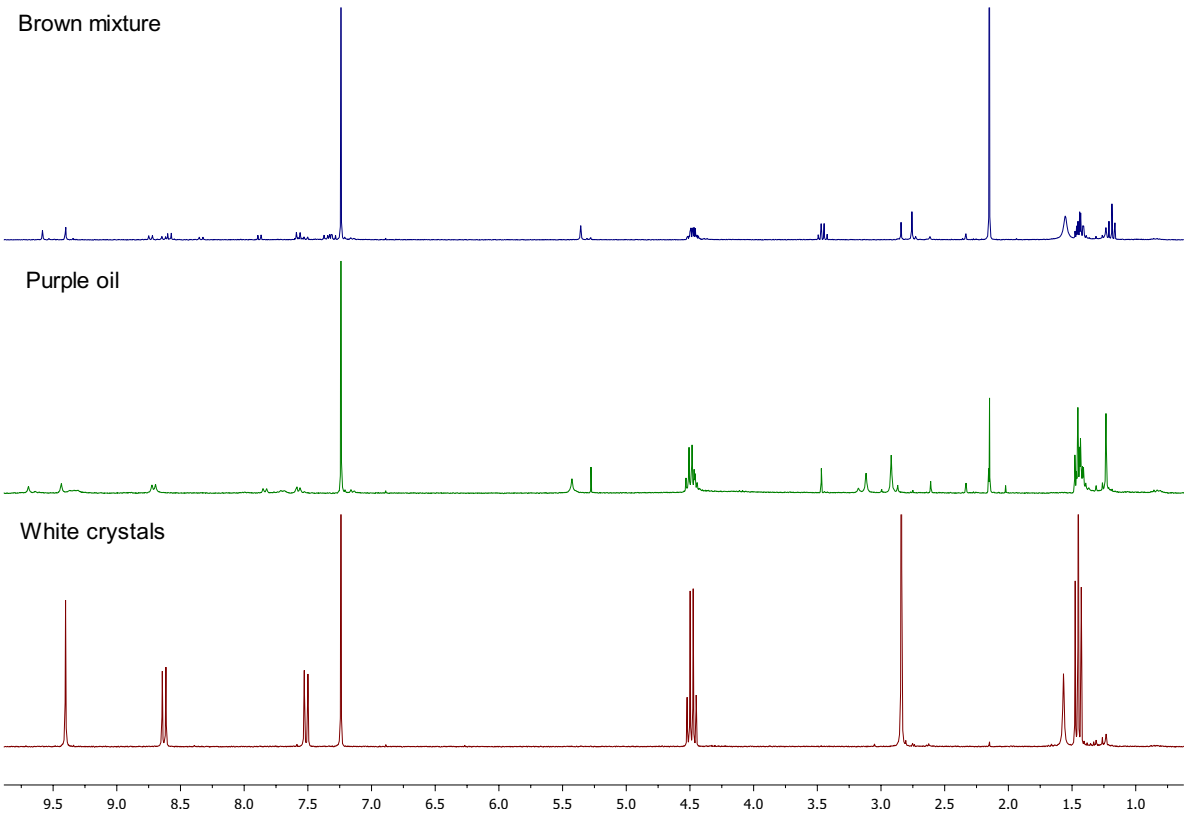

Figure 2.6: ^{1}H NMR (300 MHz, $CDCl_3$) of **23** as pure, white crystals (bottom, red spectrum) and as decomposed in the two top spectra (green and purple).

There were no attempts to purify the product mixture in order to isolate and characterize the decomposition products due to the mixtures' complexity. However, the flask containing the mixture was left open in the fume hood over days prior to cleaning. While cleaning with acetone, a precipitate appeared, which was quickly filtered and subjected to analysis by NMR spectroscopy and MS. The analyzes suggested that the analogous *quinolone* **24** in Figure 2.7 had been formed.

Conversion of 4-quinolines to 4-quinolones is not an uknown phenomenon. Non-catalyzed solvolysis (with MeOH, EtOH and *i*-PrOH) of various 4-chloroquinolines with an EWG in 3 position (-CO_2Et and -NO_2) have been reported by Heindel and Fine [8]. This was also one of the steps in the planned synthetic route to nalidixic acid (step **C** in Scheme 2.9). No alcohol was present in this work, hence, and explanation of the results is merely speculative. Considering the electron deficiency of **23**, perhaps traces of water combined with heat was enough to initiate the transformation.

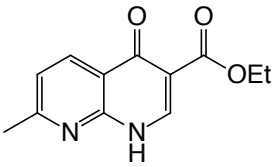

24

Figure 2.7: Ethyl 7-methyl 8-azaquinol-4-one-3-carboxylate **24**. A suggested product from the decomposition of **23**.

2.7 High conversion, low yield

As a consequence of the decomposition of **23**, the synthetic route towards nalidixic acid was not pursued further. Instead, the focus was redirected to a short investigation of the conversion of the starting material versus the yield of the product.

In all the tables from previous sections concerning cyclopropanation-ring expansion reactions between 7-azaindoles and halodiazoacetates, conversion of the starting material to the product(s) are shown. In several of the reactions, the conversion of the starting material is seemingly good, no other *obvious* by product(s) are formed, but the yield is adequate at best. As an example, the bottom crude ^{1}H NMR spectra in Figure 2.4 shows products, solvent, internal standard, trace amounts of starting material and other small peaks in the aromatic region as well as what is believed to be polymerization of the halodiazo compound. Even so, only 50 % yield of the product was obtained when 88 % of starting material was converted (entry 1, Table 2.7). Questions were raised about the faith of the starting material, optionally, the product. A plausible reasoning would be alternative reaction pathways for the starting material or degradation/further reaction of the product formed.

A control experiment was performed in order to investigate the latter suspicion. 8-azaquinoline **17** was subjected to the same conditions as the 7-azaindoles (Scheme 2.11). Compound **17** was dissolved in toluene, 2.5 mol % $Rh_2(esp)_2$ was added, followed by dropwise addition of excess Cl-EDA. An internal standard (TMB) was added prior to ^{1}H NMR analysis of the crude mixture. From the crude measurement it was evident that only 43 % of **17** was present after the reaction. This might indicate that the 8-azaquinoline-3-carboxylates are not necessarily stable under the reaction conditions, but can also be competing substrates in the $Rh_2(esp)_2$-catalyzed reactions between 7-azaindoles and halodiazoacetates.

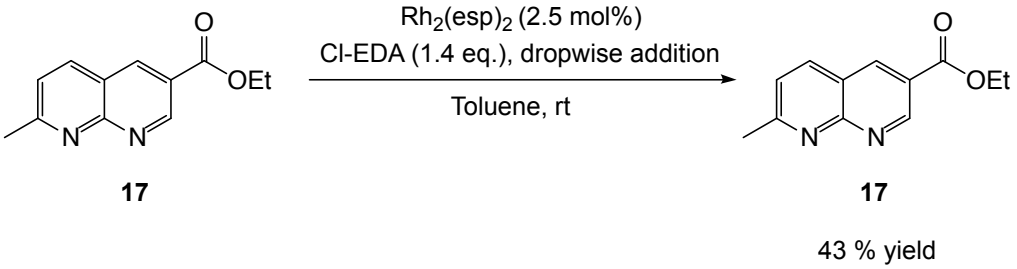

Scheme 2.11: 8-Azaquinoline **17** exposed to catalyst ($Rh_2(esp)_2$) and halodiazo (Cl-EDA) without the presence of a 7-azaindole.

The competing substrate-theory was also investigated by increasing the equivalents of the starting material. By using 2 equivalents of **20** and 1 equivalent of Cl-EDA, only 1 equivalent of product can, theoretically, be formed. This leaves a higher concentration of **20** (1 equivalent), with increased probability of undergoing the reaction, leaving more of product **23** intact. Compound **20** was subjected to equimolar amounts of NaH and stirred for approximately 1 hour, followed by addition of $Rh_2(esp)_2$, then dropwise addition of Cl-EDA (Scheme 2.12). TMB was added as an internal standard after the reaction. According to the ^{1}H NMR analysis of the crude mixture, 53 % of **23** was yielded from the reaction.

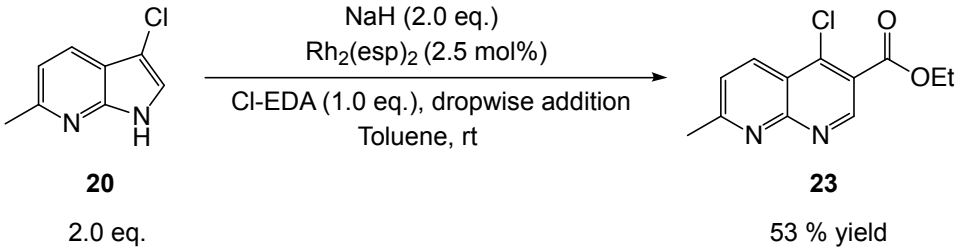

Scheme 2.12: Investigation of a reaction where **20** was used in excess.

By studying the crude spectra in Figure 2.8 from the reaction in Scheme 2.12, it was evident that only starting material (S), product (P), dimerization/polymerization (dim/poly) and, of course, the internal standard (IS) and mineral oil residue from NaH is present (0.6-1.3 ppm). The many, small peaks in the aromatic region (6.0-9.5 ppm) in Figure 2.4 can not be observed in this spectrum.

The integrals of starting material **23** (S) and product (P) in the spectra shows approximately 60 % starting material and 40 % product. This would mean that at least 40 % of **23** must have reacted. If 40 % of 2 equivalents have reacted, 1.2 equivalents should remain and 0.8 equivalent product should have been formed. In total, 2 equivalents of starting material and product combined should be present. This would indicate a yield of 80 % of **23**. Even so, the yield was measured to be 53 %. Therefore, the mass balance was checked up against the internal standard, and it showed that only 1.44 equivalents of product and starting material remained. This led us to believe that starting material could either participate in other reaction pathways and/or react with the product formed.

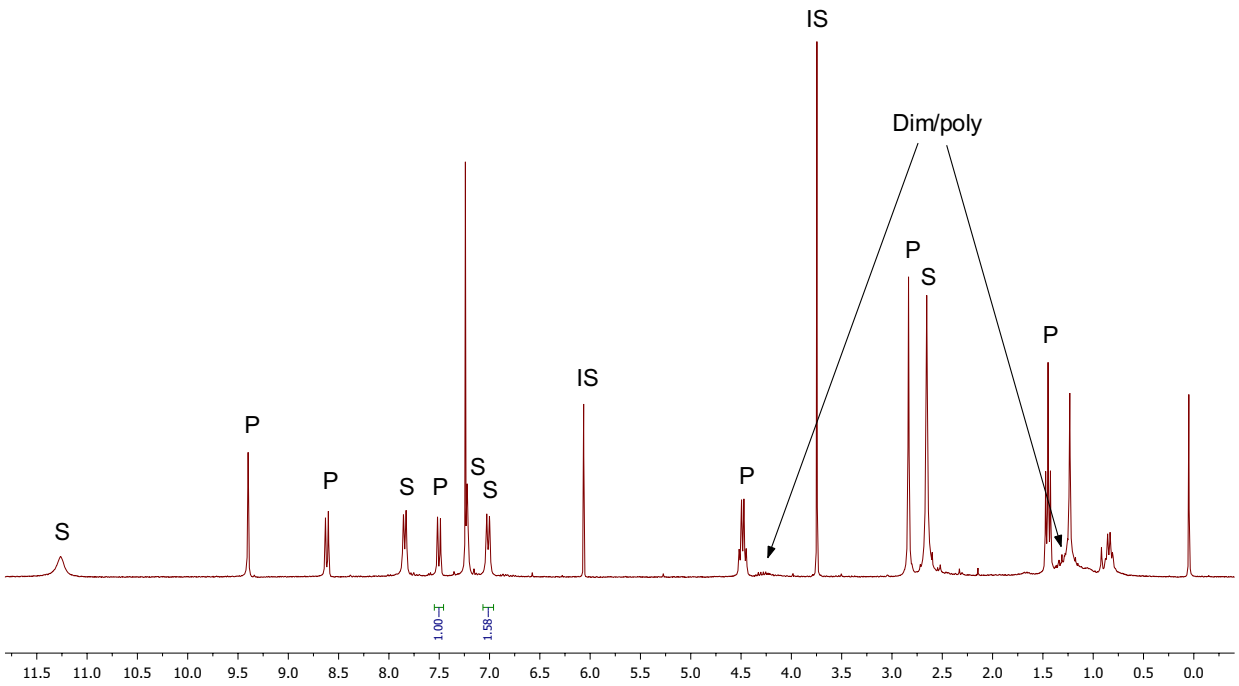

Figure 2.8: Crude ^{1}H NMR (300 MHz, $CDCl_3$) from reaction Scheme 2.12. S = starting material **20**, P = product **23**, IS = internal standard (TMB) and dim/poly = di/polymerization of the diazo.

2.7.1 Nucleophilicty of 7-azaindolates and the electron deficient nature of 8-azaquinolines

Deprotonation of a 7-azaindole results in the corresponding anion (Scheme 2.13). As the resulting negative charge on the nitrogen can be delocalized to C-3, the 7-azaindolate can be considered an ambident anion and hence, an ambident nucleophile. The preferred reaction site with an electrophile is dependent on the counter ion and solvent [22].

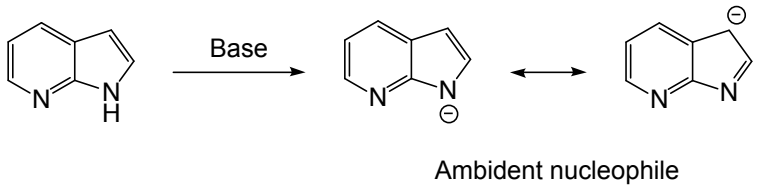

Scheme 2.13: Deprotonation of 7-azaindole and formation of an ambident nucleophile.

The two pyridine rings in 8-azaquinolines are considered electron poor, especially the carbons in α- and γ-position (Figure 2.9) [22]. Both positions are prone to nucleophilic attack, and halogens are relatively easy displaced, *i.e.* the solvolysis briefly discussed in 2.6. Compared to regular indoles the 7-azaindolate is *more* nucleophilic, and compared to quinolines, the 8-azaquinolines are *more* electrophilic. The combination of enhanced nucleophilicity and electrophilicity could lead to reactions between the starting material and the product. This could be one factor that helps explain why the conversion often is high while the yield is low. Also, if several products are formed in small amounts, they might be hard to detect in a ^{1}H NMR spectrum.

An experiment with a 7-azaindolate and a 8-azaquinoline in the absence of diazo compound and catalyst were planned to be studied briefly. However, due to shortage of time, this reaction was not carried out.

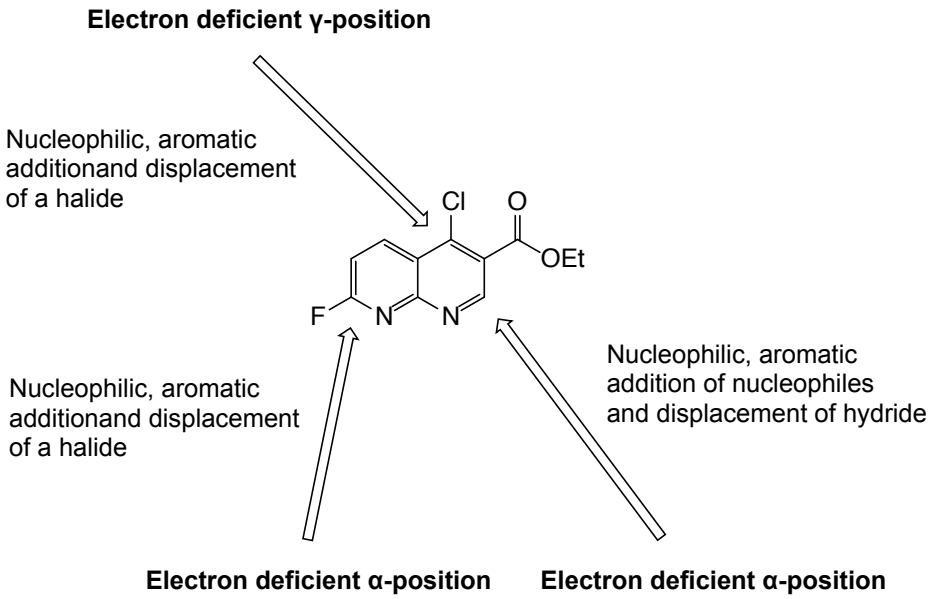

Figure 2.9: Examples of reaction sites in in a ethyl 8-azaquinoline-3-carboxylate.

2.7.2 Acidity of 2-methylpyridine type protons in 7-methyl-8-azaquinolines

As discussed in 2.5.3 and displayed in Scheme 2.8, when a methyl group is present in α/2-position of a pyridine, they are considered slightly acidic. Also discussed in 2.5.3 was the possibility of deprotonation of a methyl proton in the starting material in the presence of a strong base. What should also be considered is the possibility of deprotonation of the methyl protons in the *product* (Figure 2.10). Particularly when the base is used in excess as were the case for several of the reactions in Table 2.7. When deprotonated, subsequent reactions with electrophiles might occur. If this is the case in the reactions discussed here is not knwon, but it would be an alternative explanation of why the mass balance observed is incorrect.

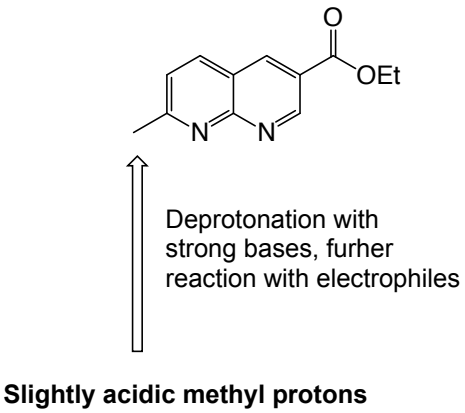

Figure 2.10: Illustration of the slightly acidic 2-methylpyridine type protons in a ethyl 7-methyl-8-azaquinoline-3-carboxylate.

2.8 Summary

What has mainly been discussed in this chapter are the challenges faced in the Rh(II)-catalyzed cyclopropanation-ring expansion reactions between various 7-azaindoles and halodiazoacetates, attempts to overcome these challenges and explanation of the results obtained. It was first discovered that the standard conditions used for the analogous reaction with indoles did not yield the same results with 7-azaindoles. With 7-azaindoles, the major product of the reactions were the N-H-insertion product with very little formation of the cyclopropanated-ring expanded product. The outcome was rationalized based on coordination of the 7-azaindoles to the Rh(II)-catalyst. Alternative catalysts were tested without success.

Attempts to suppress coordination by coordination to another metal (Zn) or by protonation of the pyridyl lone pair were unsuccessful. As was the thermal reaction. The focus was shifted towards suppression of the N-H insertion product by deprotonation of the 7-azaindoles. After several attempts, it was discovered that a combination of *n*-BuLi as base and $PhCF_3$ as solvent gave the best results. With non-chlorinated 7-azaindoles, isolated yields up to 43 % was afforded.

When chlorinated 7-azaindoles was used, *one* reaction with the new improved conditions was successful with a 50 % yield measured by internal standard (IS-yield) using ^{1}H NMR spectroscopy. Several reactions were carried out using *n*-BuLi as a base, but none of them was considered successful. Yet again, other bases were tested and NaH proved to be a good choice, with IS-yields up to 63 %. This result was only observed once as reproducibility was an issue.

Decomposition of the product that was supposed to be used further in the synthesis of nalidixic acid was observed, and the planned synthetic route could not be completed.

In most of the reactions where 7-azaindoles were deprotonated prior to cyclopropanation-ring expansion, high conversion of the starting material was observed, but seemingly low yields as no other obvious byproducts were formed. Questions were raised about what actually happens:

- Does the starting material fully convert to product (only), but the product reacts further, decreasing the yield?
- Does the starting material participate in (several) other reactions that are hard to detect in an ^{1}H NMR spectrum?

Some observations were made during experiments, and reasons why where discussed:

- Deprotonated 7-azaindoles are highly nucleophilic on N-1 and C-3, while the 8-azaquinoline-3-carboxylates formed are very electron poor.
  - If halogens are present in the product, nucleophilic aromatic substitution is a likely possibility.
- In the absence of 7-azaindoles, 8-azaquinoline-3-carboxylates react when subjected to a reaction with X-EDA and catalyst.
- If the 7-azaindole contains a methyl group in position 6 and are exposed to a strong base, deprotonation and subsequent reaction with electrophiles is a possibilty.
- The same methyl group in position 7 of the 8-azaquinoline product can, when excess of base is used, also undergo deprotonation and subsequent reaction with electrophiles.

In general, reproducibility seemed to be an issue in these reactions. Even more so when scaling up a reaction. With all the parameters (above) taken into consideration, it can perhaps help explain why these reactions are troublesome.

Chapter 3

Results and discussion - Indoles and halodiazophosphonates

In this chapter, the results of the Rh(II)-catalyzed cyclopropanation-ring expansion reaction of indoles with halodiazophosphonates will be presented. In addition, the synthesis of the EDP and C-3 chlorination of indole and substituted will be presented. The results obtained will be discussed and explained.

3.1 Introduction

The reactions of halodiazophosphonates have until now been limited to Rh(II)-catalyzed cyclopropanations [4, 5]. No cyclopropanation-ring expansion reactions with halodiazophosphonates have been reported. An investigation of the reaction between halodiazophosphonates and indoles was considered intriguing (Scheme 3.1).

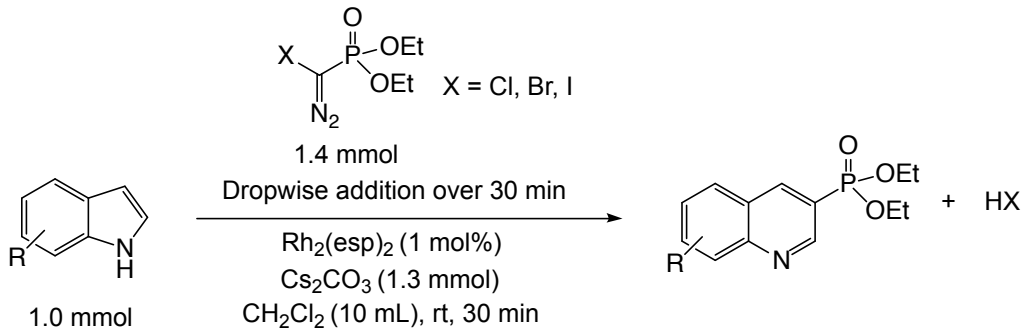

Scheme 3.1: Cyclpropanation of indole with a halodiazophosphonate and subsequent ring expansion/elimination to diethyl 3-quinolinylphosphonate under standard conditions. Anticipated reaction pathway and product formation based on literature [1, 3].

Further, it was of great interest to demonstrate the reactions usefulness as a key step in the synthesis of the phosphonic acid bioisoster of the quinolone antibacterial norfloxacin (Scheme 3.2). With the same synthetic strategy as in Scheme 2.9. No phosphonic acid bioisoster of this compound have been reported.

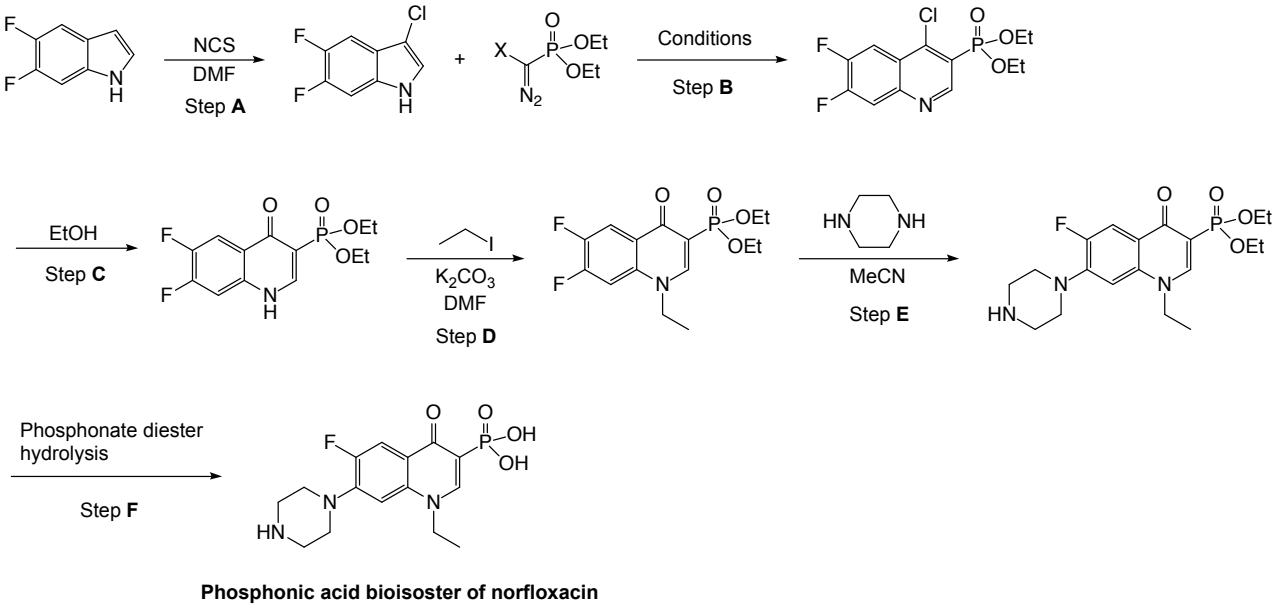

Scheme 3.2: Planned synthetic route to the phosphonic bioisoster of norfloxacin via Rh(II)-catalyzed cyclopropanation-ring expansion reaction between 3-chlorinated indoles and halodiazophosphonates.

3.2 Preparation of diethyl diazomethylphosphonate (EDP)

Diethyl diazomethylphosphonate (EDP) **27** is not as easily available as EDA, and was therefore prepared in three steps according to literature procedures. Diethyl 2-oxopropylphosphonate **25** was prepared from chloroacetone and triethylphosphite *via* the Michaelis-Arbuzov reaction [211]. Diazo transfer with tosyl azide, (TsN_3) [211, 212] afforded the Ohira-Bestmann reagent diethyl 1-diazo-2-oxopropylphosphonate **26** in 83 % yield. Deacylation *via* methanolysis with methanol and triethylamine [213] afforded EDP **27** in 70 % yield.

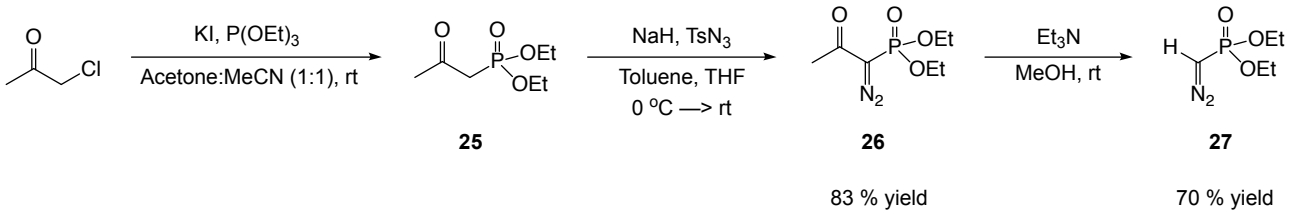

Scheme 3.3: Three step synthesis of EDP [211–213].

3.2.1 Preparation of nosyl- and tosyl azide

Para-nitrobenzenesulfonyl azide (nosyl azide) **30** and para-toluenesulfonyl azide (tosyl azide) **31** were prepared according to literature procedures (Scheme 3.4) [212] for the purpose of employing them in diazo transfer reaction (Scheme 3.3) in the synthesis of EDP. Compound **31** have been widely used as a diazo transfer reagent over the years [212, 214]. Successful diazo transfer reactions with **30** have also been reported [215]. At the time when the EDP synthesis was carried out, nosyl chloride **28** was easily accessible in the lab. Thus, it was decided to prepare **30** and use it as a diazo transfer reagent to obtain **26**. Compound **30** was afforded in 83 % yield *via* a substitution reaction from sodium azide (NaN_3) and **28**, and further used in the diazo transfer reaction. The results were not quite satisfactory with small amounts of byproduct present. It was therefore decided to prepare tosyl azide **31** instead. Compound **31** was prepared in 91 % yield from tosyl chloride **29** and NaN_3 (Scheme 3.4) and successfully employed in the diazo transfer reaction.

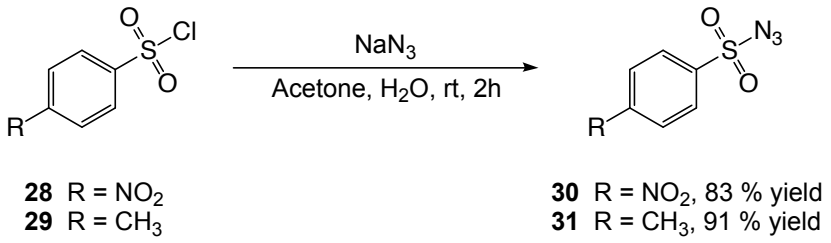

Scheme 3.4: Synthesis of nosyl azide **30** and tosyl azide **31** [212].

3.3 Halogenation of EDP: choice of halogenation method

Both nucleophilic and electrophilic halogenations to generate halogenated EDP (X-EDP) was discussed in 1.3.5.4. The yields of the Rh(II)-catalyzed cyclopropanation reactions with the X-EDPs was proven to be slightly higher in the reactions where X-EDP had been generated from EDP by electrophilic halogenation (Scheme 1.13 and Scheme 1.14) [4, 5]. For that reason, it was decided to do electrophilic halogenations with *N*-halosuccinimide. It was also demonstrated that both Cl-, Br- and I-EDP could be employed in the cyclopropanation reactions with styrene [4]. Br-EDP showed 5 % higher yield than the Cl- and I-analogue. On basis of the cyclopropanation-ring expansion reactions with I-EDA and indole, and the fact that the halogen does not end up in the final product, it was decided to exclude I-EDP and focus on Cl- and Br-EDP throughout this work.

The route in Scheme 1.14 was developed as isolation of X-EDP had proven to be unsuccessful with the same method used to isolate X-EDA [4]. The workup consisted of washing with cold $Na_2S_2O_3$, drying with $MgSO_4$, followed by silica plug filtration [1, 216]. The one-pot procedure involves an excess of NaH which have shown to be compatible with styrene derivatives in the subsequent cyclopropanation reaction. In this work, however, indoles were used as substrate and NaH is known to deprotonate indole [22]. An excess of NaH would be a potential problem as the indolate would be highly nucleophilic as were seen for the 7-azaindoles. This approach was not completely dismissed, and one reaction was carried out using the reported conditions and are briefly discussed below in 3.4 before halogenation of EDP is further discussed.

3.4 Attempt on the one-pot approach for the synthesis of diethyl 3-quinolinylphosphonate

The initial attempt of synthesizing diethyl 3-quinolinylphosphonate **34** was carried out using the reported conditions in Scheme 3.5 [4]. 5.0 equivalents of NaH was added to a solution of 1.0 equivalent of EDP **27** and 1.2 equivalents of NCS. The reaction was monitored by TLC to ensure 100 % conversion, but the EDP was still not 100 % converted after 40 min. It was, however, used further as Cl-EDP are prone to decomposition over time. Compound **34** was successfully formed according to ^{1}H NMR, but not surprisingly, only in 24 % yield. The yield was measured by ^{1}H NMR analysis of the crude product using TMB as an internal standard, and calculated over two steps from EDP. If the low yield was due to presence of NaH or possible dimerization and/or decomposition of the Cl-EDP are not known and did not warrant any further investigation.

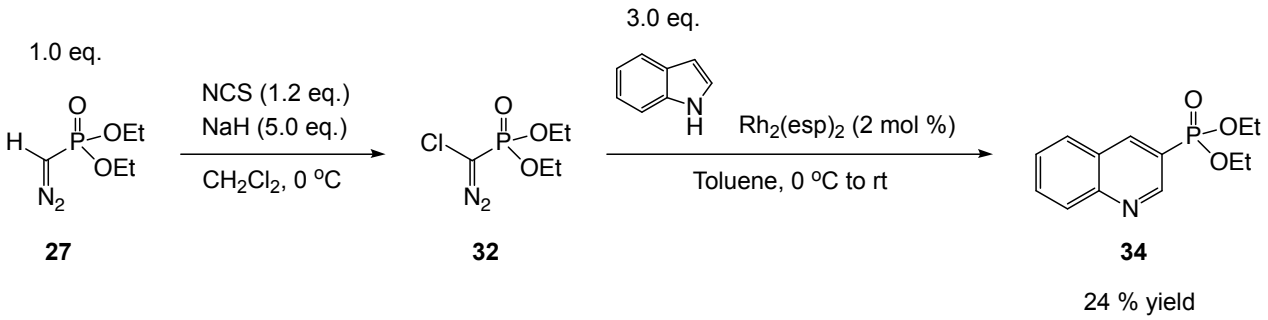

Scheme 3.5: One-pot synthesis of diethyl 3-quinolinylphosphonate **34** using the same conditions as reported for the one-pot synthesis of halocyclopropylphosphonates from X-EDP [4].

3.5 Electrophilic halogenation of EDP

The results from the one-pot approach were not quite satisfactory, as anticipated. For that reason, it was decided to use the same method used for the X-EDA, namely purification *via* silica plug filtration, with no work up prior to the filtration.

3.5.1 Quantitative analysis of Br- and Cl-EDP

As for the X-EDA, it was of interest to measure the yields of Br- and Cl-EDP. Because of the unstable (and possible explosive) nature of the X-EDPs, they were kept in solution and the yield was measured by an internal standard using ^{1}H NMR spectroscopy. The internal standard of choice was TMB as it does not react nor overlap with any of product peaks in the ^{1}H NMR spectra. Br- and Cl-EDP was prepared according to procedure 5.3.2.1. Deuterated solvent was added to the X-EDP solution, DCM was removed *in vacuo* at 0 °C and an exact amount of the internal standard was added. The solution of X-EDP was kept cold until ^{1}H NMR analysis, which was performed directly after preparation.

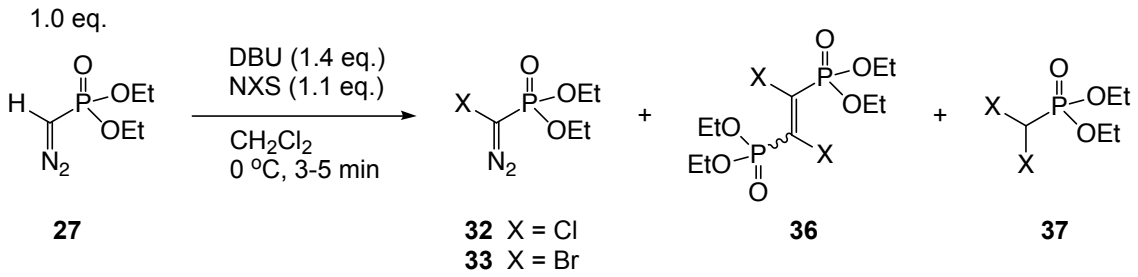

Scheme 3.6: Halogenation of EDP.

Quantitative conversion of EDP was observed in all the reactions. However, the yields could not be measured as precise as for the X-EDA analogues. Several attempts were made, and the yields varied from 75 % to > 100 %. For that reason, it was decided to calculate the yields from the cyclopropanation-ring expansion reactions (discussed further below) over two steps.

As for the halogenation of EDP, dimerization products (**36**) were observed in the halogenation of EDP. In addition, 5 - 7 % of what is believed to be the overhalogenated product **37** was observed. Diethyl dibromomethylphosphonate (X = Br in **37**) have been reported as a byproduct in the one-pot synthesis of Br-EDP and subsequent reaction with styrene [4]. Compound **37** was attempted isolated, but without success.

3.5.2 (Decomposition of) X-EDP in concentrated solutions

The halogenations of *EDA* were typically carried out in solutions of 1 mmol/10 mL DCM. The halogenations of *EDP* were carried out in slightly more diluted solutions. The reason being observations of what is believed to be decomposition of the X-EDP in concentrated solutions. As 1.1 equivalents of NCS were added to a solution of 0.3 mmol EDP in 4 mL DCM and 1.4 equivalents of DBU, gas evolution and rapid decoloration (purple or brown) was observed. In the analogous reaction with NBS, a black solution was observed together with gas evolution. It was evident that halogenations were successful, *i.e.* no gas evolution and color change to yellow/orange, in slightly more diluted solutions; 0.2 mmol in 5 mL DCM, 0.7 mmol in 10 mL DCM and 1.5 mmol in 30 mL DCM. No systematic work to determine the exact concentration of

a successful halogenation were carried out. Depicted in Figure 3.1 are examples of a successful (orange, left) and unsuccessful (brown, right) halogenation.

Figure 3.1: A successful chlorination of EDP (orange, left) and what is believed to be decomposed Cl-EDP (brown, right).

3.6 Synthesis of diethyl 3-quinolinylphosphonate *via* dropwise addition of isolated X-EDP

Based on the results from the one-pot attempt, it was decided to synthesize diethyl 3-quinolinylphosphonate **34** from indole *via* dropwise addition of the isolated X-EDP. Based on the fluctuating yield observed for the X-EDPs, it was ensured that an excess of X-EDP was used in the reactions were indole was limiting reagent. In the reactions were X-EDP was used as limiting reagent, the yield was calculated over two steps from EDP.

3.6.1 Initial reaction and optimization of reaction conditions

The initial reaction was carried out, as mentioned, by using the reported conditions in the synthesis of ethyl quinoline-3-carboxylates [3]. Compound **34** was synthesized from a solution containing 1.0 equivalent indole **38**, 1.2 equivalents Cs_2CO_3 and 1 mol % $Rh_2(esp)_2$ in DCM. 1.1-1.3 Equivalents of isolated Br-EDP was added dropwise to the solution over 20-30 min which only gave 21 % of conversion **34** (entry 1, Table 3.1). The yield was not calculated due to the low conversion.

The result from the initial reaction was not deemed satisfactory. Thus, the reaction conditions were screened in order to find better alternatives. Since the conversion of **38** was far from great, the catalyst load was increased from 1 to 2.5 mol %. Br-EDP was employed as limiting reagent and 53 % yield (calculated over two steps from EDP) was measured from the crude ^{1}H NMR spectrum. The product was isolated *via* column chromatography which afforded 48 % isolated **34** (entry 2, Table 3.1). Compound **34** have been reported in the literature [217–219]. The structure was confirmed by comparing the spectroscopic data.

As demonstrated and discussed in 2.5, toluene can be a better alternative than DCM as solvent in reactions employing halodiazoacetates. Also, in the reported procedures employing

Table 3.1: Results from the initial reaction and optimization of the conditions in the reaction between indole **38** and halodiazophosphonates.

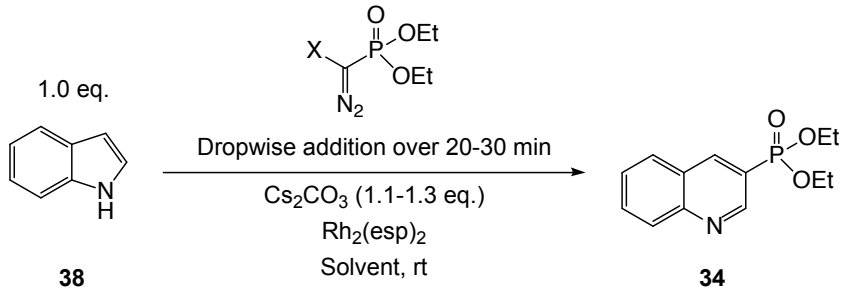

Entry	X-EDP (eq.)	Cat. load [%]	Solvent (dry)	Conversion of **38** [%][a]	Yield [%][b]
1	Br-EDP (1.3)	1.0	DCM	21	-
2	Br-EDP (0.2)	2.5	Toluene	-	53, 48[c]
3	Cl-EDP (0.2)	2.5	Toluene	-	71, 61[c]
4	Cl-EDP (0.5)	2.5	Toluene	-	53 - 63
5	Cl-EDP (1.4)	2.5	Toluene	80 - 83	51 - 60
6[d]	Cl-EDP (1.3)	2.5	Toluene	41	-

[a] Measured by ^{1}H NMR analysis of crude reaction mixture.
[b] Yield measured by ^{1}H NMR analysis of the crude product using TMB as internal standard.
[c] Isolated yield.
[d] Cl-EDP added in one portion at 0 °C.

halodiazophosphonates, a 2:1 ratio of toluene:DCM was used. Therefore, it was decided to try toluene as solvent. Br-EDP was replaced with Cl-EDP as higher yields have been afforded in cyclopropanation-ring expansion reactions when the chlorinated analogue was used [3].

A combination of large excess (5 equivalents) of **38** and Cl-EDP in toluene gave notably good results with 71 % yield measured from the ^{1}H NMR and 61 % isolated yield of **38** (entry 3, Table 3.1). By decreasing the equivalents of **38** a decrease in yield was observed as shown in entry 4, Table 3.1. The reaction was repeated several times, and yields of **34** ranging from 53 to 63 % was observed.

In the planned synthesis towards the bioisoster of norfloxacin (Scheme 3.2), it was decided to start with the 5,6-difluorinated indole. Considering the price and the fact that this starting material was used in someone else's project at the same time, it was necessary to find conditions where the amount of starting material could be reduced.

As shown in entry 5 Table 3.1, **38** was used as a limiting reagent, and yields ranging from 51 to 60 % was observed when the reaction was repeated a couple of times. The difference between a slight excess (2 equivalents) of indole and a slight excess of Cl-EDP was deemed negligible, and it was decided to continue the work using the conditions from entry 5, Table 3.1.

One attempt was made to add the Cl-EDP directly, in one portion, to the reaction mixture at 0 °C (entry 6, Table 3.1), but only 41 % conversion of **38** was afforded. The yield was not measured due to the low conversion.

3.7 Synthesis of substituted diethyl 3-quinolinyl phosphonates

Various substituted ethyl quinoline-3-carboxylates have been successfully prepared from indoles and X-EDA [3]. If substituted diethyl 3-quinolinylphosphonates also could be successfully prepared from indoles and the X-EDA analogue X-EDP was of large interest. In addition, an investigation of the substituent-effect related to the yield was also of great interest.

Several synthetic routes to unsubstituted [217–219] and substituted [220, 221] 3-quinolinyl-phosphonates have been reported. Although, there seems to be a lack of monohalogenated and halogenated derivatives without other substituents. Synthetic routes to these diethyl 3-quinolinyl-phosphonates would be of interest both synthetically as it may allow for further transformations. Also, the combination of reported antibacterial reactivity of **34** [218] and the fact that halogens are present in several drugs and drug candidates [222] are quite intriguing. None of the reported synthetic routes to 3-quinolinylphosphonates originated from indoles.

3.7.1 Substrate scope and limitations

The investigation was limited to indoles with substituents in 3, 5 and 6-position. The limitation is based on what we wanted to disclose about the substituent effects in the positions were substituents were necessary in order to synthesize the phosphonate bioisoster of norfloxacin (Scheme 3.2). 3-Substituted chloro, 5-substituted methoxy, benzyloxy, nitro, bromo and amino, 6-substituted bromo, 5,6-difluorosubstituted and 3-chloro-5,6-difluorosubstituted indoles were subjected to the conditions in Scheme 3.7

A number of the substituted indoles were successfully converted to the ring-expanded diethyl 3-quinolinylphosphonate in modest to good yields (8 - 62 %). One of the reactions was unsuccessful and yielded no desired product. Products and their corresponding yields are displayed in Figure 3.4. The yields were calculated by ^{1}H NMR spectroscopy using TMB as internal standard.

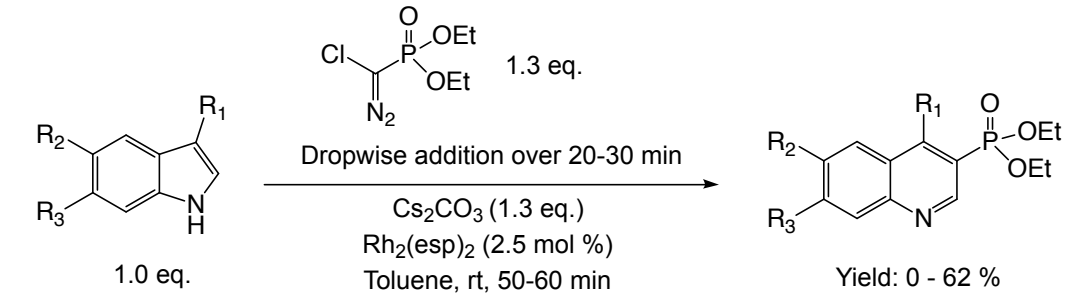

39 R_2 = OMe, R_1 = R_3 = H
40 R_2 = OBn, R_1 = R_3 = H
41 R_2 = Br, R_1 = R_3 = H
42 R_2 = R_3 = F, R_1 = H
43 R_3 = Br, R_1 = R_2 = H
44 R_2 = NO_2, R_1 = R_3 = H
45 R_1 = Cl, R_2 = R_3 = H
46 R_1 = Cl, R_2 = R_3 = F
47 R_2 = NH_2, R_1 = R_3 = H

48 R_2 = OMe, R_1 = R_3 = H
49 R_2 = OBn, R_1 = R_3 = H
50 R_2 = Br, R_1 = R_3 = H
51 R_2 = R_3 = F, R_1 = H
52 R_3 = Br, R_1 = R_2 = H
53 R_2 = NO_2, R_1 = R_3 = H
54 R_1 = Cl, R_2 = R_3 = H
55 R_1 = Cl, R_2 = R_3 = F
56 R_2 = NH_2, R_1 = R_3 = H

Scheme 3.7: Synthesis of substituted diethyl 3-quinolinylphosphonates using the new, optimalized conditions.

There were several unidentified byproducts formed in these reactions, in addition to the endless tailing of the phosphonate group on silica, which made purification a serious challenge. After purification **48**, **52** and **54** were obtained as oils, the rest as solids. Attempts were made to grow crystals suitable for single crystal X-ray diffraction. A single crystal of of **51** was successfully grown by diffusion of hexane into a solution of **51** in benzene. The crystal structure of **51** is displayed in Figure 3.2.

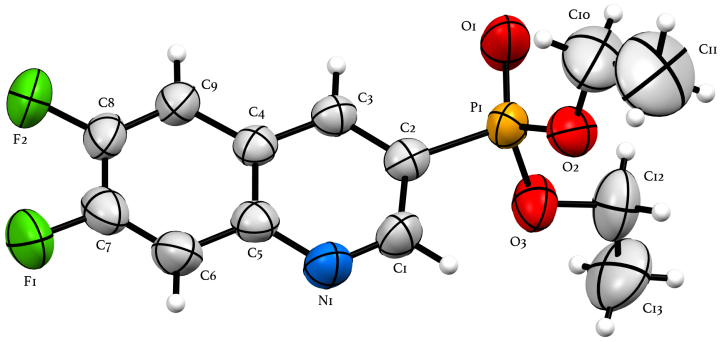

Figure 3.2: ORTEP representation of diethyl 6,7-difluoro-3-quinolinylphosphonate **51**. The atoms are color coded; hydrogen is white, carbon is grey, nitrogen is blue, fluorine is green, phosphorus is orange and oxygen is red. Ellipsoids are of 50 % probability.

A single crystal of **50** was successfully grown by slow evaporation from Et_2O. The crystal structure of **50** is displayed in Figure 3.3

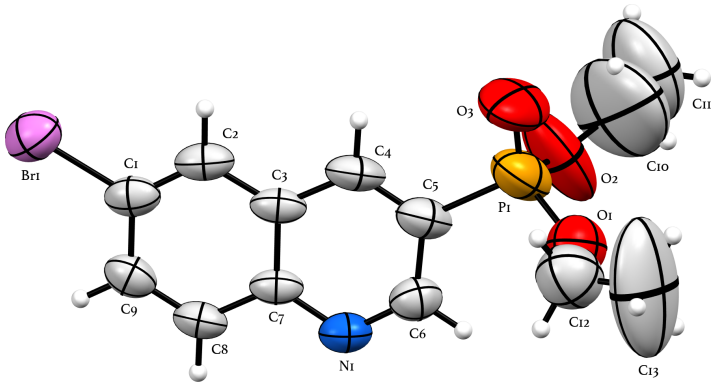

Figure 3.3: ORTEP representation of diethyl 6-bromo-3-quinolinylphosphonate **50**. The atoms are color coded; hydrogen is white, carbon is grey, nitrogen is blue, bromine is pink, phosphorus is orange and oxygen is red. Ellipsoids are of 50 % probability.

It is evident from the results in Figure 3.4 that the electron withdrawing or donating nature of the substituent in addition to its position on the indole ring affects the yield. In line with what was previously reported for the carboxylate analogues [3], the strongly withdrawing groups, such as -NO_2 in **44**, decrease the yield considerably (22 % yield). With strongly donating groups as -OMe in **39** a minor increase in yield to 62 % was observed compared to indole under the same conditions. As reported for the carboxylate analogues, **39** was deemed too reactive and several unidentified byproducts was observed when the reaction was carried out in room temperature. Therefore, the reaction with **39** was carried out at 0 °C. Suprisingly, a decrease in yield was observed from the reaction with 5-benzyloxyindole **40**.

With π-donating and σ-withdrawing abilities, the yields from the reactions of 5- and 6-halogensubstituted indoles lied somewhere in between the two extremes. Compound **50** was afforded in 50 % yield, **51** in 46 % and **52** in 45 %. This was *not* observed in the case for the 3-chloroindole **45**. The position of the substituent relative to the reaction site might explain

the rather unsatisfactory outcome. Lower yields with substituents in this position was also demonstrated for the carboxylate analogues [3], but are clearly more prominent for the phosphonates. This can be rationalized by the different geometry of the acetate and phosphonate group in the halodiazo compounds.

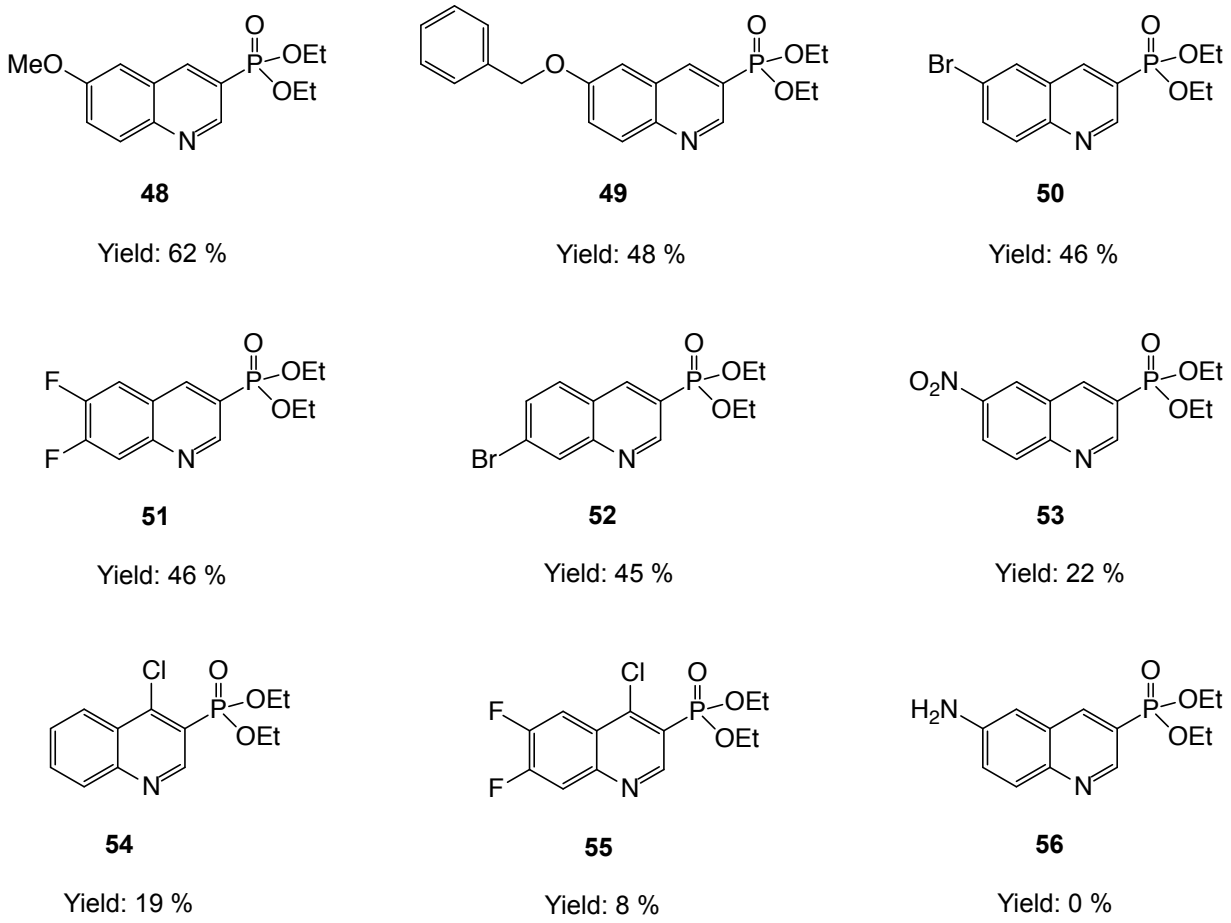

Figure 3.4: Results from the reactions in Scheme 3.7. Yields are measured by ^{1}H NMR analysis of the crude product using TMB as internal standard.

The sp^2 hybridized carbon atom in esters bond to three different groups, forcing it to adopt a trigonal planar geometry. The pentavalent phosphorus in phosphonate diesters, on the other hand, is sp^3 hybridized, and a tetrahedral structure is adopted. The non-planar geometry could give rise to steric hindrance between the more bulky phosphonate and the chlorine atom. The combination of steric effects and the σ-withdrawing effect of two flourine atoms might explain yield of **54** (19 %) and **55** (8 %). The free amino group in 5-aminoindole **47** are exposed to N-H insertion. Also, with the strongly electron donating effect of the $-NH_2$, it could be speculated that the indole becomes too reactive and favors other reaction pathways.

Based on the very poor yield of **55**, it was decided to not continue the planned synthetic route towards the bioisoster of norfloxacin.

Even though the reaction to produce **55** was displeasing and put a stop to reach the goal of the project, several of the reactions discussed above were indeed successful. The substrate scope demonstrated that the reaction was compatible with a range of substrates. Several of the substrates are commercially available and does not need to be synthesized prior to the cyclopropanation-ring expansion reactions. The availability of substituted indoles is clearly an advantage in this procedure. Also, except X-EDP, the conditions are mild and the reaction time is short. It should also be emphasized that the reactions conditions used in this substrate scope

was *not* the conditions that gave the highest yield of **34**. By using the optimized conditions, higher yields of the substituted 3-quinolinylphosphonates could perhaps be afforded.

As in every synthetic procedure, some limitations were discovered. First, a substituent in position 3 of the indole was not compatible with this reaction, which can be attributed to steric hindrance. Also, the reaction was not compatible with a free amine on the indole, and not optimal with strongly EWGs. Second, the isolation and purification of the products were a serious challenge and other methods should be revised.

3.8 X-EDA vs. X-EDP

Both X-EDA and X-EDA have now been used in cyclopropanation- and cyclopropanation-ring expansion reactions. To put it in perspective, a brief comparison of the performance of the two halodiazo compounds are given below.

Compared to the $Rh_2(esp)_2$-catalyzed cyclopropanation-ring expansion reactions between indole and Cl-EDA, the yield of the reactions performed with Cl-EDP was considerably lower. The highest yield obtained in this work was 71 % measured by internal standard using ^{1}H NMR spectroscopy, 61 % isolated. In the analogue reaction with Cl-EDA, 90 % isolated yield was reported [3]. The same "trend" has been observed in the $Rh_2(esp)_2$-catalyzed cyclopropanation reactions with styrene. Cyclopropanation with Br-EDA have been reported to give 91 % yield [1], while 82 % were reported for Br-EDP [4].

One possible explanation for these observations is the electron withdrawing ability of the ester and the phosphonate ester. The rhodium carbenoid formed in these reactions are considered electrophilic, and degree of electrophilicity and hence the reactivity is determined by the substituents on the carbenoid [132, 134, 135]. The only group that differs when using the same catalyst and halogen, are the ester and the phosphonate ester. Esters are considered more electron withdrawing than the phosphonate ester, causing the carbenoid formed more electrophilic. The more electrophilic carbenoid might show greater reactivity towards the nucleophile (being indole or styrene), which in turn might rationalize the overall lower yields obtained in the reactions employing X-EDP.

3.9 C-3 chlorination of indoles and reduction of 5-nitroindole to 5-aminoindole

The two chlorinated indoles **45** and **46** were used in the substrate scope investigation in 3.7.1. Both **45** and **46** was prepared from **38** and **42**, respectively. With slight modifications, **38** and **42** were subjected to electrophilic chlorination with NCS as reported in literature (Scheme 3.8) [206].

The reactions were tracked TLC analysis and ^{1}H NMR analysis until the starting material was fully converted and the desired products isolated using column chromatography. As for the chlorinations of the 7-azaindoles discussed in 2.6.1, full conversion of the starting material was desirable as separation of the starting material and mono-chlorinated product was practically impossible.

Crystals of **46** suitable for single crystal X-ray diffraction were successfully grown. Hexane (anti-solvent) was added to **55** and slowly heated while EtOAc (solvent) was added dropwise

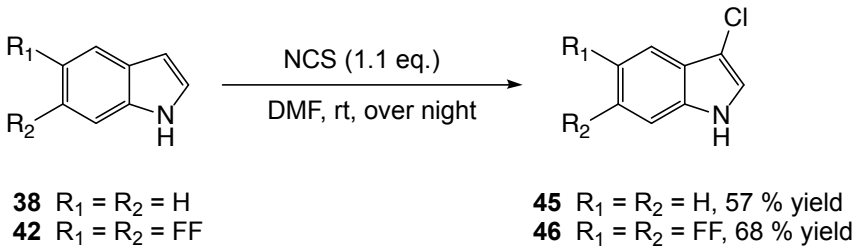

38 $R_1 = R_2 = H$
42 $R_1 = R_2 = FF$

45 $R_1 = R_2 = H$, 57 % yield
46 $R_1 = R_2 = FF$, 68 % yield

Scheme 3.8: Electrophilic chlorination of indole **38** to 3-chloroindole **45** and of 5,6-difluoroindole **42** to 3-chloro-5,6-difluoroindole **46** [206].

until **46** was fully dissolved. The solution was concentrated *in vacuo* and was left in room temperature to crystallize by slow evaporation of the remaining solvents. The crystal structure of **46** is displayed in Figure 3.5.

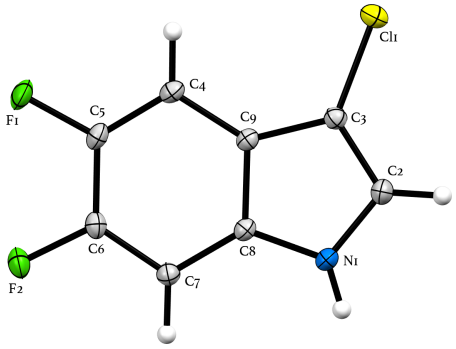

Figure 3.5: ORTEP representation of 3-chloro-5,6-difluoroindole **46**. The atoms are color coded; hydrogen is white, carbon is grey, nitrogen is blue, fluorine is green and chlorine is yellow. Ellipsoids are of 50 % probability

5-aminoindole **47** was prepared by reduction of 5-nitroindole **44** with sodium dithionite ($Na_2S_2O_4$) (Scheme 3.9) according to literature procedure [223]. Compound **47** was afforded in 62 % yield after loss of some product during work up. The presence of -NH_2 was confirmed by ^{1}H NMR spectroscopy.

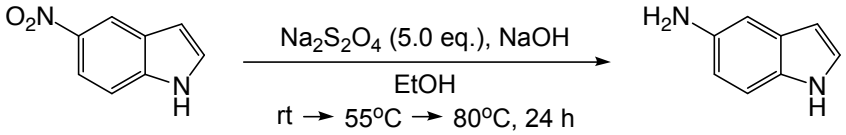

44
1.0 eq.

47
62 % yield

Scheme 3.9: Reduction of nitroindole **44** to aminoindole **47** [223].

3.10 Summary

What has mainly been discussed in this chapter is the performance of X-EDP in cyclopropanation-ring expansion reactions with indoles. Prior to these reactions, it was briefly discussed how EDP was synthesized using known literature procedures. Two halogenation methods of EDP were reported in literature (one electrophilic and one nucleophilic). Based on the results in articles, it was decided to use the electrophilic method. One cyclopropanation-ring expansion reaction with Cl-EDP and indole using the reported one pot procedure was attempted, but did not yield satisfactory results. It was therefore decided to do the halogenation and cyclopropanation-ring expansion reaction in the same manner as for EDA. The reaction conditions were optimized, and yields up to 71 % of **34** was afforded. Due to high price of the starting material that were supposed to be used in the planned synthesis of the bioisoster of norfloxacin, the conditions that were used further were not the most optimal, but more cost friendly.

Indoles with substitutens in the positions most relevant for the further synthesis was exposed to the new reactions conditions. The results showed that the reaction was compatible with a range of substrates, except the substrate that were supposed to be used further. This put a stop to the project as the goal was to synthesize the bioisoster of norfloxacin using the cyclopropanation-ring expansion reaction between Cl-EDP and **55** as a key step. The unsatisfactory results obtained were discussed and explained in terms of the phosphonate groups' geometry and steric hindrance at the reaction site. Despite this, the method developed was deemed as decent method to synthesize various substituted diethyl 3-quinolinylphosphonates. The overall performance of the halodiazophosphonates versus halodiazoacetates were shortly discussed, and the somewhat poorer performance of the halodiazophosphonates could possibly be attributed to the seemingly less electrophilic carbenoid.

Chapter 4

Conclusions and future prospects

The yields of Br-EDA (**8**) and Cl-EDA (**9**) were successfully quantified by internal standard measurements using ^{1}H NMR spectroscopy. In combination with the known amount of DCM in EDA, the determination of the exact the amount (based on average yields) of Cl- or Br-EDA used in every reaction were established.

Successful were eventually also the chlorinations of 7-azaindoles which gave **18** and **20** in very good yields.

The Rh(II)-catalyzed cyclopropanation-ring expansion reaction between halodiazoacetates and 7-azaindoles was not as successful as for regular indoles. The main issue being possible catalyst coordination and, as a consequence, major formation of the N-H-insertion product relative to the cyclopropanated-ring expanded product. 8-Azaquinoline **12** and N-H-insertion product **13** were, however, successfully isolated in poor to modest yields.

A thermal reaction was attempted without success, as were the attempts with six other catalyst. Attempts to block catalyst coordination by alternative coordination or with protonation were unsuccessful, but with new and improved conditions, formation of the N-H-insertion product was successfully prevented. With the new conditions, 8-azaquinoline **15** and **17** were synthesized and isolated in modest yields. The same conditions were only successful once in the reaction to produce the 4-chlorinated 8-azaquinoline **22** in good yields.

Again, new conditions were found and 4-chlorinated 8-azaquinoline **23** was successfully formed in 63 % yield. The successful reaction was performed at a very small scale, and once scaled up, the good results could not be reproduced. In all of reactions mentioned here, reproducibility was seemingly an issue due to a number of parameters which was briefly investigated. The highly nucleophilic nature of a deprotonated 7-azaindole in combination with a highly electrophilic product was deemed a possible explanation of the issues with reproducibility, as well as reaction/degradation of the product when exposed to the reaction conditions used.

Once formed, **23** decomposed and could not be used further in the synthesis towards nalidixic acid. One of the decomposition products was identified as the quinolone analogue **24**. With the decomposition of **23**, the planned synthetic route towards nalidixic acid could not be completed. As time were a limiting factor, the synthesis of the non-fluorinated enoxacin analogue was not attempted. Even so, solubility of chlorinated 7-azaindole **18** in appropriate solvents was an issue.

At this point, there is seemingly no point in trying to complete the synthesis of nalidixic acid, unless conditions that ensure the survival of **23** can be found. However, there are a number of other 8-azaquinolone antibacterial agents that, theoretically can be synthesized from 7-azaindoles and halodiazoacetates. As reproducibility have been an issue in this work, an alternative would be to find new conditions that does not require a rhodium catalyst that is prone to coordination. Another interesting alternative would be to generate carbenes or carbenoids from other sources than the one used here.

Br-EDP (**33**) and Cl-EDP (**32**) were successfully synthesized using the same procedure as for the halogenation of EDA. However, halogenations of EDP were less reproducible than the halogenations of EDA. Full conversion was observed but the yields seemed to vary to a certain degree. The halogenations of EDP were also seemingly more sensitive as what is believed to be decomposition of the diazo was observed in "concentrated" solution.

After some reaction optimization, diethyl 3-quinolinylphosphonate **34** was successfully formed from Cl-EDP and indole, and isolated in good yields. The substrate scope showed that the reaction was compatible with a range of substrates in the selected positions. Indoles with EDGs in 5-position and halogens in 5 and/ or 6-position; **48**, **49**, **50**, **51** and **52** gave good yields. The exception being an aminogroup in 5-position which yielded nothing of the desired product **56**. With a strongly EWG in 5-position, as in **53**, a prominent decrease in yield was observed. The reaction was not particulary successful with a chlorine atom in 3-position of the indole. Compound **54** and **55** was afforded in poor yields. The poor yields were attributed to possible steric hindrance at the reaction site as the phosphonate group is non-planar.

The future work of halodiazophosphonates should involve the development of a procedure that allows *in situ*-generation of X-EDP that are compatible with further reaction of substrates with acidic protons (*i.e.*, without excess of strong base as in the reported one-pot procedure). Further, to complete the substrate scope, indoles with substituents in positions not investigated in this work should be investigated. Preferably, with the reaction conditions that results in the best yields.

Due to the poor formation of **55**, no phosphonic bioisoster of norfloxacin was synthesized in this work. As steric hindrance seemed to be the primary reason for the bad outcome, one possibility would be to consider a different, less bulky halodiazo compound and synthesize a another bioisoster.

Chapter 5

Experimental section

General

Chemicals were used as delivered from Sigma Aldrich, Cambridge Chemicals, abcr GmbH and Fluka unless stated other wise. CH_2Cl_2, THF and DMF was dried using MB SPS-800 Solvent Purification System from MBraun. NMR-solvents were used as delivered from Sigma Aldrich and Cambridge Isotope Laboratories. Hexane was distilled prior to use. Toluene was dried using molecular sieves. Other solvents were used as delivered.

n-butyllithium was titrated against diphenylacetic acid prior to use [224] *N*-chlorosuccinimide was recrystallized from water [225] and *N*-bromoosuccinimide was recrystallized from toluene prior to use.

Thin layer chromatography was performed on 60 F_{254} silica coated aluminum plates from Merck. Flash chromatography was performed on silica gel from Merck (Silicagel 60, 0.040-0.063 mm) either manually or with Isco Inc. CombiFlash Companion with PeakTrack software (v.1.4.10).

^{1}H, ^{13}C, ^{19}F and ^{31}P NMR experiments were recorded in $CDCl_3$, benzene-d_6, DMSO-d_6, acetone-d_6, methanol-d_4 or toluene-d_8 using Bruker DPX200 operating at 200 MHz (^{1}H), DPX300 operating at 300 MHz (^{1}H) and 75 MHz (^{13}C), Bruker AVII400 or AVIIHD400 operating at 400 MHz (^{1}H), 101 MHz (^{13}C), 377 MHz (^{19}F) and 162 MHz (^{31}P), or AVI600 operating at 600 MHz (^{1}H). All spectra were recorded at 25 °C. Chemical shift (δ) are given in parts per million (ppm) relative to the solvent used.

Reference peaks: $CDCl_3$: 7.24 ppm (^{1}H), 77.0 ppm (^{13}C). Benzene-d_6: 7.16 ppm (^{1}H), 128.39 ppm (^{13}C). DMSO-d_6: 2.50 ppm (^{1}H), 39.51 ppm (^{13}C). Acetone-d_6: 2.05 ppm (^{1}H), 206.68 and 29.92 ppm (^{13}C). Toluene-d_8: 2.08, 6.97, 7.01 and 7.09 ppm (^{1}H). Methanol-d_4: 3.31 ppm (^{1}H), 49.00 ppm (^{13}C).

For some compounds ^{1}H and ^{13}C shift were assigned using DEPT135, COSY, HSQC og HMBC. Spectra are included in the appendix (6).

Mass spectra were obtained on a Bruker Daltonik GmbH MAXIS II ETD (ESI) and SCION-TQ (EI) spectrometer by Osamu Sekiguchi.

Single-crystal X-ray diffraction were performed by David Wragg or Carl-Henrik Görbitz on a Bruker D8 Venture diffractometer with Photon 100 CMOS detector.

All melting points are uncorrected and were measured by a Büchi B-545 melting point apparatus.

Nitrogen gas was used to performed reactions under inert atmosphere, and the glass wear used in the reactions were oven dried at 110 °C for at least two hours.

5.1 Preparation of reagents and starting material

In this section, chlorination of indoles and 7-azaindoles, reduction of 5-aminoindole and preparation of diazo transfer reagents are described. All compounds were prepared according to reported literature procedures. In some cases, modifications of the procedures were done and are stated in the actual procedure. In the cases were new, non-reported compounds were prepared, full characterization was performed and 2D-NMR spectra can be found in the appendix (6).

5.1.1 Preparation of sulfonyl azides

Nosyl azide and tosyl azide was prepared according to literature [212] in order to perform diazotransfer in the synthesis of diethyl diazomethylphosphonate (**27**)

5.1.1.1 Para-nitrobenzenesulfonyl azide (30)

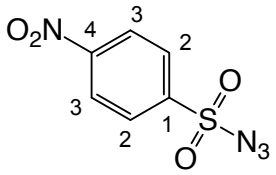

To a 100 mL erlenmeyer flask para-nitrobenzenesulfonylchloride **28** (1.99 g, 9.0 mmol 1.0 equiv.) was added and dissolved in 25 mL acetone. To another erlenmeyer flask sodium azide (NaN_3) (653.8 mg, 10.1 mmol, 1.1 equiv.) was added, dissolved in 7 mL H_2O (type 2) and diluted with 5 mL acetone. The solutions were then combined and stirred at room temperature for 2 hours and concentrated *in vacuo*. The crude mixture was then dissolved in 75 mL H_2O, transferred to a separatory funnel and extracted with EtOAc (1 x 50 mL, then 2 x 20 mL). The organic layer was dried with $MgSO_4$, filtered and concentrated *in vacuo* to afford 1.7 g of **30** as a pale yellow powder in 83 % yield.

^{1}H NMR (400 MHz, $CDCl_3$) δ 8.44 (d, J = 8.9 Hz, 2H, H-3), 8.15 (d, J = 8.9 Hz, 2H, H-2).

^{13}C NMR (101 MHz, $CDCl_3$) δ 151.18 (C-4), 143.70 (C-1), 128.87 (C-2), 124.91 (C-3).

MS (ESI): m/z (relative intensity (%)): 250.985 (M^+ + Na, 30).

Melting point: 100–102 °C Literature: 100–101 °C [226].

The spectroscopic data was in accordance with reported literature data [227]

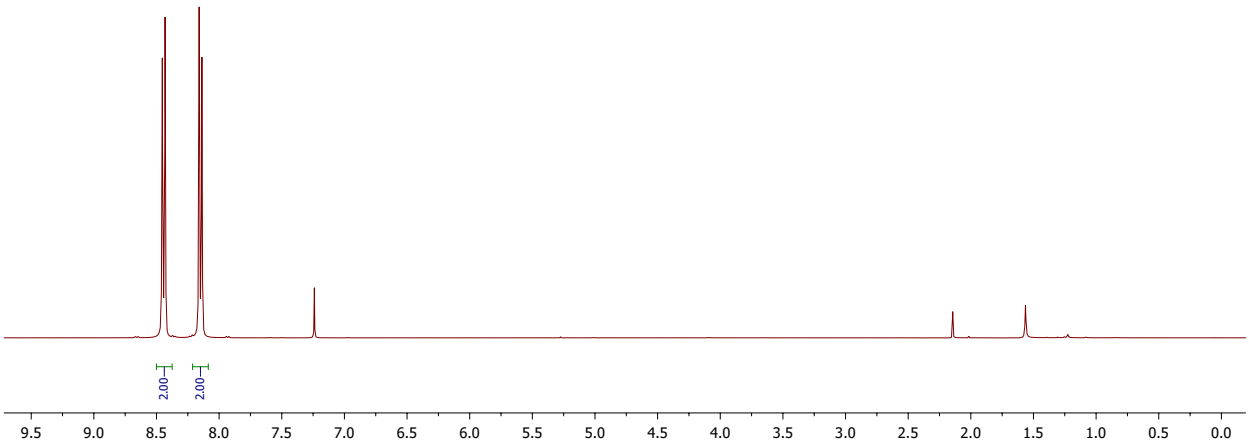

Figure 5.1: ^{1}H NMR spectrum of para-nitrobenzenesulfonyl azide (**30**) (400 MHz, $CDCl_3$).

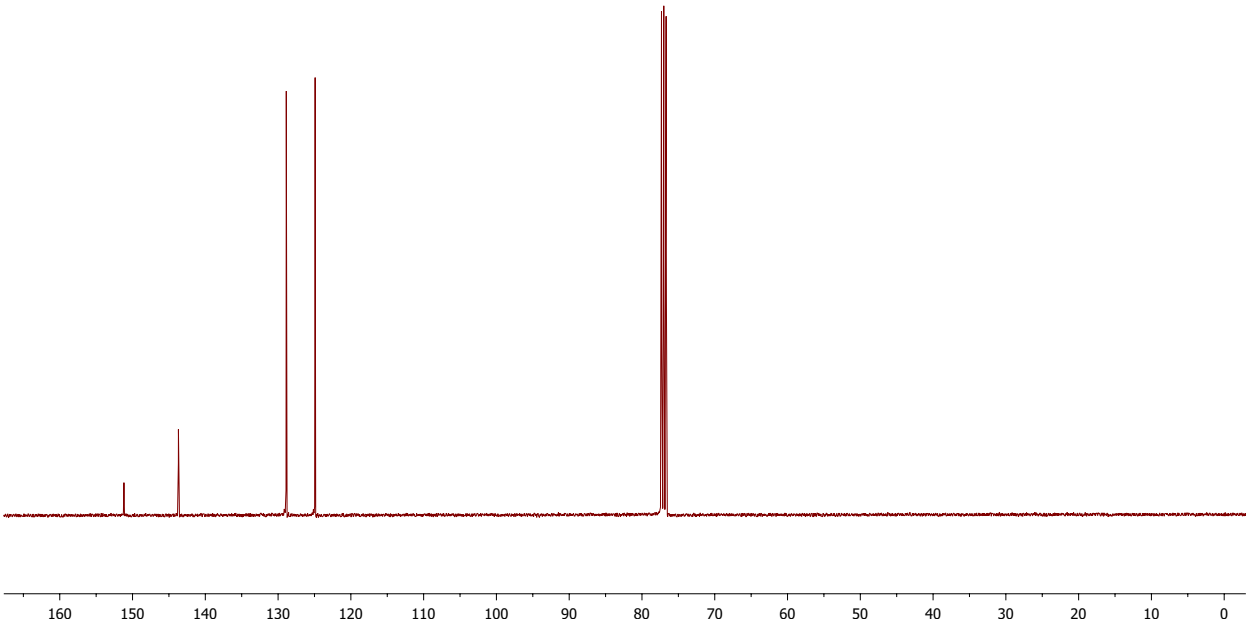

Figure 5.2: ^{13}C NMR spectrum of of para-nitrobenzenesulfonyl azide (**30**) (101 MHz, $CDCl_3$).

5.1.1.2 Para-toluenesulfonyl azide (31)

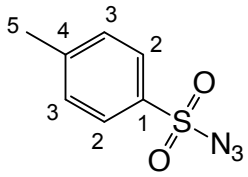

To a 500 mL round-bottom flask para-toluenesulfonylchloride **29** (25.00 g, 131 mmol 1.0 equiv.) was added and dissolved in 120 mL acetone. To another flask sodium azide (NaN_3) (9.38 g, 144 mmol, 1.1 equiv.) was added, dissolved in 45 mL H_2O (type 2) and diluted with 20 mL acetone. The solutions were then combined (in the 500 mL flask) and stirred at room temperature for 2 hours. The resulting pale yellow/orange solution was concentrated *in vacuo*, then transferred to a separatory funnel containing > 50 mL water. The organic layer was washed with water 2 x 10-20 mL, dried with Na_2SO_4, filtered and concentrated *in vacuo* to afford 23.62 g of **31** as a colorless oil in 91 % yield. The oil was stored in the fridge where it crystallizes.

^{1}H NMR (400 MHz, $CDCl_3$) δ 7.81 (d, J = 8.3 Hz, 2H, H-2), 7.38 (d, J = 8.1 Hz, 2H, H-3), 2.45 (s, 3H, H-4).

^{13}C NMR (101 MHz, $CDCl_3$) δ 146.17 (C-1), 135.39 (C-4), 130.21 (C-2), 127.43 (C-3), 21.66 (C-4).

MS (ESI): m/z (relative intensity (%)): 220.015 (M^+ + Na, 100).

The spectroscopic data was in accordance with reported literature data [212].

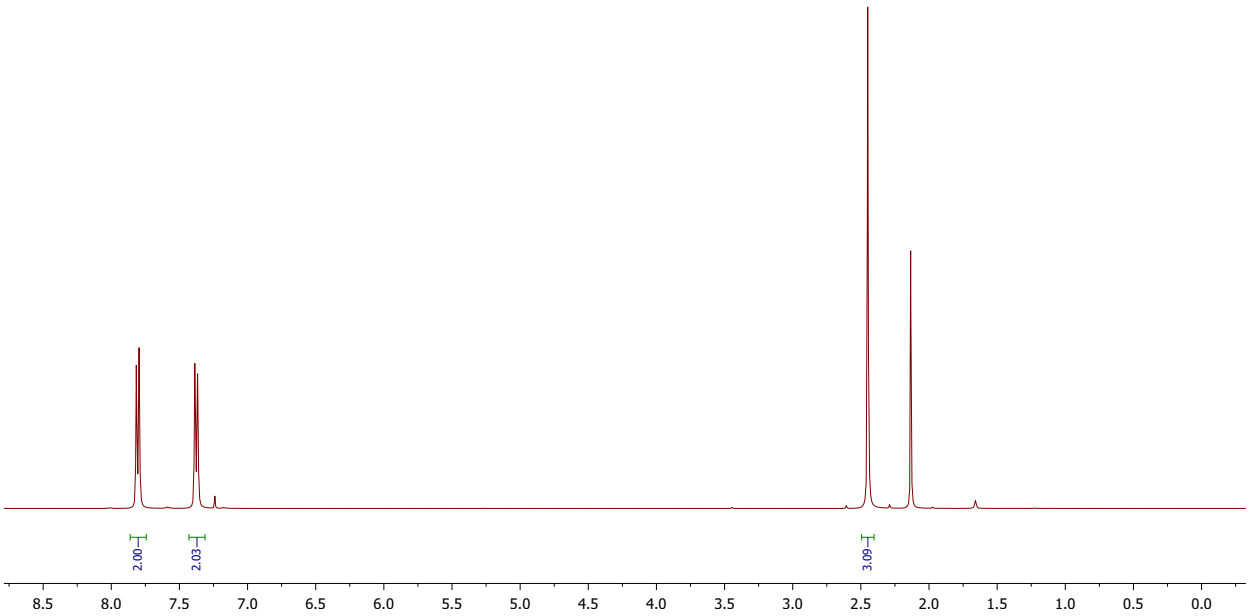

Figure 5.3: ^{1}H NMR spectrum of para-toluenesulfonyl azide (**31**) (400 MHz, $CDCl_3$).

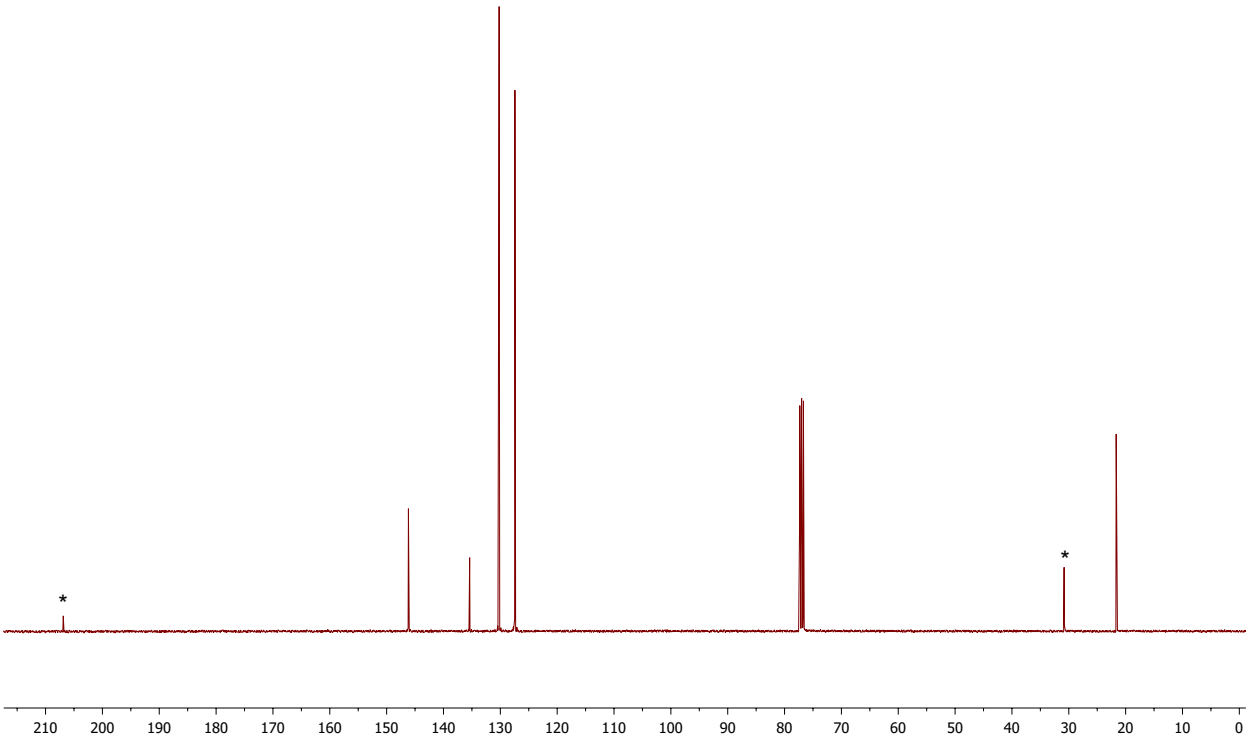

Figure 5.4: ^{13}C NMR spectrum of of para-toluenesulfonyl azide (**31**) (101 MHz, $CDCl_3$). * belongs to acetone.

5.1.2 Chlorination of indole- and 7-azaindole derivatives

Indole, 5,6-difluoroindole and 6-fluoro-7-azaindole and 6-methyl-7-azaindole was chlorinated prior to cyclopropanation-ring expansion with halodiazoacetates and halodiazophophonates. The 3-chloroindole derivatives was prepared according to literature [206] with slight modifications.

In the chlorination of 7-azaindoles byproducts were observed. Small amounts were quickly isolated as it was interesting to determine their structure, but as they were of no particular importance and was not further used, yields were not calculated.

5.1.2.1 3-chloroindole (45)

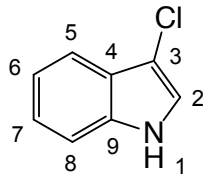

In a 100 mL round-bottom flask indole **38** (1.17 g, 10.0 mmol, 1.0 equiv.) was added and dissolved in 35 mL dry DMF. NCS (1.15 g, 11.1 mmol., 1.1 equiv.) was added, the flask was covered in aluminium foil and the solution was stirred at room temperature over night (ca. 22 hours). The resulting yellow solution was then transferred to a separatory funnel, 60 mL EtOAc was added and DMF was removed by extracting with H_2O (2 x 150 mL, 1 x 50 mL and 7 x 20 mL) and sat. NaCl (5 x 30 mL). The organic phase was collected and dried with $MgSO_4$, filtered and concentrated *in vacuo*. The extraction was repeated (mixture diluted in 20 mL EtOAC and extracted with 5 x 5-10 mL sat. NaCl) since ^{1}H NMR showed traces of DMF. The resulting red-brown mixture was then dissolved in few mL acetone and triturated with hexane. The black precipitate was filtered by vacuum filtration and the filtrate was concentrated *in vacuo*. The trituration was repeated one more time and the pink mixture was purified using column chromatography (SiO_2, EtOAc:Hex 1:4) which afforded 869 mg of **45** as pale yellow-green crystals in 57% yield.

^{1}H NMR (400 MHz, DMSO-*d*$_6$) δ 11.35 (br s, 1H, H-1), 7.51 (d, J = 2.7 Hz, 1H, H-2), 7.48 (dd, J = 7.8, 0.1 Hz, 1H, H-5), 7.42 (d, J = 8.2 Hz, 1H, H-8), 7.18 (ddd, J = 8.3, 7.0, 1.3 Hz, 1H, H-7), 7.11 (ddd, J = 8.1, 7.0, 1.1 Hz, 1H, H-6).

^{13}C NMR (101 MHz, DMSO-*d*$_6$) δ 134.90 (C-9), 124.51 (C-4), 122.36 (C-2), 122.18 (C-7), 119.68 (C-6), 117.01 (C-5), 112.15 (C-8), 103.09 (C-3).

HR-MS (ESI) m/z [M^+ - H]: Calculated for C_8H_5ClN: 150.0115/152.0086.
Found: 150.0110/152.0081 (0.4 ppm).

Melting point: 91–93 °C. Literature: 94–95 °C [228].

This compound has been reported in literature [228].

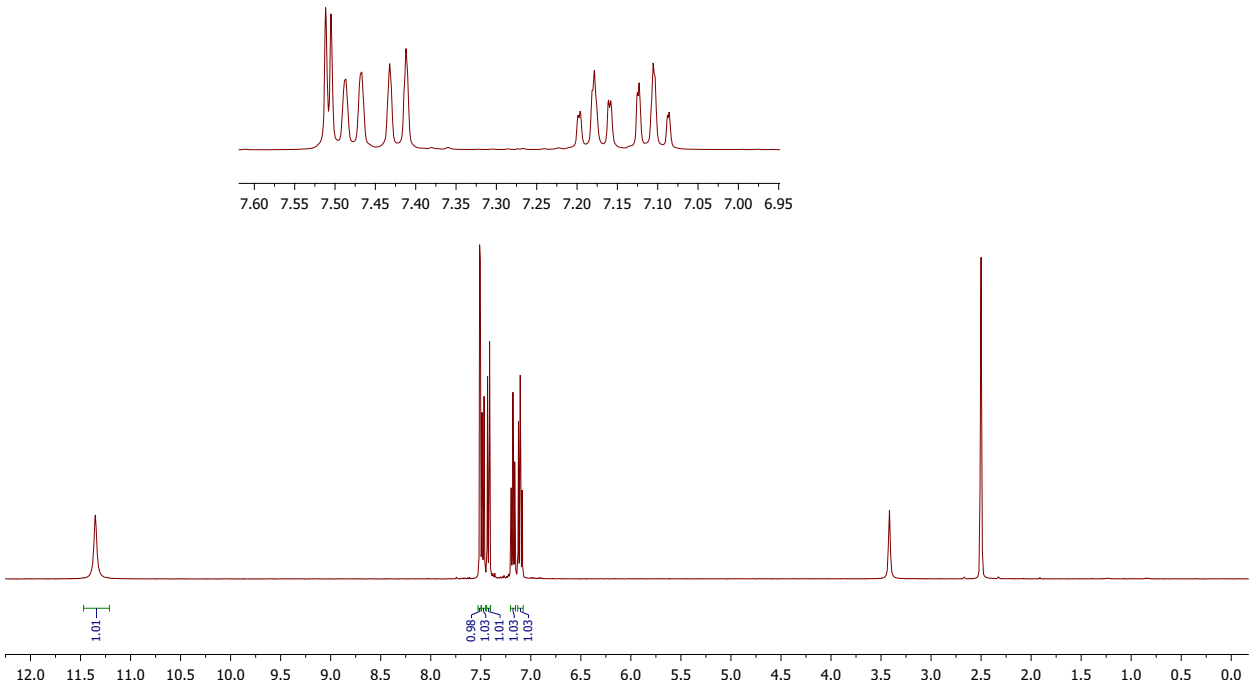

Figure 5.5: ^{1}H NMR spectrum of 3-chloroindole (**45**) (400 MHz, DMSO-d_6).

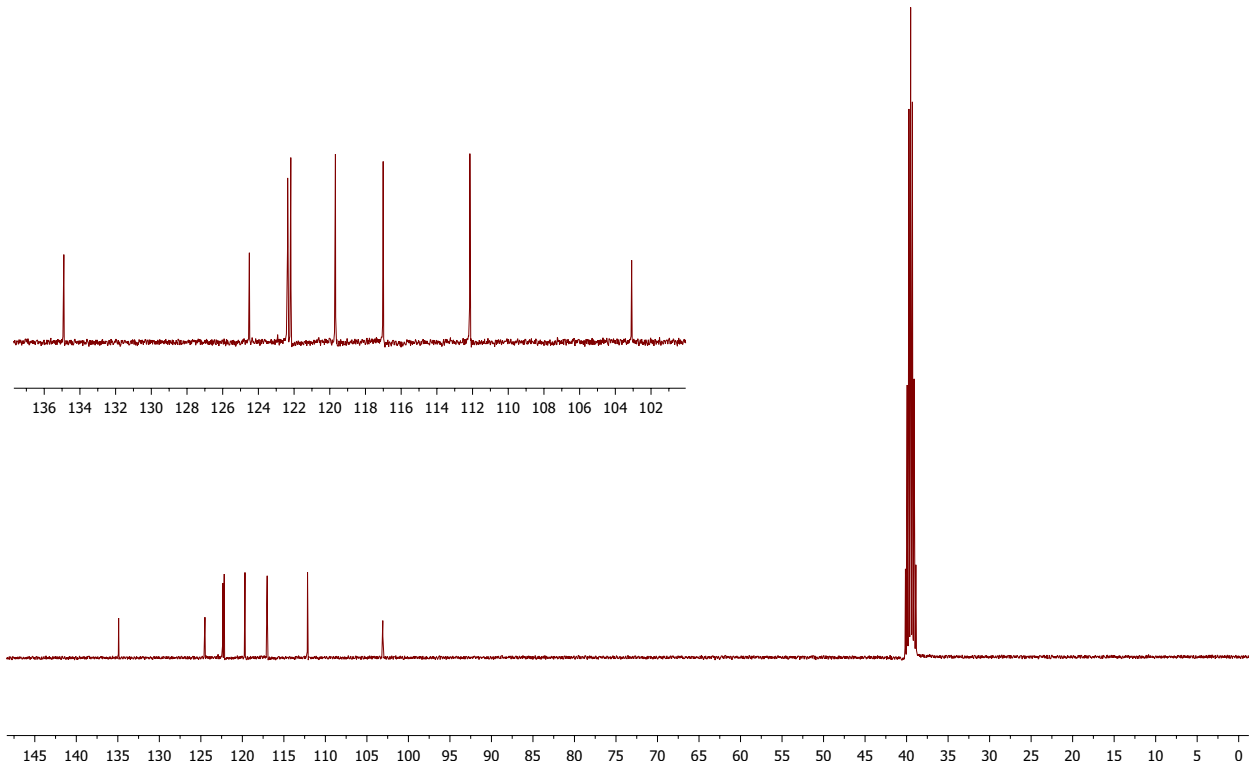

Figure 5.6: ^{13}C NMR spectrum of 3-chloroindole (**45**) (101 MHz, DMSO-d_6).

5.1.2.2 3-chloro-5,6-difluoroindole (46)

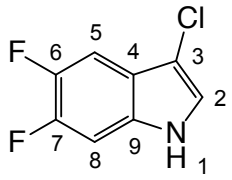

In a 100 mL round-bottom flask 5,6-difluoroindole **42** (1.53 g, 10.0 mmol, 1.0 equiv.) was added and dissolved in 35 mL dry DMF. NCS (1.47 g, 11.0 mmol., 1.1 equiv.) was added, the flask was covered in aluminium foil and the solution was stirred at room temperature over night. The resulting yellow solution was then transferred to a separatory funnel, 40 mL sat. NaCl was added, then EtOAc (2 x 35 mL) was added. The organic phase was washed with H_2O (40 mL), then sat. NaCl (5 x 10 mL) The organic phase was collected and dried with Na_2SO_4, filtered and concentrated *in vacuo*. The washing was repeated one more time, then the mixture was purified using column chromatography (SiO_2, EtOAc:Hex 1:5) which afforded 1.29 g of **46** as a pale purple-grey powder in 68% yield.

^{1}H NMR (400 MHz, $CDCl_3$) δ 8.03 (br s, 1H, H-1), 7.34 (dd, J = 10.2, 7.6 Hz, 1H, H-5), 7.17 (d, J = 2.6 Hz, 1H, H-2), 7.13 (dd, J = 10.3, 6.4 Hz, 1H, H-8).

^{13}C NMR (101 MHz, $CDCl_3$) δ 148.75 (dd, J = 243.9, 16.1 Hz, C-6), 147.05 (dd, J = 241.1, 15.1 Hz, C-7), 129.79 (d, J = 10.4 Hz, C-9), 122.18 (d, J = 3.7 Hz, C-2), 120.89 (dd, J = 8.5, 1.4 Hz, C-4), 106.65 (dd, J = 4.5, 1.8 Hz, C-3), 105.10 (dd, J = 20.2, 1.4 Hz, C-5), 99.56 (d, J = 22.3 Hz, C-8).

^{19}F NMR (decoupled) (377 MHz, $CDCl_3$) δ -141.90 (d, J = 20.7 Hz, F-7), -145.67 (d, J = 20.5 Hz, F-6).

^{19}F NMR (coupled) (377 MHz, $CDCl_3$) δ -141.90 (ddd, J = 20.5, 10.3, 7.6 Hz, F-7), -145.67 (ddd, J = 20.5, 10.2, 6.6 Hz, F-6).

MS (EI): m/z (relative intensity (%)): 187/189 (100/33, M^+/M+2), 152 (31), 125 (54).

HR-MS (ESI) m/z [M^+ - H]: Calculated for $C_7H_3ClFN_2$: 168.9969/170.9939
Found: 168.9974/170.9944 (0.4 ppm).

Melting point: 85–86 °C.

This compound has not been reported in the literature.

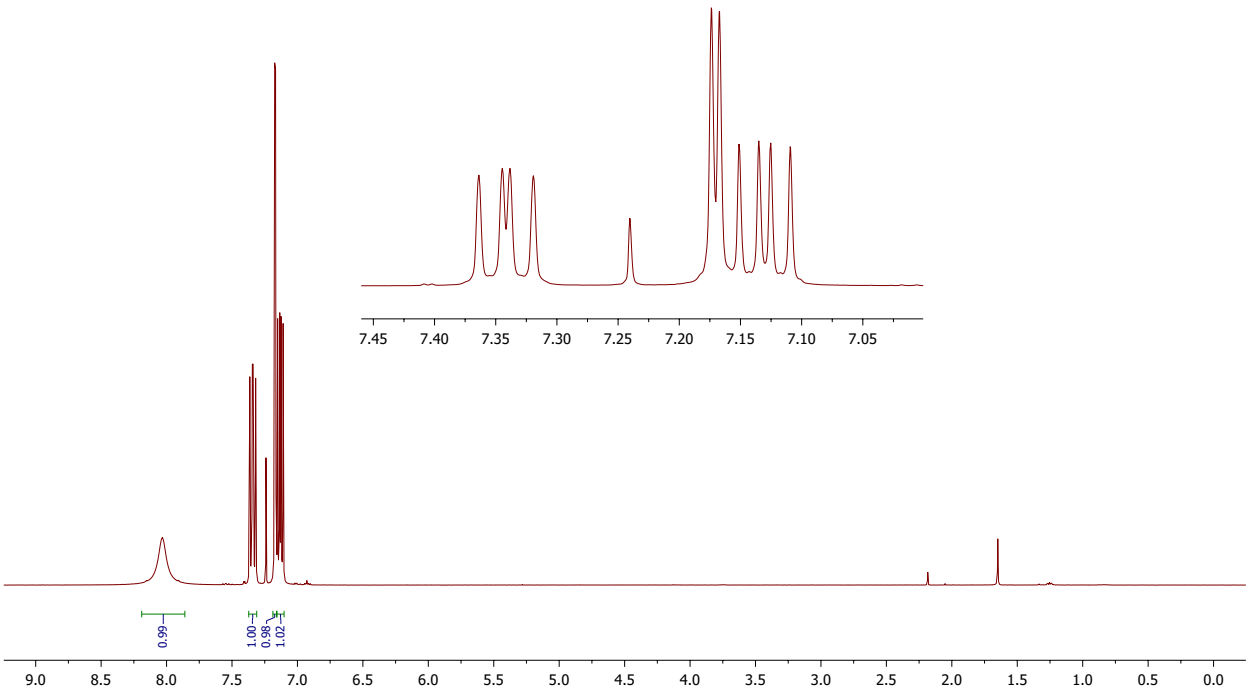

Figure 5.7: ^{1}H NMR spectrum of 3-chloro-5,6-difluoroindole (**46**) (400 MHz, $CDCl_3$).

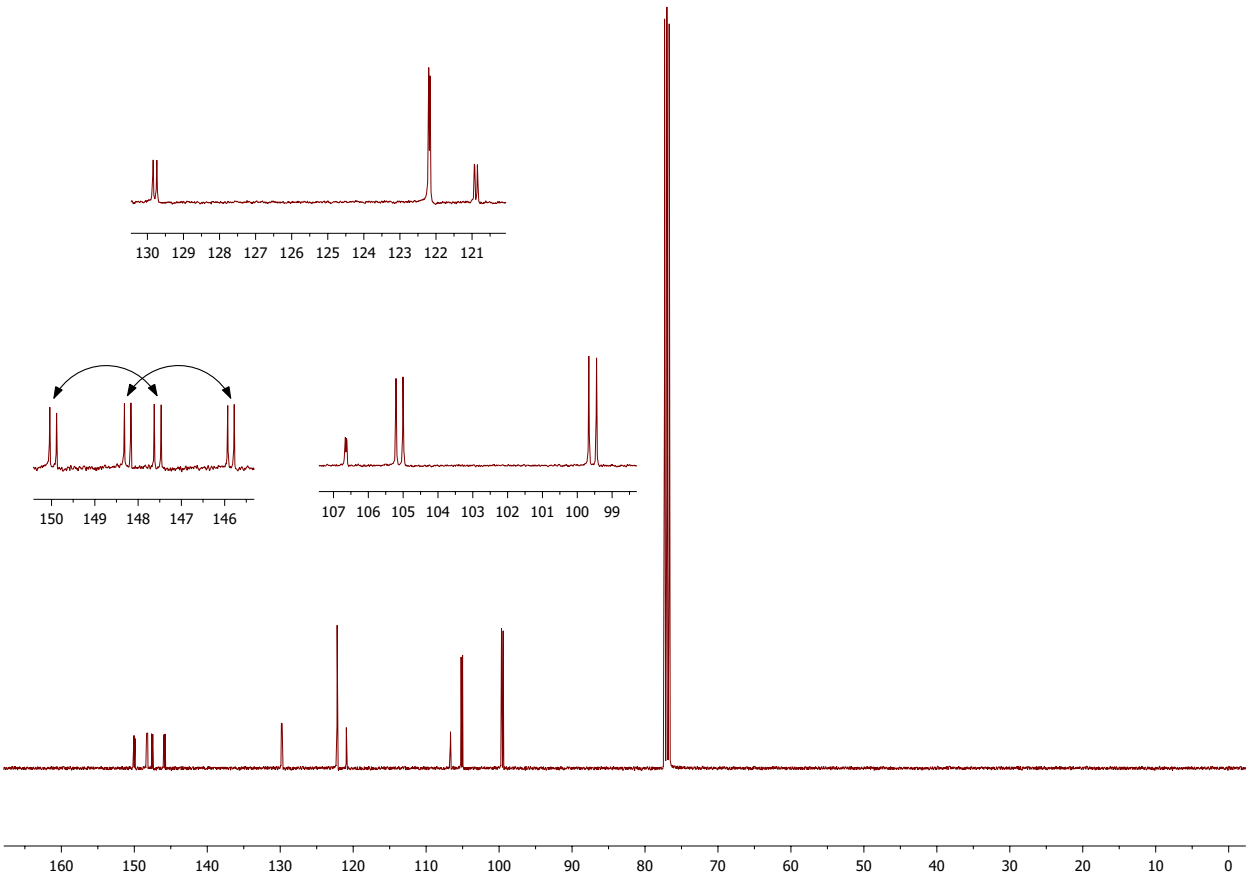

Figure 5.8: ^{13}C NMR spectrum of 3-chloro-5,6-difluoroindole (**46**) (101 MHz, $CDCl_3$). The arrows indicate which peaks correspond to one signal.

5.1.2.3 3-chloro-6-fluoro-7-azaindole (18)

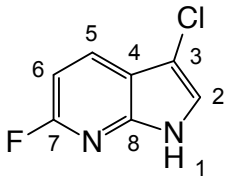

In a 100 mL round-bottom flask 6-fluoro-7-azaindole (1.00 g, 7.35 mmol, 1.0 equiv.) was added and dissolved in 40 mL dry dichloromethane (DCM). NCS (1.03 g, 7.72 mmol, 1.05 equiv.) was added, the flask was covered in aluminum foil and stirred at room temperature for 30 hours. A white, very fine-powdered precipitate was obtained and filtration was attempted, but too much product was lost during filtration (the powder was too light/fine). Instead, the DCM was removed *in vacuo*, the solid was dissolved in a minimal amount of acetone and approximately 4.0 g silica was added to the solution. The acetone was removed under reduced pressure (150 mbar) to avoid shock boiling of the silica. The product-silica mixture was then dry loaded[1] on a column (SiO_2, EtOAc:Hexane 1:2) and purification afforded 973 mg of **18** as an off-white powder in 78% yield.

^{1}H NMR (400 MHz, DMSO-*d*$_6$) δ 12.11 (br s, 1H, H-1), 8.08 (t, J = 8.1 Hz, 1H, H-5), 7.64 (d, J = 2.4 Hz, 1H, H-2), 6.93 (dd, J = 8.5, 1.0 Hz, 1H, H-6).

^{13}C NMR (101 MHz, DMSO-*d*$_6$) δ 159.79 (d, J = 234.3 Hz, C-7), 143.03 (d, J = 19.4 Hz, C-8), 131.21 (d, J = 9.8 Hz, C-5), 122.83 (d, J = 4.1 Hz, C-2), 115.23 (d, J = 2.6 Hz, C-4), 102.46 (C-3), 101.86 (d, J = 39.5 Hz, C-6).

^{19}F NMR (377 MHz, DMSO-*d*$_6$) δ -74.37

MS (EI): m/z (relative intensity (%)): 170/172 (100/33, M^+/M+2), 143 (31), 108 (49).

HR-MS (ESI) m/z [M^+ - H]: Calculated for $C_7H_3ClFN_2$: 168.9969/170.9939
Found: 168.9974/170.9944 (0.4 ppm).

Melting point: 90 °C (subl.).

This compound has not been reported in the literature.

[1] Wet loading had been attempted without success

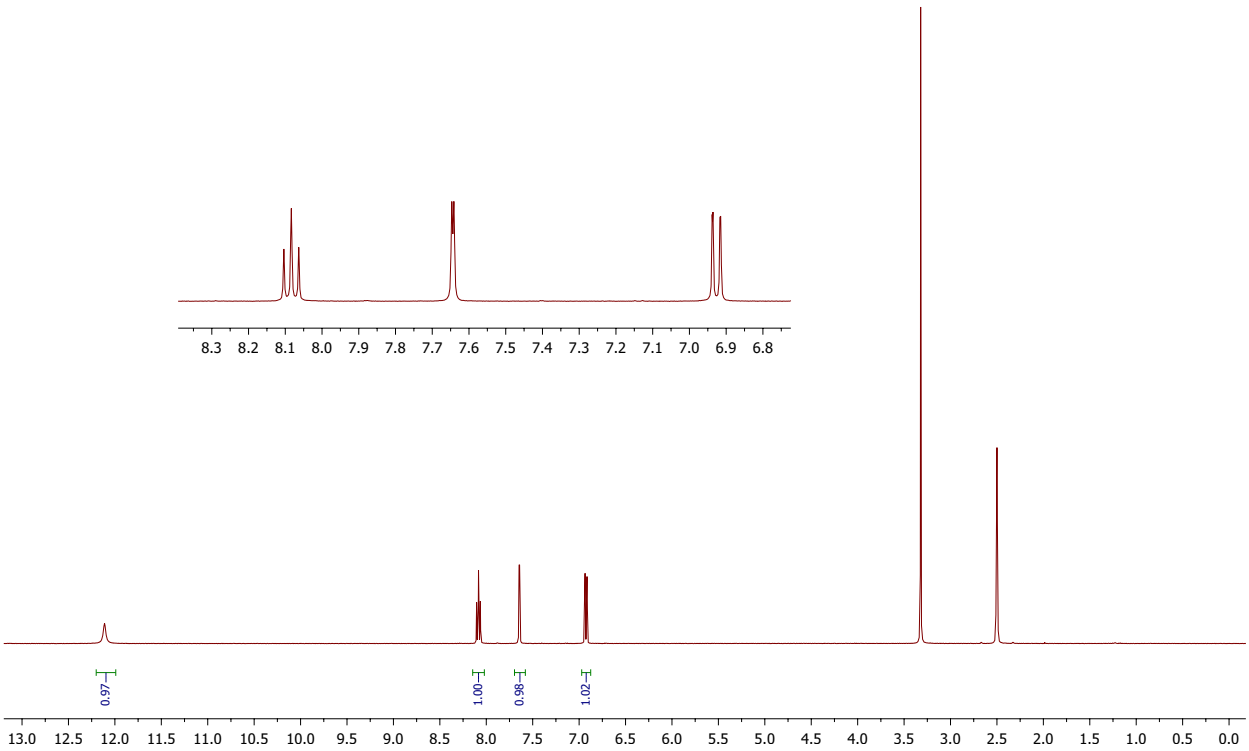

Figure 5.9: ^{1}H NMR spectrum of 3-chloro-6-fluoro-7-azaindole (**18**) (400 MHz, DMSO-d_6).

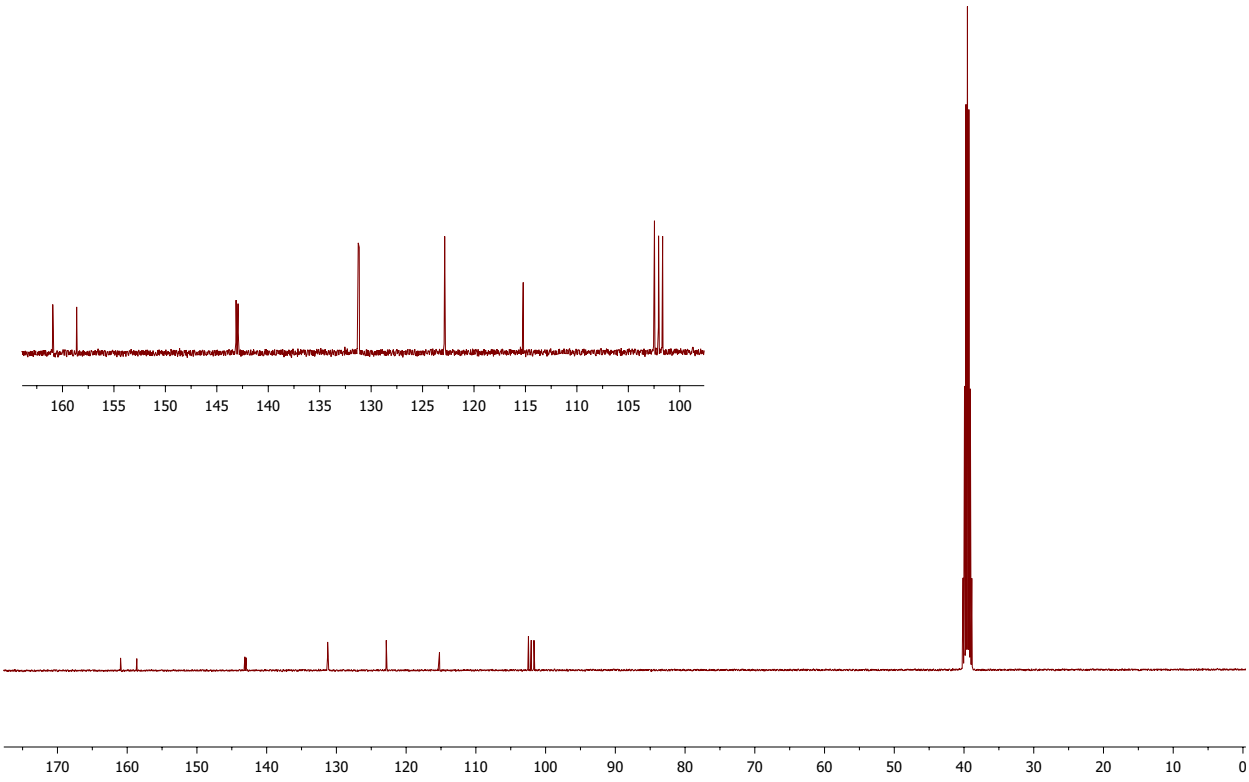

Figure 5.10: ^{13}C NMR spectrum of 3-chloro-6-fluoro-7-azaindole (**18**) (400 MHz, DMSO-d_6).

5.1.2.4 2,3-dichloro-6-fluoro-7-azaindole (19)

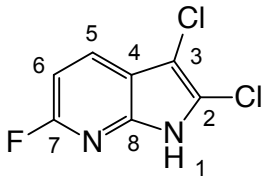

In a 100 mL round-bottom flask 6-fluoro-7-azaindole (1.00 g, 7.35 mmol, 1.0 equiv.) was added and dissolved in 40 mL dry DMF. NCS (2.17 g, 16.72 mmol, 2.2 equiv.) was added, the flask was covered in aluminum foil and stirred at room temperature over night. DMF was removed *in vacuo*, the crude mixture was triturated with chloroform and the precipitate was filtered by vacuum filtration. A pale, pink very fine powder of **19** was afforded. Yield was not calculated as much of the product was lost during the filtration and was not to be used any further.

^{1}H NMR (400 MHz, acetone-*d*$_6$) δ 11.83 (br s, 1H, H-1), 8.06 (dd, J = 8.5, 7.5 Hz, 1H, H-5), 6.95 (dd, J = 8.5, 1.0 Hz, 1H, H-6).

^{13}C NMR (101 MHz, acetone-*d*$_6$) δ 161.67 (d, J = 236.6 Hz, C-7), 142.97 (d, J = 19.6 Hz, C-8), 131.70 (d, J = 9.7 Hz, C-5), 121.62 (d, J = 3.9 Hz, C-2), 116.85 (d, J = 3.0 Hz, C-4), 103.89 (d, J = 39.5 Hz, C-6), 102.14 (C-3).

^{19}F NMR (377 MHz, acetone-*d*$_6$) δ -74.78.

MS (EI): m/z (relative intensity (%)): 204/206/208 (100/63/11, M^+/M+2/M+4)

HR-MS (ESI) m/z [M^+ - H]: Calculated for $C_7H_2Cl_2FN_2$: 202.9579/204.9550/206.9520
Found: 202.9584/204.9554/206.9525 (0.3 ppm).

Melting point: 109 °C (subl.).

This compound has not been reported in the literature.

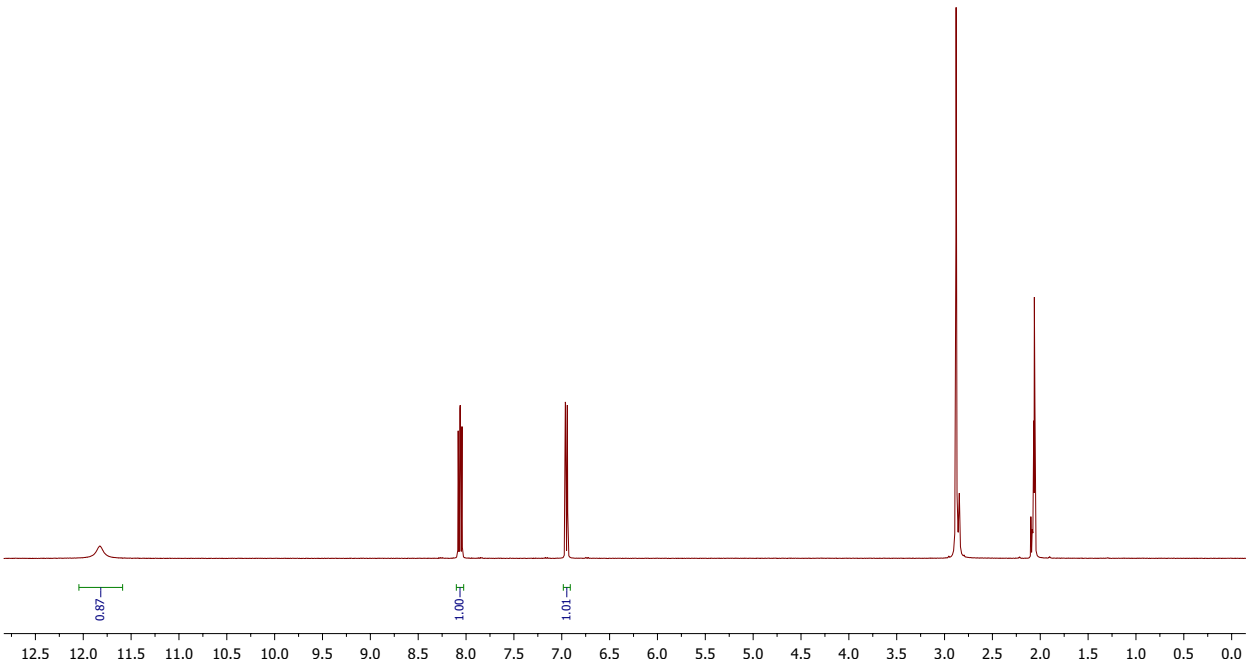

Figure 5.11: ^{1}H NMR spectrum of 2,3-dichloro-6-fluoro-7-azaindole (**19**) (400 MHz, acetone-d_6).

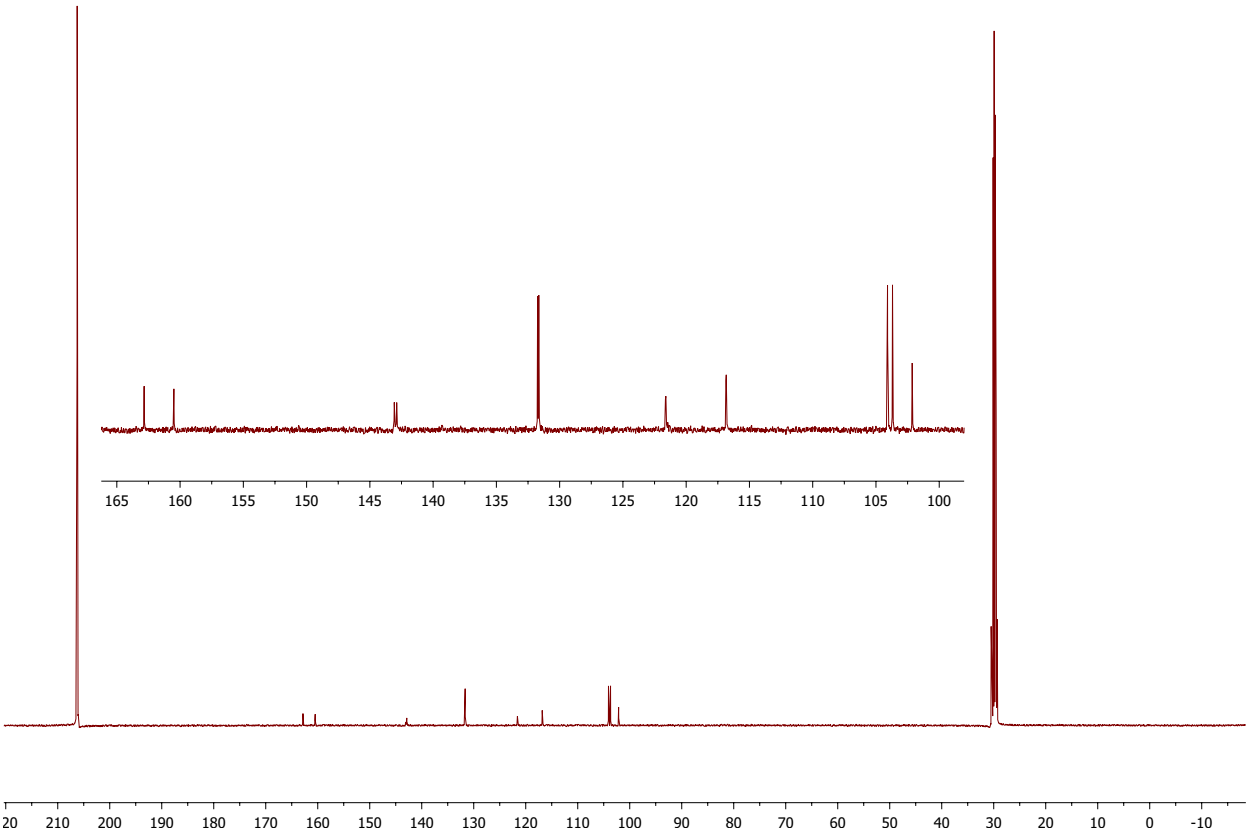

Figure 5.12: ^{13}C NMR spectrum of 2,3-dichloro-6-fluoro-7-azaindole (**19**) (400 MHz, acetone-d_6).

5.1.2.5 3-chloro-6-methyl-7-azaindole (20)

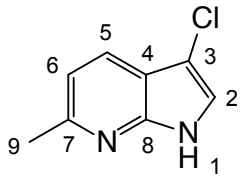

In a 50 mL round-bottom flask 6-methyl-7-azaindole (500 mg, 3.78 mmol 1.0 eqiuiv) was dissolved in 20 mL dry dichloromethane. NCS (350 mg 3.97 mmol 1.05 equiv) was added, the flask was covered with aluminum foil and the mixture was refluxed at 43 0 °C for 8.5 h. The solution was allowed to cool before it was concentrated *in vacuo*. The crude was dissolved in 40 mL EtOAc and washed with saturated $NaHCO_3$ (1 x 20 mL then 3 x 10 mL). The organic phase was dried with $MgSO_4$, filtered and concentrated *in vacuo*. The product mixture was purified using column chromatography (SiO_2, EtOAC:Hexane 1:1) which afforded 470 mg of **20** as a white powder[2] in 75 % yield.

^{1}H NMR (400 MHz, DMSO-*d*$_6$) δ 11.78 (br s, 1H, H-1) 7.79 (d, J = 8.0 Hz, 1H, H-5), 7.56 (d, J = 2.6 Hz, 1H, H-2), 7.04 (d, J = 8.0 Hz, 1H, H-6), 2.53 (s, 3H, H-9).

^{13}C NMR (101 MHz, DMSO-*d*$_6$) δ 152.42 (C-7), 146.39 (C-8), 125.90 (C-5), 121.92 (C-2), 116.09 (C-6), 114.69 (C-4), 101.64 (C-3), 23.97 (C-9).

MS (EI): m/z (relative intensity (%)): 166/168 (100/33, M^+/M+2), 131 (71), 104 (34).

HR-MS (ESI) m/z $[M + H]^+$: Calculated for $C_8H_8ClN_2$: 167.0376/169.0347
Found: 167.0371/169.0341 (0.0 ppm).

Melting point: 106 °C (subl.).

This compound has not been reported in the literature.

[2] Slight color variations may occur as the same procedure afforded a slightly more yellow powder in another experiment

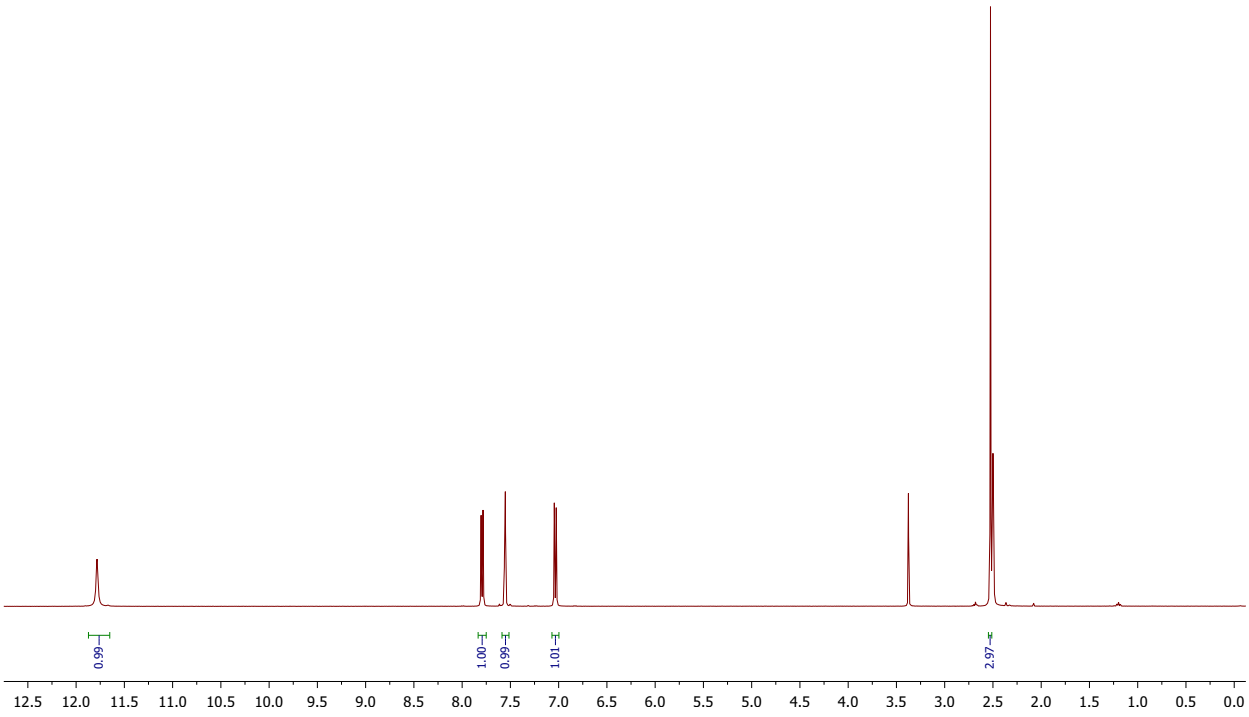

Figure 5.13: ^{1}H NMR spectrum of 3-chloro-6-methyl-7-azaindole (**20**) (400 MHz, DMSO-d_6).

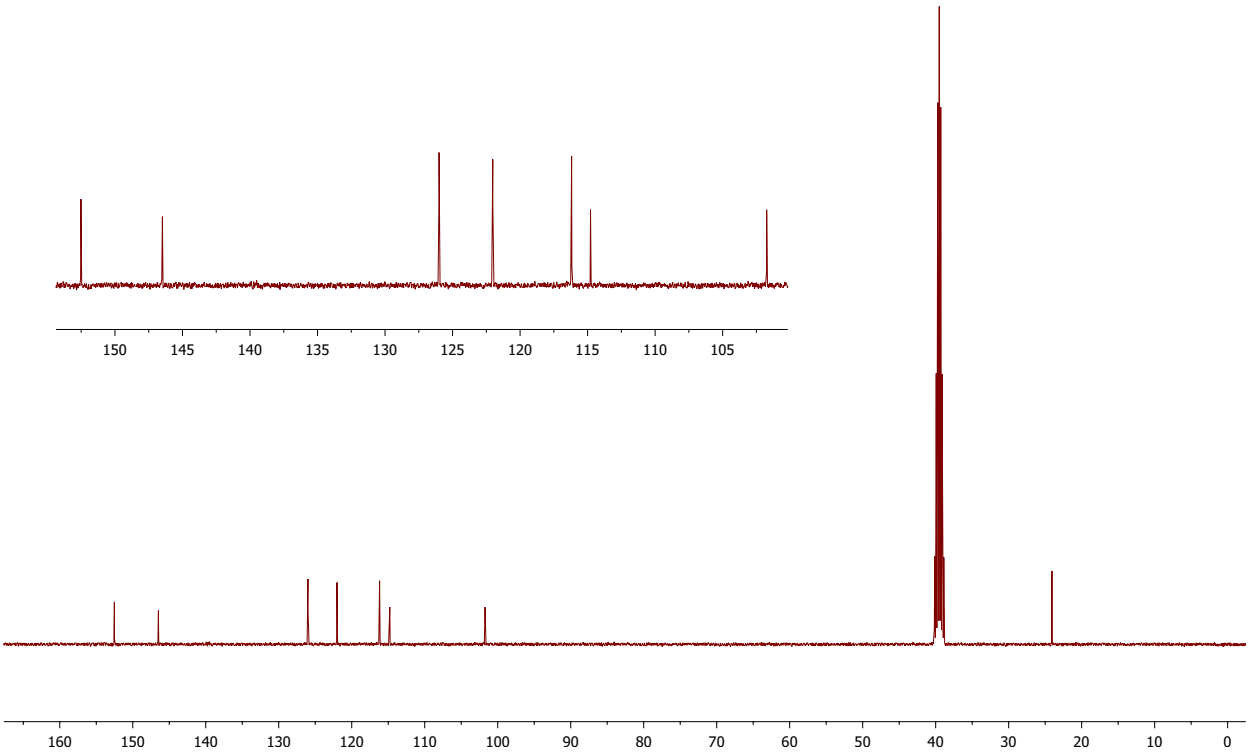

Figure 5.14: ^{13}C NMR spectrum of 3-chloro-6-methyl-7-azaindole (**20**) (400 MHz, DMSO-d_6).

5.1.2.6 2,3-dichloro-6-methyl-7-azaindole (21)

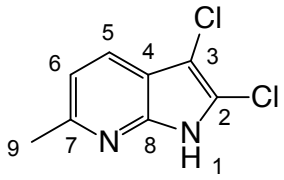

See procedure 5.1.2.5. **21** was a byproduct in the reaction and isolated during column chromatography of **20**. No yield was calculated.

^{1}H NMR (400 MHz, acetone-*d*$_6$) δ 11.55 (bs, 1H, H-1), 7.77 (d, J = 8.1 Hz, 1H, H-5), 7.11 (d, J = 8.1 Hz, 1H, H-6), 2.55 (s, 3H, H-9).

^{13}C NMR (101 MHz, acetone-*d*$_6$) δ 154.02 (C-7), 145.57 (C-8), 125.96 (C-5), 120.60 (C-2), 117.41 (C-6), 115.94 (C-4), 100.80 (C-3), 23.84 (C-9).

MS (EI): m/z (relative intensity (%)): 200/202/204 (100/65/11, M^+/M+2/M+4), 165/167 (52/17)

HR-MS (ESI) m/z [M^+ + H]: Calculated for $C_8H_7Cl_2N_2$: 200.9986/202.9957/204.9927. Found: 200.9981/202.9957/204.9932 (-0.3 ppm).

Melting point: 92 °C (subl.).

This compound has not been reported in the literature.

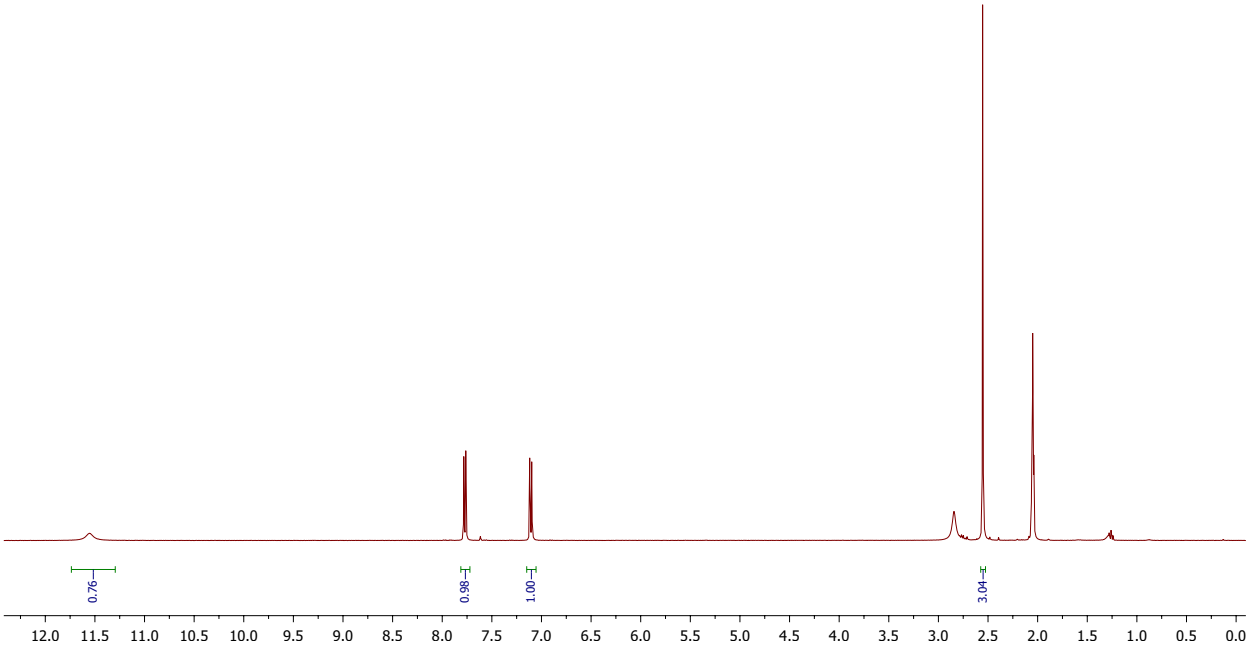

Figure 5.15: ^{1}H NMR spectrum of 2,3-dichloro-6-methyl-7-azaindole (**21**) (400 MHz, acetone-d_6).

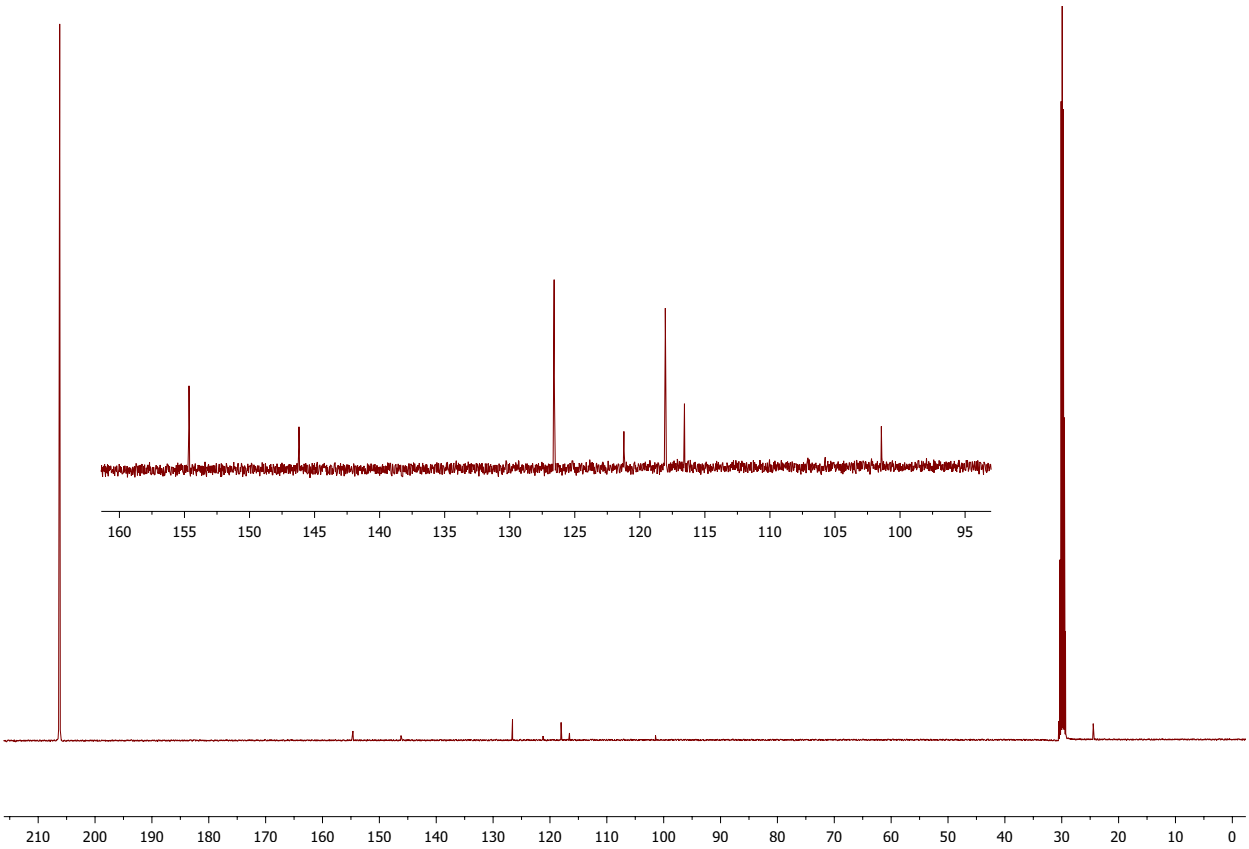

Figure 5.16: ^{13}C NMR spectrum of 2,3-dichloro-6-methyl-7-azaindole (**21**) (400 MHz, acetone-d_6).

5.1.3 Reduction of 5-nitroindole

5-nitroindole was reduced to 5-aminoindole prior to cyclopropanation and ring expansion with halodiazophophonates. 5-aminoindole was prepared according to literature [223].

5.1.3.1 5-aminoindole (47)

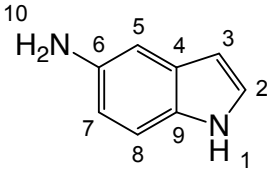

In a 250 mL two-neck round-bottom flask 5-nitroindole (1.00 g, 6.18 mmol, 1.0 equiv.) was added and dissolved in 27 mL EtOH. While stirred at room temperature, 25 mL 1M NaOH was added. The resulting deep red mixture was heated to 55 °C and sodium dithionite ($Na_2S_2O_4$) (5.37 g, 30.85 mmol, 5.0 equiv.) in 25 mL 1M NaOH was added dropwise via an addition funnel to the stirring solution over 15-20 min. The resulting yellow mixture was heated to 80 °C and refluxed for 24 hours. The resulting brown mixture was filtered hot, then allowed to (almost)[3] reach room temperature before it was concentrated *in vacuo*. The mixture was then transferred to a separatory funnel and extracted with Et_2O (3 x 20-50 mL), dried with $MgSO_4$, filtered and concentrated *in vacuo*. This afforded 510 mg of **47** as a brown solid in 62 % yield.

^{1}H NMR (300 MHz, $CDCl_3$) δ 7.93 (br s, 1H, H-1), 7.18 (dt, J = 8.5, 0.8 Hz, 1H, H-8), 7.11 (t, J = 2.8 Hz, 1H, H-2), 6.93 (dt, J = 2.3, 0.7 Hz, 1H, H-5), 6.65 (ddd, J = 8.5, 2.2, 0.5 Hz, 1H. H-7), 6.36 (ddd, J = 3.1, 2.0, 1.0 Hz, 1H, H-3), 3.49 (br s, 2H, H-10).

Melting point: 128–131 °C. Literature: 126–135 °C [223].

This compound has been reported in literature [229].

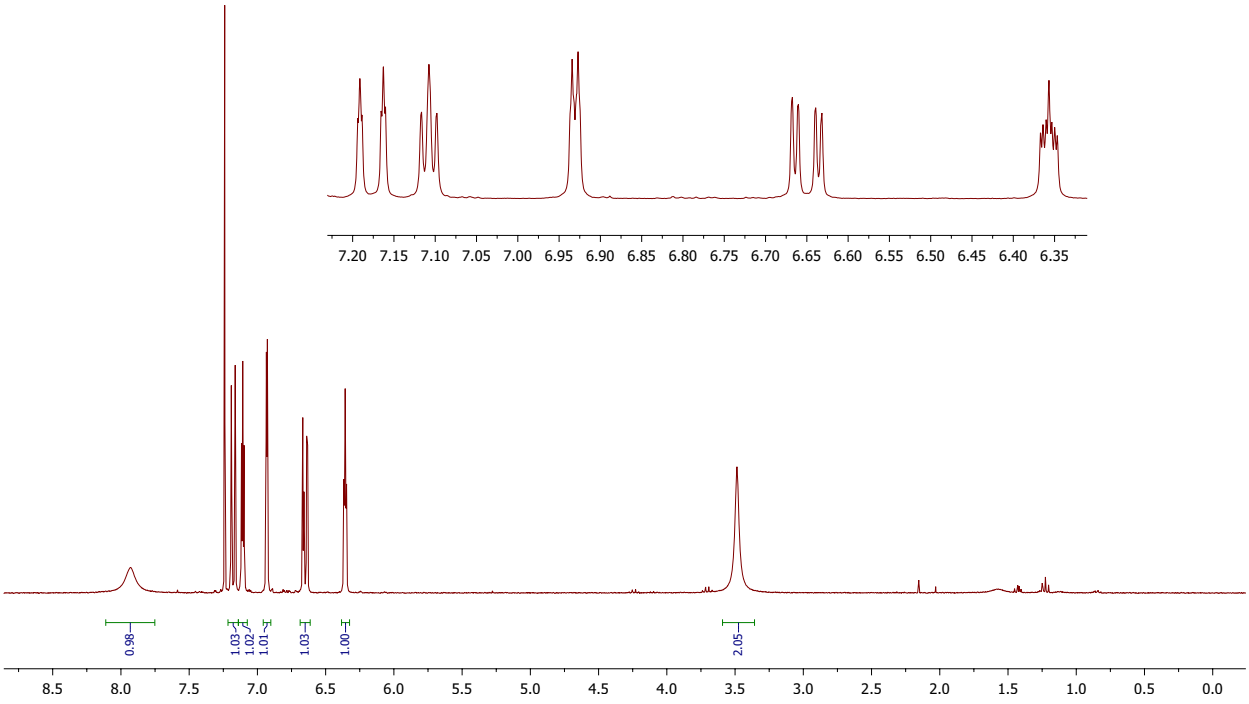

Figure 5.17: ^{1}H NMR spectrum of 5-aminoindole (**47**) (300 MHz, $CDCl_3$). Residual solvent peaks from EtOAc and Et_2O are present between 1.10 and 4.20 ppm.

[3] A considerable amount of the crude mixture was lost on the rotary evaporator due to shock boiling of a solution that was too hot

5.2 Halodiazoacetates and ethyl 8-azaquinoline-3-carboxylates

5.2.1 Ethyl halodiazoacetates

Preparation of Cl- and Br-EDA from EDA was performed according to the following general procedure 5.2.1.1, which is based on reported literature procedure [3]. In all experiments where X-EDA was employed as a reactant, the reactions were performed immediately after preparation due to their thermal instability. The X-EDAs were always kept in a cold (0 °C) solution and never evaporated to dryness. In procedures employing X-EDA, the amount of X-EDA (based on ^{1}H NMR yield measurements) as well as the volume of the solution will be stated.

5.2.1.1 General procedure for the preparation of ethyl halodiazoacetates (X-EDA)

EDA (114.10 mg, 1.0 mmol, 1.0 equiv.) was diluted with cold CH_2Cl_2 (10 mL). DBU (213.14 mg, 1.4 mmol, 1.4 equiv.) was added to the solution and stirring was continued for 5 min at 0 °C before NXS (1.1 mmol, 1.1 equiv. NCS, or NCS) of choice was added. There was an immediate color change from yellow to orange/red (shade dependent on the NXS). The solution was stirred for an additional 5 minutes at 0 °C, then filtered through a pre-cooled (0 °C) plug of silica gel, eluting with cold CH_2Cl_2. This afforded a dark yellow (X = Cl) or orange (X = Br) solution of X-EDA.

If CH_2Cl_2 was the solvent of choice for reactions employing X-EDA as a reactant, the volume of CH_2Cl_2 was reduced to 10 mL *in vacuo* at 0 °C. If another solvent was to be used, 10 mL of the solvent was added and CH_2Cl_2 was removed *in vacuo* at 0 °C.

5.2.1.2 Ethyl bromodiazoacetate (8)

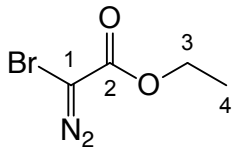

Compound **8** was prepared according to procedure 5.2.1.1.

EDA (30.0 mg, 0.23 mmol, 1.0 equiv.), DBU (54.2 mg, 0.34 mmol, 1.5 equiv.) and NBS (49.5 mg, 0.28 mmol, 1.2 equiv.), gave **8** as an orange solution in 95 % yield.

^{1}H NMR (300 MHz, benzene-d_6) δ 3.88 (q, J = 7.1 Hz, 2H, C-3), 0.87 (t, J = 7.1 Hz, 3H, C-4).

^{13}C NMR (75 MHz, benzene-d_6) δ 162.70 (C-2), 62.69 (C-3), 14.54 (C-4)

The spectroscopic data was in accordance with reported literature data [1].

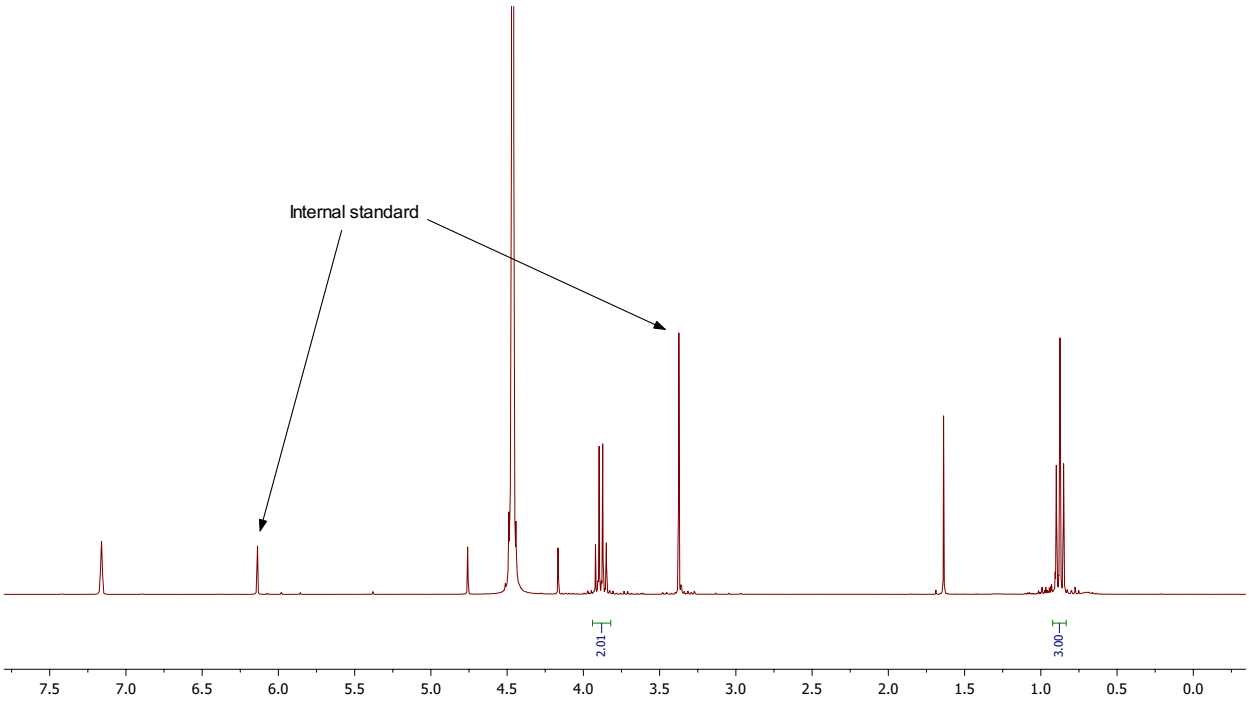

Figure 5.18: ^{1}H NMR spectrum of ethyl bromodiazoacetate (**8**) (300 MHz, benzene-d_6). The large peak close to 4.50 ppm belongs to DCM.

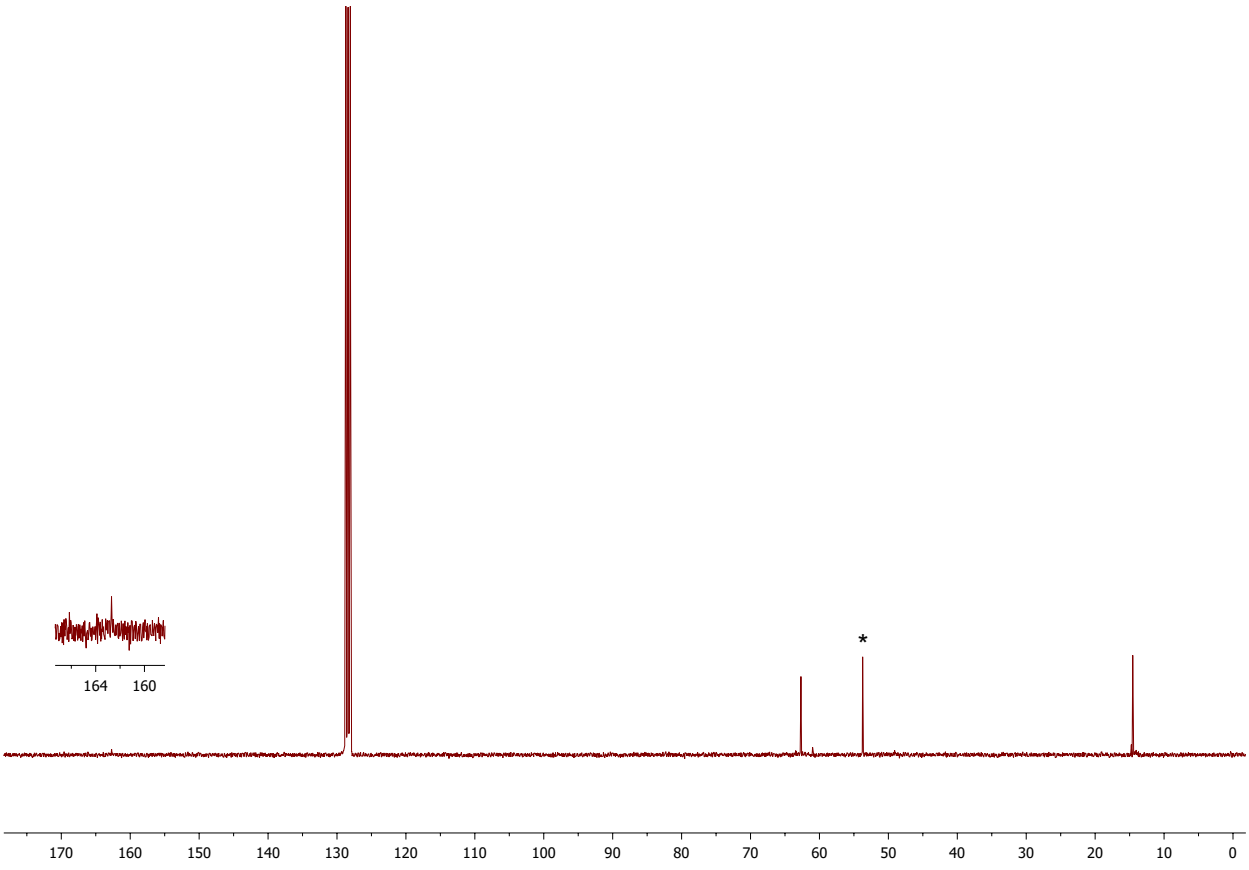

Figure 5.19: ^{13}C NMR spectrum of ethyl bromodiazoacetate (**8**) (75 MHz, benzene-d_6). * belongs to DCM.

5.2.1.3 Ethyl chlorodiazoacetate (9)

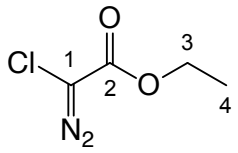

Compound **9** was prepared according to procedure 5.2.1.1.

EDA (54.6 mg, 0.48 mmol, 1.0 equiv.), DBU (110.7 mg, 0.73 mmol, 1.5 equiv.) and NCS (73.2 mg, 0.55 mmol, 1.1 equiv.), gave **9** as a yellow solution in 93 % yield.

^{1}H NMR (300 MHz, benzene-d_6) δ 3.87 (q, J = 7.1 Hz, 2H, H-3), 0.84 (t, J = 7.1 Hz, 3H, H-4).

^{13}C NMR (75 MHz, benzene-d_6) δ 162.62 (C-2), 62.56 (C-3), 14.55 (C-4).

The spectroscopic data was in accordance with reported literature data [1].

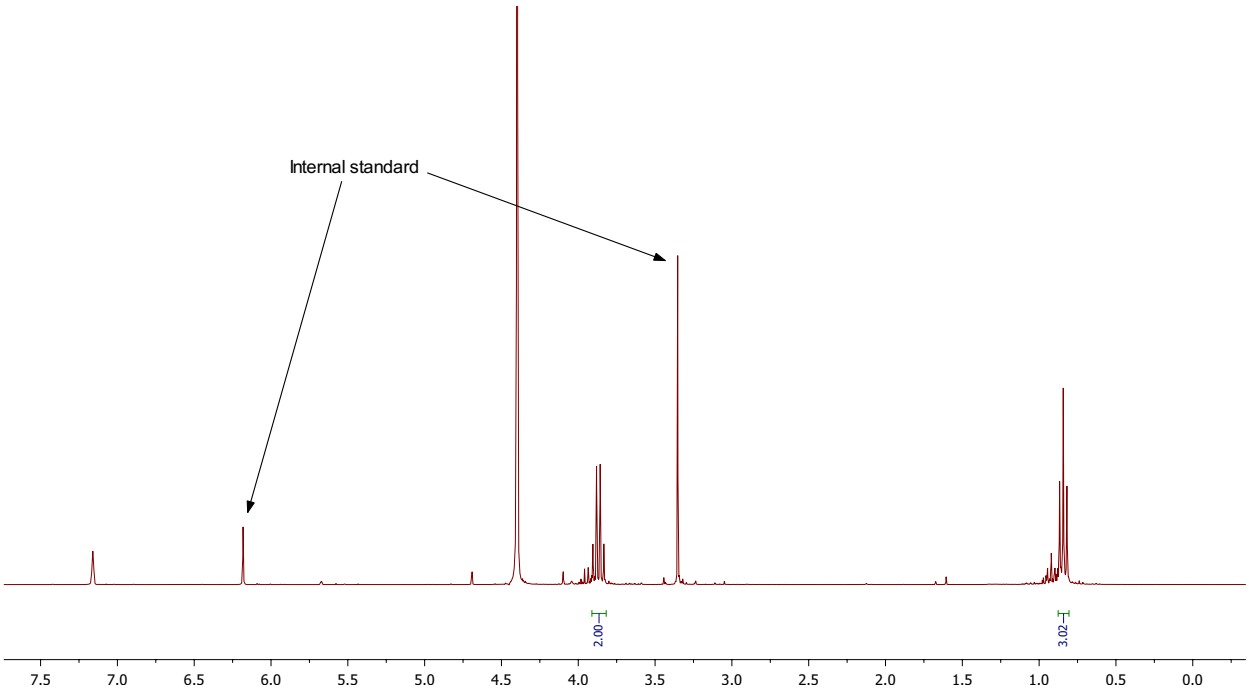

Figure 5.20: ^{1}H NMR spectrum of ethyl chlorodiazoacetate (**9**) (300 MHz, benzene-d_6). The large peak close to 4.50 ppm belongs to DCM.

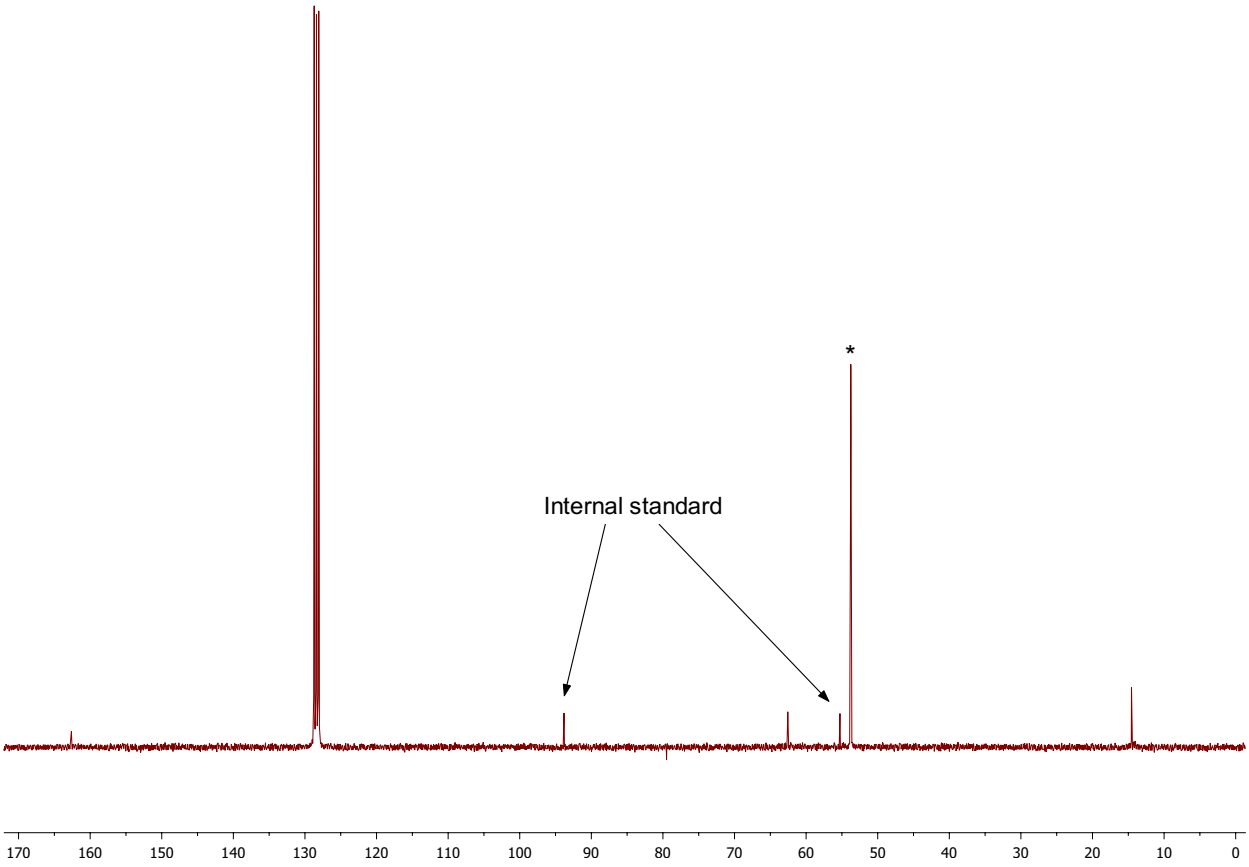

Figure 5.21: ^{13}C NMR spectrum of ethyl chlorodiazoacetate (**9**) (75 MHz, benzene-d_6). * belongs to DCM.

5.2.2 Synthesis of ethyl 8-azaquinoline-3-carboxylate derivaties from halodiazoacetates and 7-azaindoles

Ethyl 8-azaquinoline-3-carboxylates were synthesized from Br- or Cl-EDA and 7-azaindoles based on the reported literature procedure [3]. Several modifications to the reported procedure have been made. Thus, the procedures are described in full detail under each experiment.

5.2.2.1 Ethyl 8-azaquinoline-3-carboxylate (12)

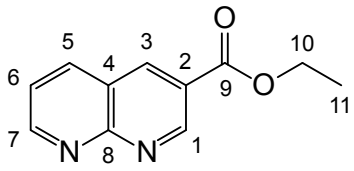

Br-EDA was prepared according to procedure 5.2.1.1. This afforded Br-EDA (0.82 mmol, 1.2 equiv in 8 mL DCM) which was transferred to a cooled addition funnel (0 °C) and added dropwise over 25 min to a mixture of 7-azaindole (84.5 mg, 0.72 mmol, 1.0 equiv.), CS_2CO_3 (303.3 mg, 0.93 mmol, 0.9 equiv.) and $Rh_2(esp)_2$ (5.7 mg, 0.008 mmol, 0.01 equiv.) in 8 mL CH_2Cl_2 at room temperature. With addition of the green $Rh_2(esp)_2$, the solution turned pink. The reaction mixture changed color from pink to orange during the first few minutes of addition of Br-EDA and then to a dark brown color. The mixture was stirred for an additional 30 min and concentrated *in vacuo*. The crude was re-dissolved in 20 mL EtOAc, transferred to a separatory funnel and washed with H_2O (2 x 4 mL), then sat. NaCl (3 mL). The organic phase was dried with $MgSO_4$, filtered and concentrated *in vacuo*. Isolation using column chromatography (SiO_2, EtOAc) afforded **12** as a brown oil in 9 % yield.

^{1}H NMR (400 MHz, $CDCl_3$) δ 9.63 (d, J = 2.4 Hz, 1H, H-1), 9.19 (dd, J = 4.2, 2.1 Hz, 1H, H-7), 8.85 (d, J = 2.2 Hz, 1H, H-3), 8.29 (dd, J = 8.2, 2.1 Hz, 1H, H-5), 7.55 (dd, J = 8.1, 4.1 Hz, 1H, H-6), 4.46 (q, J = 7.2 Hz, 2H, H-10), 1.43 (t, J = 7.1 Hz, 3H, H-11).

^{13}C NMR (101 MHz, $CDCl_3$) δ 164.57 (C-9), 157.39 (C-8), 155.59 (C-7), 153.35 (C-1), 139.79 (C-3), 138.26 (C-5), 124.35 (C-2), 122.94 (C-6), 121.49 (C-4), 61.79 (C-10), 14.26 (C-11).

MS (EI): m/z (relative intensity (%)): 202 (49, M^+), 174 (48), 157 (91), 129 (56), 102 (100).

This compound has been reported in literature [230].

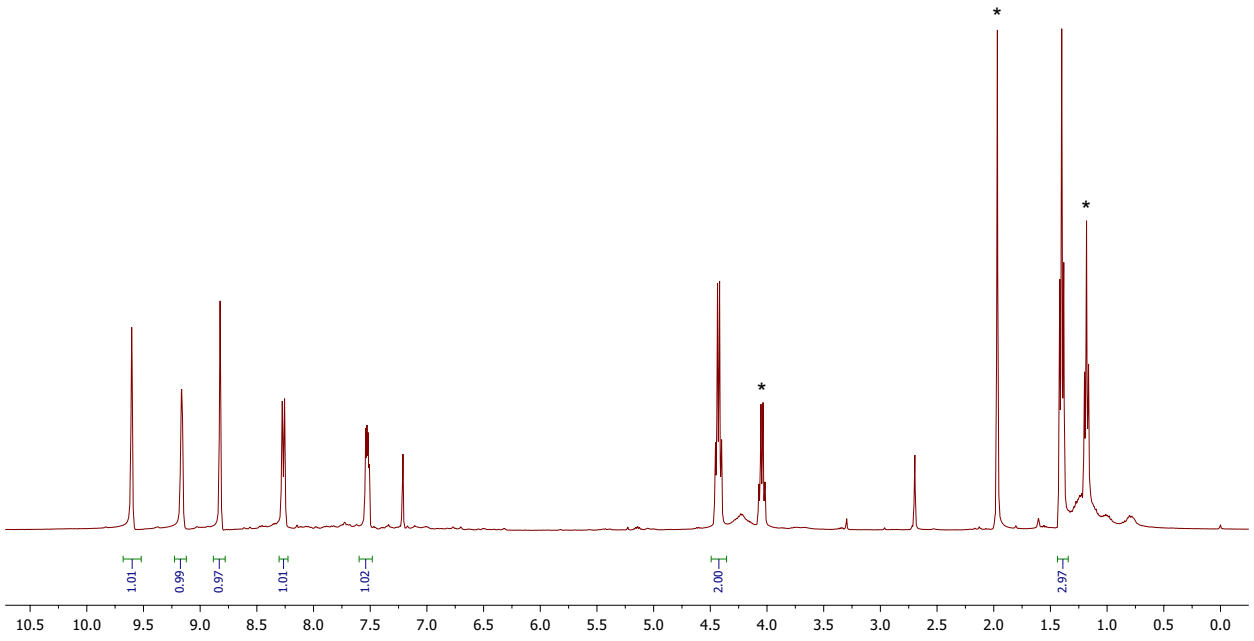

Figure 5.22: ^{1}H NMR spectrum of of ethyl 8-azaquinoline-3-carboxylate (**12**) (400 MHz, $CDCl_3$). * belongs to EtOAc.

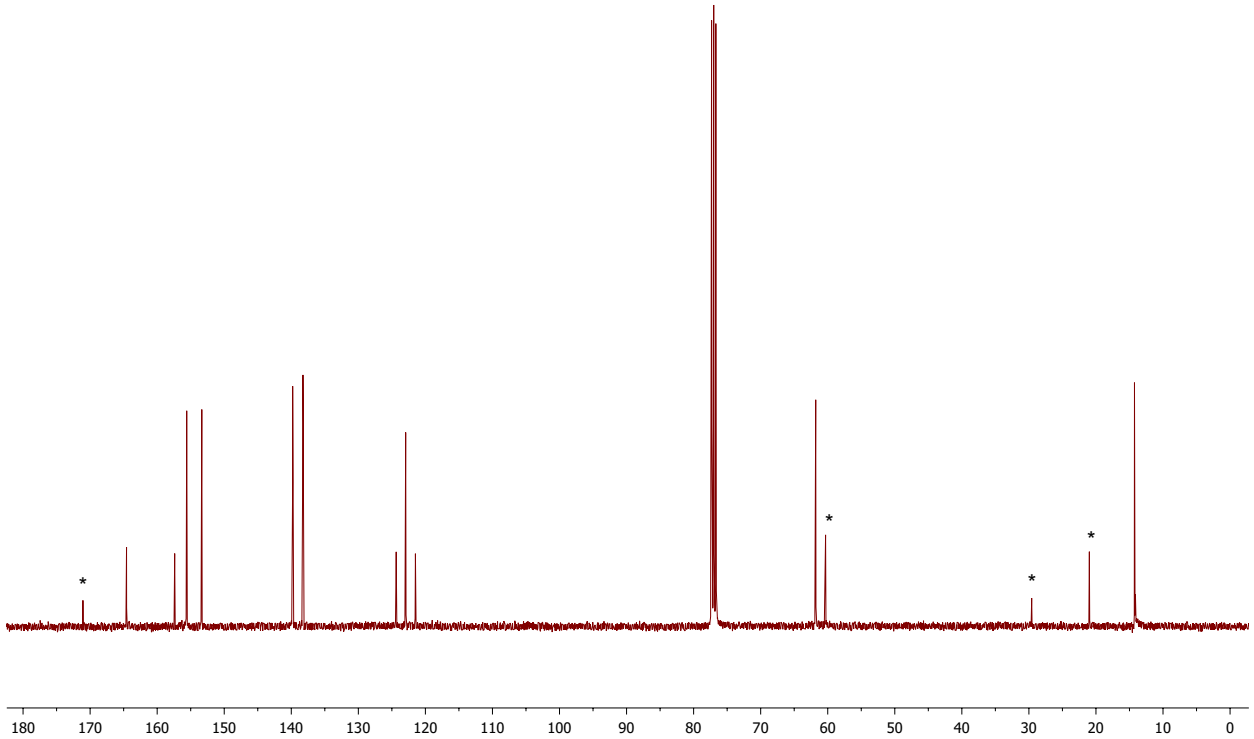

Figure 5.23: ^{13}C NMR spectrum of ethyl 8-azaquinoline-3-carboxylate (**12**) (101 MHz, $CDCl_3$). * belongs to EtOAc.

5.2.2.2 Ethyl 2-bromo-2-(7-aza-1-indolyl) acetate (13)

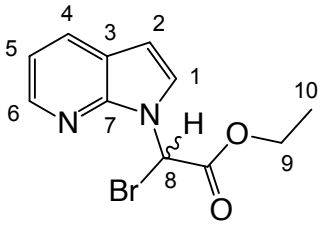

Br-EDA was prepared according to procedure 5.2.1.1. This afforded Br-EDA (0.55 mmol, 1.2 equiv. in 6 mL) which was transferred to a cooled addition funnel (0 °C) and added dropwise over 30 min to a mixture of 7-azaindole (52.7 mg, 0.45 mmol, 1.0 equiv.), CS_2CO_3 (166.3 mg, 0.5 mmol, 1.1 equiv.) and $Rh_2(esp)_2$ (3.9 mg, 0.005 mmol, 0.01 equiv.) in 6 mL CH_2Cl_2 at room temperature. With addition of the green $Rh_2(esp)_2$, the solution turned pink. The reaction mixture changed color from pink to orange during the first few minutes of addition of Br-EDA and then to a dark brown color. The mixture was stirred for an additional 30 min and concentrated *in vacuo*. The crude was re-dissolved in 20 mL EtOAc, transferred to a separatory funnel and washed with H_2O (2 x 4 mL), then sat. NaCl (3 mL). The organic phase was dried with $MgSO_4$, filtered and concentrated *in vacuo*. Isolation using column chromatography (SiO_2, EtOAc) afforded **13** as a brown oil in 24 % yield. **13** decomposes in room temperature.

^{1}H NMR (200 MHz, $CDCl_3$) δ 8.18 (dt, J = 6.7, 0.8 Hz, 1H, H-4), 8.12 (s, 1H, H-8), 8.08 (dd, J = 7.3, 1.1 Hz, 1H, H-6), 7.82 (d, J = 2.7 Hz, 1H, H-1), 6.96 (t, J = 7.0 Hz, 1H, H-5), 6.69 (d, J = 2.7 Hz, 1H, H-2), 4.32 (qd, J = 7.2, 2.5 Hz, 2H, H-9), 1.32 (t, J = 7.1 Hz, 3H, H-10).

^{13}C NMR (101 MHz, $CDCl_3$) δ 165.06 (C-9), 143.51 (C-1), 132.58 (C-6), 130.32 (C-7), 129.50 (C-4), 124.68 (C-3), 110.28 (C-5), 102.93 (C-2), 63.94 (C-10), 51.32 (C-8), 13.81 (C-11).

MS (ESI): m/z (relative intensity (%)): 285.006/283.008 (M^+ + H, 100/100), 268.992/270.990 (45/45), 249.123 (55), 225.064 (69).

This compound has not been reported in the literature.

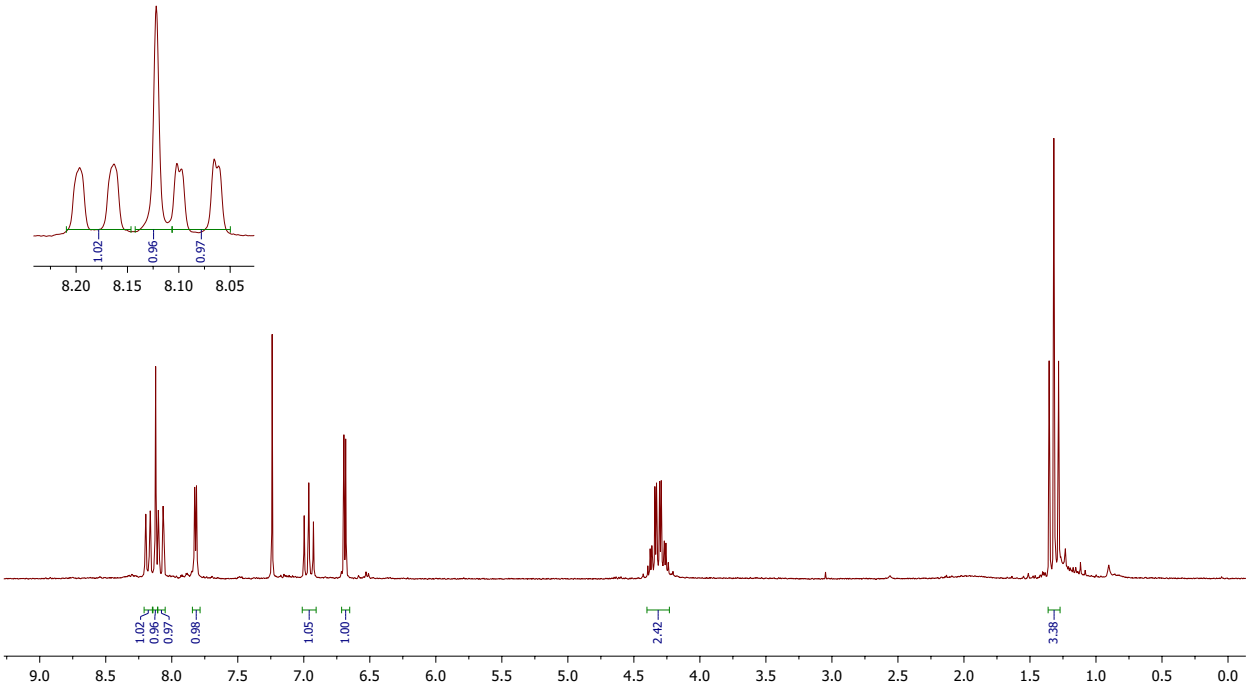

Figure 5.24: ^{1}H NMR spectrum of ethyl 2-bromo-2-(7-aza-1-indolyl) acetate (**13**) (200 MHz, $CDCl_3$).

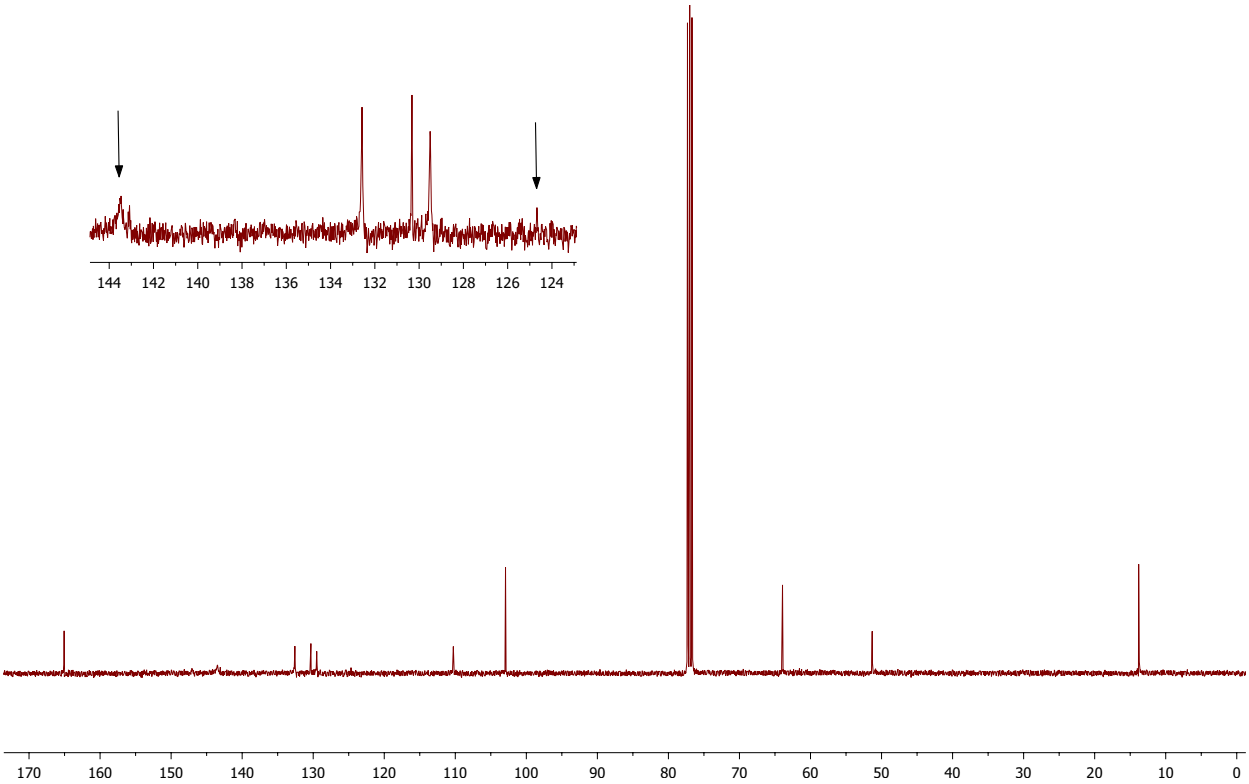

Figure 5.25: ^{13}C NMR spectrum of ethyl 2-bromo-2-(7-aza-1-indolyl) acetate (**13**) (101 MHz, $CDCl_3$). The black arrows indicate the presence of peaks.

5.2.2.3 Ethyl 7-fluoro-8-azaquinoline-3-carboxylate (15)

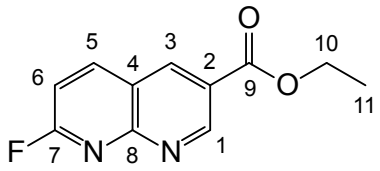

6-fluoro-7-azaindole (40.9 mg, 0.3 mmol, 1.0 equiv.) was dissolved 4 mL anhydrous α-α-α-trifluorotoluene ($PhCF_3$) and cooled down to 0 °C. The solution was purged with nitrogen gas while Cl-EDA was prepared (for approximately 30 min) according to procedure 5.2.1.1. *n*-BuLi (187 µL, 0.3 mmol, 1.0 equiv.) was carefully added *via* a syringe to the stirring solution causing immediate formation of a pale yellow precipitate. The reaction mixture was allowed to stir for 5-10 minutes, then the inert atmosphere was removed and $Rh_2(esp)_2$ (8.7 mg, 0.01 mmol, 0.033 equiv.) in a few drops $PhCF_3$ was added. A rapid color change from yellow to light brown could be observed. Cl-EDA (0.38 mmol, 1.3 equiv. in 4 mL anhydrous $PhCF_3$) was added dropwise to the reaction mixture from a cooled addition funnel (0 °C) over 20-25 min. The ice bath was removed and the dark brown solution was stirred in room temperature for an addition 30 min and concentrated *in vacuo*. The crude was re-dissolved in 15 mL EtOAc, transferred to a separatory funnel and washed with H_2O (2 x 5 mL), then sat. NaCl (2 x 5 mL). The organic phase was dried with $MgSO_4$, filtered and concentrated *in vacuo*. The product mixture was purified using column chromatography (SiO_2, EtOAc:Hex 1:1) and then washed carefully 5 times with small amounts of hexane to wash away oily impurities. The process afforded 28.2 mg of **15** as a yellow-orange solid in 43 % yield.

^{1}H NMR (400 MHz, $CDCl_3$) δ 9.63 (d, J = 2.3 Hz, 1H, H-1), 8.88 (d, J = 2.3 Hz, 1H, H-3), 8.40 (t, J = 8.5 Hz, 1H, H-5), 7.27 (dd, J = 8.7, 2.8 Hz, 1H, H-6), 4.48 (q, J = 7.2 Hz, 2H, H-10), 1.45 (t, J = 7.1 Hz, 3H, H-11).

^{13}C NMR (101 MHz, $CDCl_3$) δ 164.45 (d, J = 251.2 Hz, C-7) 164.35 (C-9), 156.03 (d, J = 19.5 Hz, C-8), 154.17 (C-1), 143.49 (d, J = 11.0 Hz, C-5), 139.11 (C-3), 124.25 (C-2), 120.15 (C-4), 112.52 (d, J = 42.0 Hz, C-6), 61.88 (C-10), 14.24 (C-11).

^{19}F NMR (377 MHz, $CDCl_3$) δ -52.21

MS (EI): m/z (relative intensity (%)): 220 (35, M^+), 192 (57), 175 (100), 147 (61), 120 (76).

MS (ESI) m/z $[M + Na]^+$: Calculated for $C_7H_7N_3NaO_2S$: 220.016. Found: 220.015 (0. ppm).

This compound has not been reported in literature

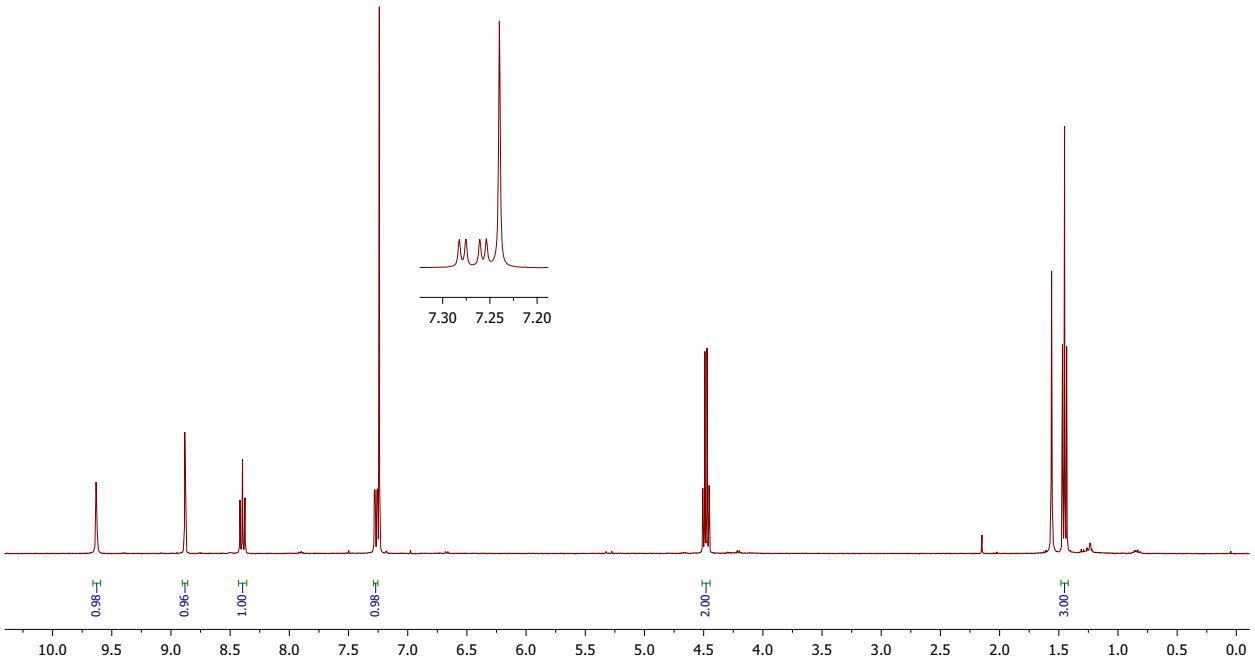

Figure 5.26: ^{1}H NMR spectrum of ethyl 7-fluoro-8-azaquinoline-3-carboxylate **15** (400 MHz, $CDCl_3$).

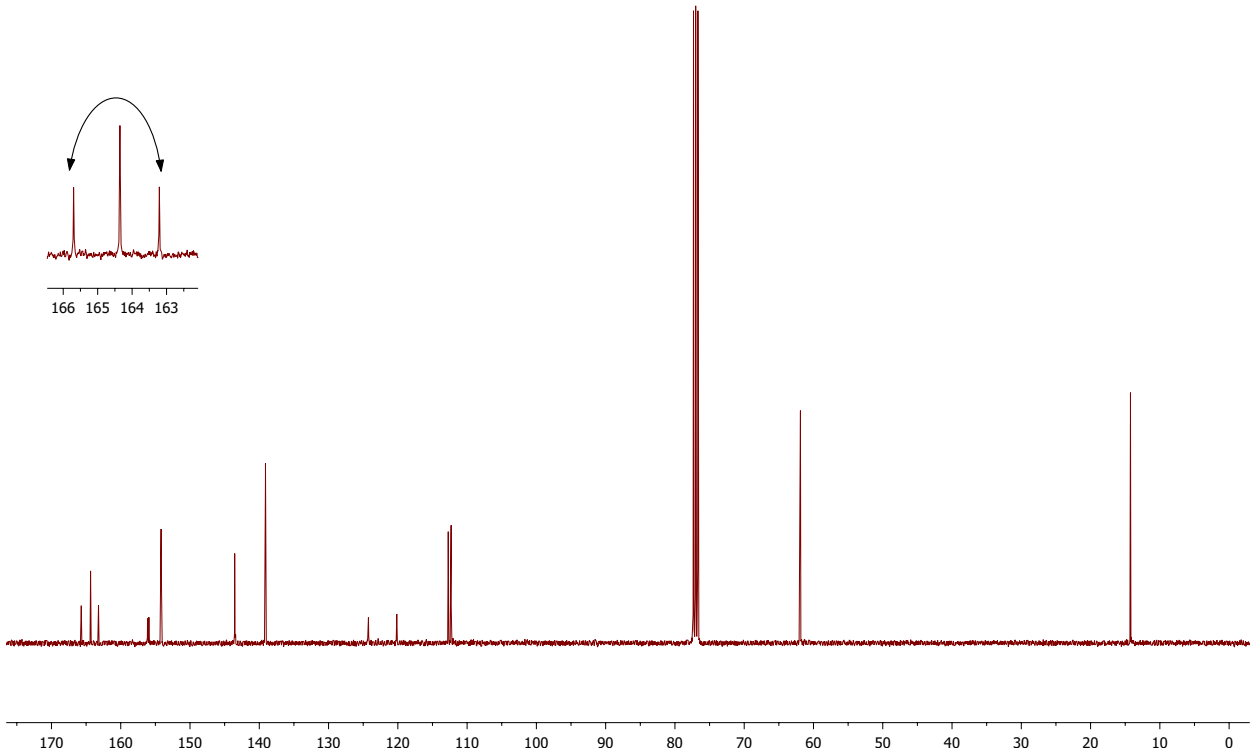

Figure 5.27: ^{13}C NMR spectrum of ethyl 7-fluoro-8-azaquinoline-3-carboxylate **15** (101 MHz, $CDCl_3$). The arrow indicates that the two peaks belong to one signal.

5.2.2.4 Ethyl 4-chloro-7-fluoro-8-azaquinoline-3-carboxylate (22)

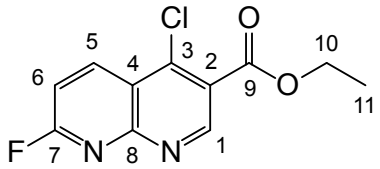

3-chloro-6-fluoro-7-azaindole **18** (85.3 mg, 0.5 mmol, 1.0 equiv.) was dissolved[4] 7 mL anhydrous $PhCF_3$), cooled down to 0 °C and purged with nitrogen gas while Cl-EDA was prepared (approximately 30 min) according to procedure 5.2.1.1. *n*-BuLi (310 µL, 0.5 mmol, 1.0 equiv.) was carefully added *via* a syringe, causing immediate formation of a pale yellow precipitate. The reaction mixture was allowed to stir for 5-10 minutes, then the inert atmosphere was removed and $Rh_2(esp)_2$ (13.3 mg, 0.018 mmol, 0.036 equiv.) in 1 mL $PhCF_3$ was added. A rapid color change from yellow to light brown could be observed. Cl-EDA (0.58 mmol, 1.2 equiv. in 7 mL anhydrous $PhCF_3$) was added dropwise to the reaction mixture from a cooled addition funnel (0 °C) over 25-30 min. The ice bath was removed and the dark solution was stirred in room temperature for an addition 30 min and concentrated *in vacuo*. The crude was then re-dissolved in 20 mL $CHCl_3$, transferred to a separatory funnel and washed with H_2O (5 mL), then sat. NaCl (10 mL). The organic phase was dried with $MgSO_4$, filtered, concentrated *in vacuo*, and triturated with EtOAc. The pink/orange precipitate was removed by vacuum filtration, and the remaining brown oil was purified using column chromatography (SiO_2, Et_2O:Hex 2:1 → 1:1) and washed carefully with small amounts of Et_2O to afford **22** as a white powder.

IS-yield: 50 %

^{1}H NMR (400 MHz, $CDCl_3$) δ 9.42 (s, 1H, H-1), 8.87 (t, J = 8.4 Hz, 1H, H-5), 7.33 (dd, J = 9.0, 3.0 Hz, 1H, H-6), 4.49 (q, J = 7.1 Hz, 2H, H-10), 1.44 (t, J = 7.1 Hz, 3H, H-11).

^{13}C NMR (101 MHz, $CDCl_3$) δ 164.58 (d, J = 249.4 Hz, C-7) 163.45 (C-9), 155.64 (d, J = 19.6 Hz, C-8), 154.57 (C-1), 144.12 (C-3), 140.78 (d, J = 10.9 Hz, C-5), 123.64 (C-2), 120.29 (C-4), 113.09 (d, J = 41.5 Hz, C-6), 62.44 (C-10), 14.19 (C-11).

^{19}F NMR (377 MHz, $CDCl_3$) δ -52.93

MS (EI): m/z (relative intensity (%)): 254/256 (33/12, M^+/M+2), 226/228 (42/14), 209/211 (100/34), 181/183 (32/12). 154/156 (46/14), 119 (10).

HR-MS (ESI) m/z $[M + Na]^+$: Calculated for $C_{11}H_8ClFN_2NaO_2$: 277.0156/279.0127. Found: 277.0151/279.0122 (-0.2 ppm).

This compound has not been reported in literature.

[4] poorly soluble

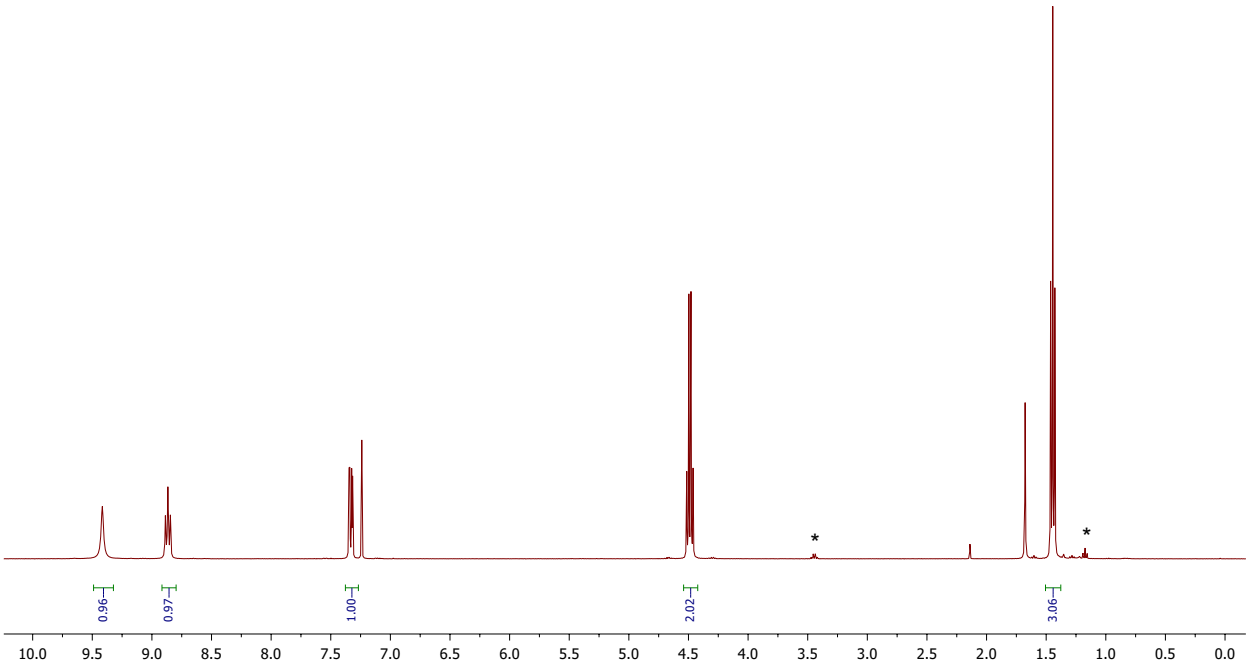

Figure 5.28: ^{1}H NMR spectrum of ethyl 4-chloro-7-fluoro-8-azaquinoline-3-carboxylate (**22**) (400 MHz, $CDCl_3$). * Belongs to residual Et_2O.

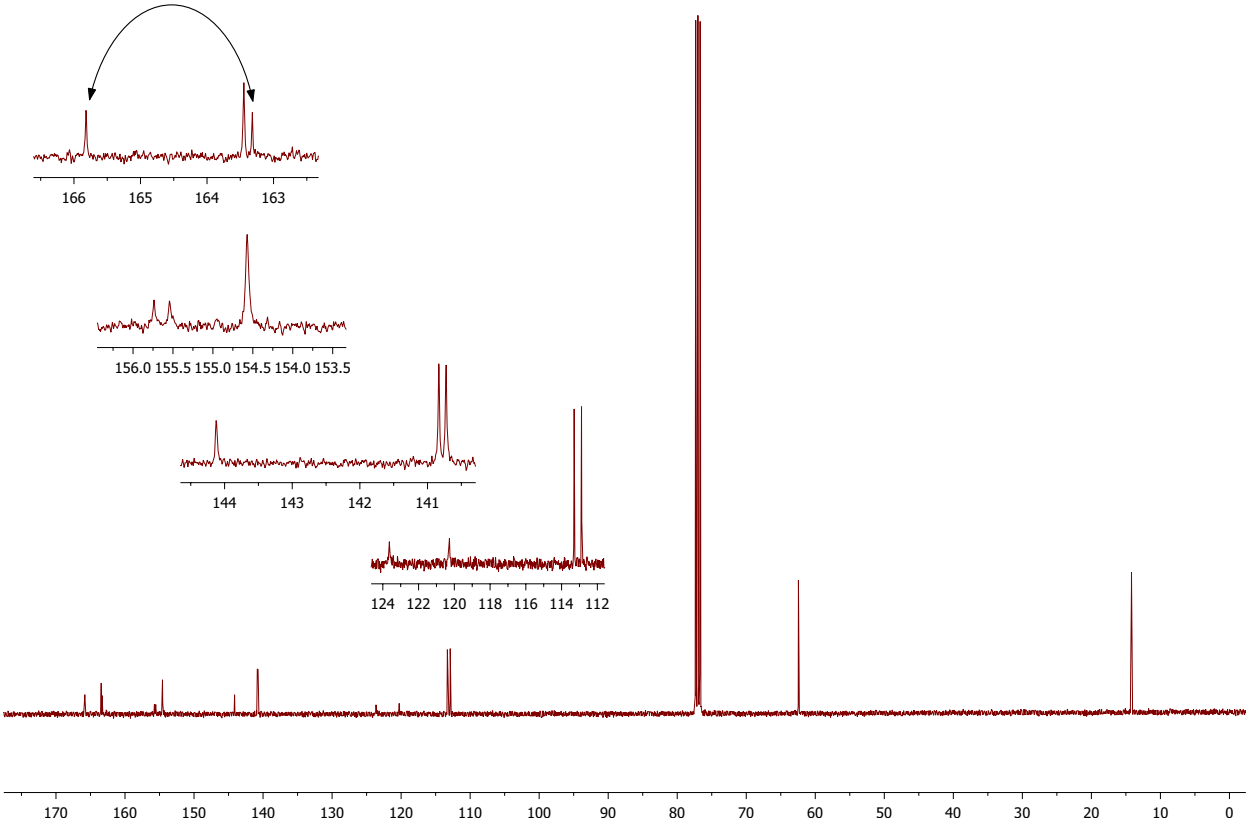

Figure 5.29: ^{13}C NMR spectrum of ethyl 4-chloro-7-fluoro-8-azaquinoline-3-carboxylate (**22**) (101 MHz, $CDCl_3$). The arrow indicate that the two peaks belong to one signal.

5.2.2.5 Ethyl 7-methyl-8-azaquinoline-3-carboxylate (17)

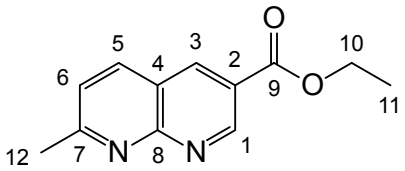

6-methyl-7-azaindole (89.6 mg, 0.68 mmol, 1.0 equiv.) was dissolved in 7 mL anhydrous $PhCF_3$), cooled down to 0 °C and purged with nitrogen gas while Cl-EDA was prepared according to procedure 5.2.1.1 (for approximately 30 min). *n*-BuLi (340 µL, 0.68 mmol, 1.0 equiv.) was carefully added to the stirring solution *via* a syringe, causing formation of a pale yellow precipitate after 30-60 sec. The reaction mixture was allowed to stir for 5-10 minutes, then the inert atmosphere was removed and $Rh_2(esp)_2$ (18.8 mg, 0.025 mmol, 0.036 equiv.) in 1 mL $PhCF_3$ was added. A rapid color change from yellow to light brown could be observed. Cl-EDA (0.83 mmol, 1.2 equiv. in 5 mL anhydrous $PhCF_3$) was added dropwise to the reaction mixture from a cooled addition funnel (0 °C) over 25-30 min. The ice bath was removed and the dark brown solution was stirred in room temperature for an additional 30 min and concentrated *in vacuo*. The crude was then re-dissolved in 25 mL EtOAc, transferred to a separatory funnel and washed with sat. NaCl (3 x 5 mL). The organic phase was dried with $MgSO_4$, filtered, concentrateed *in vacuo*. The desired product was isolated using column chromatography (SiO_2, EtOAc:Hex 3:1) and carefully washed with small amounts of Et_2O which afforded 34.5 mg of **17** as a pale yellow solid in 24 % yield.

^{1}H NMR (600 MHz, $CDCl_3$) δ 9.59 (d, J = 2.3 Hz, 1H, H-1), 8.80 (d, J = 2.4 Hz, 1H, H-3), 8.16 (d, J = 8.3 Hz, 1H, H-5), 7.43 (d, J = 8.3 Hz, 1H, H-6), 4.46 (q, J = 7.1 Hz, 2H, H-10), 2.83 (s, 3H, H-12), 1.44 (t, J = 7.1 Hz, 3H, H-11).

^{13}C NMR (101 MHz, $CDCl_3$) δ 165.63 (C-9), 164.85 (C-7), 157.32(C-8), 153.20 (C-1), 139.30 (C-3), 137.84 (C-5), 123.85 (C-6), 123.59 (C-2), 119.43 (C-4), 61.65 (C-10), 25.93 (C-12), 14.30 (C-11).

MS (EI) m/z (relative intensity (%)): 216 (66, M^+), 188 (57), 171 (100), 143 (34), 116 (59).

HR-MS (ESI) m/z $[M + Na]^+$: Calculated for $C_{12}H_{12}N_2NaO_2$: 239.0797. Found: 239.0791 (0.1 ppm).

Melting point: 142–144 °C.

This compound has not been reported in the literature.

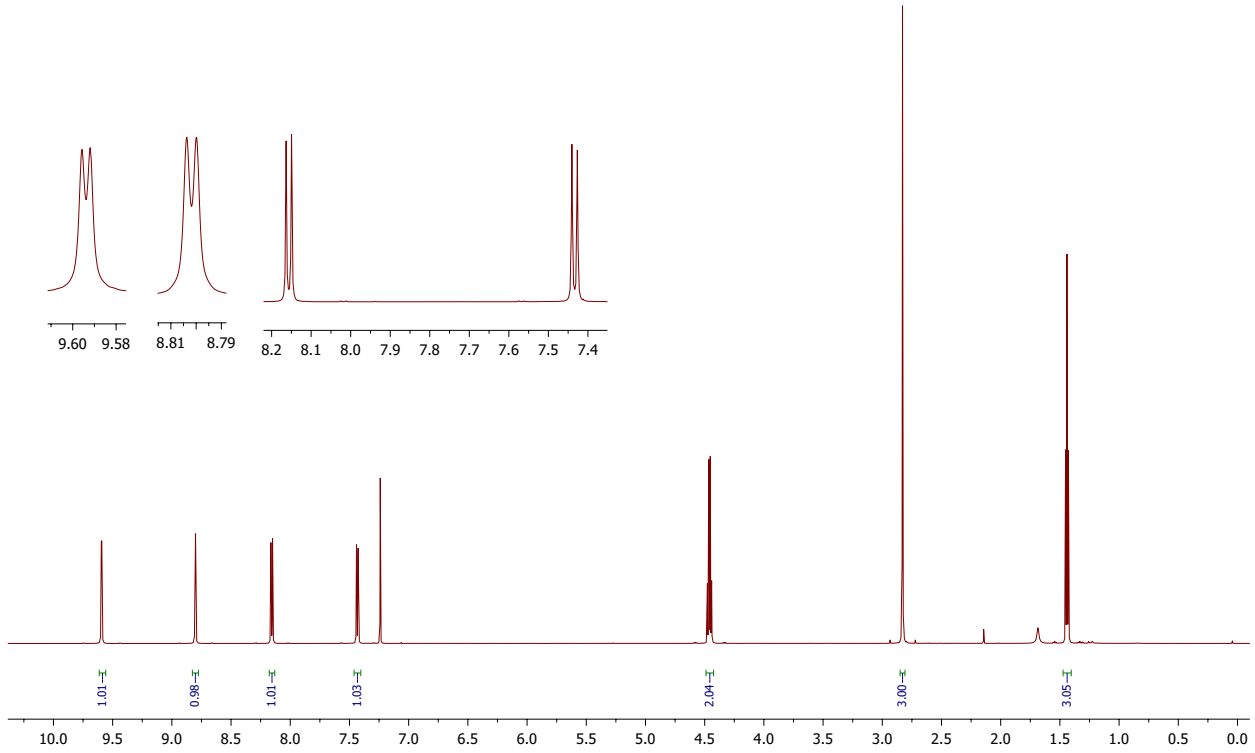

Figure 5.30: ^{1}H NMR spectrum of ethyl 7-methyl-8-azaquinoline-3-carboxylate (**17**) (600 MHz, $CDCl_3$).

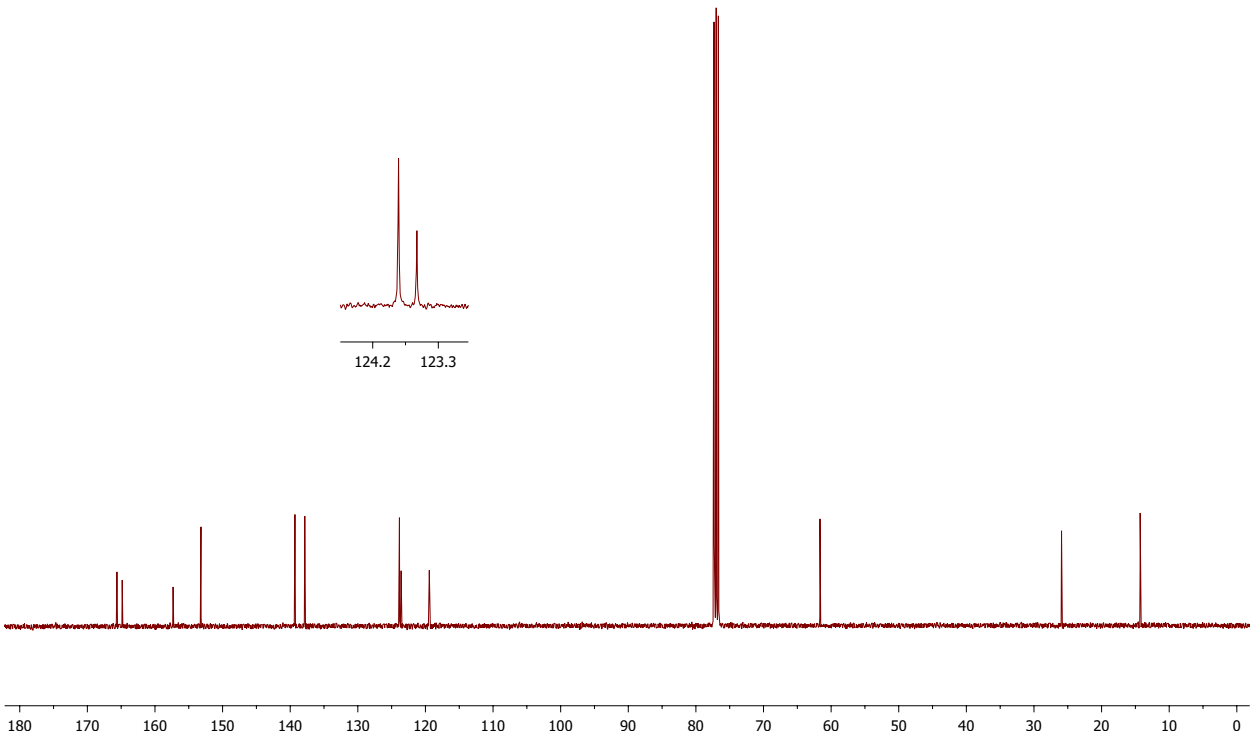

Figure 5.31: ^{13}C NMR spectrum of ethyl 7-methyl-8-azaquinoline-3-carboxylate (**17**) (101 MHz, $CDCl_3$).

5.2.2.6 Ethyl 4-chloro-7-methyl-8-azaquinoline-3-carboxylate (23)

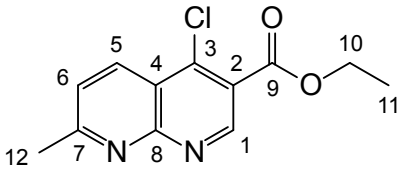

3-chloro-6-methyl-7-azaindole **20** (20.1 mg, 0.12 mmol, 1.0 equiv.) was dissolved in 2.5 mL dry toluene. The flask was gently heated with a heating gun to ensure full dissolution of **20**. NaH (60 % on mineral oil, 14.6 mg, 0.37 mmol, 3 equiv.) was added to the solution and stirred for approximately 60 min. A slight color change from pale yellow to yellow-green was observed during the 60 minutes. $Rh_2(esp)_2$ (3.3 mg, 0.004 mmol, 0.03 equiv.) was then added, and the solution turned purple. Cl-EDA (0.14 mmol, 1.2 equiv. in 2 mL dry toluene), prepared according to procedure 5.2.1.1 was added dropwise to the reaction mixture from a cooled addition funnel (0 °C) over 15 min. The resulting orange-brown solution was stirred for an additional 30 minutes, then concentrated *in vacuo*. The crude was then re-dissolved in 15 mL EtOAc, transferred to a separatory funnel and washed with H_2O (2 x 5 mL) sat. NaCl (3 x 5 mL). The organic phase was dried with $MgSO_4$, filtered, concentrated *in vacuo*. Isolation using column chromatography (SiO_2, EtOAc:Hex 3:1), and careful washing with small amounts of Et_2O afforded **23** as white crystals.

IS-yield: 63 %

While removing the last bit of solvent after the spectroscopic analysis, the white crystals decomposed to a purple oil. Thus, no isolated yield was calculated, nor were any MS-data obtained.

^{1}H NMR (400 MHz, $CDCl_3$) δ 9.40 (s, 1H, H-1), 8.63 (d, J = 8.6 Hz, 1H. H-5), 7.51 (d, J = 8.6 Hz, 1H, H-6), 4.49 (q, J = 7.1 Hz, 2H, H-10), 2.84 (s, 3H, H-12), 1.45 (t, J = 7.1 Hz, 3H, H-11).

^{13}C NMR (101 MHz, $CDCl_3$) δ 165.81 (C-9), 163.87 (C-7), 156.71 (C-8), 153.39 (C-1), 144.06 (C-3), 134.72 (C-5), 124.52 (C-6), 122.88 (C-2), 119.51 (C-4), 62.20 (C-10), 25.67 (C-12), 14.22 (C-11).

This compound has been reported in the literature [231].

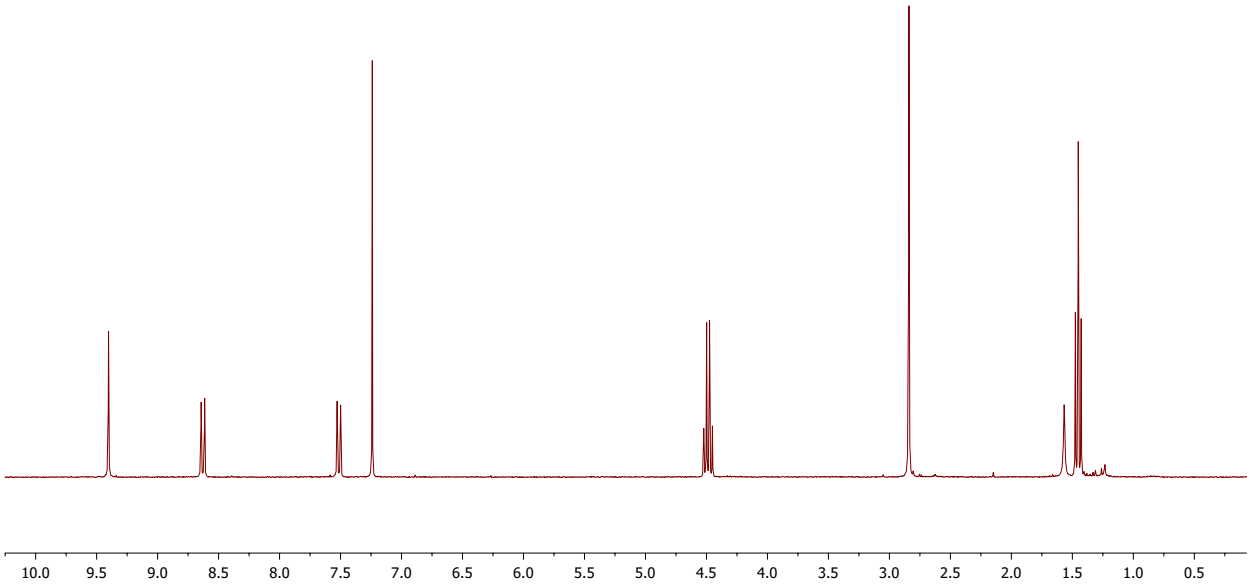

Figure 5.32: ^{1}H NMR spectrum of ethyl 4-chloro-7-methyl-8-azaquinoline-3-carboxylate (**23**) (400 MHz, $CDCl_3$).

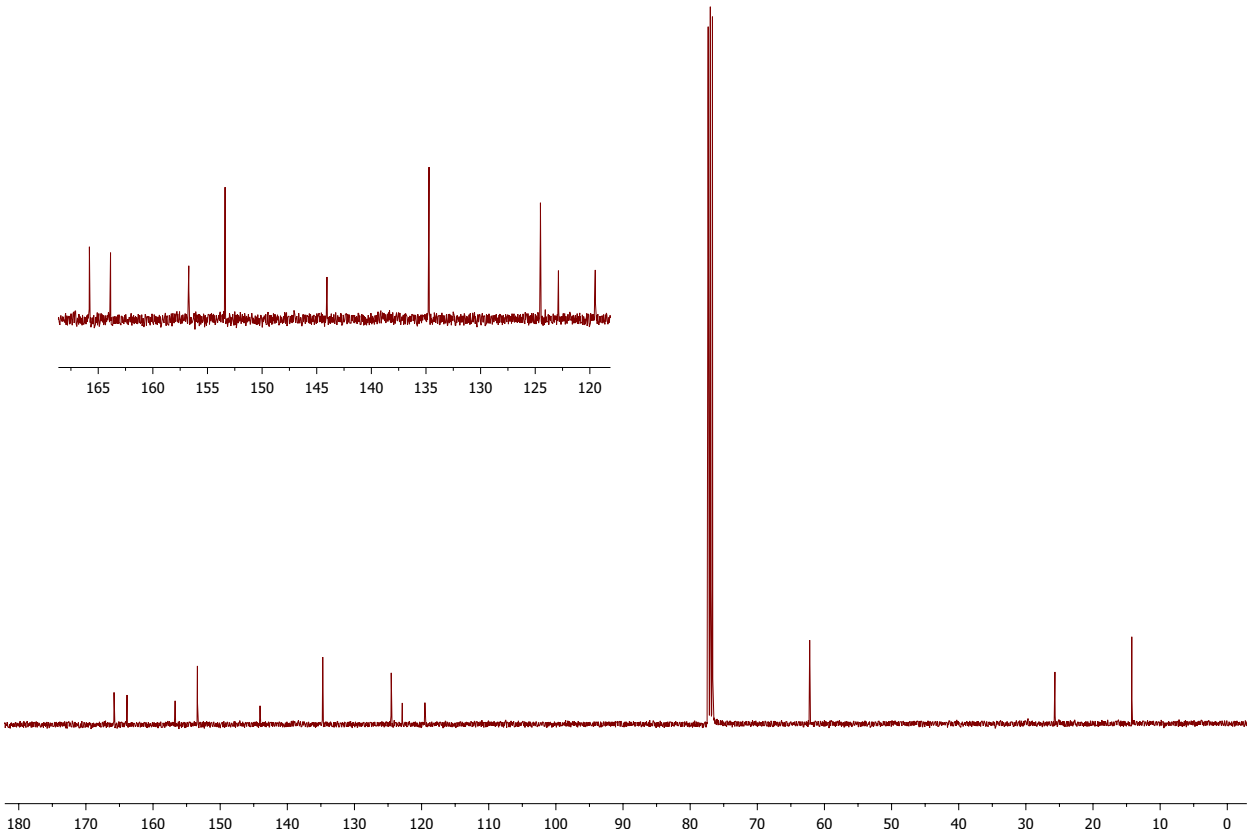

Figure 5.33: ^{13}C NMR spectrum of ethyl 4-chloro-7-methyl-8-azaquinoline-3-carboxylate (**23**) (101 MHz, $CDCl_3$).

5.2.2.7 Ethyl 7-methyl-8-azaquinol-4-one-3-carboxylate (24)

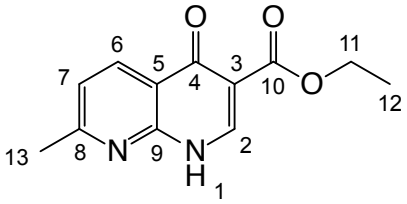

Compound **24** was one of the decomposition products from procedure 5.2.2.6. The decomposed mixture was left in the fume hood over several days and a brown/red/orange mixture was observed. The mixture was attempted cleaned out with acetone. An insoluble part of the mixture was transferred to a vial and washed further with acetone. The washing process afforded an orange powder.

^{1}H NMR (400 MHz, methanol-d_4) δ 8.68 (s, 1H, H-2), 8.54 (d, J = 8.2 Hz, 1H, H-6), 7.38 (d, J = 8.2 Hz, 1H, H-7), 4.34 (q, J = 7.1 Hz, 2H, H-11), 2.65 (s, 3H, H-13), 1.37 (t, J = 7.1 Hz, 3H, H-12).

HR-MS (ESI) m/z [M + Na]$^+$: Calculated for $C_{12}H_{12}N_2NaO_3$: 255.0746. Found: 255.0740 (0.1 ppm).

This compound has been reported in the literature [232].

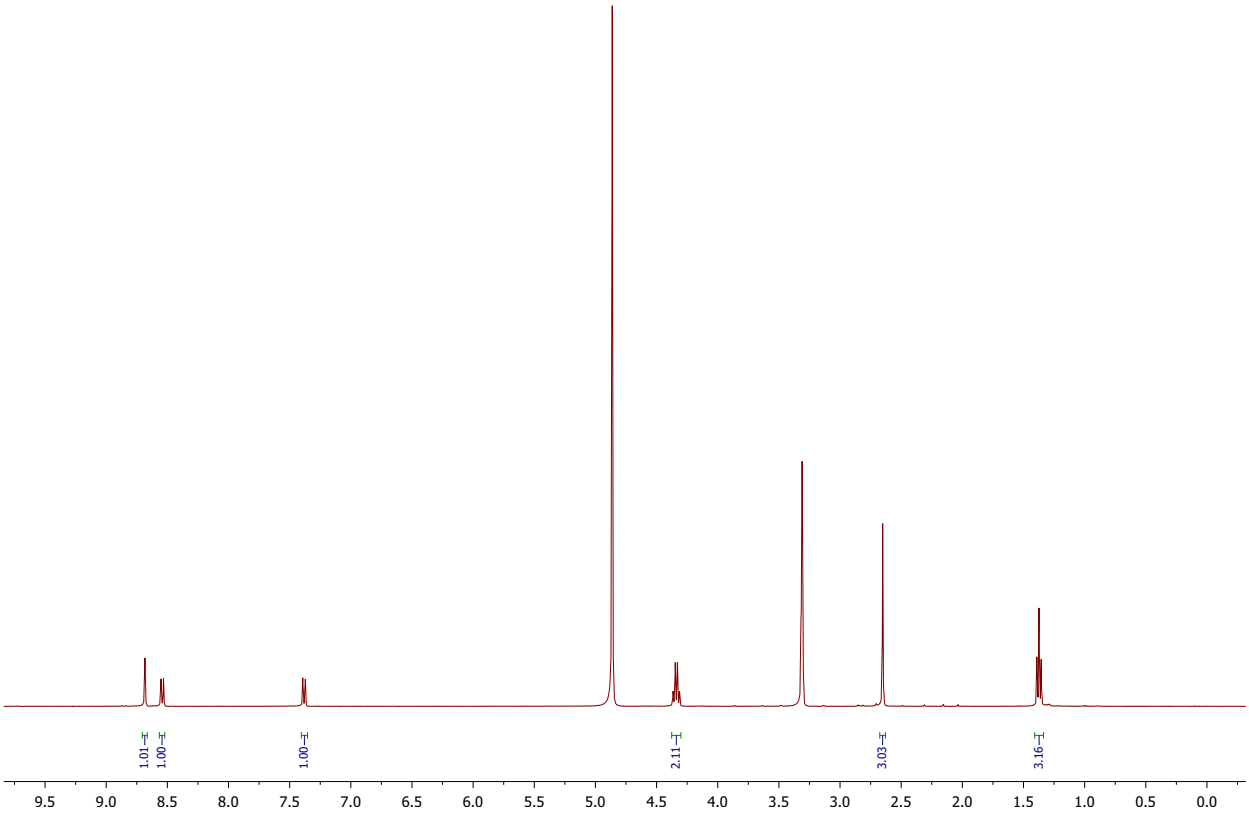

Figure 5.34: ^{1}H NMR spectrum of ethyl 7-methyl-8-azaquinol-4-one-3-carboxylate (**24**) (400 MHz, methanol-d_4).

5.3 Halodiazophosphonates and diethyl 3-quinolinylphosphonates

5.3.1 Preparation of diethyl diazomethylphosphonate (27)

Diethyl diazomethylphosphonate (EDP) was prepared according to literature [211–213].

5.3.1.1 Diethyl 2-oxopropylphosphonate (25)

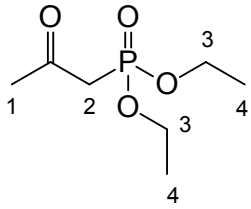

To a 500 mL round-bottom flask potassium iodide (45.83 g, 276 mmol, 1.1 eqiuv.) and acetone/acetonitrile (100 mL/100 mL) was added and stirred. Chloroacetone (20 mL, 250 mmol, 1.0 eqiuv.) was added to the suspension, and the yellow mixture was stirred at room temperature for 1.5 h. Triethylphosphite (43 mL, 250 mmol, 1.0 eqiuv.) was then added dropwise over 45 min via an addition funnel. The orange mixture was stirred at room temperature over night, and the resulting white mixture was then filtered through a plug of celite and concentrated *in vacuo*, which afforded a pale yellow liquid. In an attempt to remove KCl from the solution, the crude was transferred to a separatory funnel and ethyl acetate was added. A sudden color change appeared, and the crude turned brown. It was extracted three times with CH_2Cl_2, then washed three times with brine. Some of brown crude was purified using column chromatography (SiO_2, Hexane:EtOAc 1:1) which afforded **25** as a colorless liquid. No yield was calculated in this step as only parts of the crude were purified.

^{1}H NMR (300 MHz, $CDCl_3$) δ 4.15 - 4.00 (m, 4H, H-3), 3.02 (d, J = 22.9 Hz, 2H, H-2), 2.25 (s, 3H, H-1), 1.27 (t, J = 7.1 Hz, 6H, H-4).

The spectroscopic data was in accordance with reported literature data [233].

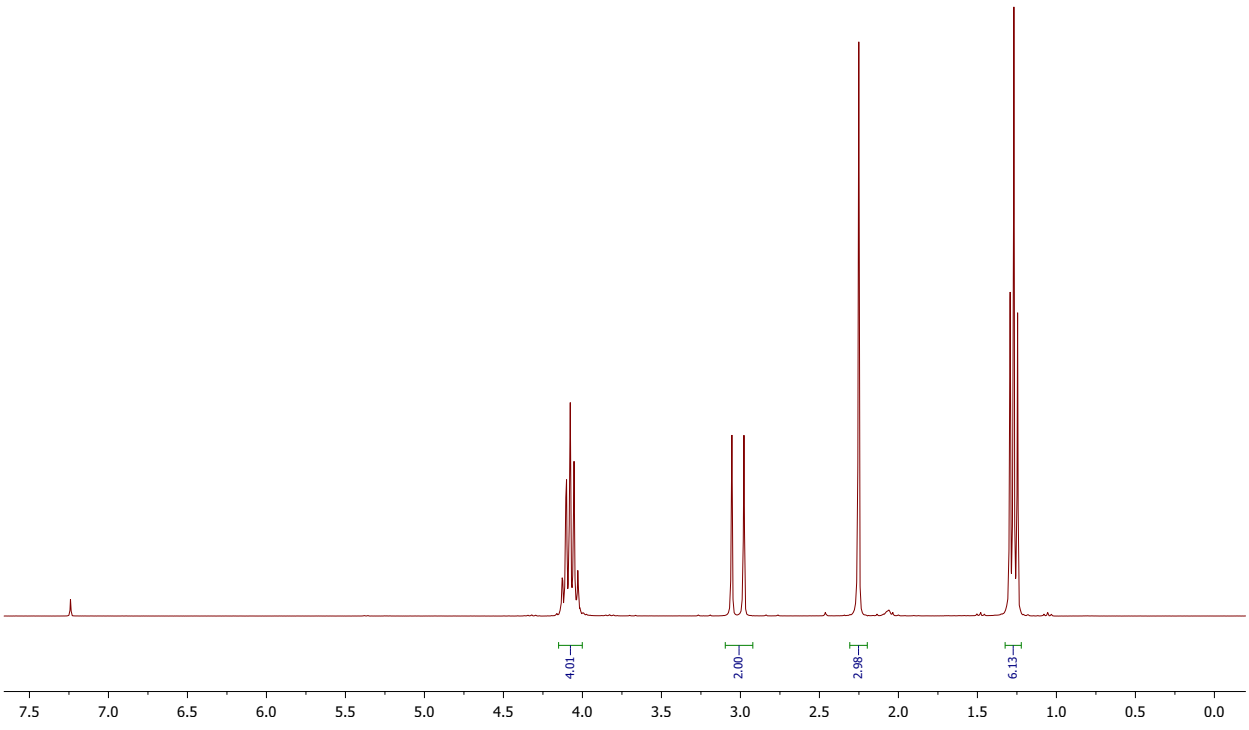

Figure 5.35: ^{1}H NMR spectrum of diethyl 2-oxopropylphosphonate (**25**) (300 MHz, $CDCl_3$).

5.3.1.2 Diethyl 1-diazo-2-oxopropylphosphonate (26)

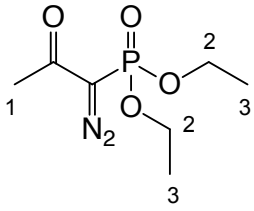

Diethyl 2-oxopropylphosphonate **25** (20.29 g, 105 mmol, 1.0 equiv.) was diluted in 120 mL dry toluene and cooled down to 0 °C. NaH (60% on mineral oil, 4.60 g, 115 mmol, 1.1 equiv.) was then added portionwise until gas evolution ceased. Tosyl azide (22.68 g, 115 mmol, 1.0 equiv.) in 50 mL dry THF was added to the mixture yellow mixture over 15-20 min via an addition funnel at 0 °C. The orange solution was stirred at 0 °C for 1 h then at room temperature over night. The resulting chocolate brown mixture was diluted with hexane and filtered through a pad of celite. The celite was washed with a few portions of toluene. The resulting orange filtrate was concentrated *in vacuo*, and triturated with hexane (to force precipitation of *p*-toluenesulfonyl amide) prior to separation. Column chromatography (SiO_2, EtOAc:hexane 1:1) afforded 19.95 g of **26** as a pale yellow liquid in 83 % yield.

^{1}H NMR (300 MHz, $CDCl_3$) δ 4.41 - 3.87 (m, 4H, H-2), 2.25 (s, 3H, H-1), 1.36 (td, J = 7.1, 0.8 Hz, 6H, H-3).

The spectroscopic data was in accordance with reported literature data [233].

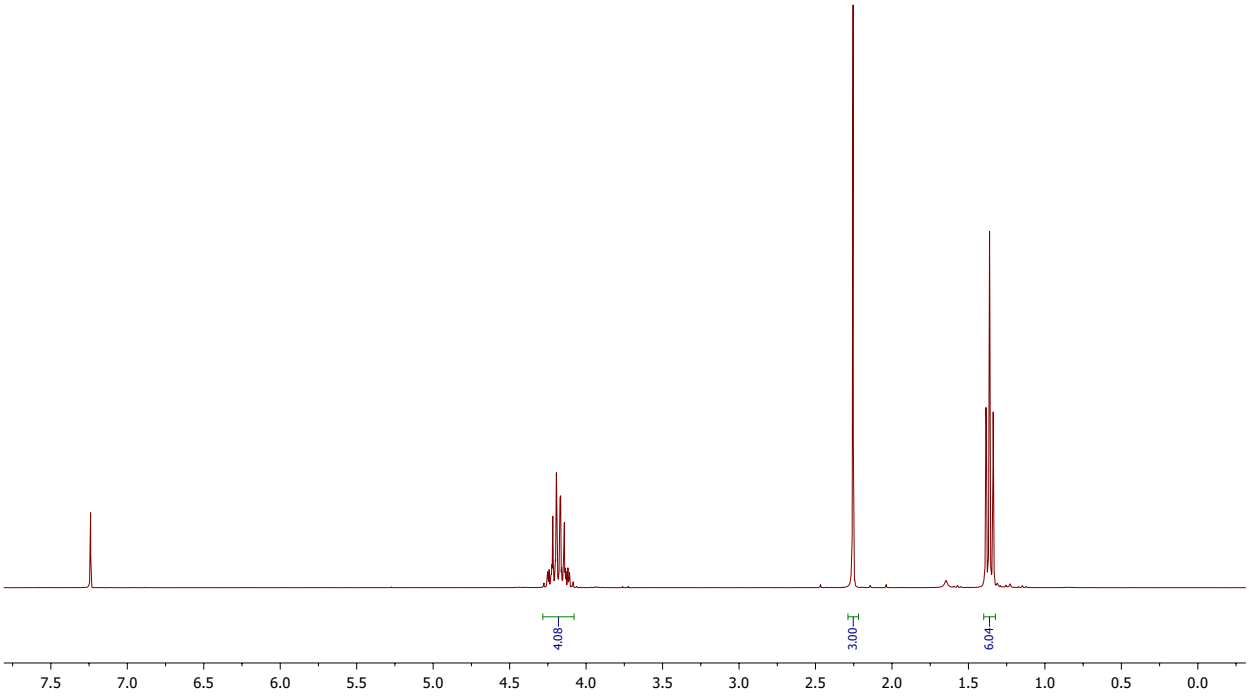

Figure 5.36: ^{1}H NMR spectrum of diethyl 1-diazo-2-oxopropylphosphonate (**26**) (300 MHz, $CDCl_3$).

5.3.1.3 Diethyl diazomethylphosphonate (EDP) (27)

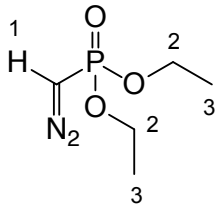

Diethyl 1-diazo-2-oxopropylphosphonate **26** (19.95 g, 105 mmol, 1.0 equiv.) was diluted in 100 mL MeOH and triethylamine (18.9 mL, 136 mmol, 1.3 equiv.) was added to the solution and stirred at room temperature over night. The mixture was concentrated *in vacuo*. Isolation using column chromatography (SiO_2, EtOAc:hexane 1:1) afforded 13.10 g of **27** as a yellow liquid in 70 % yield. The liquid was stored in the fridge.

^{1}H NMR (400 MHz, $CDCl_3$) δ 4.24 - 3.92 (m, 4H, H-2), 3.74 (d, J = 11.1 Hz, 1H, H-1), 1.33 (td, J = 7.1, 0.7 Hz, 6H, H-3).

^{13}C NMR (101 MHz, $CDCl_3$) δ 62.60 (d, J = 5.4 Hz, C-2), 29.57 (d, J = 231.2 Hz, C-1), 16.18 (d, J = 6.9 Hz, C-3).

The spectroscopic data was in accordance with reported literature data [233].

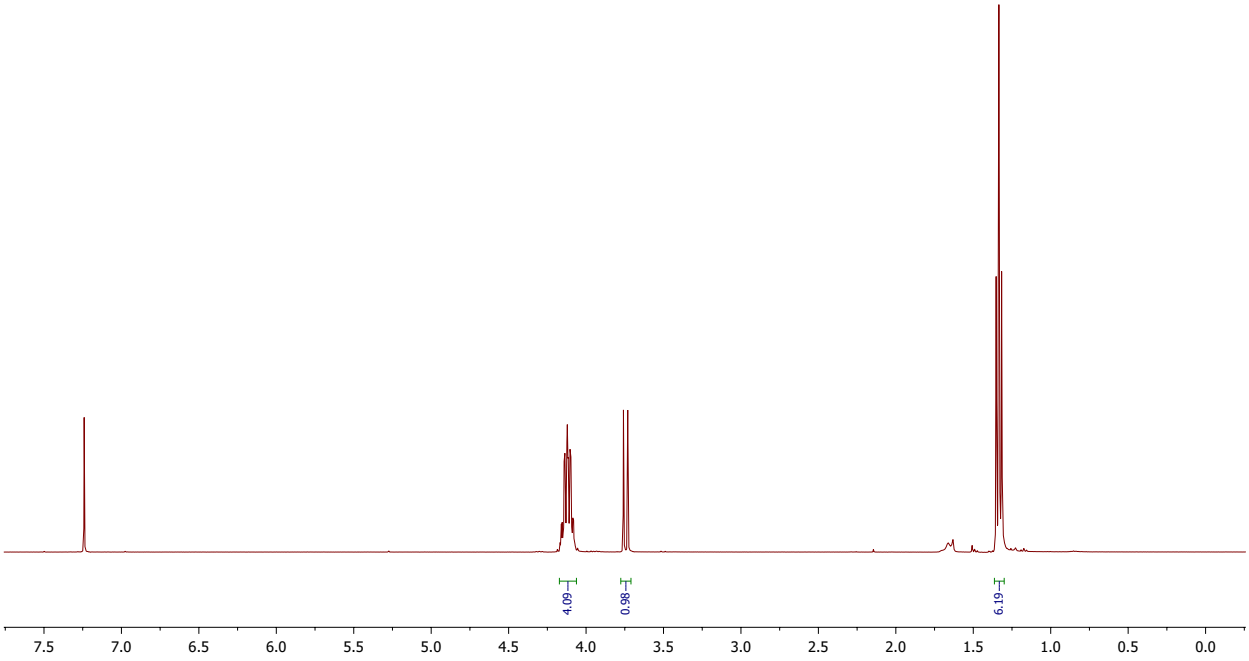

Figure 5.37: ^{1}H NMR spectrum of diethyl diazomethylphosphonate (**27**) (400 MHz, $CDCl_3$).

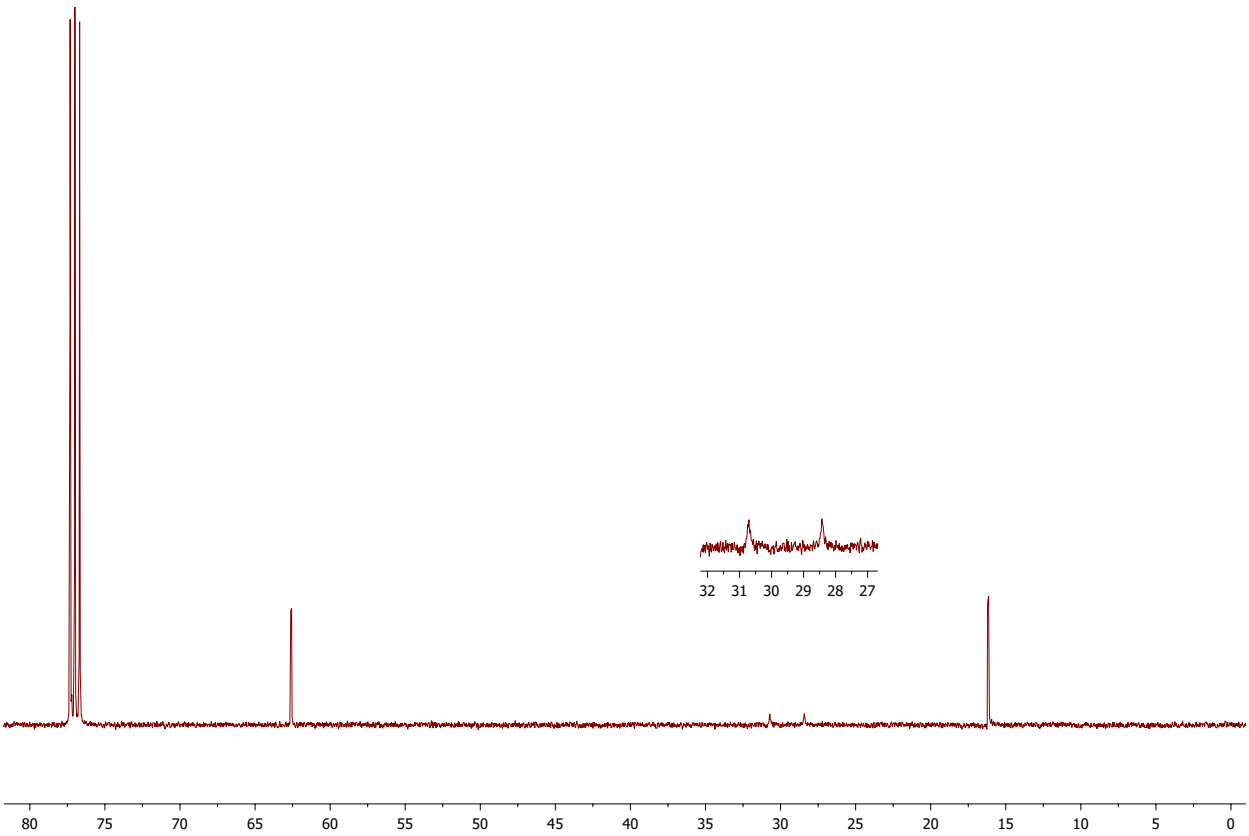

Figure 5.38: ^{13}C NMR spectrum of diethyl diazomethylphosphonate (**27**) (101 MHz, $CDCl_3$).

5.3.2 Diethyl halodiazophosphonates

The reported one-pot procedure for halogenation of EDP and subsequent intermolecular Rh(II)-catalyzed cyclopropanation by Schnaars *et al.* [4] did not seem compatible with indole as a substrate due to excess of NaH. Therefore, preparation of Cl- and Br-EDP from EDP was performed according to the following general procedure (5.3.2.1), which is based on reported literature procedure of halogenation of EDA [3]. In all experiments where X-EDP was employed as a reactant, the reactions were performed immediately after preparation due to their thermal instability. The X-EDPs were always kept in a cold (0 °C) and never evaporated to dryness. Due to the varying results in yield measurements, yields of the halogenated EDPs will not be stated.

5.3.2.1 General procedure for the preparation of diethyl halodiazophosphonates (X-EDP)

EDP (178.13 mg, 1.0 mmol, 1.0 equiv.) was diluted with cold CH_2Cl_2 (12-14 mL). DBU (213.14 mg, 1.4 mmol, 1.4 equiv.) was added to the solution and stirring was continued for 5 min at 0 °C before NXS (1.1 mmol, 1.1 equiv. NBS, or NCS) of choice was added. There was an immediate color change from yellow to orange (shade dependent on the NXS). The solution was stirred for an additional 2-3 minutes at 0 °C, then filtered through a pre-cooled (0 °C) plug of silica gel, eluting with cold CH_2Cl_2. This afforded a yellow (X = Cl) or orange (X = Br) solution of X-EDA. 10 mL dry toluene was added and CH_2Cl_2 was removed *in vacuo* at 0 °C.

5.3.2.2 Diethyl chlorodiazomethylphosphonate (32)

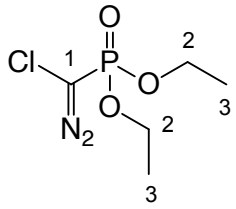

Compound **32** was prepared according to procedure 5.3.2.1.

EDP (54.7 mg, 0.31 mmol, 1.0 equiv.), DBU (67.7 mg, 0.44 mmol, 1.4 equiv.) and NCS (48.0 mg, 0.36 mmol, 1.2 equiv.), gave **32** as yellow solution.

^{1}H NMR (300 MHz, toluene-d_8) δ 3.93-3.72 (m, 4H, H-2), 1.01 (td, J = 7.1, 0.7 Hz, 6H, H-3).

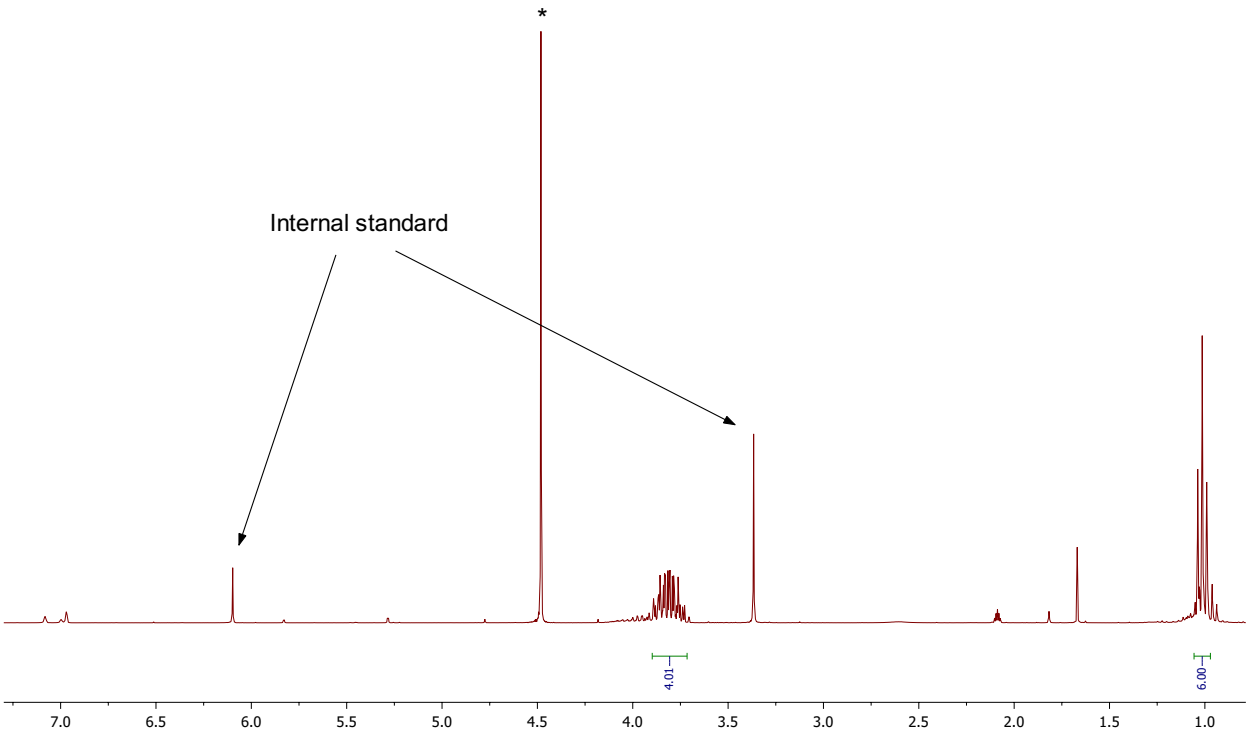

Figure 5.39: ^{1}H NMR spectrum of diethyl chlorodiazomethylphosphonate (**32**) (300 MHz, $CDCl_3$). * belongs to DCM.

5.3.2.3 Diethyl bromodiazomethylphosphonate (33)

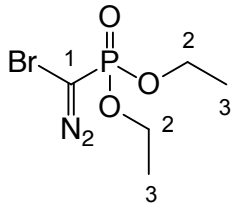

Compound **33** was prepared according to procedure 5.3.2.1.

EDP (89.6 mg, 0.50 mmol, 1.0 equiv.), DBU (106.4 mg, 0.70 mmol, 1.4 equiv.) and NBS (98.1 mg, 0.55 mmol, 1.1 equiv.), gave **32** as an orange solution.

No good ^{1}H NMR spectrum could be obtained.

5.3.3 Synthesis of diethyl quinolinyl-3-phosphonates from halodiazophosphonates and indoles

Diethyl 3-quinolinylphosphonates were synthesized from Br- or Cl-EDP and indoles based on the reported literature procedure for Rh(II)-catalyzed cyclopropanation-ring expansion between halodiazoacetates and indoles [3]. Some modifications to the reported procedure have been made.

Unless stated otherwise, all yields were measured by ^{1}H NMR analysis using TMB as internal standard from the respective crude ^{1}H NMR spectra.

In procedures where Cl-EDP were used as the limiting reagent, yields were calculated over two steps from EDP.

5.3.3.1 Diethyl 3-quinolinylphosphonate (34)

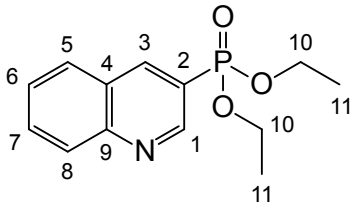

Cl-EDP was prepared according to procedure 5.3.2.1. This afforded Cl-EDP (0.51 mmol, 1.0 equiv in 5 mL dry toluene) which was transferred to a cooled addition funnel (0 °C) and added dropwise over 20-25 min to a mixture of indole (293.4 mg, 2.50 mmol, 5.0 equiv.), CS_2CO_3 (171.0 mg, 0.53 mmol, 1.0 equiv.) and $Rh_2(esp)_2$ (9.5 mg, 0.013 mmol, 0.025 equiv.) in 5 mL dry toluene at room temperature. The dark mixture was stirred for an additional 30 min and concentrated *in vacuo*. The crude was re-dissolved in 20 mL EtOAc, transferred to a separatory funnel and washed with H_2O (2 x 4 mL), then sat. NaCl (2 x 3 mL). The organic phase was dried with $MgSO_4$, filtered and concentrated *in vacuo*. Isolation twice using column chromatography (SiO_2, EtOAc:DCM 1:20, then EtOAc:EtOH 9:1) afforded 82.52 mg of **34** as an orange oil in 61 % isolated yield.

^{1}H NMR (400 MHz, $CDCl_3$) 9.12 (dd, J = 4.5, 2.0 Hz, 1H, H-1), 8.67 (ddd, J = 15.2, 2.0, 0.9 Hz, 1H, H-3), 8.12 (dd, J = 8.5, 1.1 Hz, 1H, H-8), 7.88 (dd, J = 8.2, 1.4 Hz, 1H, H-5), 7.80 (ddd, J = 8.5, 6.9, 1.5 Hz, 1H, H-7), 7.60 (ddd, J = 8.1, 6.9, 1.1 Hz, 1H, H-6), 4.26 – 4.06 (m, 5H, H-10), 1.32 (t, J = 7.0 Hz, 6H, H-11).

^{13}C NMR (101 MHz, $CDCl_3$) 150.54 (d, J = 12.3 Hz, C-1), 149.31 (d, J = 1.5 Hz, C-9), 141.95 (d, J = 8.6 Hz, C-3), 131.78 (C-7), 129.45 (d, J = 1.4 Hz, C-8), 128.63 (C-5), 127.53 (d, J = 1.3 Hz, C-6), 126.64 (d, J = 13.5 Hz, C-4), 121.83 (d, J = 189.2 Hz, C-2), 62.52 (d, J = 5.5 Hz, C-10), 16.32 (d, J = 6.3 Hz, C-11).

^{31}P NMR (162 MHz, $CDCl_3$) 16.14.

MS (EI): m/z (relative intensity (%)): 265 (56, M^+), 236 (56), 209 (100), 192 (49), 156 (71) 128 (57), 101 (30).

HR-MS (ESI) m/z $[M + Na]^+$: Calculated for $C_{13}H_{16}NNaO_3P$: 288.0766. Found: 288.0760 (-0.1 ppm)

This compound has been reported in the literature [234].

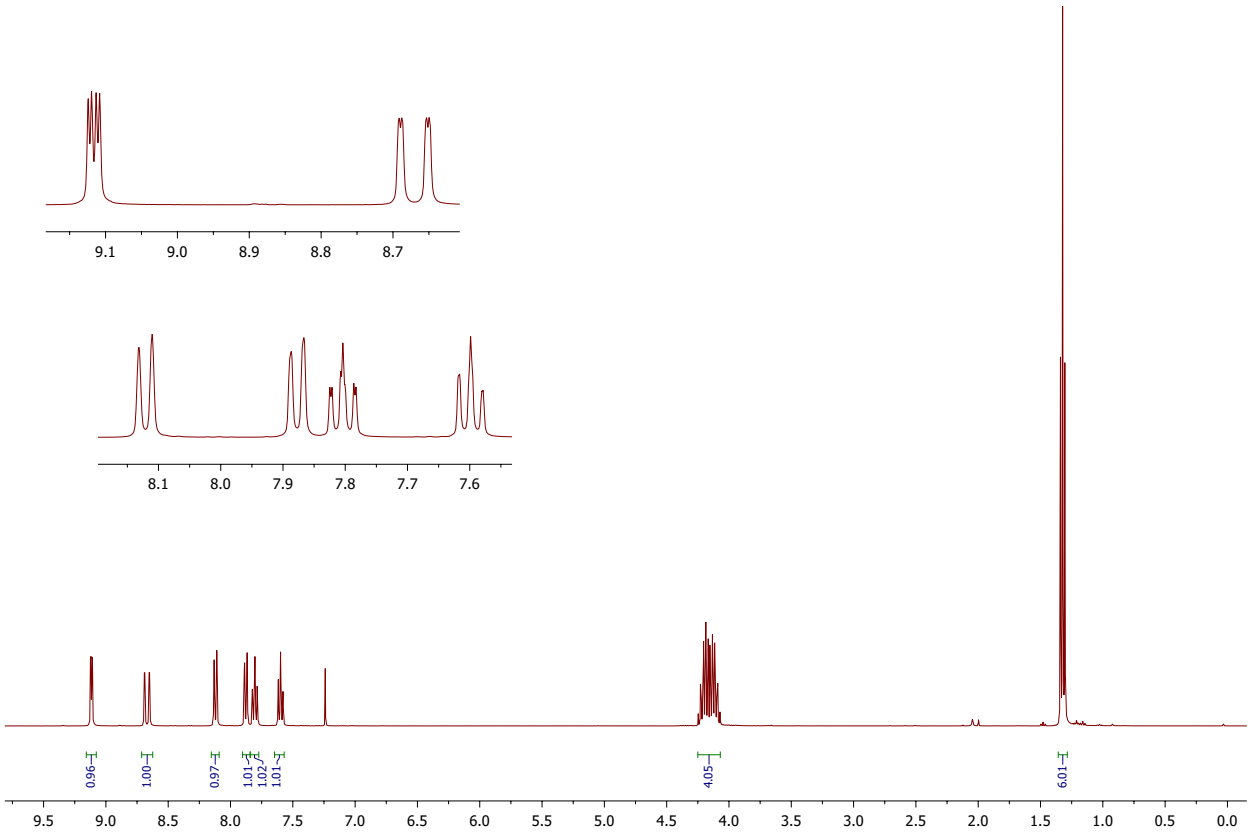

Figure 5.40: ^{1}H NMR spectrum of diethyl 3-quinolinylphosphonate (**34**) (400 MHz, $CDCl_3$).

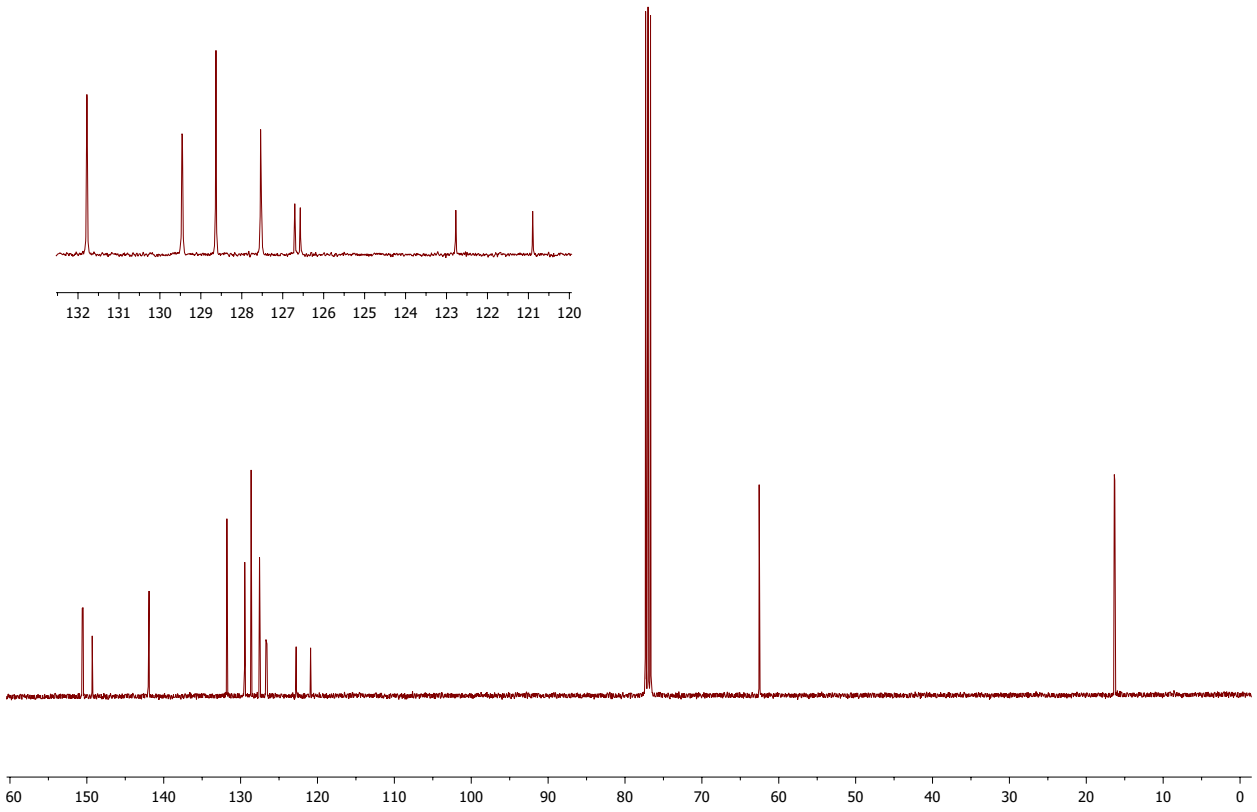

Figure 5.41: ^{13}C NMR spectrum of of diethyl 3-quinolinylphosphonate (**34**) (101 MHz, $CDCl_3$).

5.3.3.2 Diethyl 6-methoxy-3-quinolinylphosphonate (48)

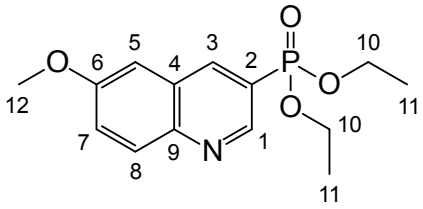

Cl-EDA was prepared according to procedure 5.3.2.1. This afforded Cl-EDA (0.72 mmol, 1.4 equiv in 8 mL dry toluene) which was transferred to a cooled addition funnel (0 °C) and added dropwise over 20-25 min to a mixture of 5-methoxyindole **39** (73.6 mg, 0.50 mmol, 1.0 equiv.), CS_2CO_3 (209.3 mg, 0.64 mmol, 1.3 equiv.) and $Rh_2(esp)_2$ (13.5 mg, 0.018 mmol, 0.036 equiv.) in 5 mL dry toluene at (0 °C). The ice bath was removed, and the dark brown mixture was allowed to reach room temperature before it was concentrated *in vacuo*. The crude was then dissolved in 10 mL EtOAc, transferred to a separatory funnel and washed with 2 x 4 mL H_2O, 1 x 4 mL sat. NaCl, dried with $MgSO_4$, filtered and concentrated *in vacuo*. The remaining oily mixture was then triturated with EtOAc:Hex (1:1), the precipitate (a red solid) was filtered off by vacuum filtration, the filtrate was collected and concentrated *in vacuo*. Isolation thrice using column chromatography (SiO_2, EtOAc:Hex 1:1, then EtOAc:MeOH 10:1, then 5 % EtOH in EtOAc) which afforded **48** as a orange oil.

IS-yield: 62 %

^{1}H NMR (400 MHz, $CDCl_3$) δ 8.98 (dd, J = 4.6, 1.9 Hz, 1H, H-1), 8.57 (dd, J = 15.3, 1.8 Hz, 1H, H-3), 8.03 (d, J = 9.2 Hz, 1H, H-8), 7.46 (dd, J = 9.2, 2.8 Hz, 1H, H-7), 7.12 (d, J = 2.8 Hz, 1H, H-5), 4.32 – 4.04 (m, 5H, H-11), 3.93 (s, 3H, H-13), 1.34 (t, J = 7.1 Hz, 6H, H-12).

^{13}C NMR (101 MHz, $CDCl_3$) δ 158.42 (d, J = 1.7 Hz, C-6), 148.21 (d, J = 11.8 Hz, C-1), 145.62 (C-9), 140.46 (d, J = 8.9 Hz, C-3), 130.87 (d, J = 1.6 Hz, C-8), 127.86 (d, J = 13.7 Hz, C-4), 124.75 (C-7), 122.00 (d, J = 188.5 Hz, C-2), 105.63 (C-5), 62.51 (d, J = 5.5 Hz, C-11), 55.66 (C-13), 16.36 (d, J = 6.4 Hz, C-12).

^{31}P NMR (162 MHz, $CDCl_3$) δ 16.57.

MS (EI): m/z (relative intensity (%)): 295 (99, M^+), 267 (85), 239 (100), 221 (74), 186 (73) 158 (43).

HR-MS (ESI) m/z $[M + Na]^+$: Calculated for $C_{14}H_{18}NNaO_4P$: 318.0871 Found: 318.0866 (0.0 ppm).

This compound has not been reported in literature.

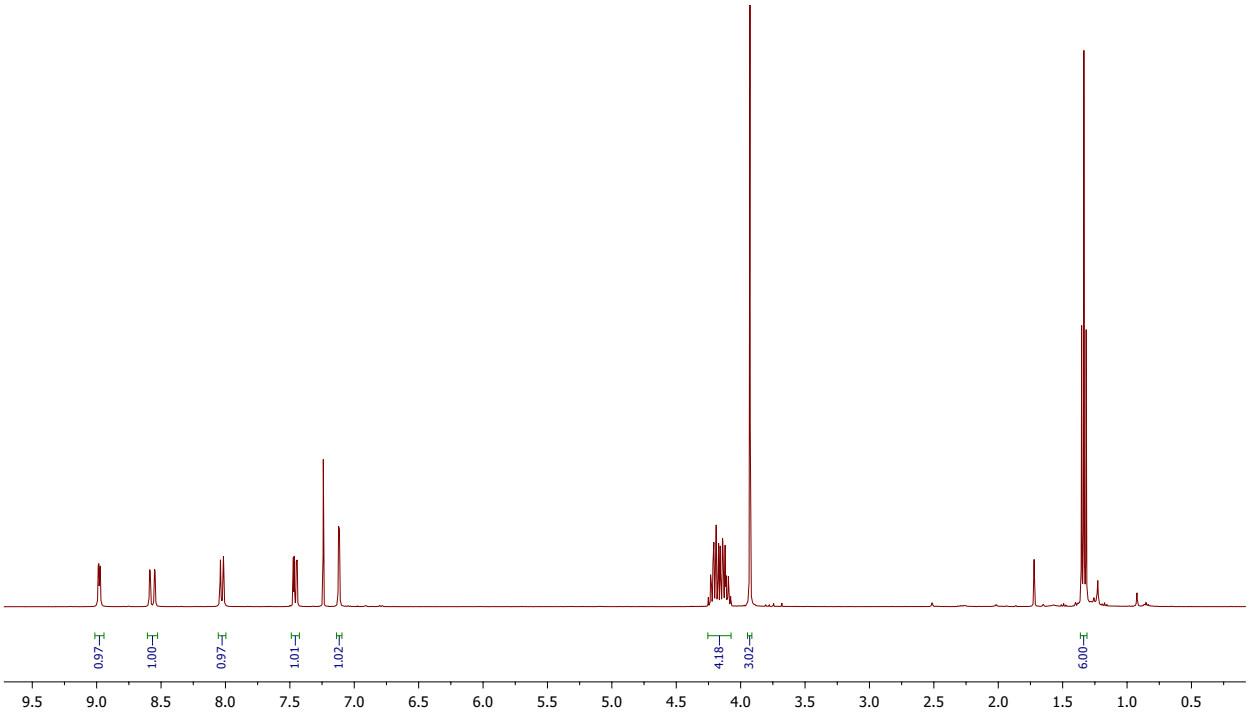

Figure 5.42: ^{1}H NMR spectrum of diethyl 6-methoxy-3-quinolinylphosphonate (**48**) (400 MHz, $CDCl_3$).

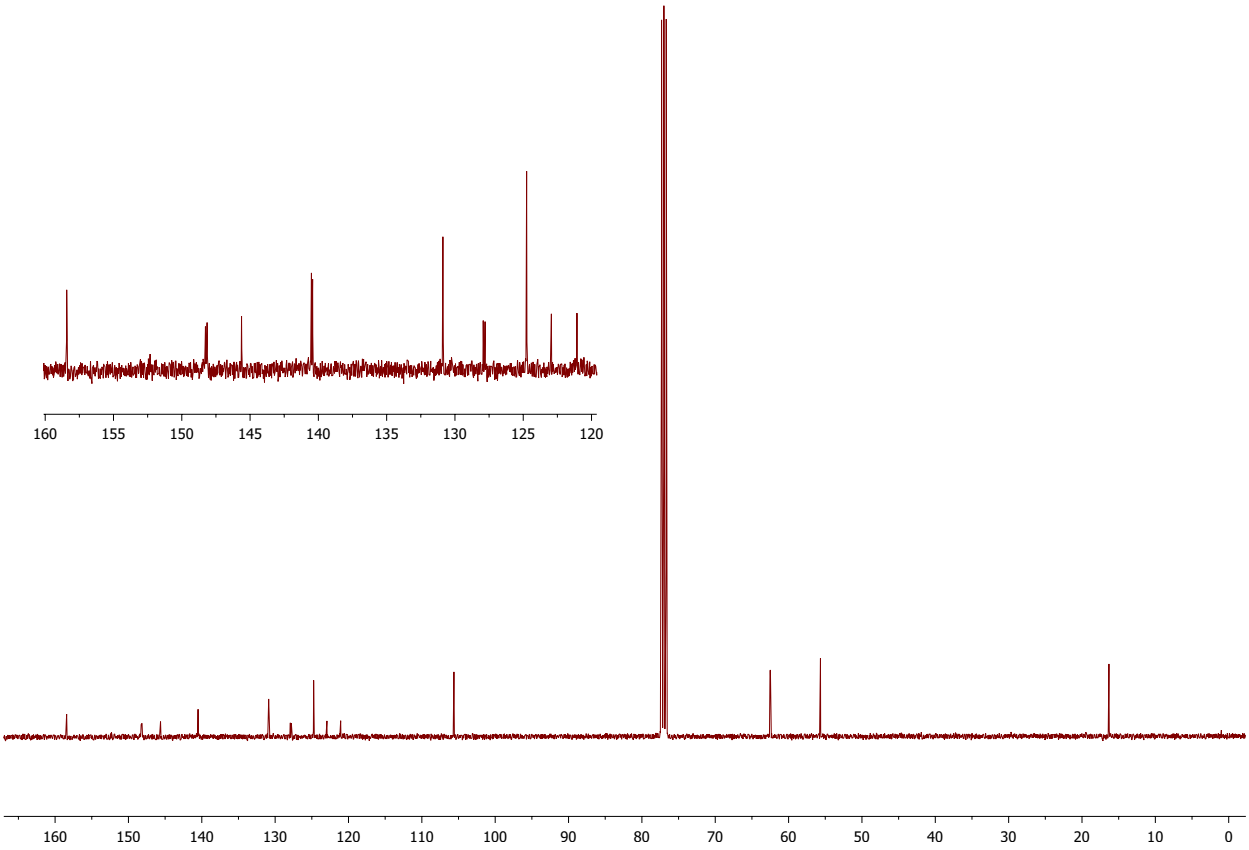

Figure 5.43: ^{13}C NMR spectrum of diethyl 6-methoxy-3-quinolinylphosphonate (**48**) (101 MHz, $CDCl_3$).

5.3.3.3 Diethyl 6-benzyloxy-3-quinolinylphosphonate (49)

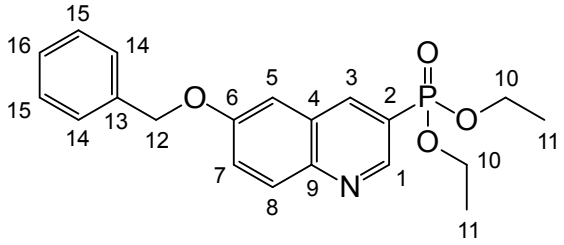

Cl-EDP was prepared according to procedure 5.3.2.1. This afforded Cl-EDP (1.00 mmol, 1.4 equiv in 10 mL dry toluene) which was transferred to a cooled addition funnel (0 °C) and added dropwise over 25 min to a mixture of 5-benzyloxyindole **40** (156.7 mg, 0.70 mmol, 1.0 equiv.), CS_2CO_3 (295.0 mg, 0.91 mmol, 1.3 equiv.) and $Rh_2(esp)_2$ (17.1 mg, 0.023 mmol, 0.033 equiv.) in 10 mL dry toluene at (0 °C). The resulting dark mixture was stirred for an additional 30 min and concentrated *in vacuo*. *in vacuo*. The crude was then dissolved in 10 mL EtOAc, transferred to a separatory funnel and washed with 2 x 4 mL H_2O, 1 x 4 mL sat. NaCl, dried with $MgSO_4$, filtered and concentrated *in vacuo*. The crude was then dissolved in 15 mL EtOAc, transferred to a separatory funnel and washed with 2 x 5 mL H_2O, 2 x 5 mL sat. NaCl, dried with $MgSO_4$, filtered and concentrated *in vacuo*. The mixture was triturated with hexane twice, and the precipitate (a brown solid) was filtered off by vacuum filtration, and the filtrate was concentraed *in vacuo*. Isolation using column chromatography (SiO_2, EtOAc:Hexane 1:1 –> EtOAc:Hexane 2:1) afforded pink-orange crystals that were washed in a minimal amount of Et_2O to afford **49** as a white crystals.

IS-yield: 48 %

^{1}H NMR (400 MHz, $CDCl_3$): δ 8.98 (dd, J = 4.6, 1.9 Hz, 1H, H-1), 8.54 (dd, J = 15.3, 1.9 Hz, 1H, H-3), 8.04 (d, J = 9.2 Hz, 1H, H-8), 7.55 (dd, J = 9.2, 2.8 Hz, 1H, H-7), 7.50 – 7.30 (m, 5H, H-14, H-15, H-16), 7.19 (d, J = 2.8 Hz, 1H, H-5), 5.19 (s, 2H, H-12), 4.26 – 4.06 (m, 4H, H-10), 1.34 (t, J = 7.1 Hz, 6H, H-11).

^{13}C NMR (101 MHz, $CDCl_3$): δ 157.47 (d, J = 1.8 Hz, C-6), 148.26 (d, J = 12.3 Hz, C-1), 145.63 (d, J = 1.4 Hz, C-9), 140.56 (d, J = 8.9 Hz, C-3), 136.09 (C-14), 130.96 (d, J = 1.5 Hz, C-8), 128.74 (C-15), 128.29 (C-17), 127.78 (d, J = 13.8 Hz, C-4), 127.51 (C-14), 125.08 C-7), 122.01 (d, J = 188.4 Hz, C-2), 107.09 (C-5), 70.43 (C-13), 62.52 (d, J = 5.5 Hz, C-10), 16.36 (d, J = 6.4 Hz, C-11).

^{31}P NMR (162 MHz, $CDCl_3$) δ 16.56

MS (EI) m/z (relative intensity (%)): 371 (14, M^+), 343 (1), 208 (2), 91 (100), 65 (7).

HR-MS (ESI) m/z $[M + Na]^+$: Calculated for $C_{20}H_{22}NNaO_4P$: 394.1184.
Found: 394.1179 (0.0 ppm).

Melting point: 113–117 °C.

This compound has not been reported in the literature.

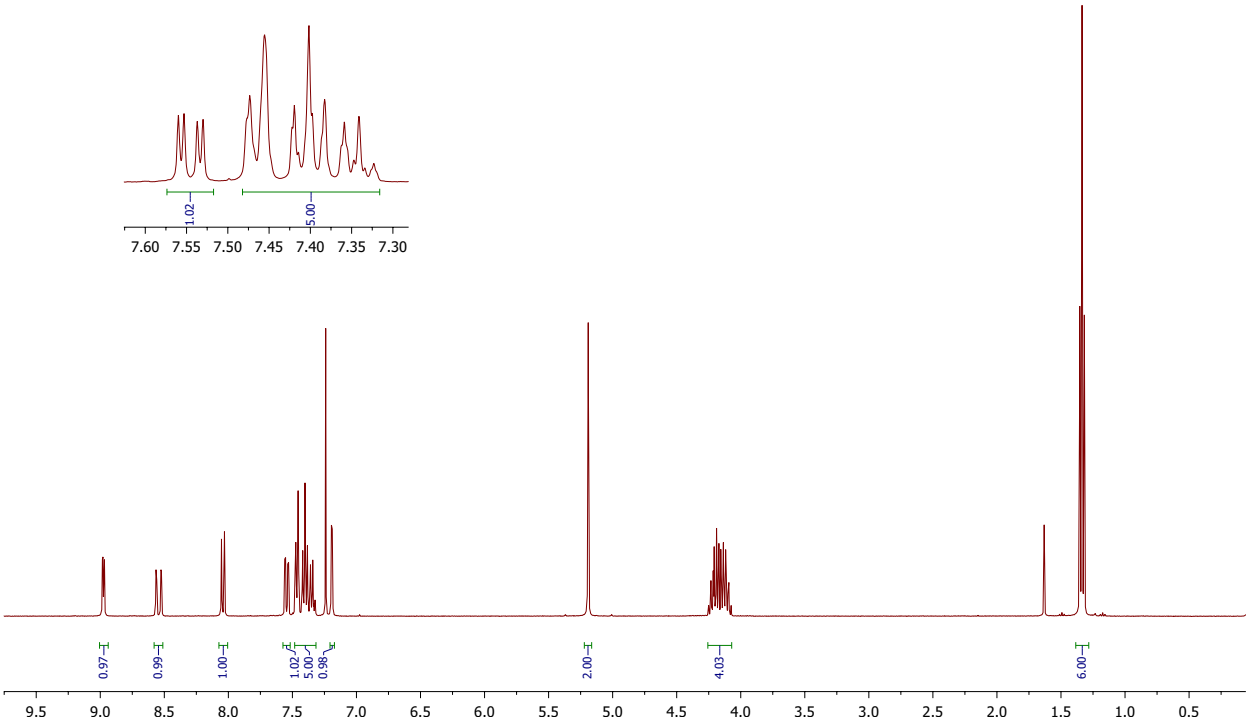

Figure 5.44: ^{1}H NMR spectrum of diethyl 6-benzyloxy-3-quinolinylphosphonate (**49**) (400 MHz, $CDCl_3$).

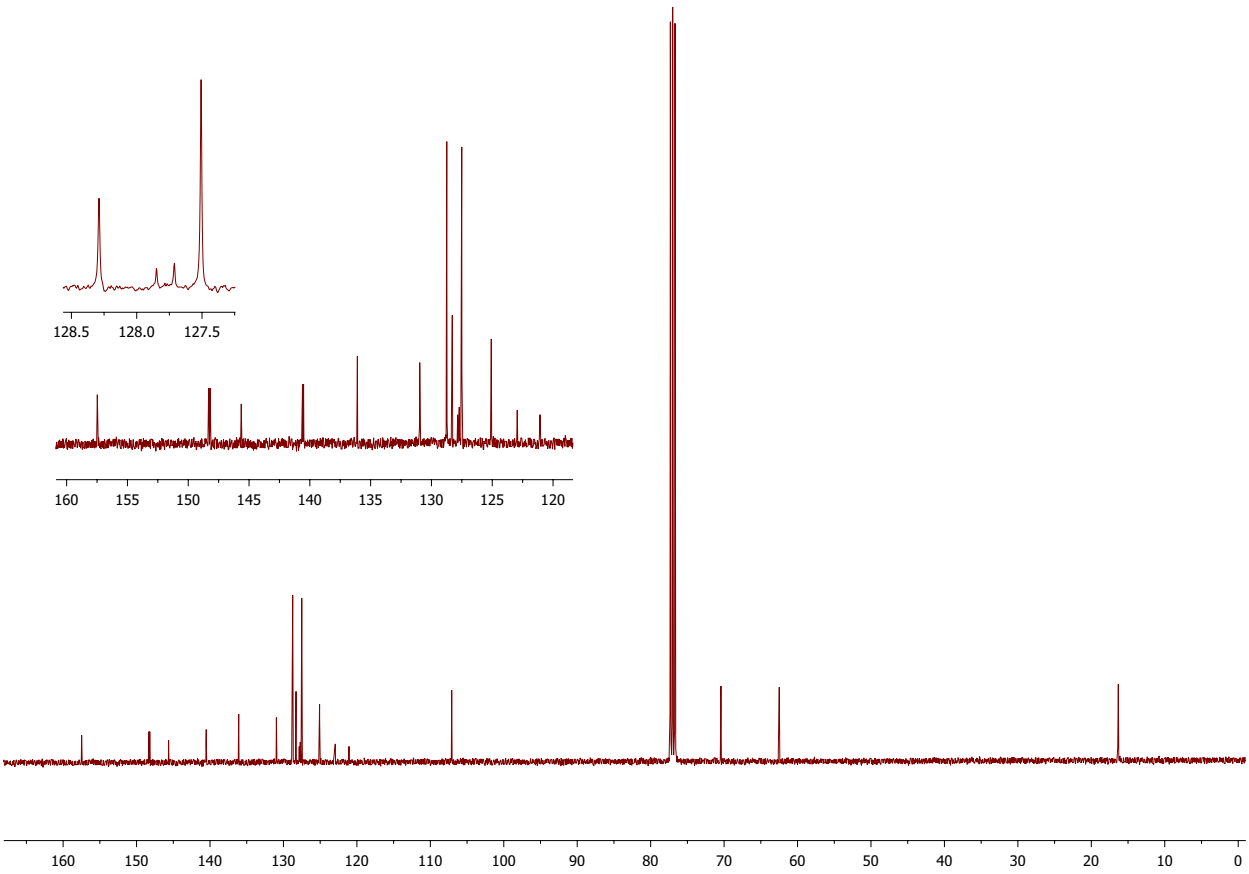

Figure 5.45: ^{13}C NMR spectrum of diethyl 6-benzyloxy-3-quinolinylphosphonate (**49**) (101 MHz, $CDCl_3$).

5.3.3.4 Diethyl 6-bromo-3-quinolinylphosphonate (50)

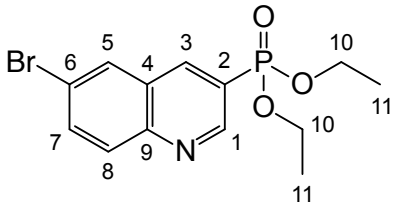

Cl-EDA was prepared according to procedure 5.3.2.1. This afforded Cl-EDA (0.72 mmol, 1.4 equiv in 8 mL dry toluene) which was transferred to a cooled addition funnel (0 °C) and added dropwise over 20-25 min to a mixture of 5-bromoindole **41** (98.4 mg, 0.50 mmol, 1.0 equiv.), CS_2CO_3 (209.9 mg, 0.64 mmol, 1.3 equiv.) and $Rh_2(esp)_2$ (13.8 mg, 0.018 mmol, 0.036 equiv.) in 5 mL dry toluene at (0 °C). The resulting dark mixture was stirred for an additional 30 min and concentrated *in vacuo*. *in vacuo*. The crude was then dissolved in 10 mL EtOAc, transferred to a separatory funnel and washed with 2 x 4 mL H_2O, 1 x 4 mL sat. NaCl, dried with $MgSO_4$, filtered and concentrated *in vacuo*. The crude was then dissolved in 10 mL EtOAc, transferred to a separatory funnel and washed with 2 x 4 mL H_2O, 1 x 4 mL sat. NaCl, dried with $MgSO_4$, filtered and concentrated *in vacuo*. The remaining oily mixture was then triturated with EtOAc:Hex (1:1), the precipitate (a red solid) was filtered off by vacuum filtration, the filtrate was collected and concentrated *in vacuo*. Isolation twice using column chromatography (SiO_2, EtOAc:Hex 2:1 and EtOAc:EtOH 20:1) afforded an oil that was diluted in hexane and the hexane soluble fraction was decanted. The remaining non-hexane soluble precipitate formed crystals. The crystals were washed three times with 2-3 mL hexane, which afforded **50** as orange crystals.

IS-yield: 46 %

^{1}H NMR (400 MHz, $CDCl_3$) δ 9.13 (dd, J = 4.8, 2.0 Hz, 1H, H-1), 8.59 (dd, J = 15.2, 1.4 Hz 1H, H-3), 8.05 (d, J = 2.2 Hz, 1H, H-5), 8.02 (d, J = 9.0 Hz, 1H, H-8), 7.88 (dd, J = 9.0, 2.2 Hz, 1H, H-7), 4.30-4.04 (m, 4H, H-10), 1.34 (t, J = 7.1 Hz, 6H, H-11).

^{13}C NMR (101 MHz, $CDCl_3$) δ 150.93 (d, J = 12.0 Hz, C-1), 147.91 (C-9), 140.75 (d, J = 8.7 Hz, C-3), 135.23 (C-7), 131.21 (d, J = 1.6 Hz, C-8), 130.57 (C-5), 127.79 (d, J = 14.0 Hz, C-4), 123.08 (d, J = 189.0 Hz, C-2), 121.55 (d, J = 2.1 Hz, C-6), 62.72 (d, J = 5.6 Hz, C-10), 16.36 (d, J = 6.4 Hz, C-11).

^{31}P NMR (162 MHz, $CDCl_3$) δ 15.30.

MS (EI): m/z (relative intensity (%)): 343/345 (58/58, M^+/M+2), 315/317 (27/26), 287/289 (81/80), 236 (78), 208 (62) 127 (100), 100 (75).

HR-MS (ESI) m/z $[M + Na]^+$: Calculated for $C_{13}H_{15}BrNNaO_3P$: 365.9871/367.9850. Found: 365.9865/367.9845 (0.0 ppm).

This compound has not been reported in the literature.

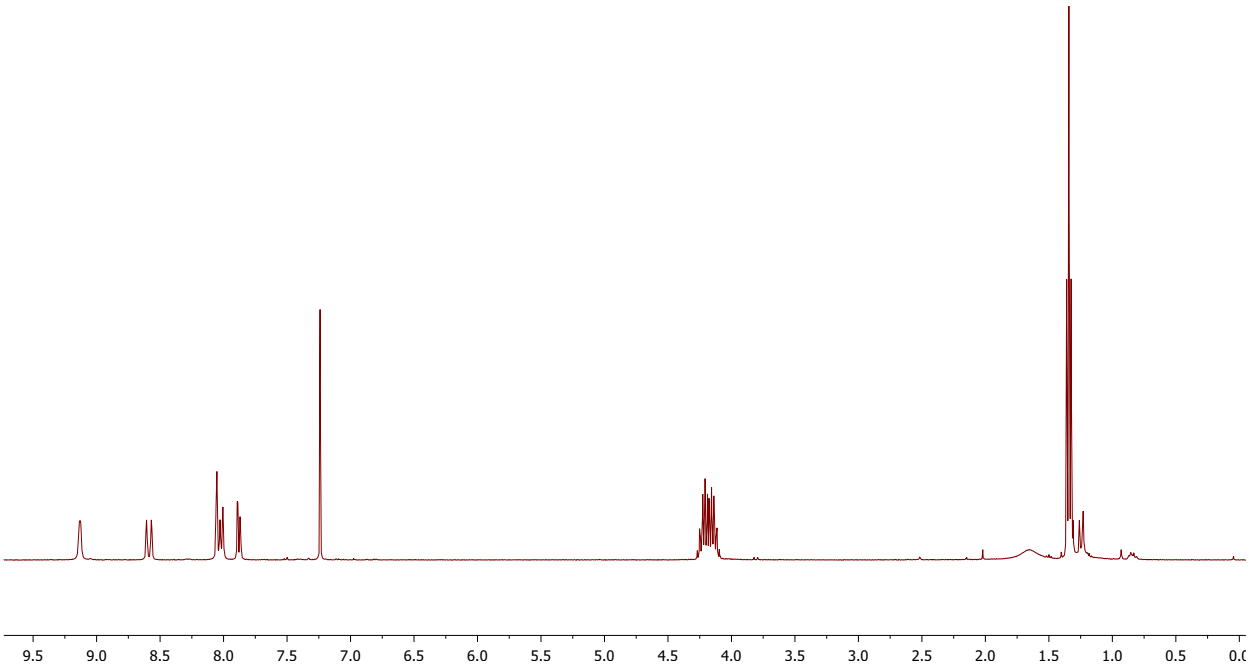

Figure 5.46: ^{1}H NMR spectrum of diethyl 6-bromo-3-quinolinylphosphonate (**50**) (400 MHz, $CDCl_3$).

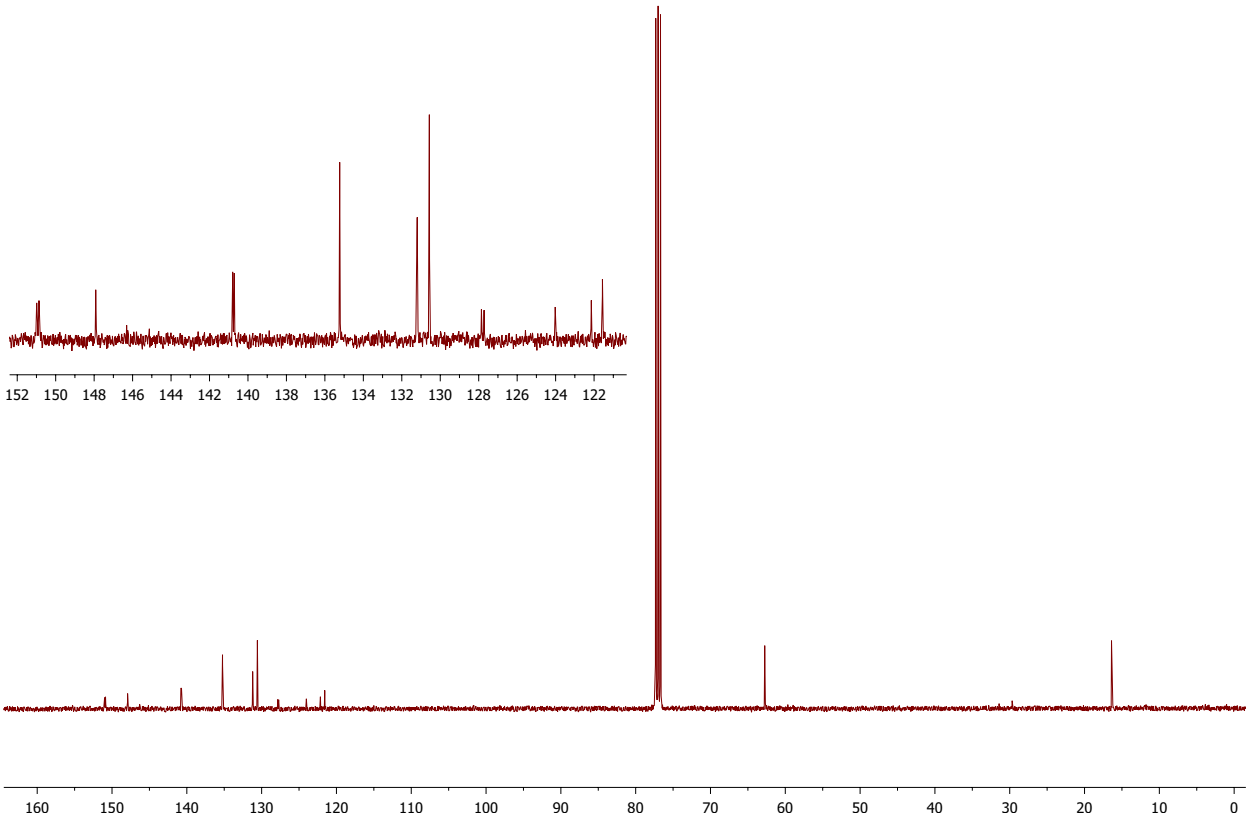

Figure 5.47: ^{13}C NMR spectrum of diethyl 6-bromo-3-quinolinylphosphonate (**50**) (101 MHz, $CDCl_3$).

5.3.3.5 Diethyl 6,7-difluoro-3-quinolinylphosphonate (51)

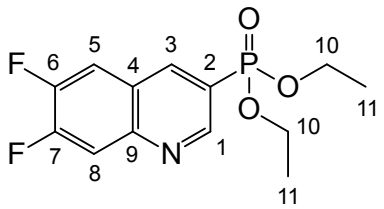

Cl-EDP was prepared according to procedure 5.3.2.1. This afforded Cl-EDP (1.02 mmol, 1.4 equiv in 10 mL dry toluene) which was transferred to a cooled addition funnel (0 °C) and added dropwise over 20-25 min to a mixture of 5,6-difluoroindole **42** (107.3 mg, 0.70 mmol, 1.0 equiv.), CS_2CO_3 (295.2 mg, 0.91 mmol, 1.3 equiv.) and $Rh_2(esp)_2$ (19.0 mg, 0.025 mmol, 0.036 equiv.) in 10 mL dry toluene at (0 °C). The resulting dark mixture was stirred for an additional 30 min and concentrated *in vacuo*. *in vacuo*. The crude was then dissolved in 10 mL EtOAc, transferred to a separatory funnel and washed with 2 x 4 mL H_2O, 1 x 4 mL sat. NaCl, dried with $MgSO_4$, filtered and concentrated *in vacuo*. The crude was then dissolved in 15 mL EtOAc, transferred to a separatory funnel and washed with 2 x 5 mL H_2O, 2 x 5 mL sat. NaCl, dried with $MgSO_4$, filtered and concentrated *in vacuo*. The mixture was triturated with hexane twice, and the precipitate (a brown solid) was filtered off by vacuum filtration, and the filtrate was concentraed *in vacuo*. Isolation using column chromatography (SiO_2, EtOAc:Hex 1:1) afforded **51** as a off-white/pale yellow crystals.

IS-yield: 46 %

^{1}H NMR (400 MHz, $CDCl_3$) δ 9.09 (dd, J = 4.6, 1.9 Hz, 1H, H-1) , 8.60 (ddd, J = 15.1, 2.0, 0.7 Hz, 1H, H-3), 7.88 (dd, J = 10.9, 7.6 Hz, 1H, H-5), 7.62 (dd, J = 9.8, 8.3 Hz, 1H, H-8), 4.28 – 4.05 (m, 4H, H-10), 1.34 (td, J = 7.0, 0.6 Hz, 6H, H-11).

^{13}C NMR (101 MHz, $CDCl_3$) δ 153.73 (dd, J = 258.4, 16.0 Hz, C-6), 150.92 (dd, J = 12.0, 2.9 Hz, C-1), 150.69 (ddd, J = 256.2, 16.0, 2.0 Hz, C-7), 146.73 (d, J = 11.2 Hz, C-9), 140.86 (ddd, J = 8.9, 5.3, 1.8 Hz, C-3) , 123.74 (ddd, J = 13.8, 8.1, 1.0 Hz, C-4), 122.47 (dd, J = 190.3, 2.8 Hz, C-2), 115.96 (d, J = 16.7 Hz, C-5), 113.84 (dd, J = 17.6, 2.1 Hz, C-8), 62.71 (d, J = 5.6 Hz, C-10), 16.34 (d, J = 6.4 Hz, C-11).

^{19}F NMR (decoupled) (377 MHz, $CDCl_3$) δ -127.10 (d, J = 20.5 Hz, F-6), -132.98 (d, J = 20.6 Hz, F-7).

^{19}F NMR (coupled) (377 MHz, $CDCl_3$) δ -127.10 (ddd, J = 19.8, 10.7, 8.3 Hz, F-6), -132.98 (dt, J = 20.6, 8.6 Hz, F-7).

^{31}P NMR (162 MHz, $CDCl_3$) δ 15.34.

MS (EI): m/z (relative intensity (%)): 301 (42, M^+), 272 (45), 245 (92), 228 (53), 192 (92), 165 (100), 164 (95).

HR-MS (ESI) m/z $[M + Na]^+$: Calculated for $C_{13}H_{14}F_2NNaO_3P$: 324.0577. Found: 324.0572 (0.0 ppm).

Melting point: 94–96 °C.

This compound has not been reported in the literature.

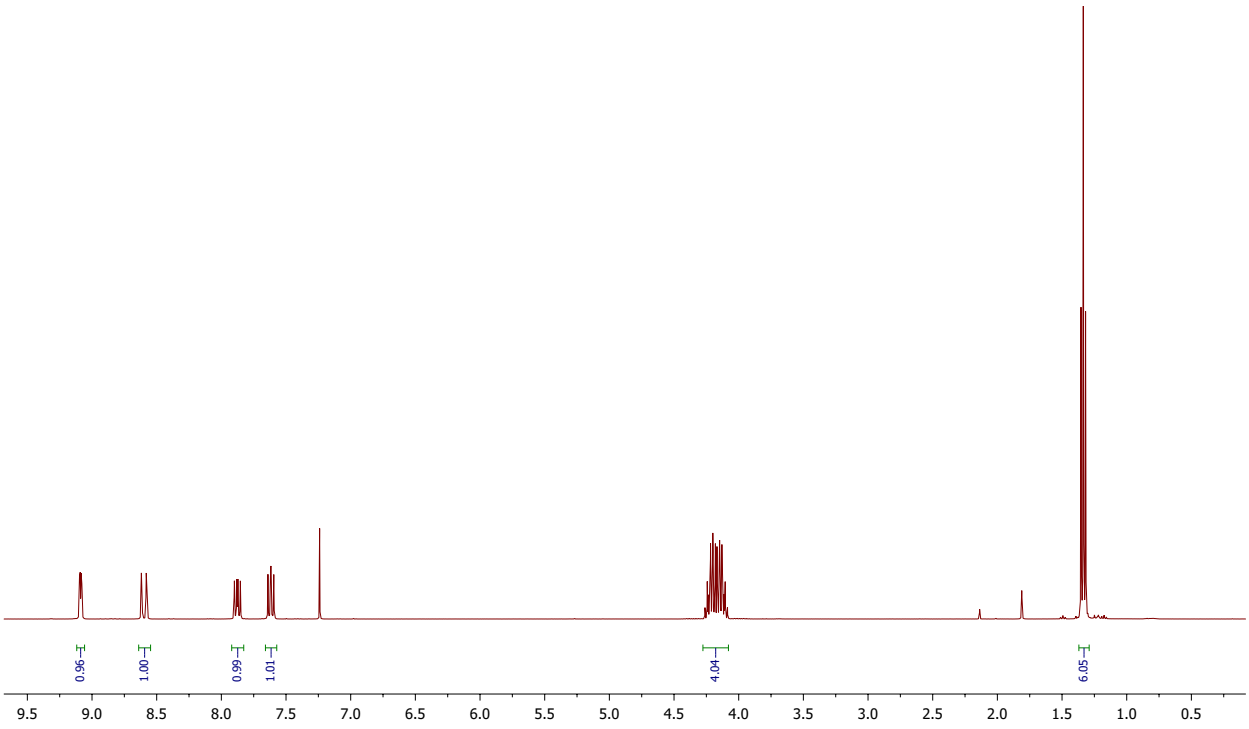

Figure 5.48: ^{1}H NMR spectrum of diethyl 6,7-difluoro-3-quinolinylphosphonate (**51**) (400 MHz, $CDCl_3$).

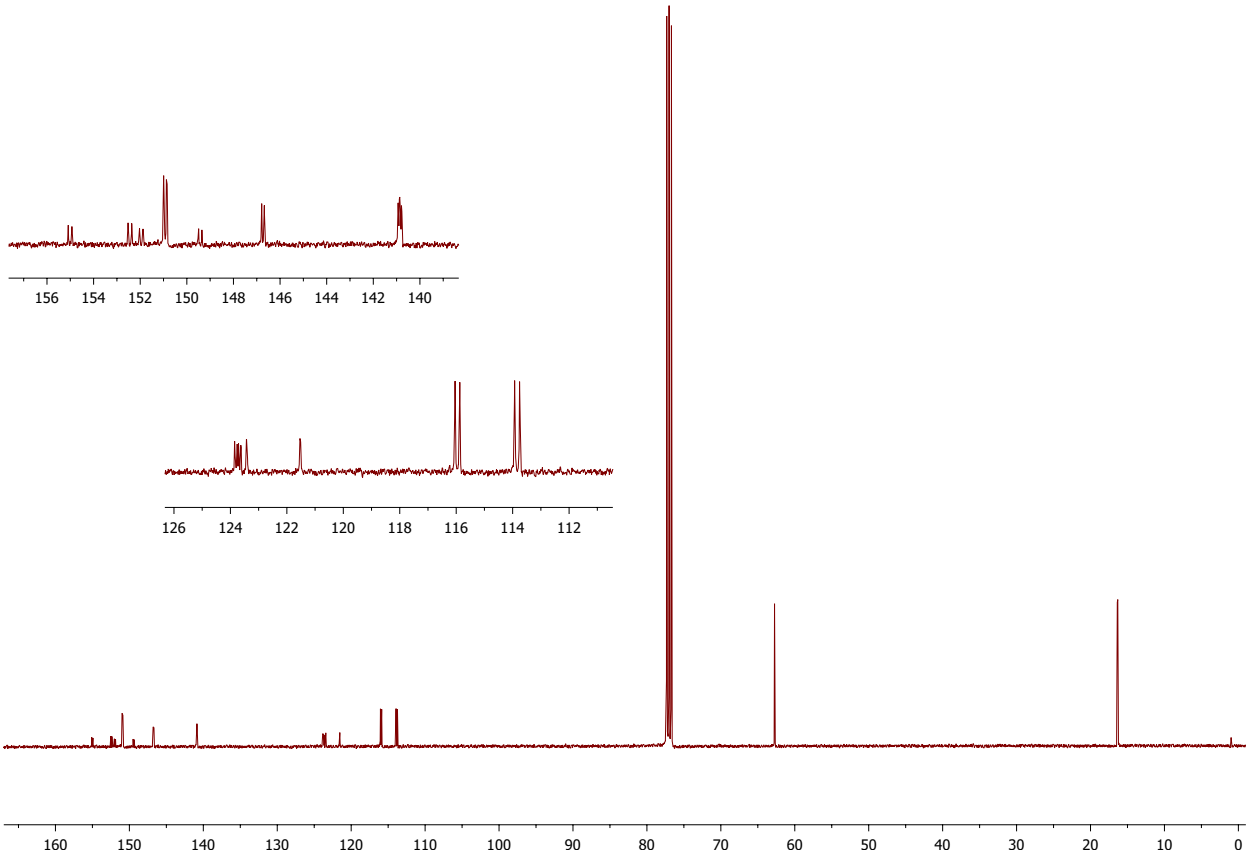

Figure 5.49: ^{13}C NMR spectrum of diethyl 6,7-difluoro-3-quinolinylphosphonate (**51**) (101 MHz, $CDCl_3$).

5.3.3.6 Diethyl 7-bromo-3-quinolinylphosphonate (52)

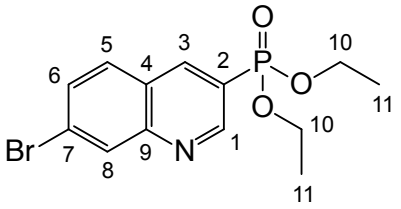

Cl-EDA was prepared according to procedure 5.3.2.1. This afforded Cl-EDA (0.72 mmol, 1.4 equiv in 8 mL dry toluene) which was transferred to a cooled addition funnel (0 °C) and added dropwise over 20-25 min to a mixture of 6-bromoindole **43** (96.1 mg, 0.50 mmol, 1.0 equiv.), CS_2CO_3 (206.5 mg, 0.63 mmol, 1.3 equiv.) and $Rh_2(esp)_2$ (14.0 mg, 0.018 mmol, 0.036 equiv.) in 5 mL dry toluene at (0 °C). The resulting dark mixture was stirred for an additional 30 min and concentrated *in vacuo*. *in vacuo*. The crude was then dissolved in 10 mL EtOAc, transferred to a separatory funnel and washed with 2 x 4 mL H_2O, 1 x 4 mL sat. NaCl, dried with $MgSO_4$, filtered and concentrated *in vacuo*. The crude was then dissolved in 10 mL EtOAc, transferred to a separatory funnel and washed with 2 x 4 mL H_2O, 1 x 4 mL sat. NaCl, dried with $MgSO_4$, filtered and concentrated *in vacuo*. The remaining oily mixture was then triturated with EtOAc:Hex (1:1), the precipitate (a red solid) was filtered off by vacuum filtration, the filtrate was collected and concentrated *in vacuo*. Isolation twice[5] using column chromatography (SiO_2, EtOAc:Hex 1:1, then EtOAc:Hex 3:1) afforded **52** as an orange oil.

IS-yield: 45 %

^{1}H NMR (400 MHz, $CDCl_3$) δ 9.11 (dd, J = 4.5, 2.0 Hz, 1H, H-1), 8.64 (ddd, J = 15.2, 2.0, 0.8 Hz, 1H, H-3), 8.32 (d, J = 1.8 Hz, 1H, H-8), 7.75 (d, J = 8.7 Hz, 1H, H-5), 7.69 (dd, J = 8.7, 1.9 Hz, 1H, H-6), 4.29 – 4.04 (m, 4H, H-11), 1.33 (td, J = 7.1, 0.6 Hz, 6H, H-12).

^{13}C NMR (101 MHz, $CDCl_3$) δ 151.49 (d, J = 12.1 Hz, C-1), 149.73 (d, J = 1.4 Hz, C-9), 141.66 (d, J = 8.7 Hz, C-3), 131.89 (d, J = 1.5 Hz, C-8), 131.19 (d, J = 1.4 Hz, C-6), 129.74 (C-5), 126.22 (C-7), 125.25 (d, J = 13.6 Hz, C-4), 122.40 (d, J = 189.8 Hz, C-2), 62.63 (d, J = 5.6 Hz, C-11), 16.31 (d, J = 6.3 Hz, C-12).

^{31}P NMR (162 MHz, $CDCl_3$) δ 15.53.

MS (EI): m/z (relative intensity (%)): 343/345 (38/37, M^+/M+2), 315/317 (25/25), 287/289 (80/79), 236 (100) 127 (51), 100 (38).

HR-MS (ESI) m/z $[M + Na]^+$: Calculated for $C_{13}H_{15}BrNNaO_3P$: 365.9871/367.9850. Found: 365.9865/367.9845 (0.1 ppm).

This compound has not been reported in the literature.

[5] Much co-elution during the first column

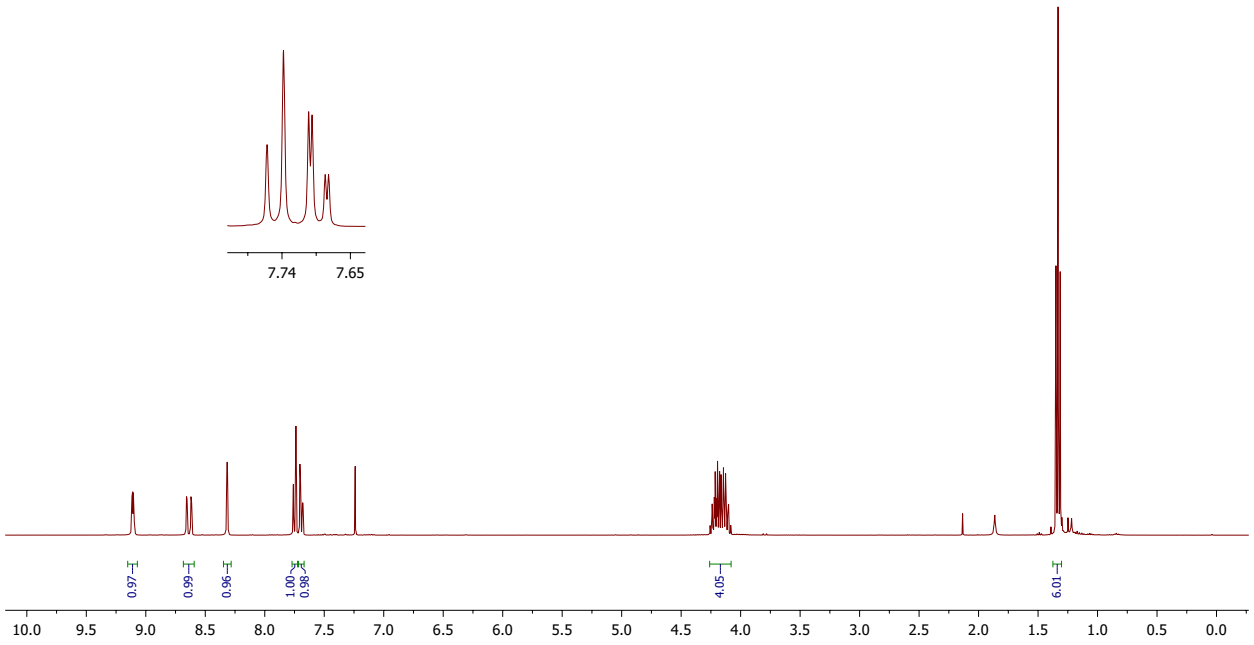

Figure 5.50: ^{1}H NMR spectrum of diethyl 7-bromo-3-quinolinylphosphonate (**52**) (400 MHz, $CDCl_3$).

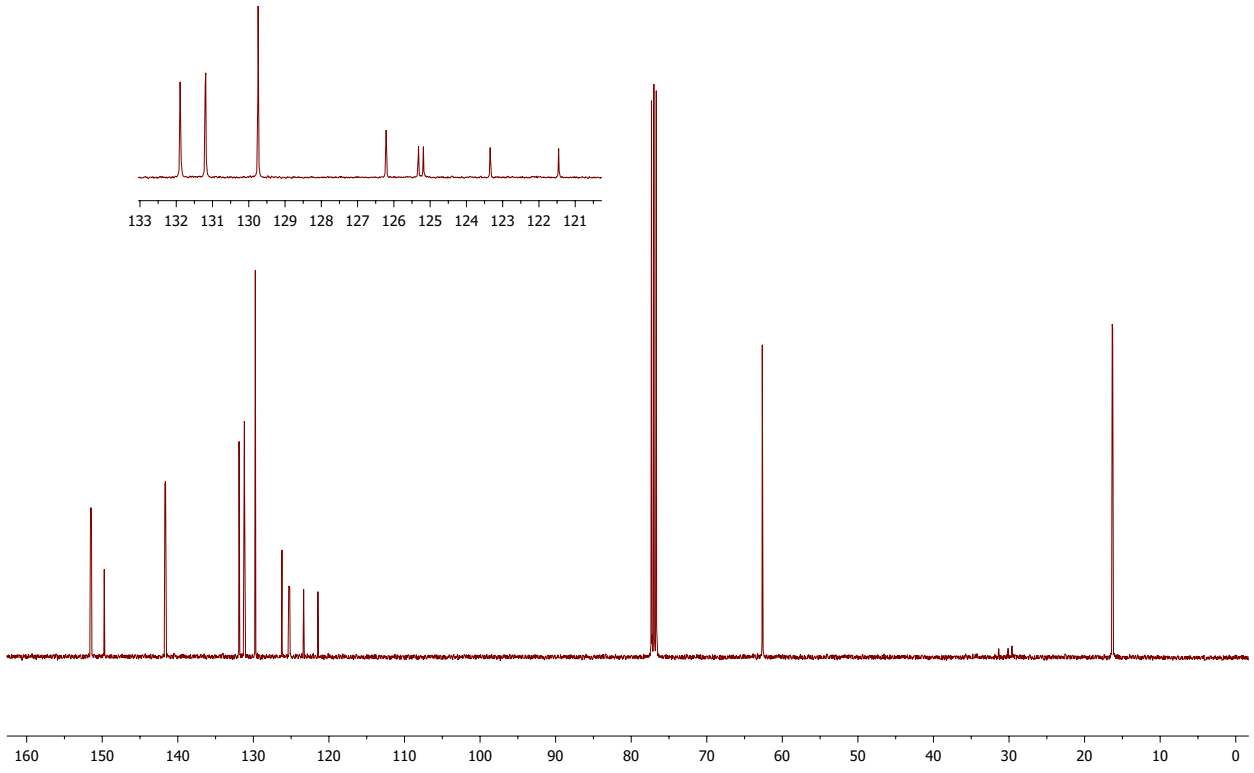

Figure 5.51: ^{13}C NMR spectrum of diethyl 7-bromo-3-quinolinylphosphonate (**52**) (101 MHz, $CDCl_3$).

5.3.3.7 Diethyl 6-nitro-3-quinolinylphosphonate (53)

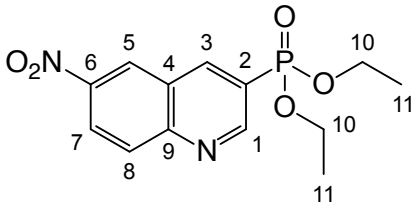

Cl-EDA was prepared according to procedure 5.3.2.1. This afforded Cl-EDA (0.72 mmol, 1.4 equiv in 8 mL dry toluene) which was transferred to a cooled addition funnel (0 °C) and added dropwise over 20-25 min to a mixture of 5-nitroindole **44** (81.3 mg, 0.50 mmol, 1.0 equiv.), CS_2CO_3 (207.2 mg, 0.64 mmol, 1.3 equiv.) and $Rh_2(esp)_2$ (13.8 mg, 0.018 mmol, 0.036 equiv.) in 5 mL dry toluene at (0 °C). The dark mixture brown mixture was stirred for an additional 30 min and concentrated *in vacuo*. The crude was then dissolved in 10 mL EtOAc, transferred to a separatory funnel and washed with 2 x 4 mL H_2O, 1 x 4 mL sat. NaCl, dried with $MgSO_4$, filtered and concentrated *in vacuo*. The remaining oily mixture was then triturated twice; first with EtOAc:Hexane (1:1). The precipitate (a red solid) was filtered by vacuum filtration, the filtrate was collected and concentrated *in vacuo*. Then with hexane, which cause a yellow solid (unconverted starting material) to precipitate. Isolation using column chromatography (SiO_2, EtOAc:Hex 5:1) afforded crystals that were washed with a few mL hexane, then the crystals was dissolved in Et_2O and transferred to another flask, leaving some impurities behind. This process afforded **53** as yellow crystals.

IS-yield: 22 %

^{1}H NMR (400 MHz, $CDCl_3$) δ 9.29 (dd, J = 4.5, 2.0 Hz, 1H, H-1), 8.85 (d, J = 2.7 Hz, 1H, H-3), 8.84 (dd, J = 3.7 Hz, 0.5 Hz, H-5) 8.57 (dd, J = 9.2, 2.5 Hz, 1H, H-7), 8.29 (d, J = 9.2 Hz, 1H, H-8), 4.32 – 4.12 (m, 4H, H-10), 1.36 (td, J = 7.1, 0.5 Hz, 6H, H-11).

^{13}C NMR (101 MHz, $CDCl_3$) δ 153.97 (d, J = 12.1 Hz, C-1), 151.09 (d, J = 1.3 Hz, C-9), 146.12 (d, J = 1.2 Hz, C-6), 143.26 (d, J = 8.5 Hz, C-3), 131.54 (d, J = 1.6 Hz, C-8), 125.65 (d, J = 14.2 Hz, C-4) 125.21 (C-5), 124.96 (C-7), 124.63 (d, J = 191.4 Hz, C-2), 62.98 (d, J = 5.8 Hz, C-10), 16.39 (d, J = 6.4 Hz, C-11).

^{31}P NMR (162 MHz, $CDCl_3$) δ 27.43.

MS (EI): m/z (relative intensity (%)): 310 (25, M^+), 281 (34), 254 (47), 238 (58), 201 (100) 127 (58), 100 (41).

HR-MS (ESI) m/z $[M + Na]^+$: Calculated for $C_{13}H_{15}N_2NaO_5P$: 333.0616 Found: 333.0610 (0.1 ppm)

Melting point: 99–101 °C.

This compound has not been reported in the literature.

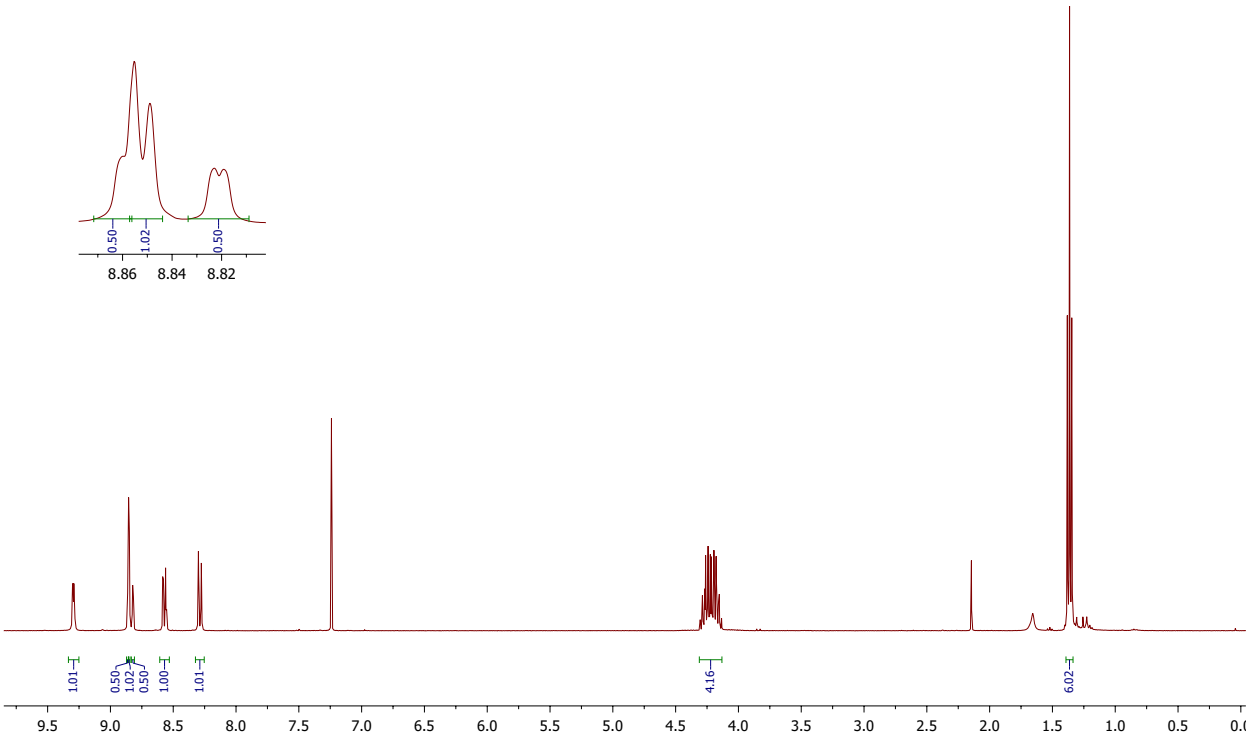

Figure 5.52: ^{1}H NMR spectrum diethyl 6-nitro-3-quinolinylphosphonate (**53**) (400 MHz, $CDCl_3$).

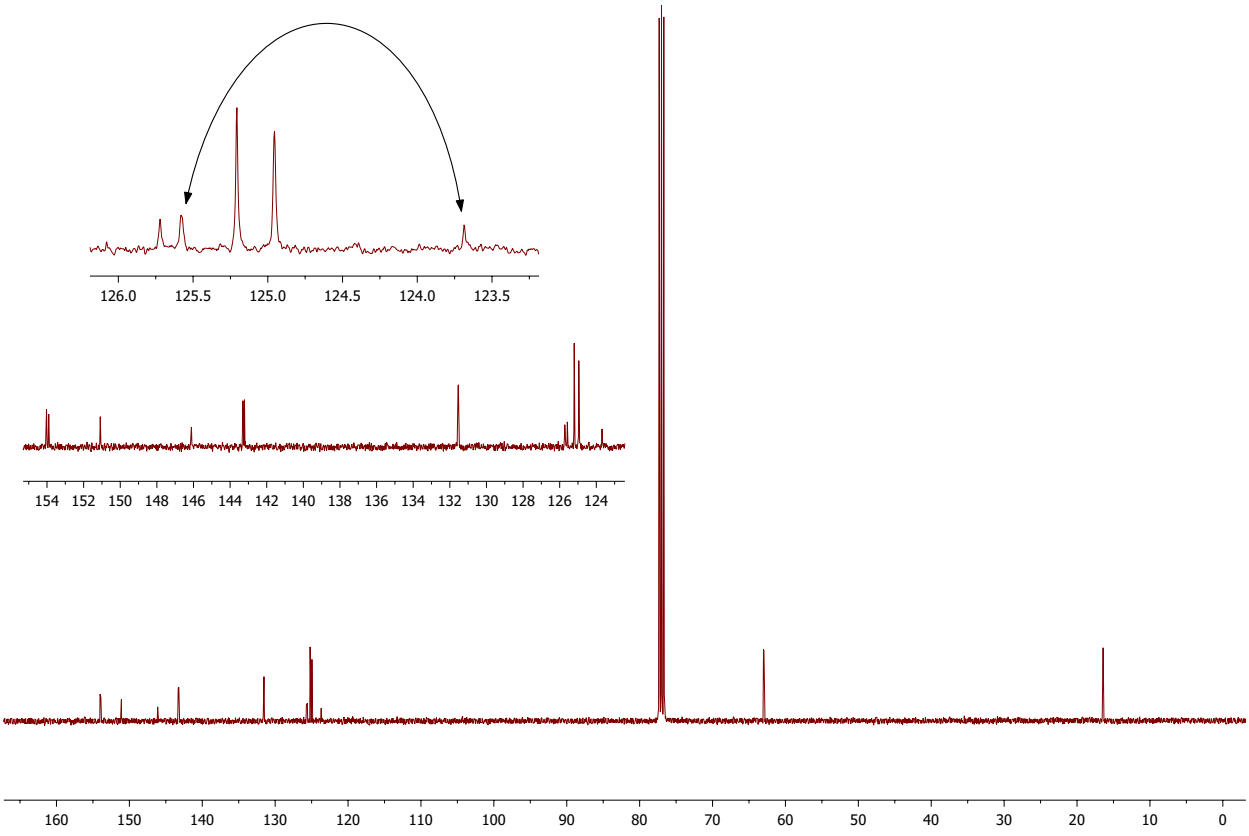

Figure 5.53: ^{13}C NMR spectrum of diethyl 6-nitro-3-quinolinylphosphonate (**53**) (101 MHz, $CDCl_3$). The arrow indicates that the two peaks belong to one signal.

5.3.3.8 Diethyl 4-chloro-3-quinolinylphosphonate (54)

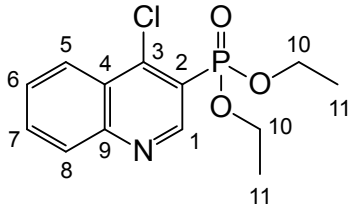

Cl-EDP was prepared according to procedure 5.3.2.1. This afforded Cl-EDP (2.14 mmol, 1.4 equiv in 15 mL dry toluene) which was transferred to a cooled addition funnel (0 °C) and added dropwise over 30 min to a mixture of 3-chloroindole **45** (228.4 mg, 1.50 mmol, 1.0 equiv.), CS_2CO_3 (629.9 mg, 1.90 mmol, 1.3 equiv.) and $Rh_2(esp)_2$ (37.6 mg, 0.05 mmol, 0.033 equiv.) in 15 mL dry toluene at (0 °C). The resulting dark mixture was stirred for an additional 30 min and concentrated *in vacuo*. *in vacuo*. The crude was then dissolved in 35 mL EtOAc, transferred to a separatory funnel and washed with 2 x 7 mL H_2O, 3 x 7 mL sat. NaCl, dried with $MgSO_4$, filtered and concentrated *in vacuo*. The crude was then dissolved in 10 mL EtOAc, transferred to a separatory funnel and washed with 2 x 4 mL H_2O, 1 x 4 mL sat. NaCl, dried with $MgSO_4$, filtered and concentrated *in vacuo*. Isolation thrice using column chromatography (SiO_2, EtOAc:Hex 4:1 twice, then EtOAc:EtOH 9:1) afforded **54** as a yellow oil.

IS-yield: 19 %

^{1}H NMR (400 MHz, $CDCl_3$) δ 9.24 (d, J = 5.4 Hz, 1H, H-1), 8.36 (dd, J = 8.5, 1.3 Hz, 1H, H-5), 8.13 (d, J = 8.4 Hz, 1H, H-8), 7.84 (ddd, J = 8.4, 6.9, 1.4 Hz, 1H, H-7), 7.68 (ddd, J = 8.2, 6.9, 1.1 Hz, 1H, H-6), 4.35 - 4.08 (m, 4H, H-10), 1.36 (t, J = 7.1 Hz, 6H, H-11).

^{13}C NMR (101 MHz, $CDCl_3$) δ 152.41 (d, J = 10.7 Hz, C-1), 150.20 (C-9), 147.58 (d, J = 1.8 Hz, C-3), 132.32 (C-7), 129.87 (C-8), 128.34 (d, J = 1.7 Hz, C-6), 125.95 (d, J = 9.6 Hz, C-4), 124.91 (C-5), 120.68 (d, J = 190.6 Hz, C-2), 62.94 (d, J = 6.0 Hz, C-11), 16.28 (d, J = 6.9 Hz, C-12).

^{31}P NMR (162 MHz, $CDCl_3$) δ 12.24.

MS (EI): m/z (relative intensity (%)): 299/301 (14/5, M^+/M+2), 264 (51), 236 (50), 208 (20), 190 (100), 163 (53).

HR-MS (ESI) m/z $[M + Na]^+$: Calculated for $C_{13}H_{15}ClNNaO_3P$: 322.0376/324.0346. Found: 322.0371/324.0343 (-0.1 ppm)

This compound has not been reported in the literature.

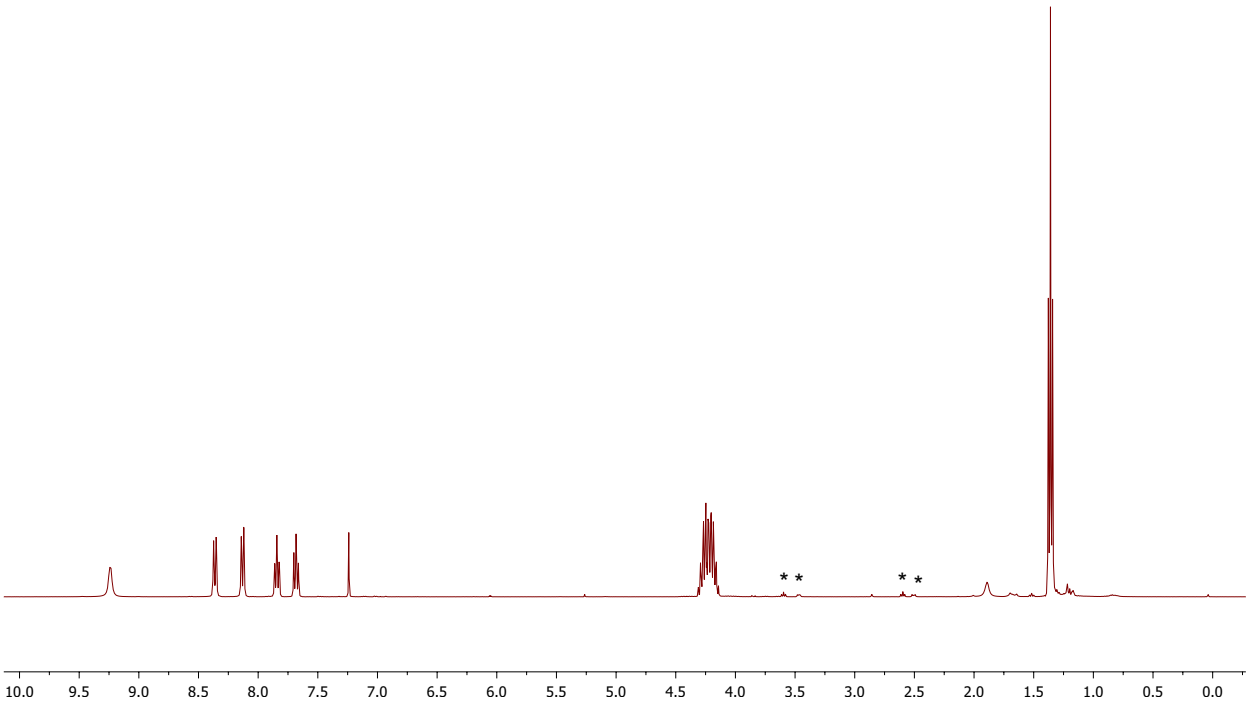

Figure 5.54: ^{1}H NMR spectrum of of diethyl 4-chloro-3-quinolinylphosphonate (**54**) (101 MHz, $CDCl_3$). * belongs to an unknown impurity that appeared after purification.

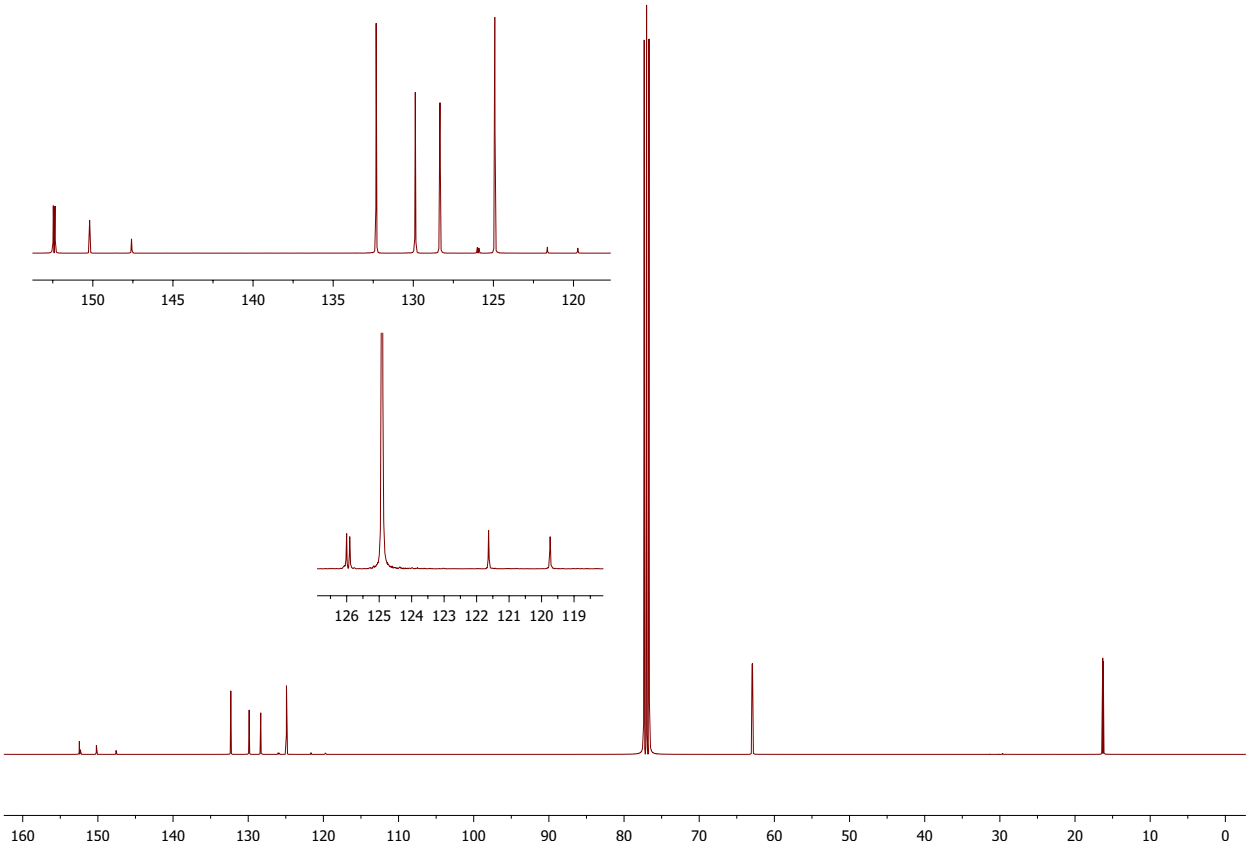

Figure 5.55: ^{13}C NMR spectrum of of diethyl 4-chloro-3-quinolinylphosphonate (**54**) (101 MHz, $CDCl_3$).

5.4 Attempted syntheses

12 was attempted prepared at several occasions with using various conditions. The detailed experimental procedures of the unsuccessful preparations are given below.

The 3-quinolinylphosphonates **55** and **56** were synthesized in very poor yields and were not isolated. The detailed experimental procedures are given below.

5.4.1 Ethyl 8-azaquinoline-3-carboxylate (12)

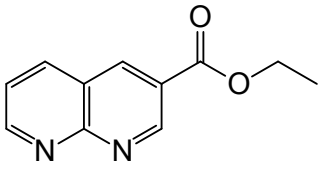

5.4.1.1 Thermal reaction

Br-EDA was prepared according to procedure 5.2.1.1. This afforded Br-EDA (0.51 mmol, 1.3 equiv. in 8 mL DCM). 7-azaindole (50.0 mg, 0.4 mmol, 1.0 equiv.) was added directly to the cold Br-EDA solution and stirred at room temp over night.

Conversion of the starting material: 15 %

5.4.1.2 Addition of para-toluenesulfonic acid

7-azaindole (49.5 mg, 0.42 mmol, 1.0 equiv.) was dissolved in 5 mL DCM. Para-toluenesulfonic acid (PTSA) (68.5 mg, 0.40 mmol, 1.0 equiv.) was added to the solution and stirred while Br-EDA was prepared according to procedure 5.2.1.1. The procedure afforded Br-EDA (0.51 mmol, 1.3 equiv. in 6 mL DCM). $Rh_2(esp)_2$ (3.3 mg, 0.004 mmol, 0.01 equiv.) was added to the 7-azaindole solution, then Br-EDA was added dropwise from a cooled addition funnel (0 °C) over 40 min. The resulting reaction mixture was stirred for an additional 30 min.

Conversion of the starting material: 0 %

5.4.1.3 Addition of trifluoroacetic acid

7-azaindole (25.5 mg, 0.22 mmol, 1.0 equiv.) was dissolved in 4 mL toluene. Trifluoroacetic acid (TFA) (16 µL, 0.21 mmol, 1.0 equiv.) was added to the solution and stirred while Cl-EDA was prepared according to procedure 5.2.1.1. The procedure afforded Cl-EDA (0.25 mmol, 1.1 equiv. in 4 mL toluene). $Rh_2(esp)_2$ (9.6 mg, 0.013 mmol, 0.006 equiv.) was added to the 7-azaindole solution, then Cl-EDA was added dropwise from a cooled addition funnel (0 °C) over 30 min. The resulting reaction mixture was stirred for an additional 30 min.

Conversion of the starting material: 0 %

5.4.1.4 Addition of $ZnCl_2$

7-azaindole (41.6 mg, 0.35 mmol, 1.0 equiv.) was dissolved in 10 mL DCM. $ZnCl_2$ in 1.0 M Et_2O (0.39 mL, 0.39 mmol, 1.1 equiv.) was added to the solution and stirred while Br-EDA was prepared according to procedure 5.2.1.1. The procedure afforded Br-EDA (0.41 mmol, 1.2 equiv. in 6 mL toluene). Cs_2CO_3 (146.6 mg, 0.45 mmol, 13. equiv.) and $Rh_2(esp)_2$ (3.0 mg, 0.004 mmol, 0.001 equiv.) was added to the 7-azaindole solution, then Br-EDA was added dropwise from a cooled addition funnel (0 °C) over 30 min. The resulting reaction mixture was stirred for an additional 30 min.

Conversion of the starting material: 0 %

5.4.1.5 Cu_2O as catalyst

See procedure 5.2.2.1.

Br-EDA (0.52 mmol, 1.2 equiv. in 8 mL DCM), 7-azaindole (51.5 mg, 0.44 mmol, 1.0 equiv.), Cs_2CO_3 (188.6 mg, 0.58 mmol, 1.3 equiv.) and Cu_2O (14.7 mg, 0.10 mmol, 0.23 equiv.).

Conversion of the starting material: 0 %

5.4.1.6 $Fe(ClO_4)_3$ as catalyst

See procedure 5.2.2.1. The solution was stirred over night after dropwise addition of Br-EDA.

Br-EDA (0.26 mmol, 1.2 equiv. in 4 mL DCM), 7-azaindole (25.5 mg, 0.22 mmol, 1.0 equiv.), Cs_2CO_3 (86.5 mg, 0.27 mmol, 1.2 equiv.) and $Fe(ClO_4)_3$ (16.0 mg, 0.046 mmol, 0.2 equiv.) in 7 mL DCM

Conversion of the starting material: 7 %

5.4.1.7 $Rh_2(4\,VBA)_4$ as catalyst

See procedure 5.2.2.1.

Br-EDA (0.21 mmol, 1.2 equiv. in 4 mL DCM), 7-azaindole (20.6 mg, 0.17 mmol, 1.0 equiv.), Cs_2CO_3 (73.5 mg, 0.23 mmol, 1.3 equiv.) and $Rh_2(4\,VBA)_4$ (2.1 mg, 0.003 mmol, 0.02 equiv.) in 4 mL DCM.

Conversion of the starting material: 83 %

The ratio of **12** and **13** was compared using ^1H NMR spectroscopy:

$$\frac{\mathbf{12}}{\mathbf{13}} = \frac{1}{7}$$

5.4.1.8 $Rh_2(MCES)_4$ as catalyst

See procedure 5.2.2.1.

Br-EDA (0.21 mmol, 1.2 equiv. in 4 mL DCM), 7-azaindole (20.7 mg, 0.17 mmol, 1.0 equiv.), Cs_2CO_3 (73.3 mg, 0.23 mmol, 1.3 equiv.) and $Rh_2(4\,VBA)_4$ (3.8 mg, 0.0035 mmol, 0.02 equiv.) in 4 mL DCM.

Conversion of the starting material: 49 %

The ratio of **12** and **13** was compared using ^1H NMR spectroscopy:

$$\frac{\mathbf{12}}{\mathbf{13}} = \frac{1}{2}$$

5.4.1.9 Pol(II)-$Rh_2(4\,VBA)_4$ as catalyst

See procedure 5.2.2.1.

Cat. load pol(II)-$Rh_2(4\,VBA)_4$: 0.150 mmol/g.

Br-EDA (0.21 mmol, 1.2 equiv. in 4 mL DCM), 7-azaindole (20.6 mg, 0.17 mmol, 1.0 equiv.), Cs_2CO_3 (73.3 mg, 0.23 mmol, 1.3 equiv.) and pol(II)-$Rh_2(4\,VBA)_4$ (18.8 mg, 0.003 mmol, 0.02 equiv.) in 4 mL DCM.

Conversion of the starting material: 27 %

The ratio of **12** and **13** was compared using ^1H NMR spectroscopy:

$$\frac{\mathbf{12}}{\mathbf{13}} = \frac{1}{2}$$

5.4.1.10 Pol(II)-$Rh_2(MCES)_4$ as catalyst

See procedure 5.2.2.1.

Cat. load pol(II)-$Rh_2(MCES)_4$: 0.0659 mmol/g.

Br-EDA (0.21 mmol, 1.2 equiv. in 4 mL DCM), 7-azaindole (21.0 mg, 0.18 mmol, 1.0 equiv.), Cs_2CO_3 (74.0 mg, 0.23 mmol, 1.3 equiv.) and pol(II)-$Rh_2(MCES)_4$ (38.9 mg, 0.003 mmol, 0.02 equiv.) in 4 mL DCM.

Conversion of the starting material: 23 %

The ratio of **12** and **13** was compared using ^1H NMR spectroscopy:

$$\frac{\mathbf{12}}{\mathbf{13}} = \frac{1}{3}$$

5.4.1.11 KHMDS as base

7-azaindole (49.0 mg, 0.41 mmol, 1.0 equiv) was dissolved in 5 mL DCM. KHMDS (80.3 mg, 0.40 mmol, 1.0 equiv) was added to the solution and stirred while Br-EDA was prepared according to procedure 5.2.1.1. The procedure afforded Br-EDA (0.51 mmol, 1.3 equiv. in 5 mL DCM). Cs_2CO_3 (68.88 mg, 0.21 mmol, 0.5 equiv.) $Rh_2(esp)_2$ (3.1 mg, 0.004 mmol, 0.01 equiv.) was added to the 7-azaindole solution, then Br-EDA was added dropwise from a cooled addition funnel (0 °C) over 30 min. The resulting reaction mixture was stirred for an additional 30 min.

Conversion of the starting material: 88 %

The ratio of **12** and **13** was compared using ^{1}H NMR spectroscopy:

$$\frac{\mathbf{12}}{\mathbf{13}} = \frac{1}{2.6}$$

5.4.1.12 NaHMDS as base

See procedure 5.4.1.11

Br-EDA (0.41 mmol, 1.2 equiv. in 5 mL DCM), 7-azaindole (41.7 mg, 0.35 mmol, 1.0 equiv), 1.0 M NaHMDS in THF (0.42 mL mg, 0.42 mmol, 1.2 equiv), $Rh_2(esp)_2$ (2.9 mg, 0.0038 mmol, 0.01 equiv.) in 6 mL DCM.

Conversion of the starting material: 49 %

The ratio of **12** and **13** was compared using ^{1}H NMR spectroscopy:

$$\frac{\mathbf{12}}{\mathbf{13}} = \frac{1}{1}$$

5.4.1.13 *t*-BuOLi as base

See procedure 5.4.1.11. *t*-BuOLi was slowly added to the solution over 1-2 min.

Br-EDA (0.41 mmol, 1.2 equiv. in 5 mL DCM), 7-azaindole (49.9 mg, 0.42 mmol, 1.0 equiv), 1.0 M *t*-BuOLi in THF (0.50 mL mg, 0.50 mmol, 1.2 equiv), $Rh_2(esp)_2$ (8.0 mg, 0.01 mmol, 0.024 equiv.) in 6 mL DCM.

The crude reaction mixture was re-dissolved in EtOAc, transferred to a separatory funnel and washed with H_2O (3-5 mL x 3) then $NaHCO_3$ (3 mL). The organic phase was dried with $MgSO_4$, filtered, concentrated *in vacuo*. Isolation using column chromatography (SiO_2, EtOA) afforded **12** in 13 % yield.

5.4.2 Diethyl 4-chloro-6,7-difluoro-3-quinolinylphosphonate (55)

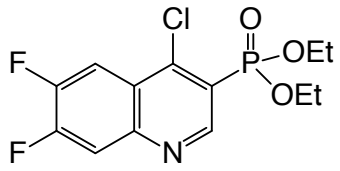

3-chloro-5,6-difluoroindole **46** (93.8 mg, 0.50 mmol, 1.0 equiv) was dissolved in 5 mL $PhCF_3$. The solution was purged while Cl-EDP was prepared according to procedure 5.3.2.1. The procedure afforded Cl-EDP (0.72 mmol, 1.4 equiv. in 5 mL $PhCF_3$). *n*-BuLi (µL, 0.50 mmol, 1.0 equiv) was added to the solution and stirred for 10 min before $Rh_2(esp)_2$ (13.9 mg, 0.018 mmol, 0.037 equiv.) was added. Cl-EDP was added dropwise from a cooled addition funnel (0 °C) over 30 min. The resulting reaction mixture was stirred for an additional 30 min.

IS-yield: 8 %

5.4.3 Diethyl 6-amino-3-quinolinylphosphonate (56)

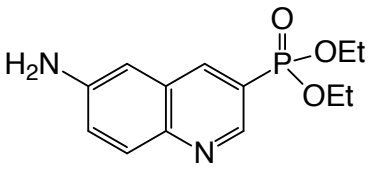

See procedure 5.3.3.1.

Cl-EDP (0.61 mmol, 1.4 equiv. in 8 mL dry toluene), 5-aminoindole **47** (57.4 mg, 0.43 mmol, 1.0 equiv.), CS_2CO_3 (181.6 mg, 0.56 mmol, 1.3 equiv.) and $Rh_2(esp)_2$ (11.7 mg, 0.015 mmol, 0.035 equiv.) in 8 mL dry toluene.

TMB was added as an internal standard prior to ^{1}H NMR analysis of the crude reaction mixture.

IS-yield: 0.3 %

Chapter 6

Appendix

6.1 The dichloromethane content of ethyl diazoacetate

The commercially available EDA contains ≥ 13 wt % DCM [184]. The exact amount was calculated from the ^{1}H NMR spectrum in Figure 6.1 as shown below.

$$\text{wt \% DCM} = \left(\frac{\frac{Integral_{\text{DCM}}}{H_{\text{DCM}}}}{\frac{Integral_{\text{DCM}}}{H_{\text{DCM}}} + \frac{Integral_{\text{EDA}}}{H_{\text{EDA}}}} \right) \times 100\ \% = \left(\frac{\frac{0.27}{2}}{\frac{0.27}{2} + \frac{2.00}{2}} \right) \times 100\ \% = 12\ \%$$

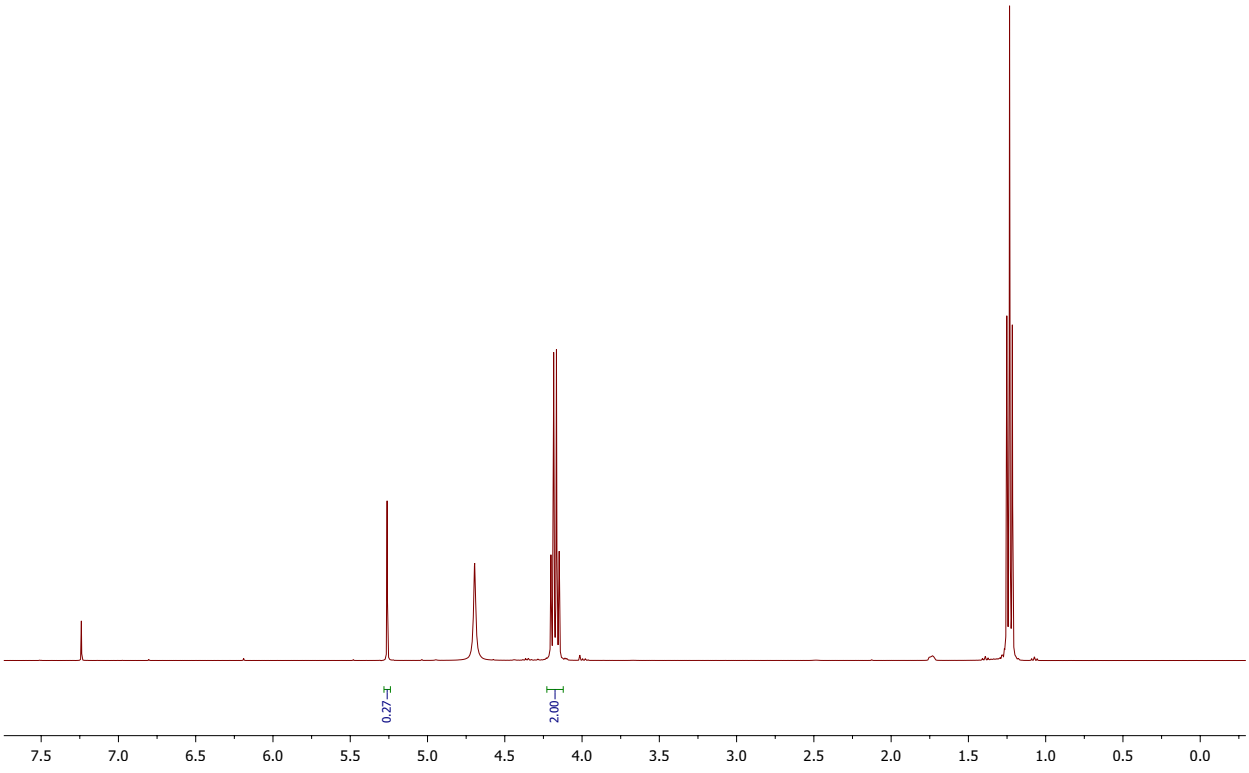

Figure 6.1: ^{1}H NMR spectrum of EDA **7** (300 MHz, $CDCl_3$).

6.2 3-chloro-5,6-difluoroindole (46)

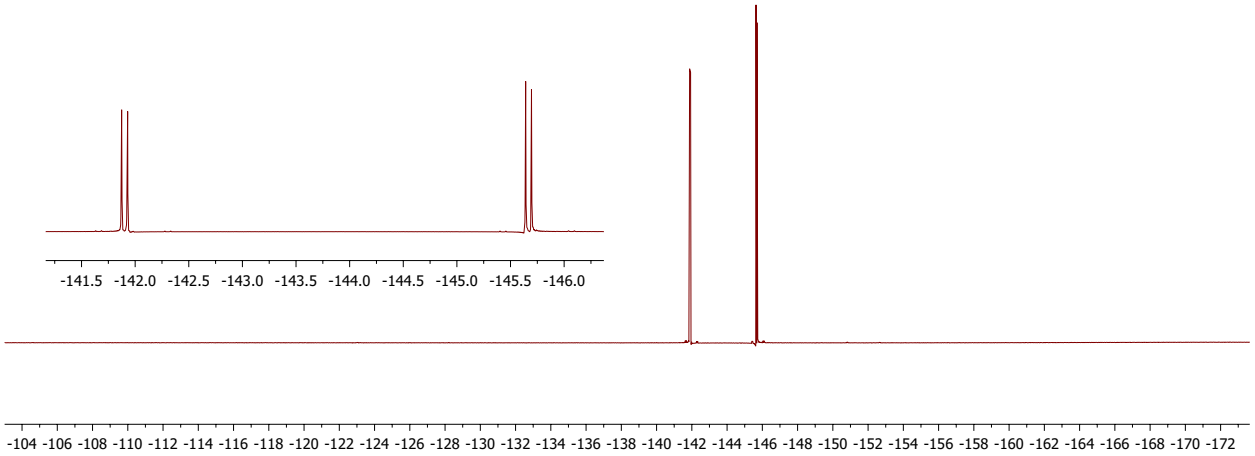

Figure 6.2: ^{19}F NMR (decoupled) of **46** (377 MHz, $CDCl_3$).

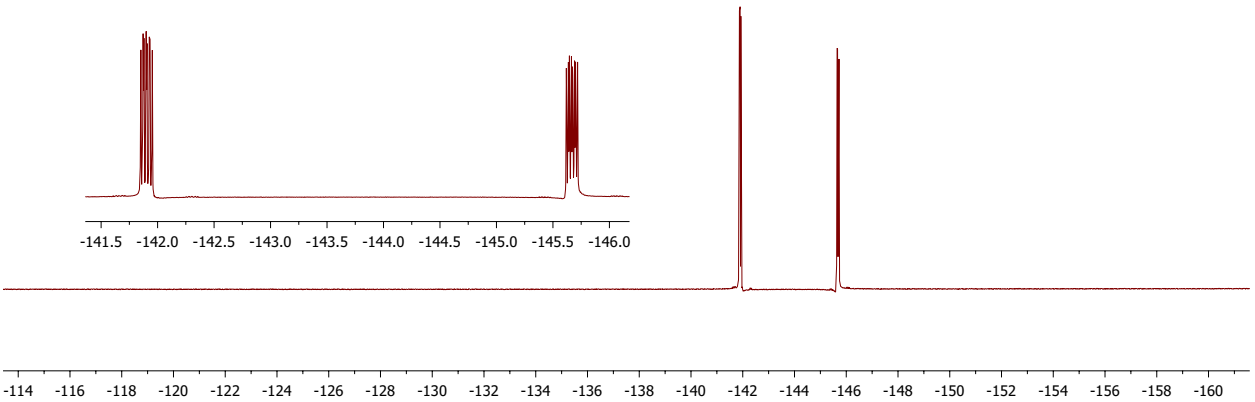

Figure 6.3: ^{19}F NMR (coupled) of **46** (377 MHz, $CDCl_3$).

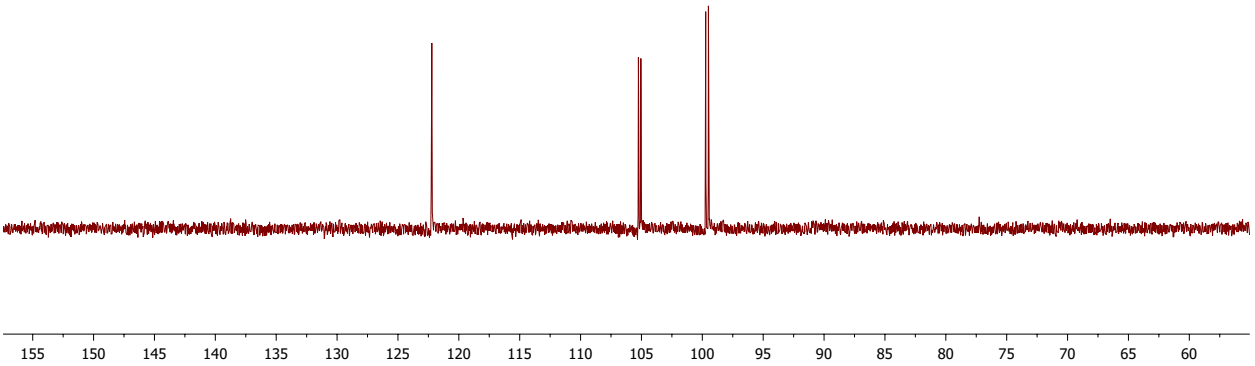

Figure 6.4: DEPT135 of **46** (101 MHz, $CDCl_3$).

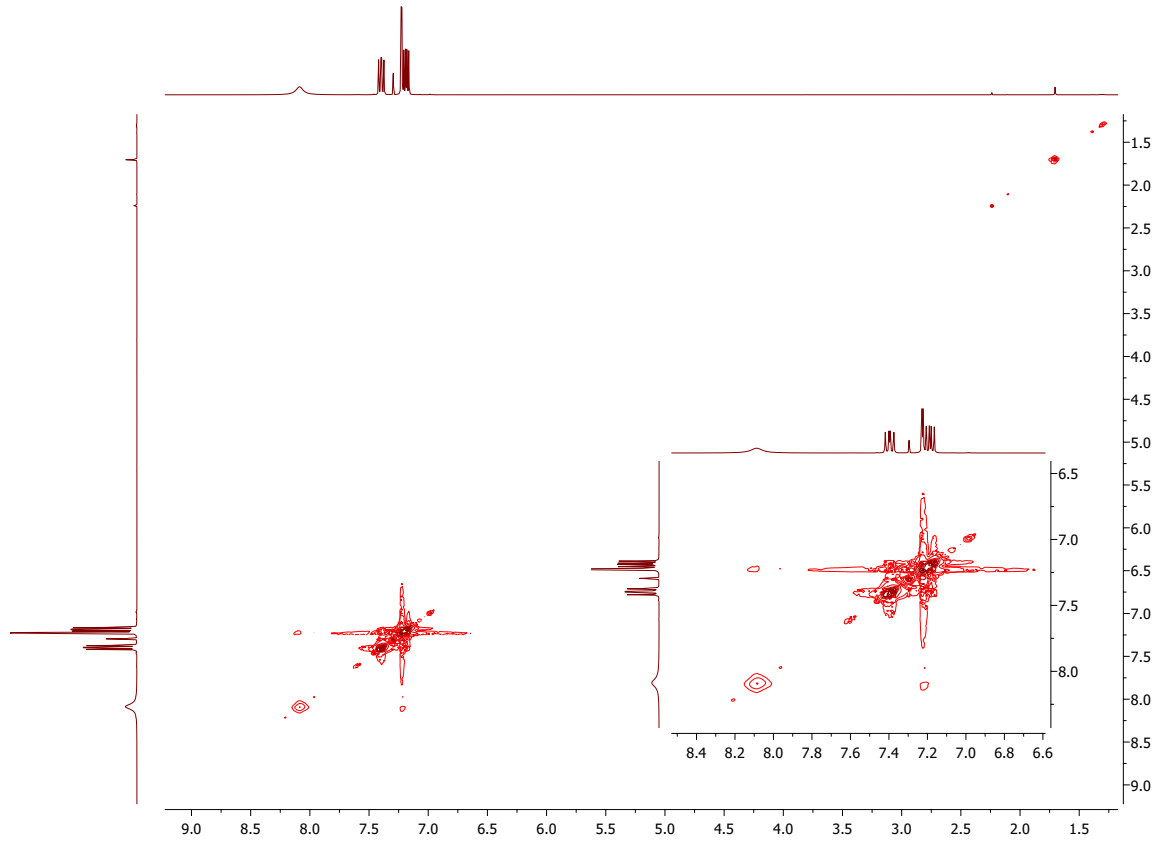

Figure 6.5: COSY of **46** (400 MHz, $CDCl_3$).

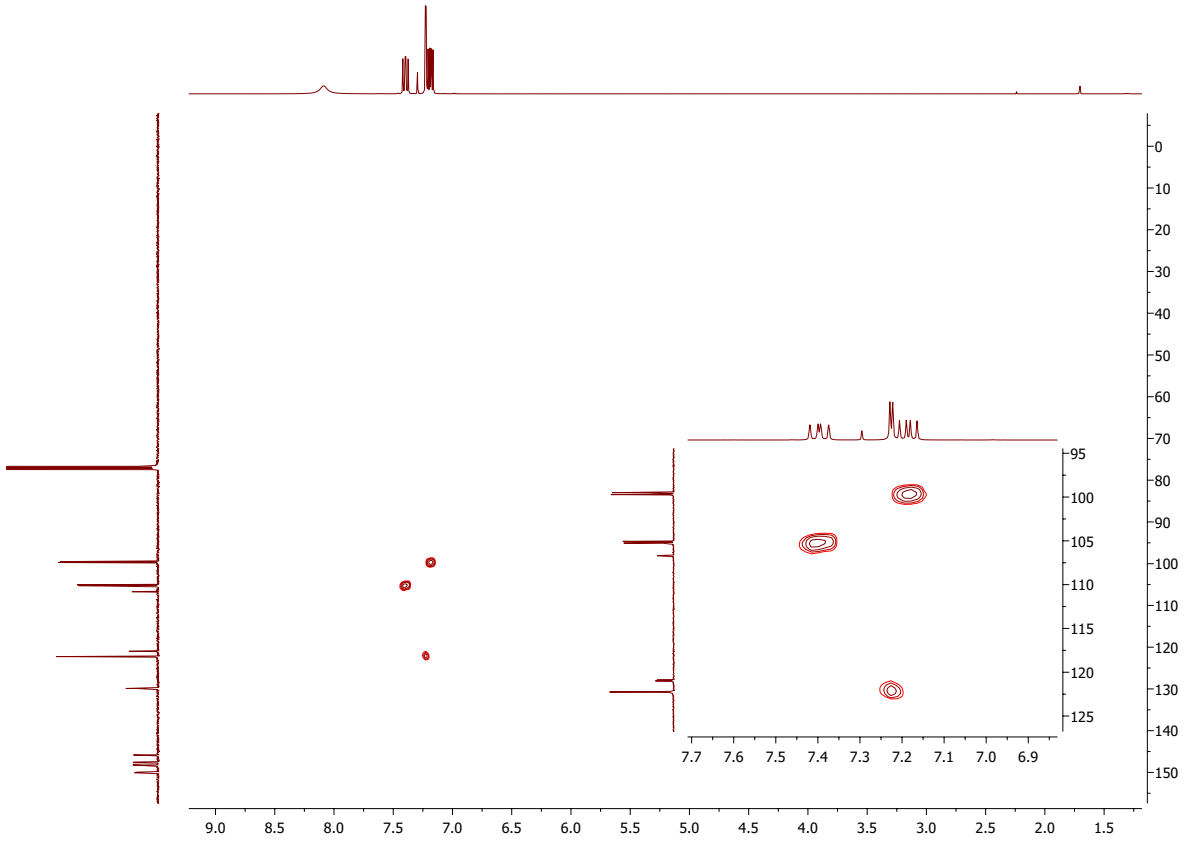

Figure 6.6: HSQC of **46** (400 MHz, $CDCl_3$).

6.3 3-chloro-6-fluoro-7-azaindole (18)

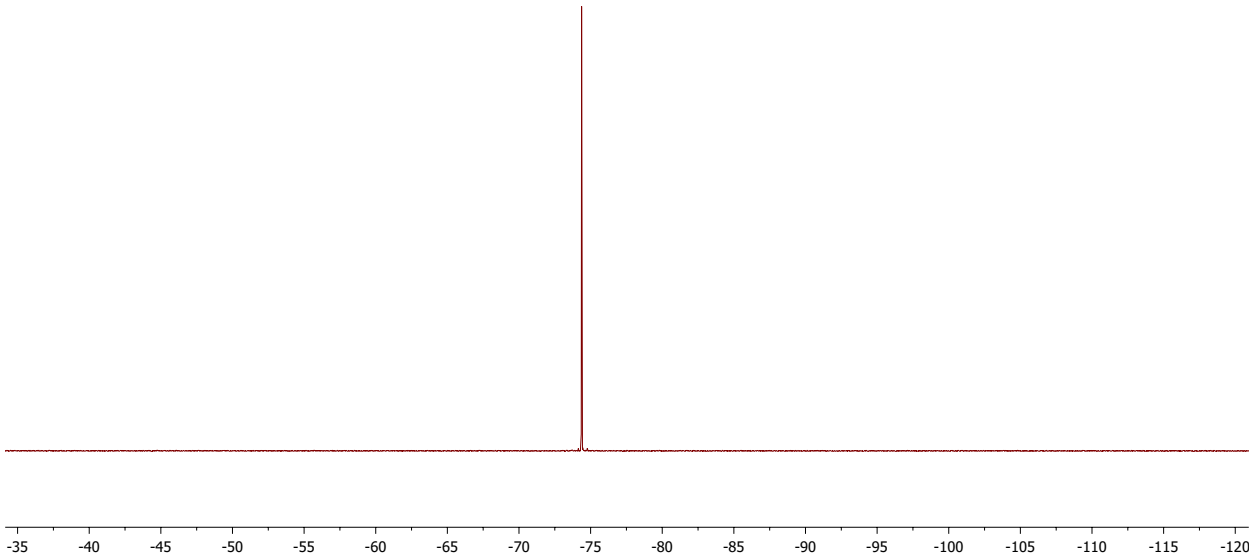

Figure 6.7: ^{19}F NMR (decoupled) of **18** (400 MHz, DMSO-d_6).

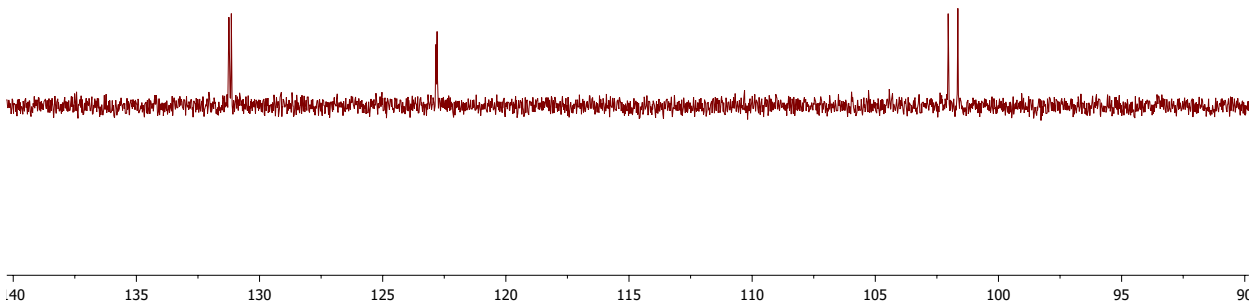

Figure 6.8: DEPT135 of **18** (101 MHz, DMSO-d_6).

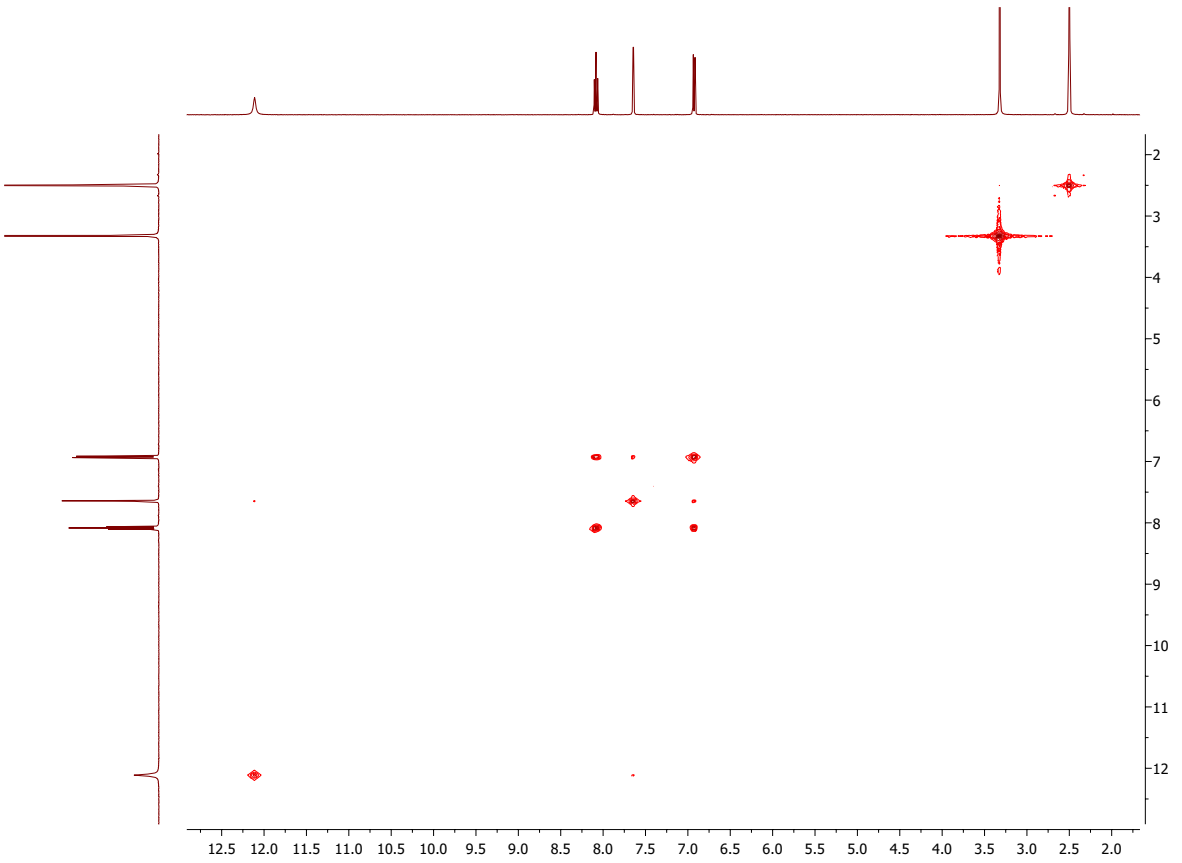

Figure 6.9: COSY of **18** (400 MHz, DMSO-d_6).

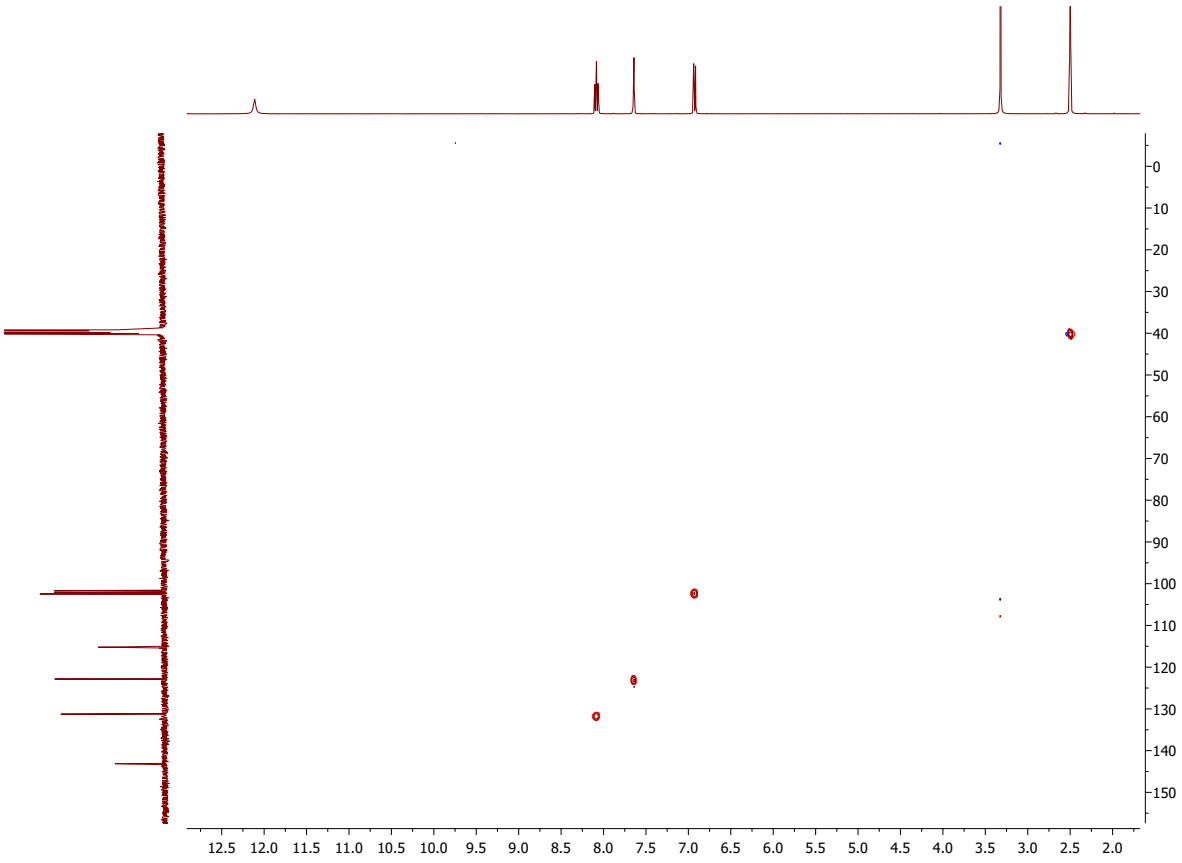

Figure 6.10: HSQC of **18** (400 MHz, DMSO-d_6).

6.4 2,3-dichloro-6-fluoro-7-azaindole (19)

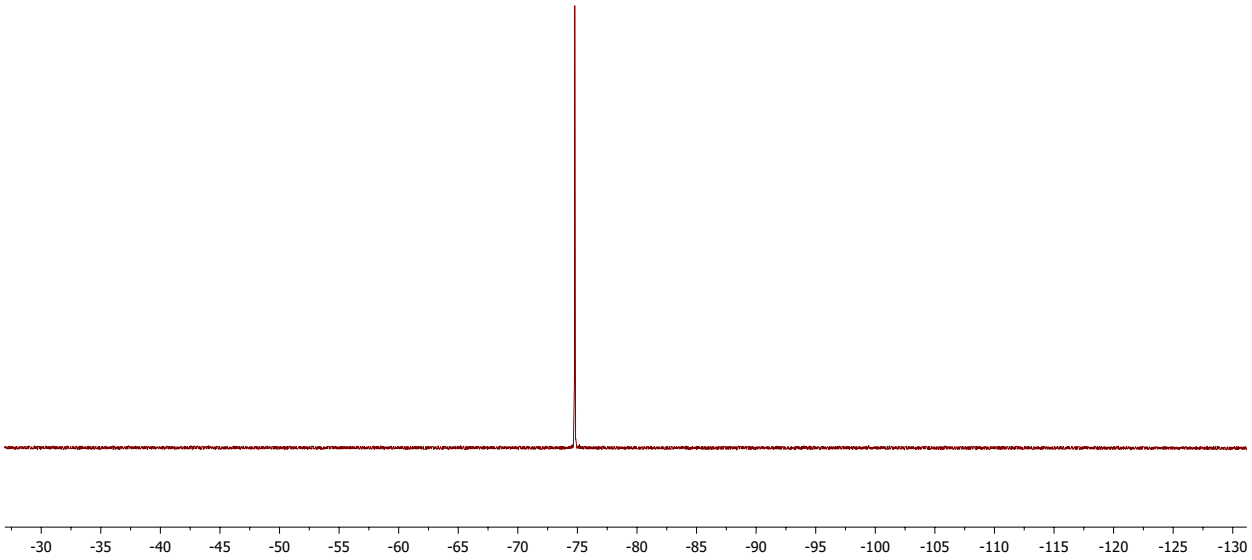

Figure 6.11: ^{19}F NMR (decoupled) of **19** (400 MHz, acetone-d_6).

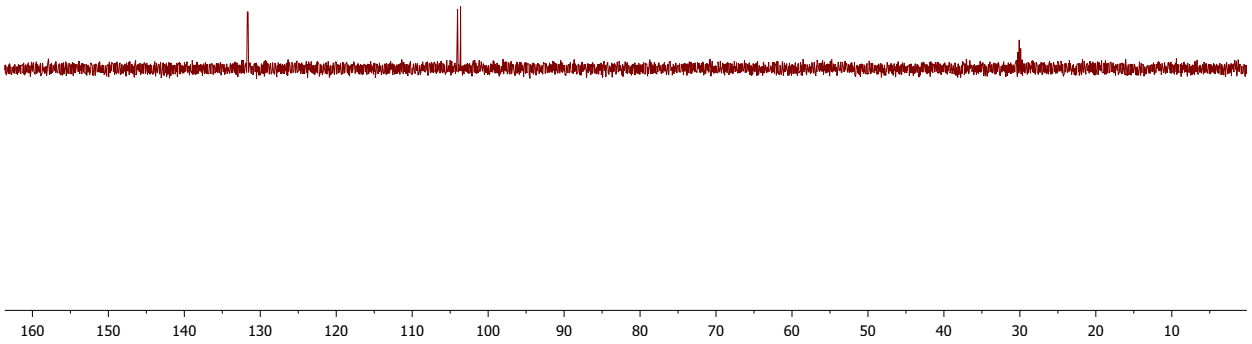

Figure 6.12: DEPT135 of **19** (101 MHz, acetone-d_6).

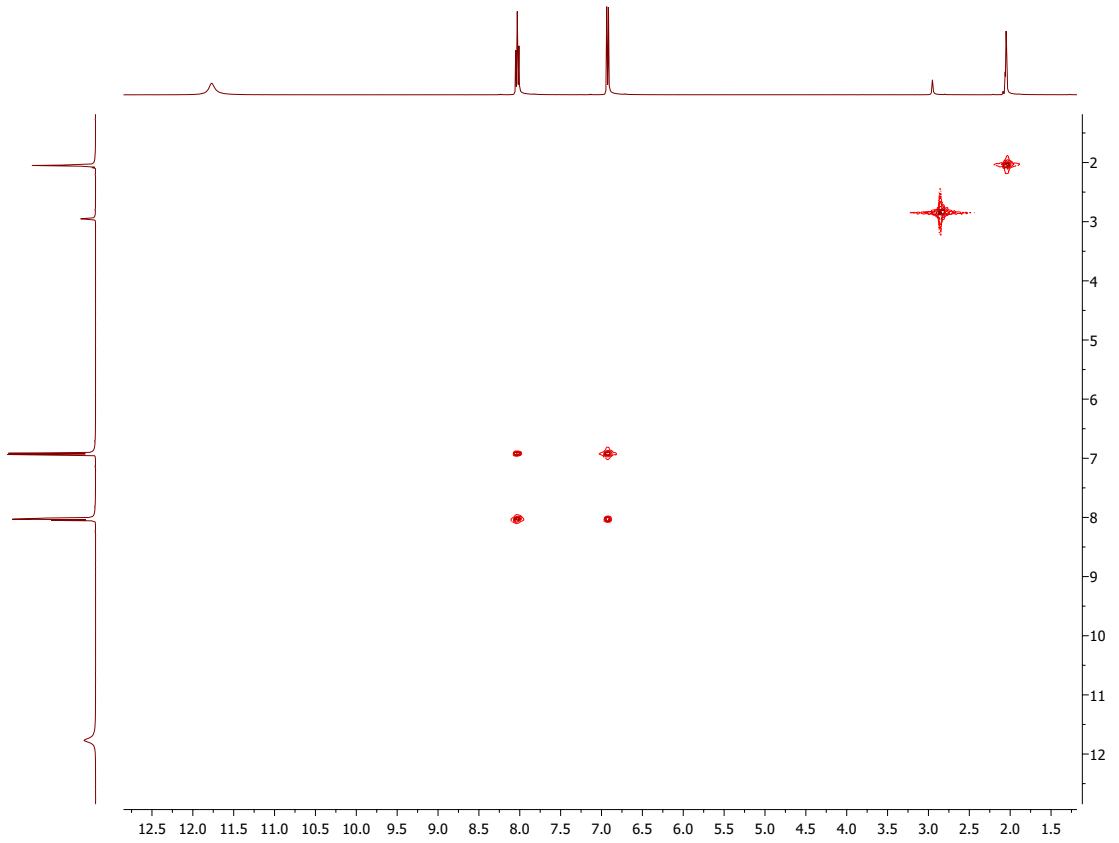

Figure 6.13: COSY of **19** (400 MHz, acetone-d_6).

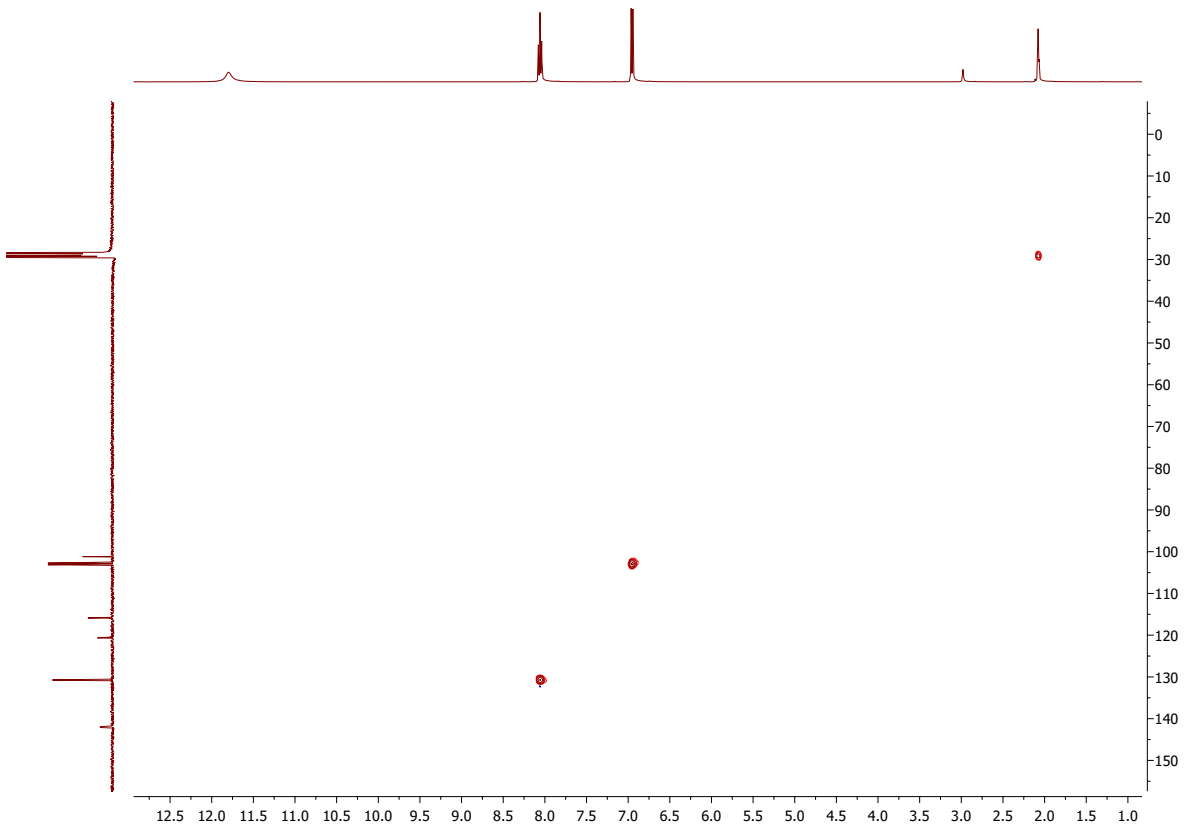

Figure 6.14: HSQC of **19** (400 MHz, Acetone-d_6).

6.5 3-chloro-6-methyl-7-azaindole (20)

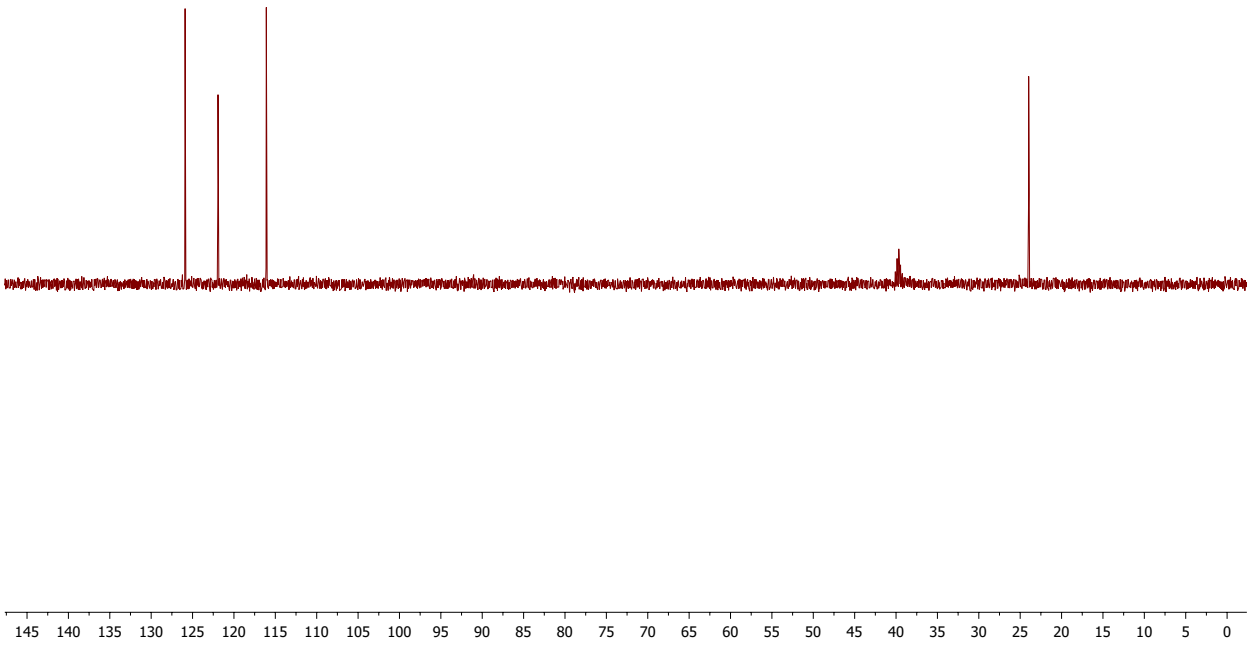

Figure 6.15: DEPT135 of **20** (101 MHz, DMSO-d_6).

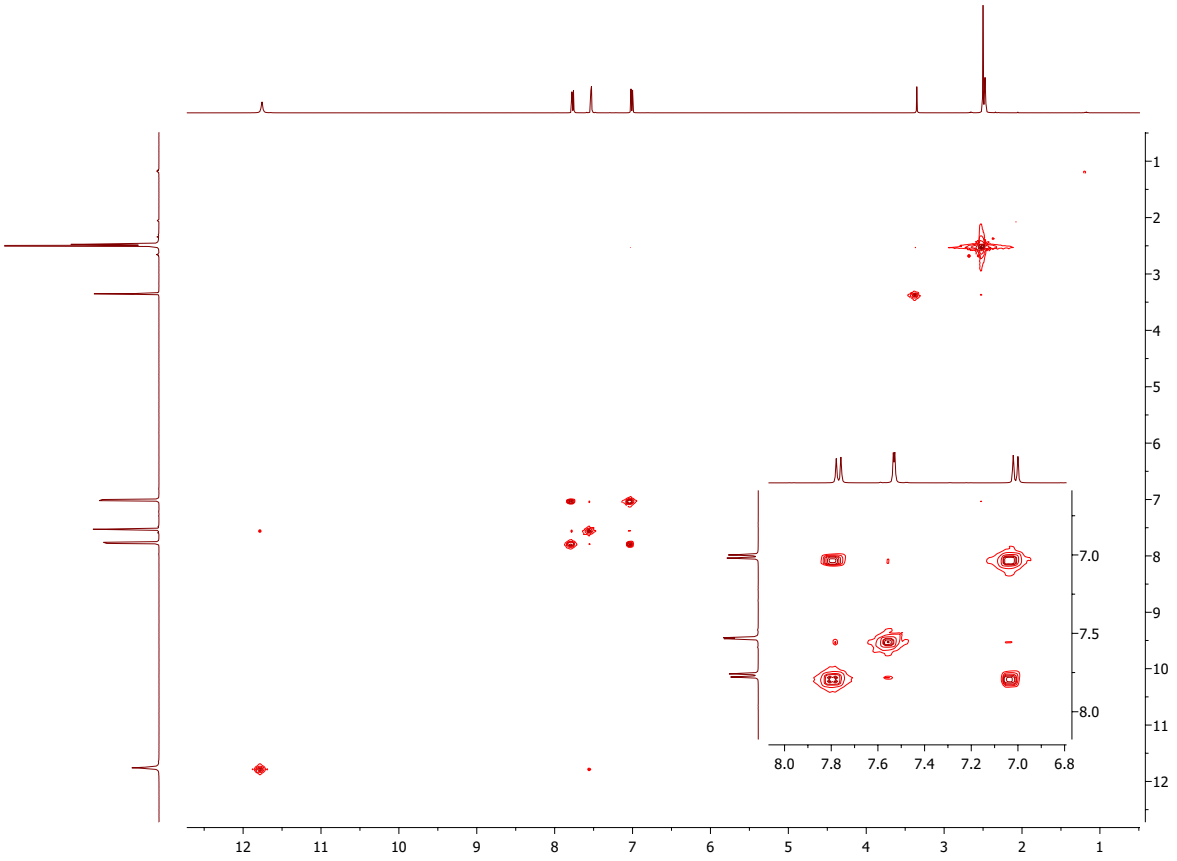

Figure 6.16: COSY of **20** (400 MHz, DMSO-d_6).

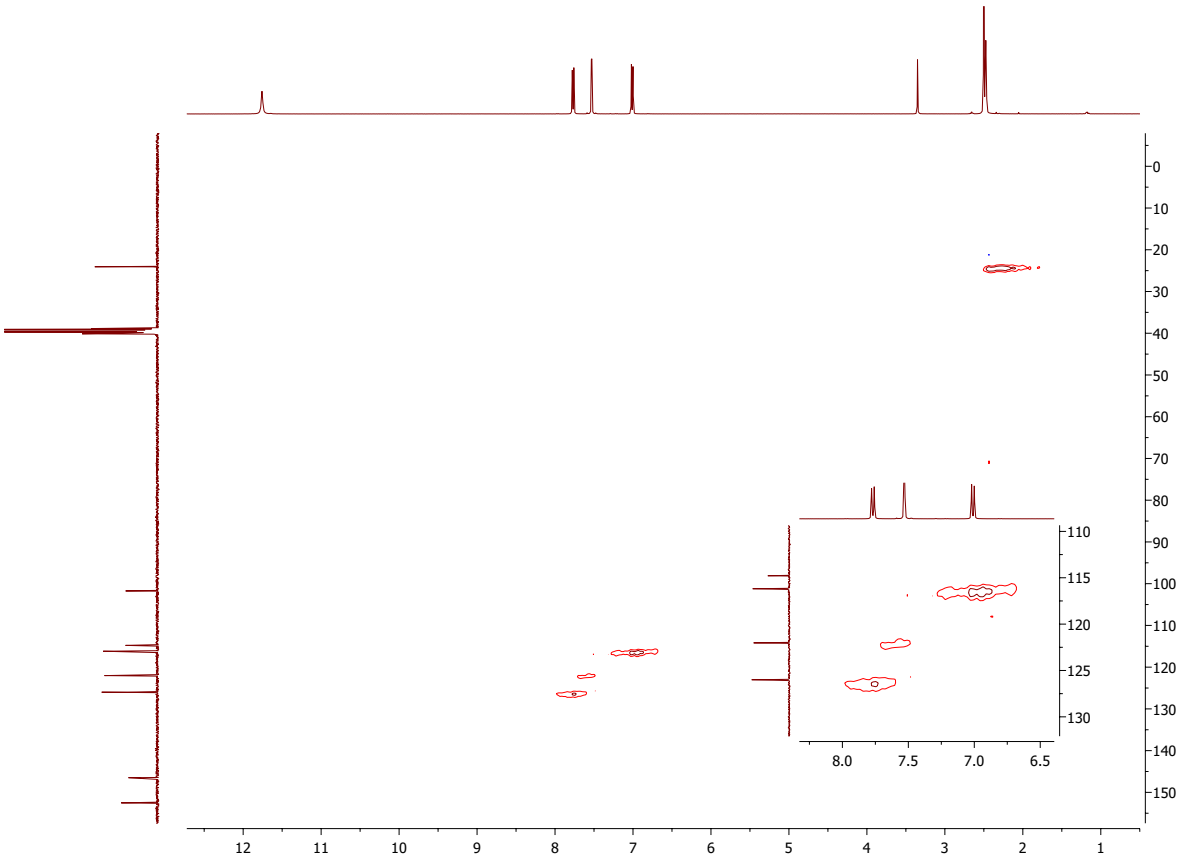

Figure 6.17: HSQC of **20** (400 MHz, DMSO-d_6).

6.6 2,3-dichloro-6-methyl-7-azaindole (21)

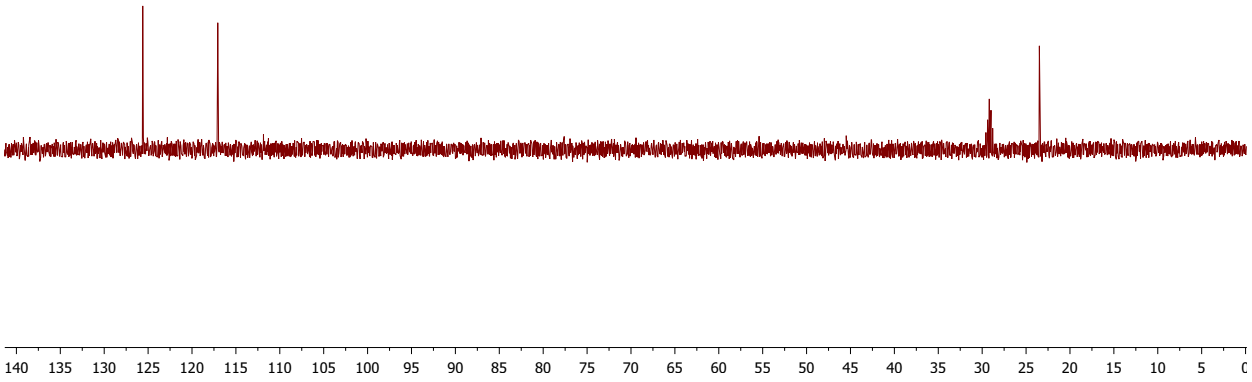

Figure 6.18: DEPT135 of **21** (101 MHz, acetone-d_6).

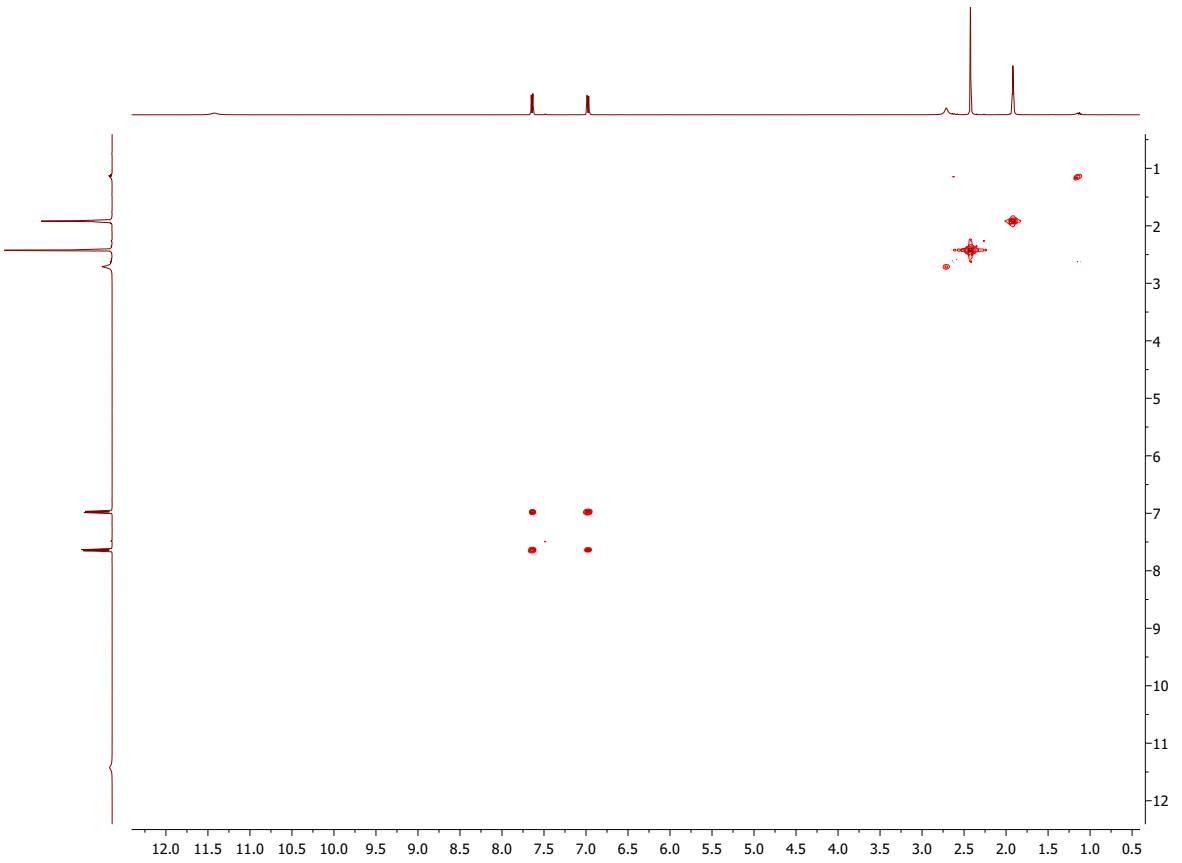

Figure 6.19: COSY of **21** (400 MHz, acetone-d_6).

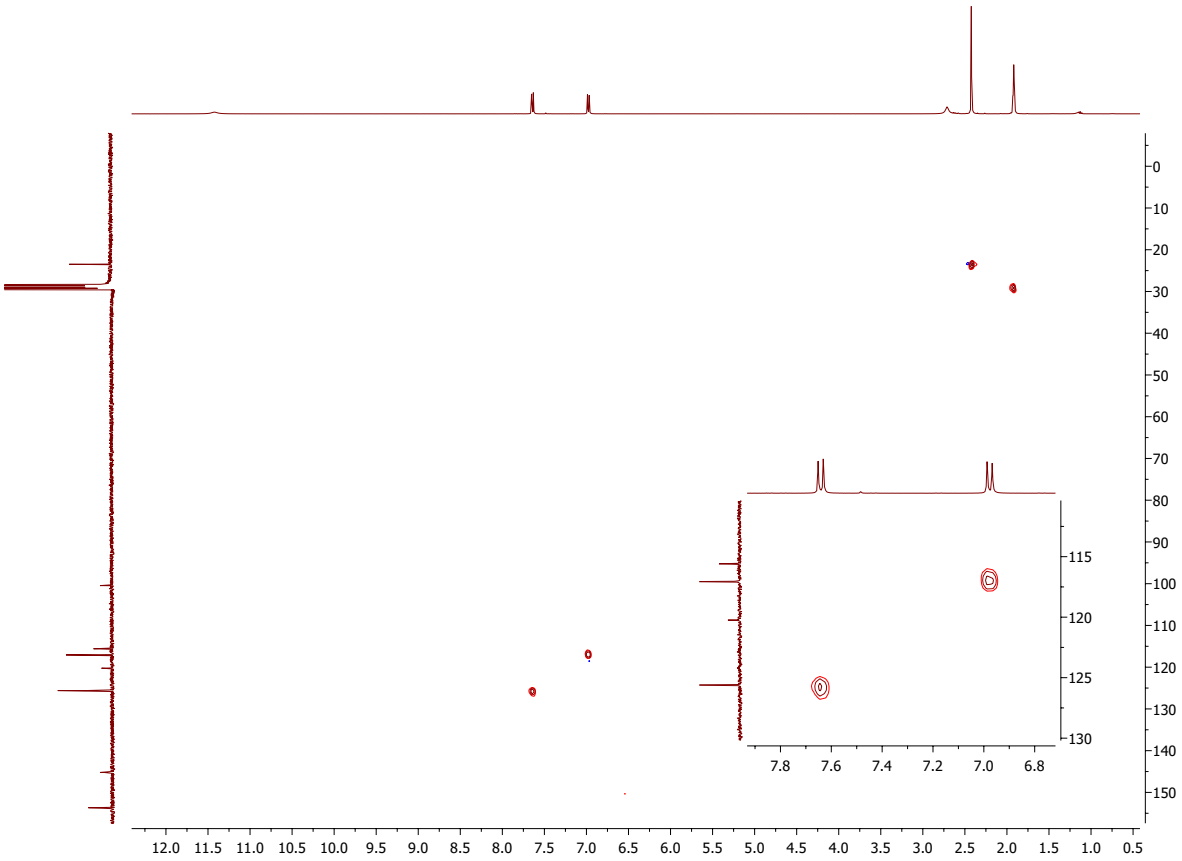

Figure 6.20: HSQC of **21** (400 MHz, acetone-d_6).

6.7 Ethyl 8-azaquinoline-3-carboxylate (12)

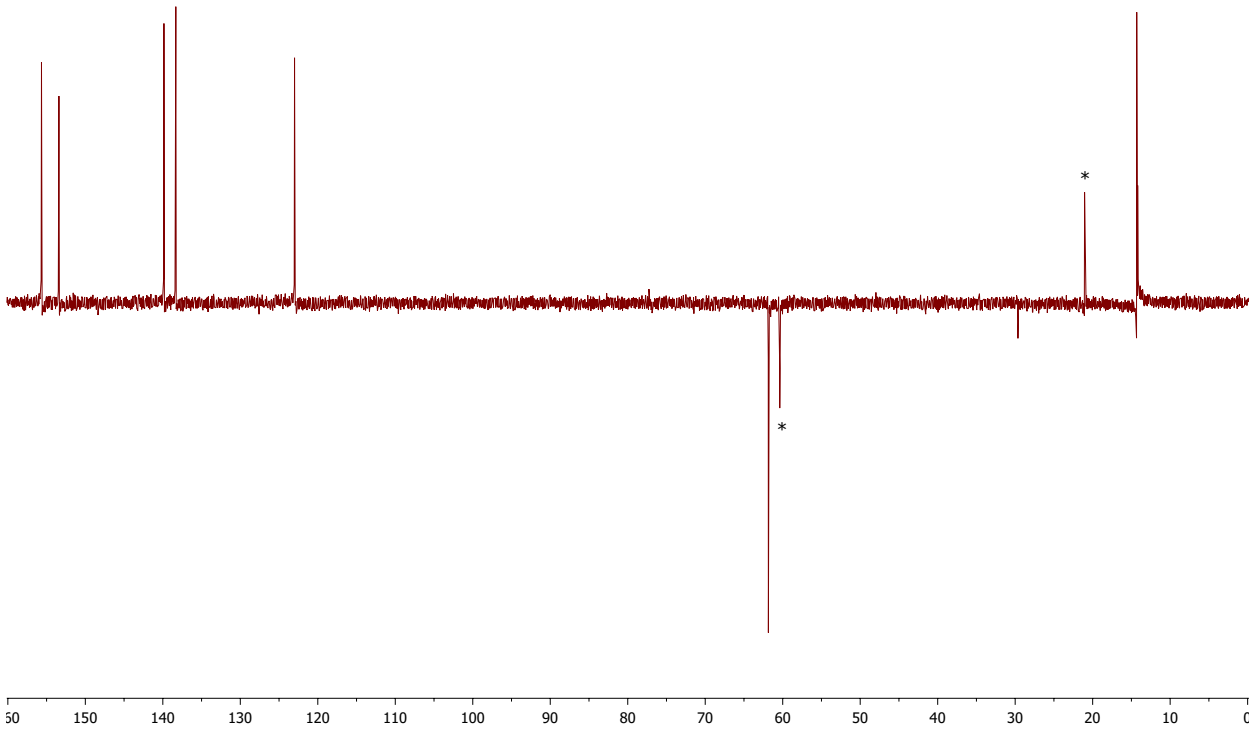

Figure 6.21: DEPT135 of **12** (101 MHz, $CDCl_3$).

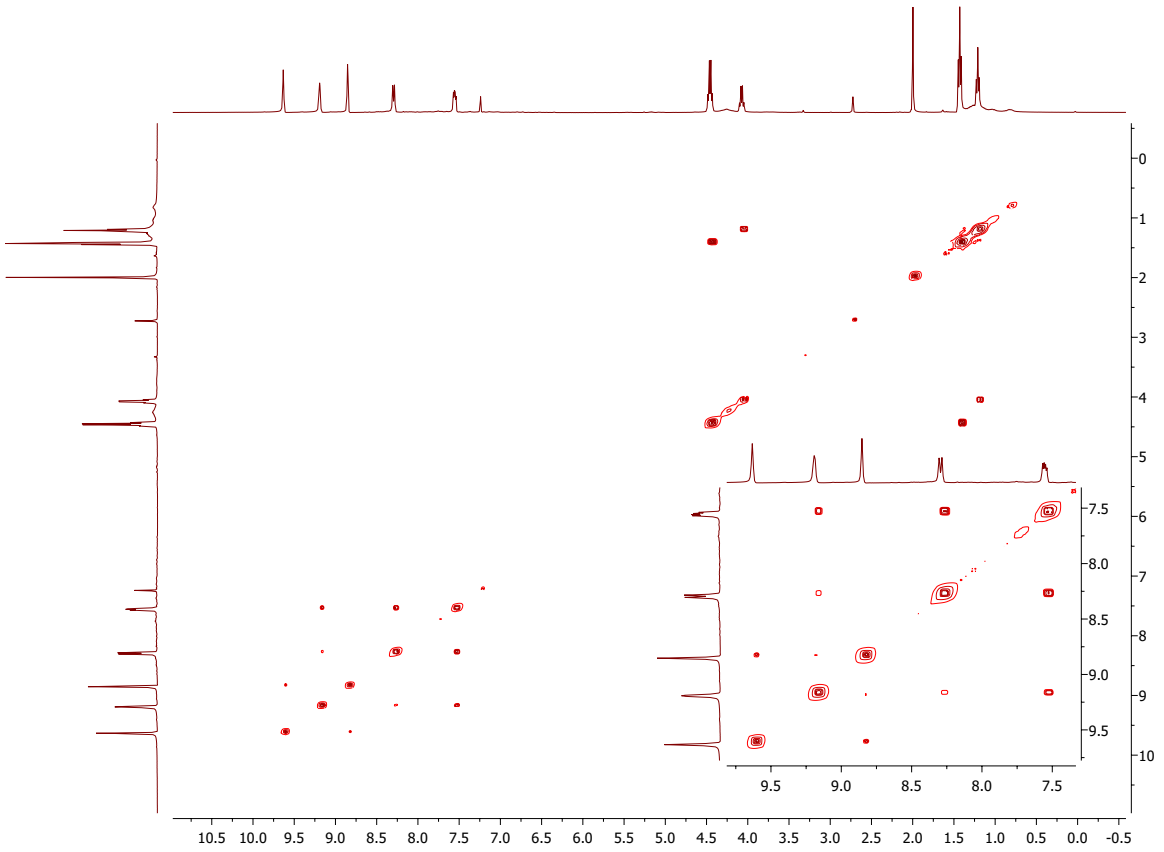

Figure 6.22: COSY of **12** (400 MHz, $CDCl_3$).

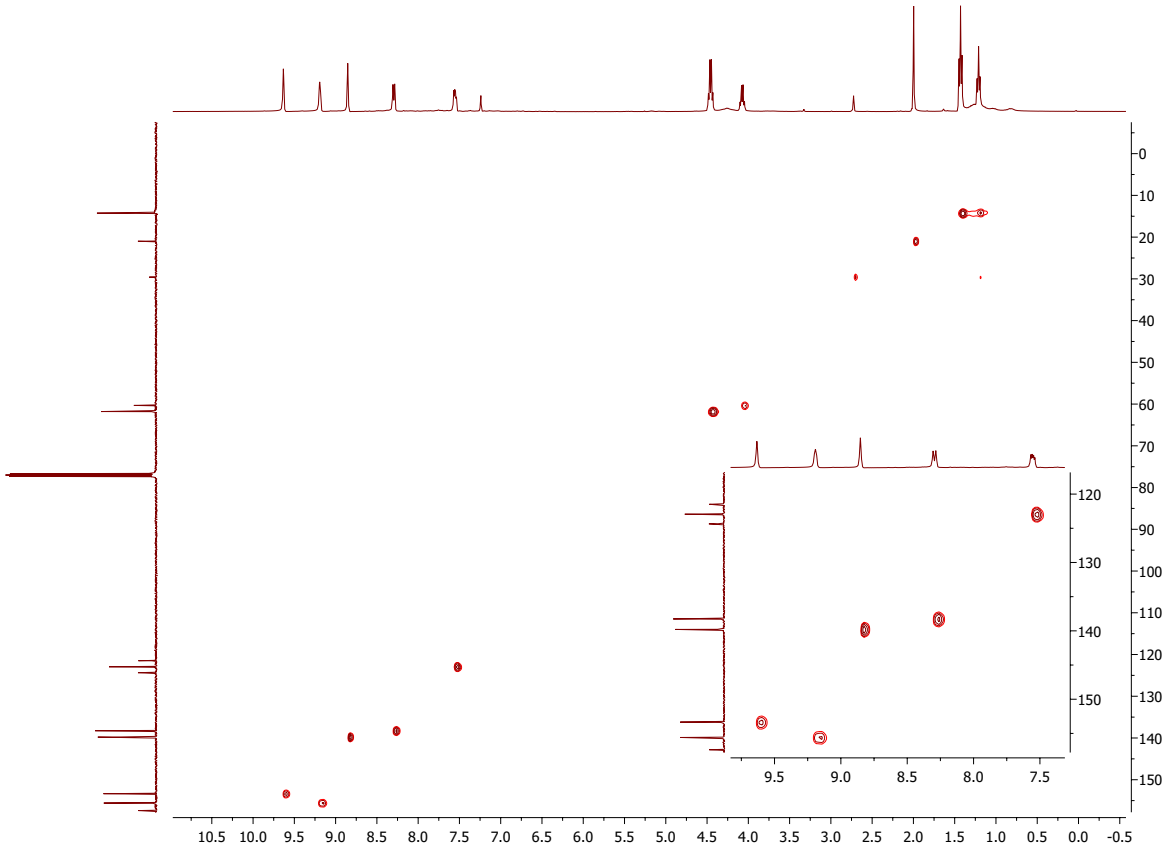

Figure 6.23: HSQC of **12** (400 MHz, $CDCl_3$).

6.8 Ethyl 2-bromo-2-(7-azaindol-1-yl) acetate (13)

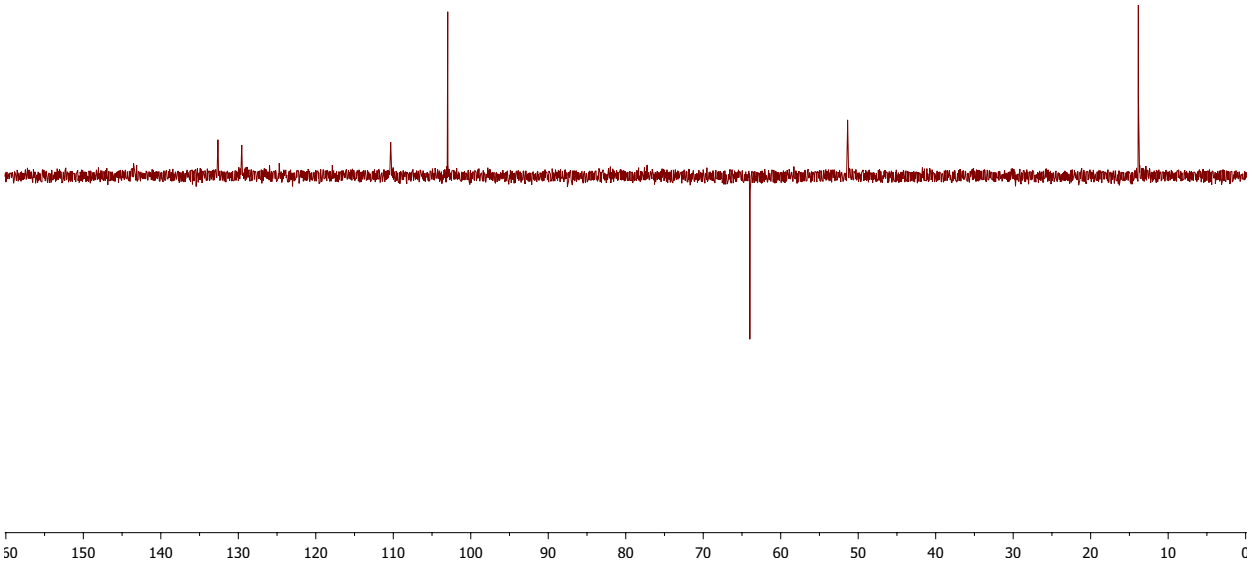

Figure 6.24: DEPT135 of **13** (101 MHz, $CDCl_3$).

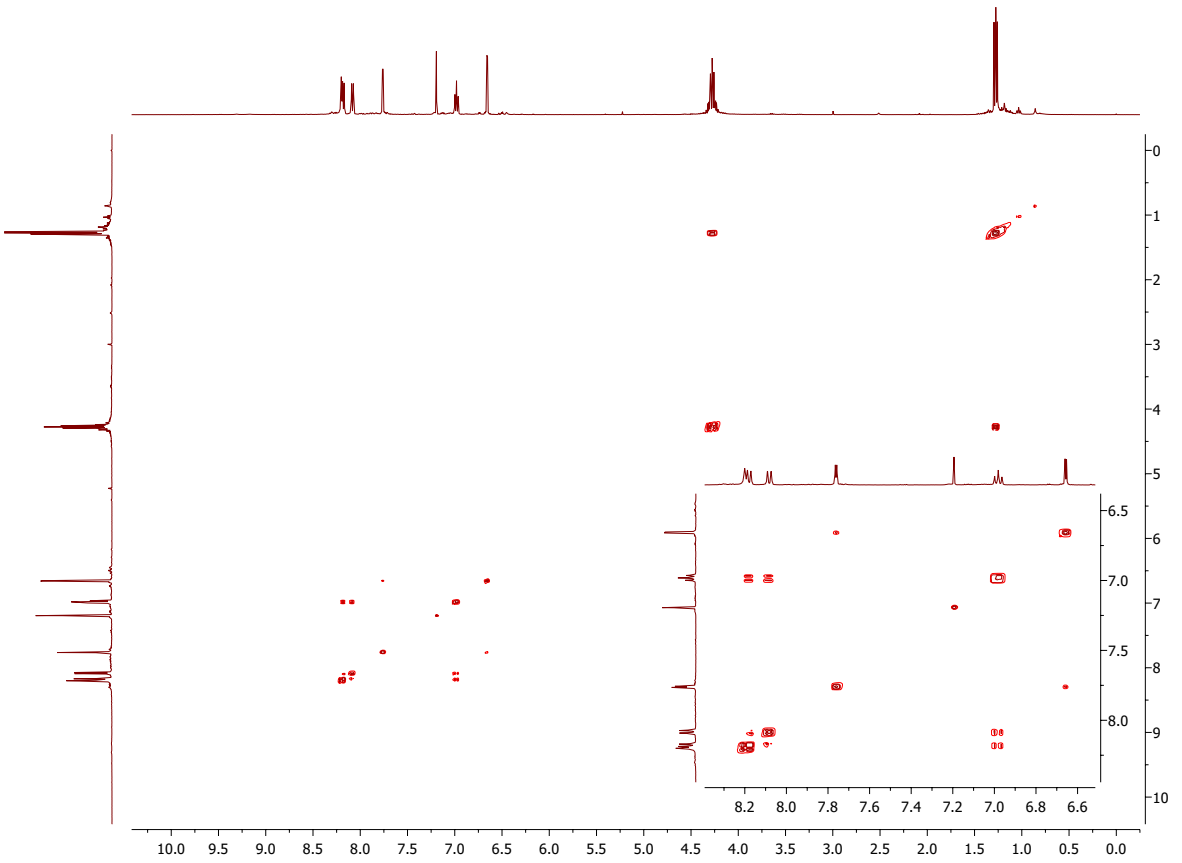

Figure 6.25: COSY of **13** (400 MHz, $CDCl_3$).

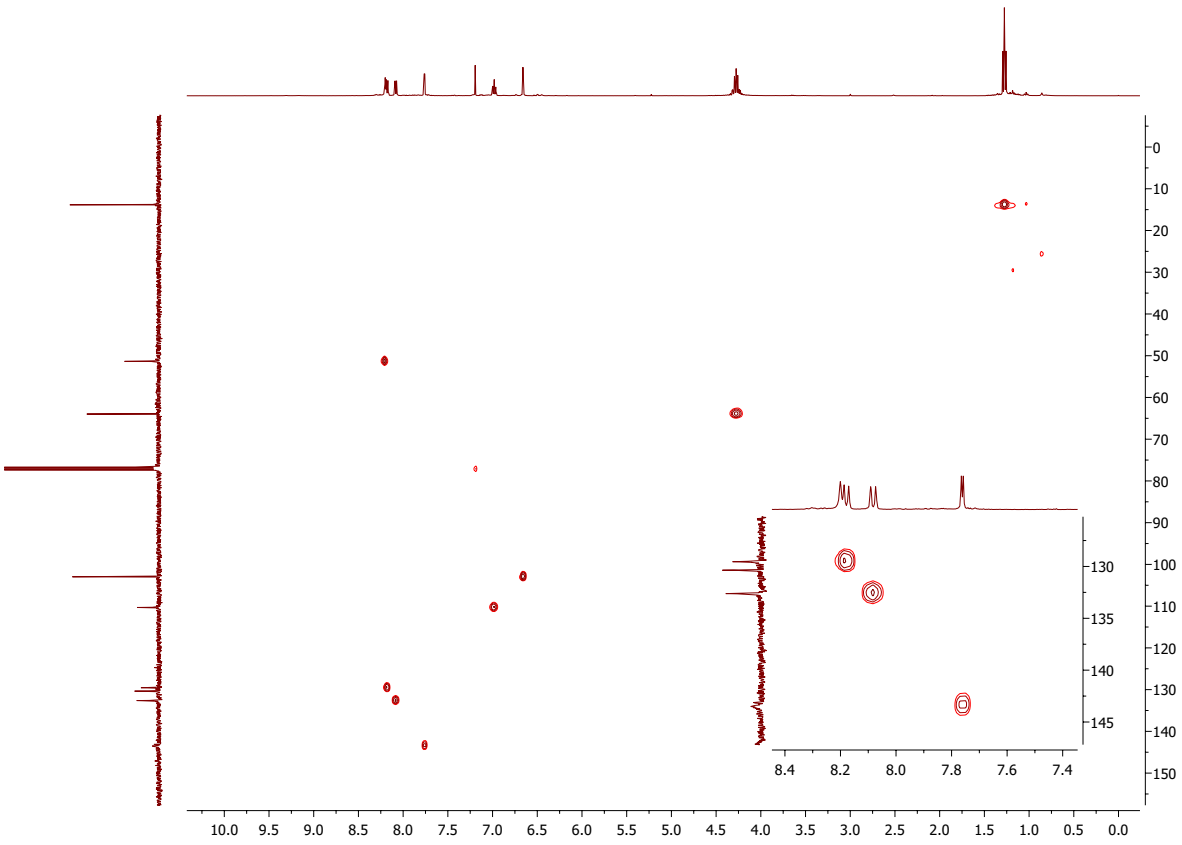

Figure 6.26: HSQC of **13** (400 MHz, $CDCl_3$).

6.9 Ethyl 7-fluoro-8-azaquinoline-3-carboxylate (15)

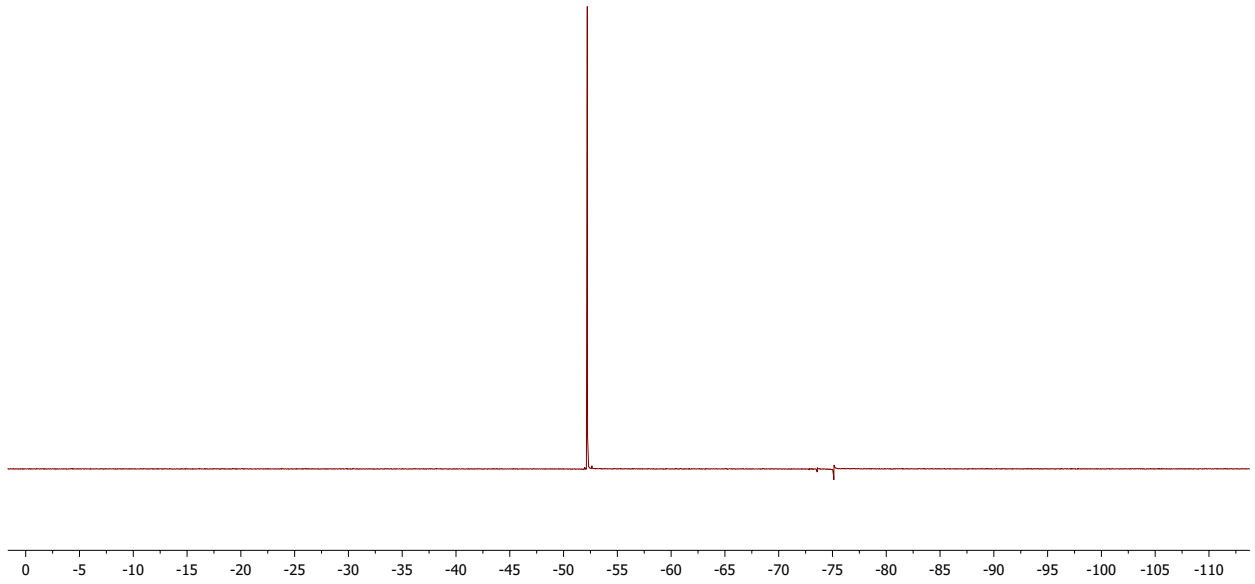

Figure 6.27: ^{19}F NMR (decoupled) of **15** (377 MHz, $CDCl_3$).

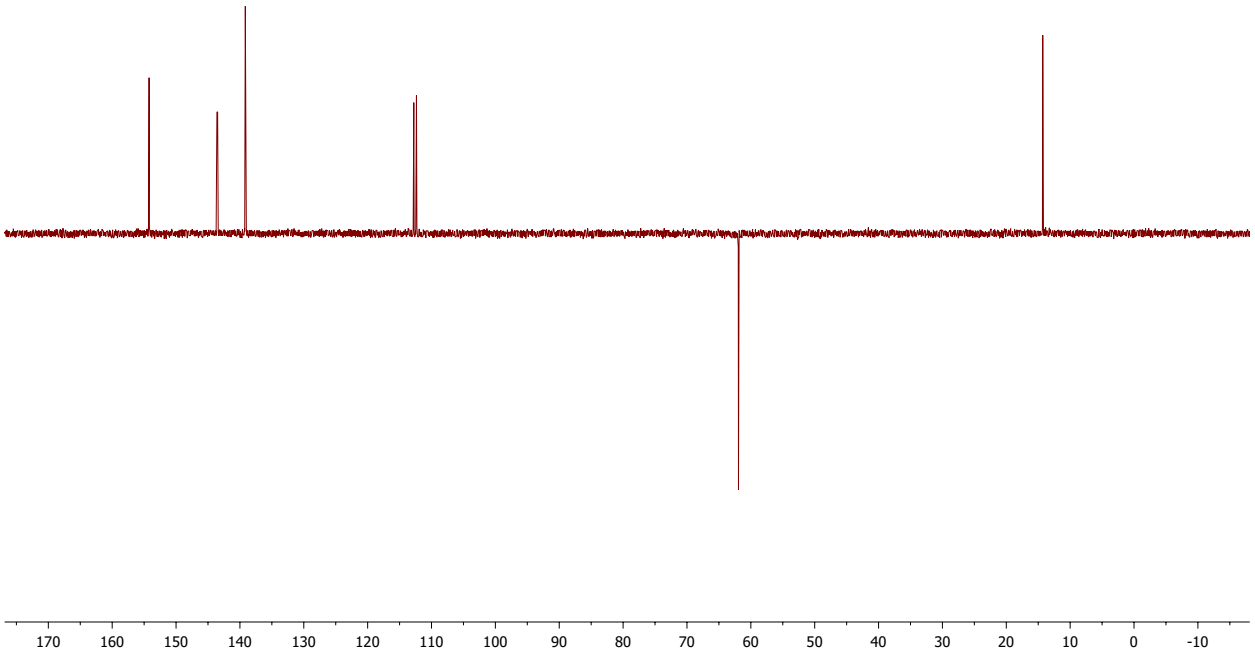

Figure 6.28: DEPT135 of **15** (101 MHz, $CDCl_3$).

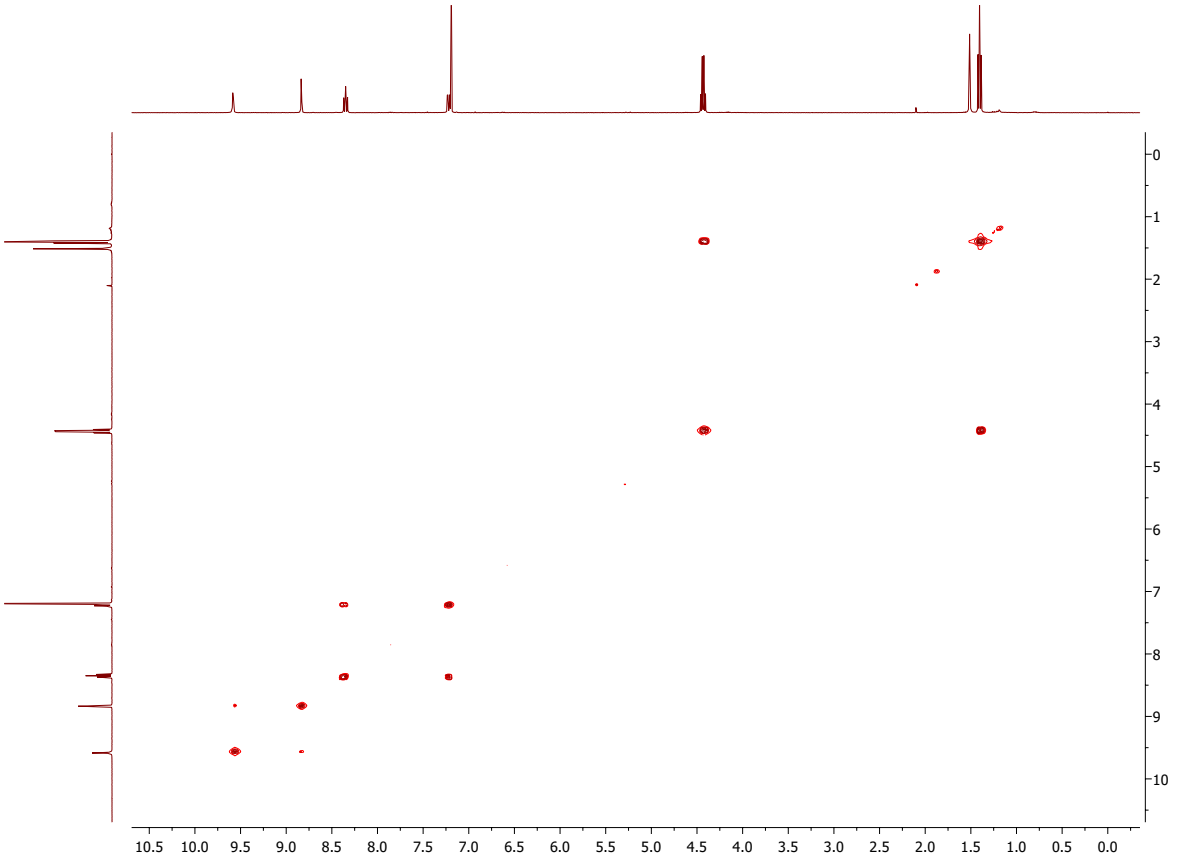

Figure 6.29: COSY of **15** (400 MHz, $CDCl_3$).

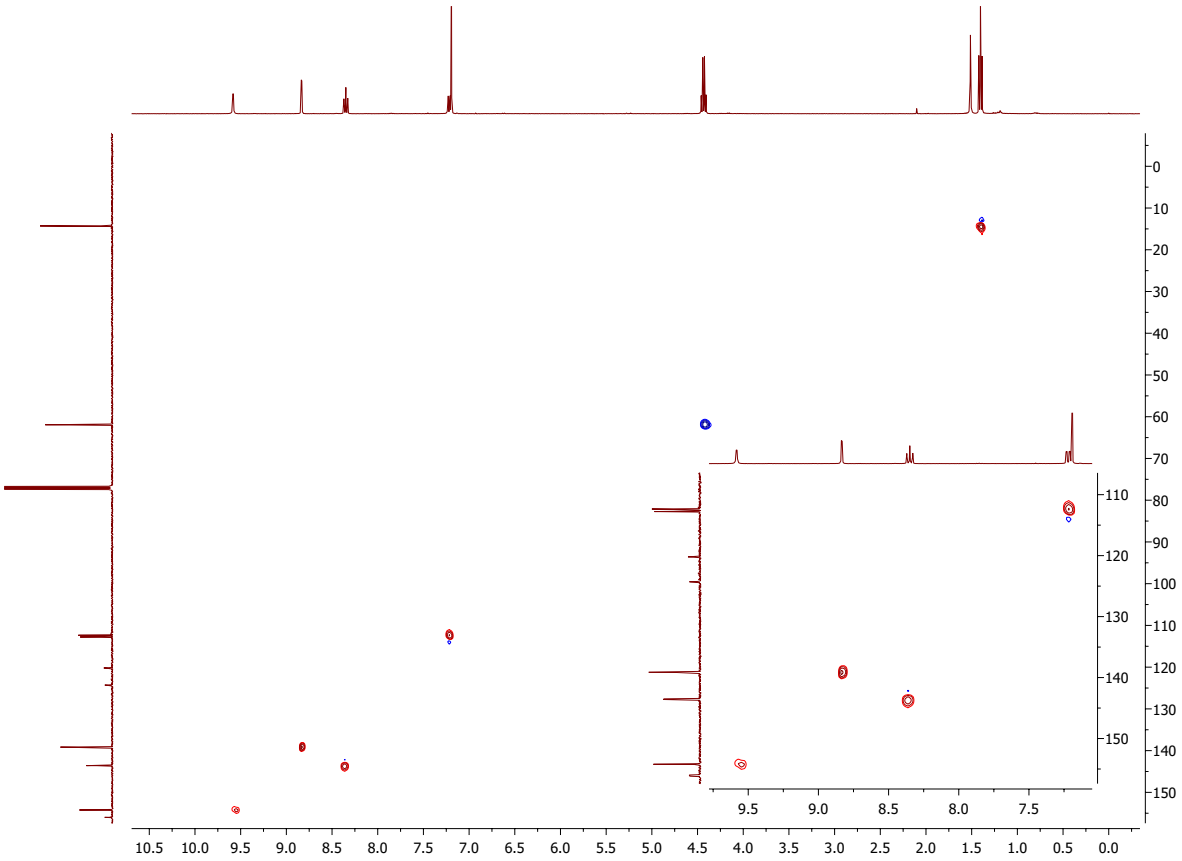

Figure 6.30: HSQC of **15** (400 MHz, $CDCl_3$).

6.10 Ethyl 4-chloro-7-fluoro-8-azaquinoline-3-carboxylate (22)

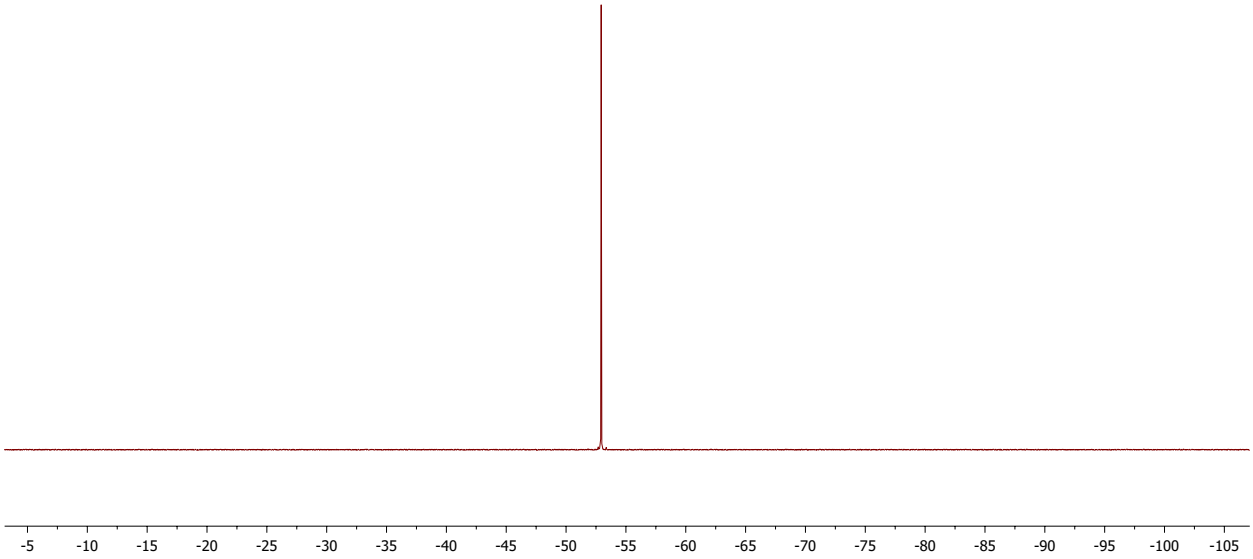

Figure 6.31: ^{19}F NMR (decoupled) of **22** (377 MHz, $CDCl_3$).

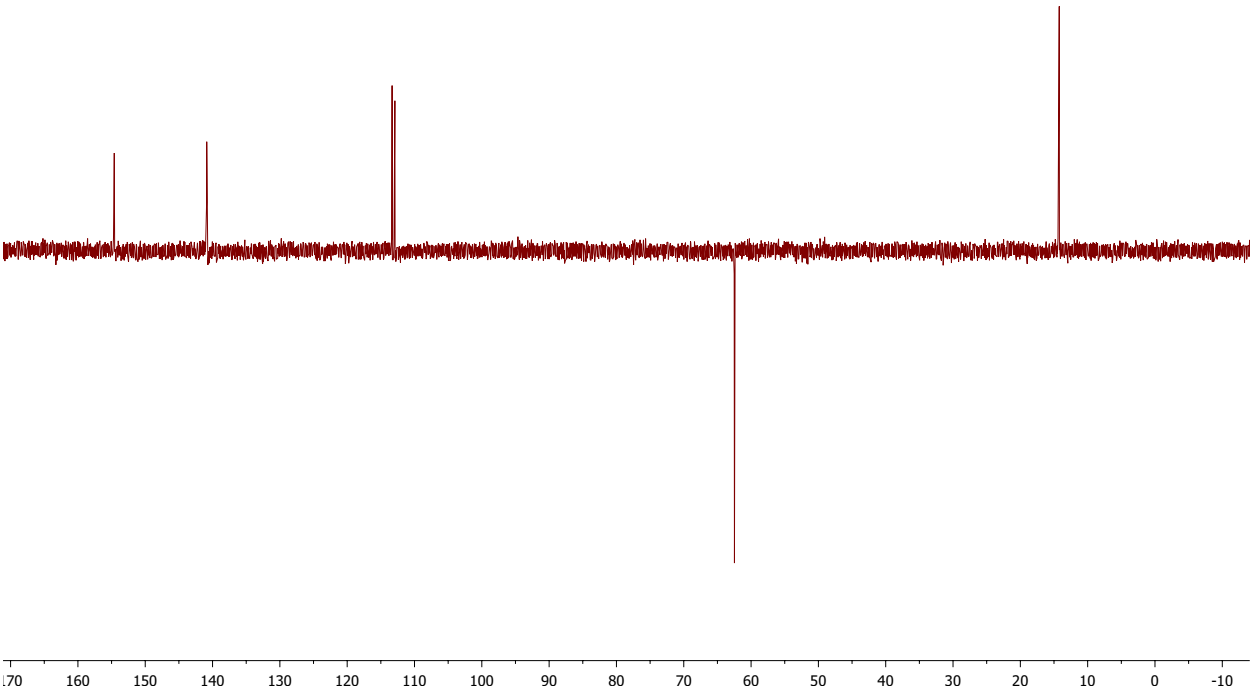

Figure 6.32: DEPT135 of **22** (101 MHz, $CDCl_3$).

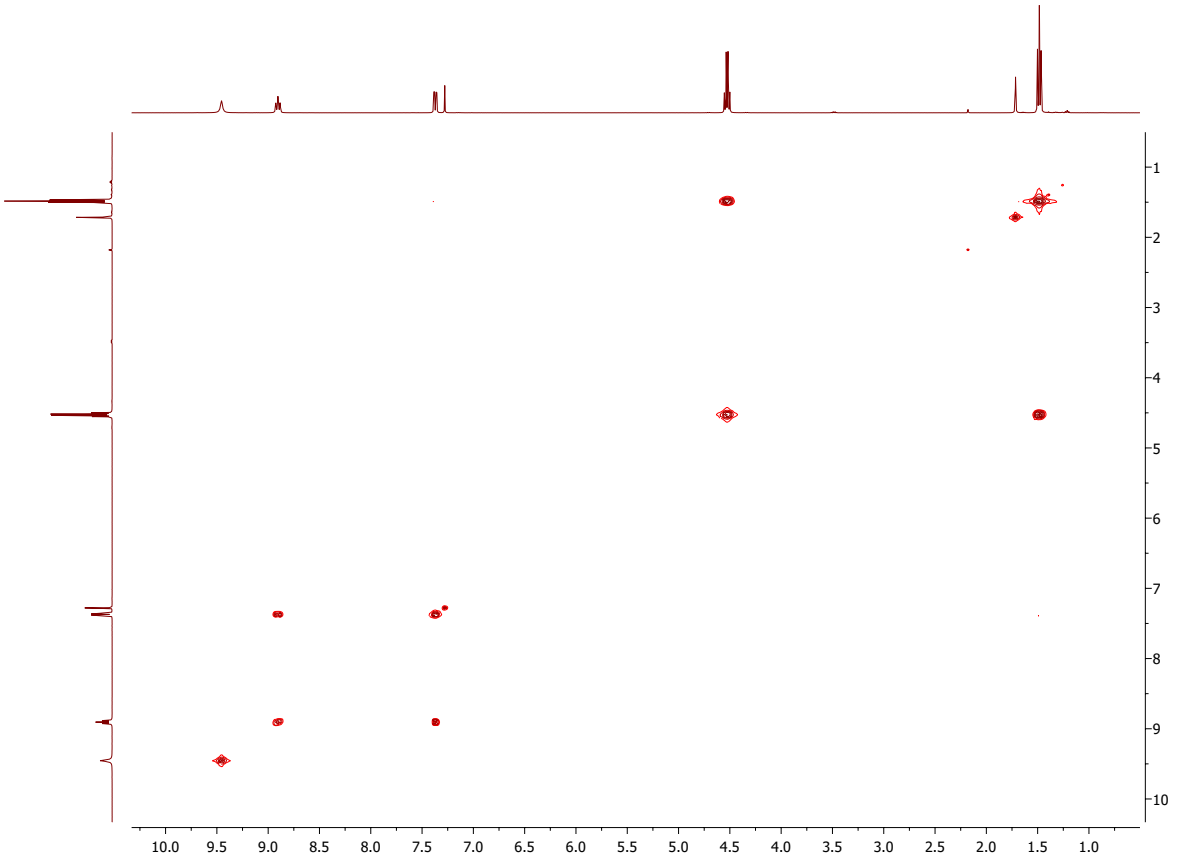

Figure 6.33: COSY of **22** (400 MHz, $CDCl_3$).

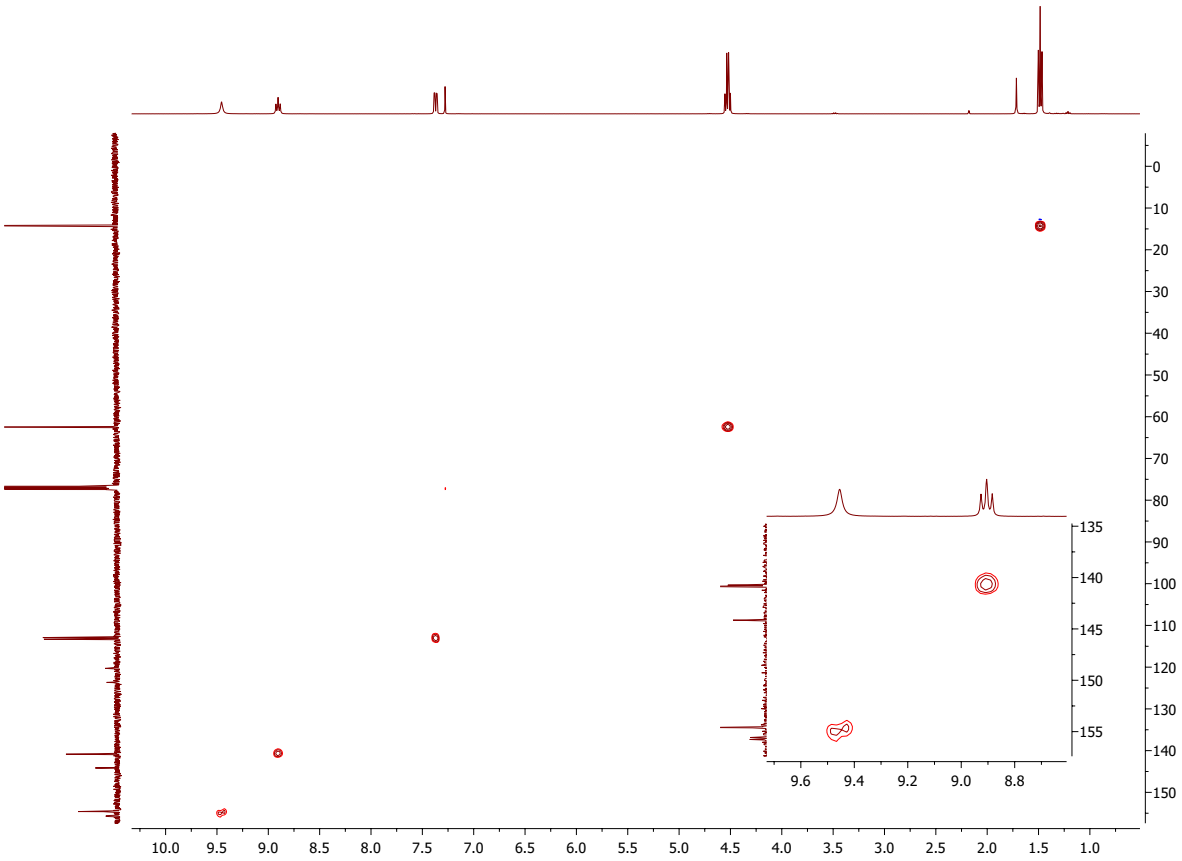

Figure 6.34: HSQC of **22** (400 MHz, $CDCl_3$).

6.11 Ethyl 7-methyl-8-azaquinoline-3-carboxylate (17)

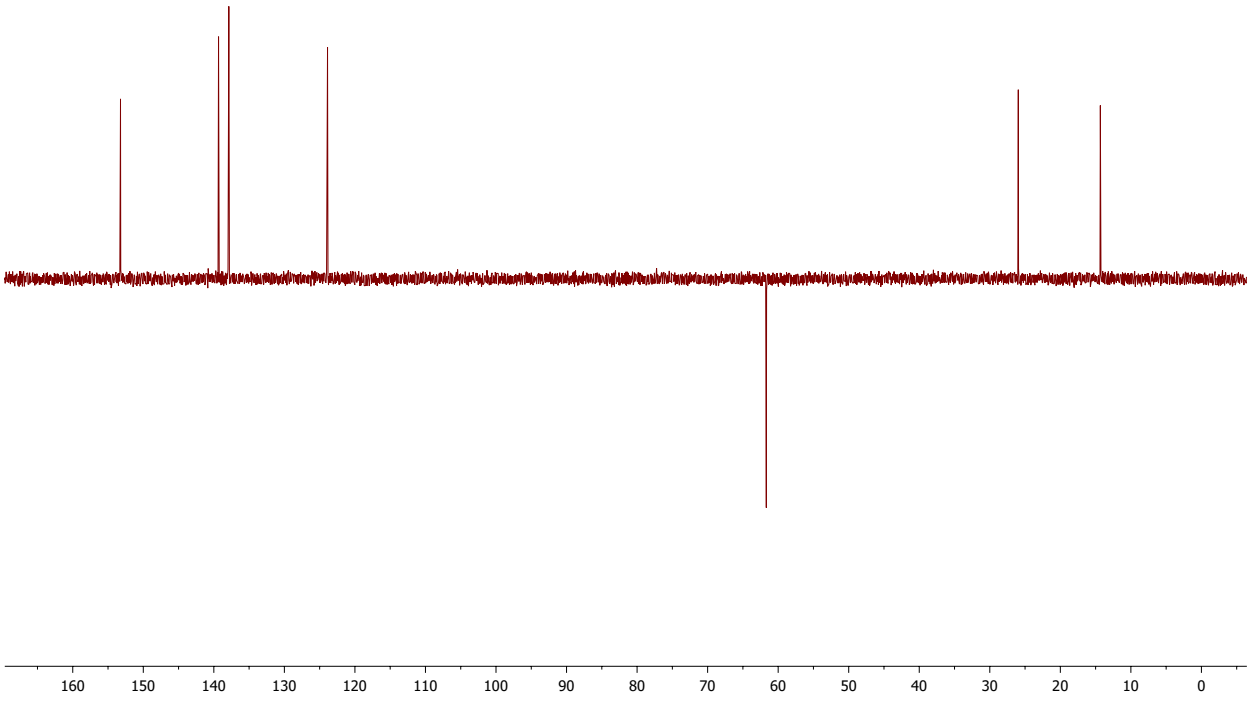

Figure 6.35: DEPT135 of **17** (101 MHz, $CDCl_3$).

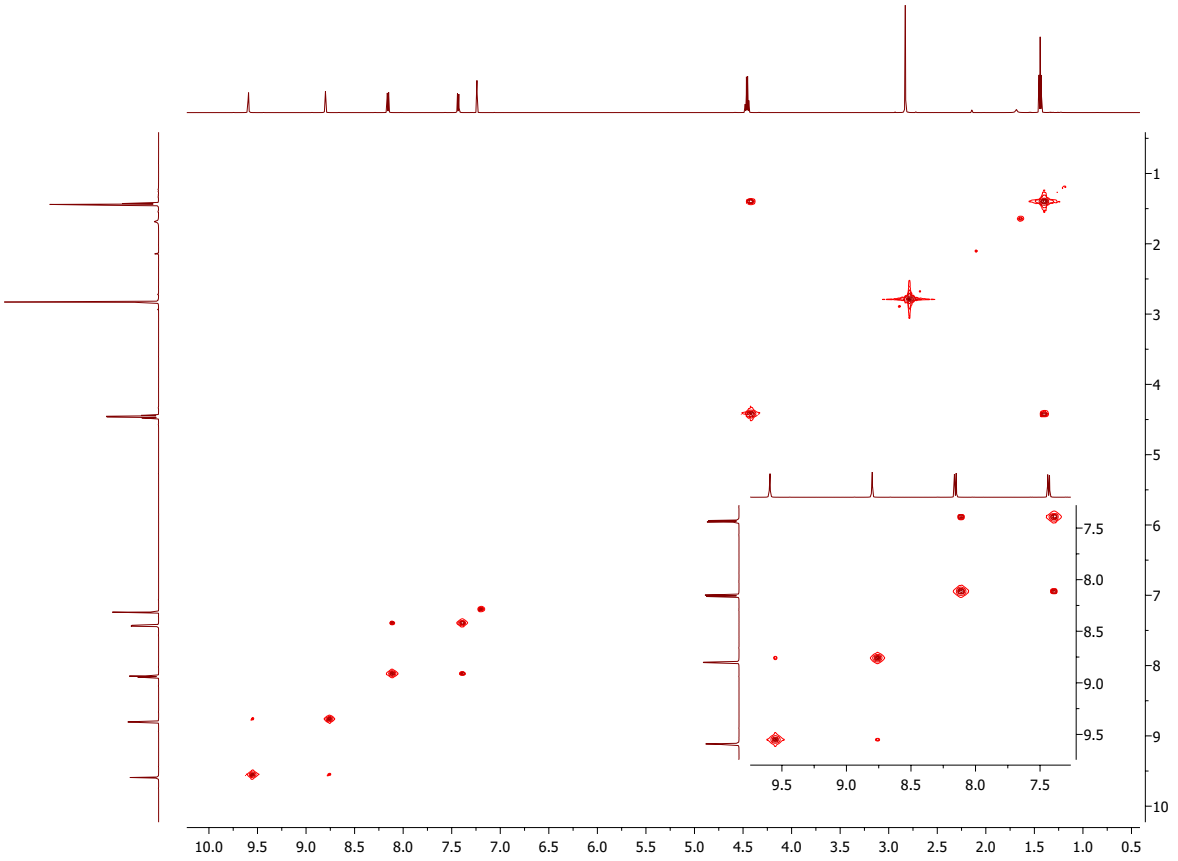

Figure 6.36: COSY of **17** (400 MHz, $CDCl_3$).

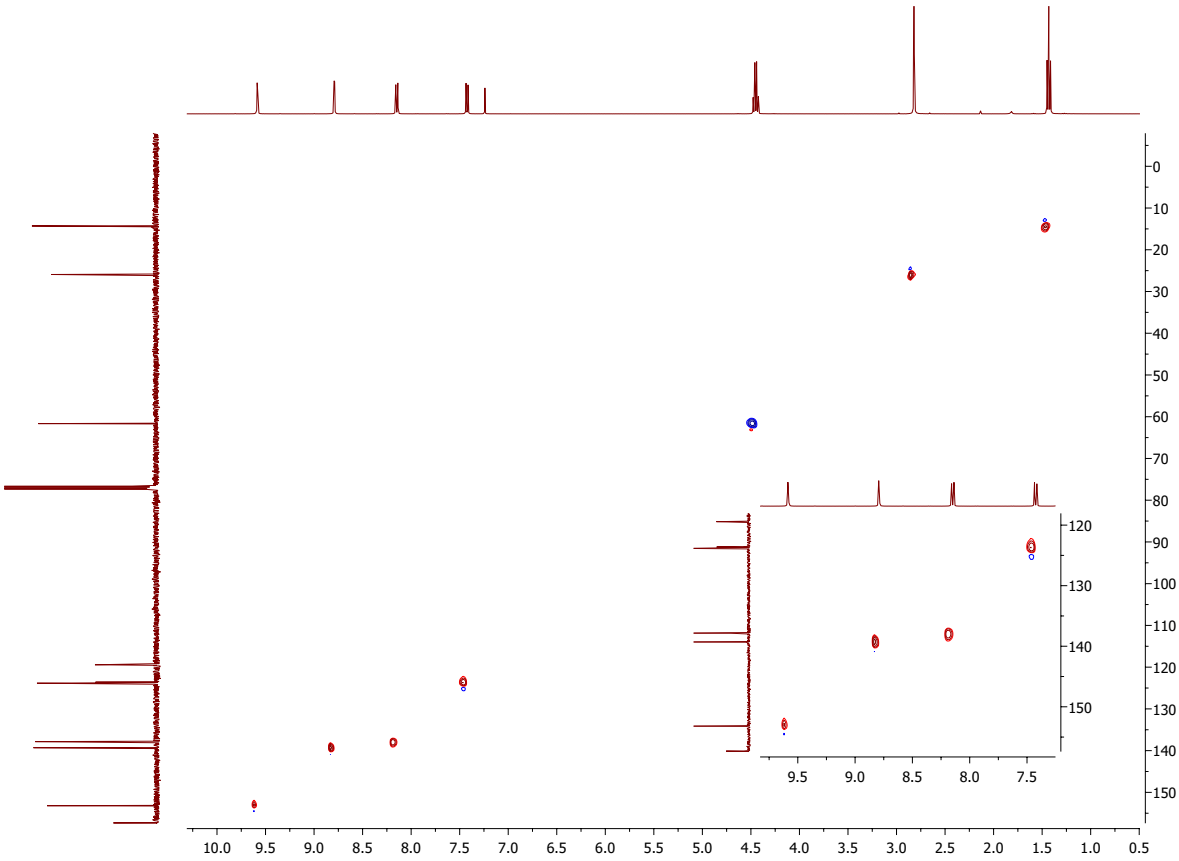

Figure 6.37: HSQC of **17** (400 MHz, $CDCl_3$).

6.12 Ethyl 4-chloro-7-methyl-8-azaquinoline-3-carboxylate (23)

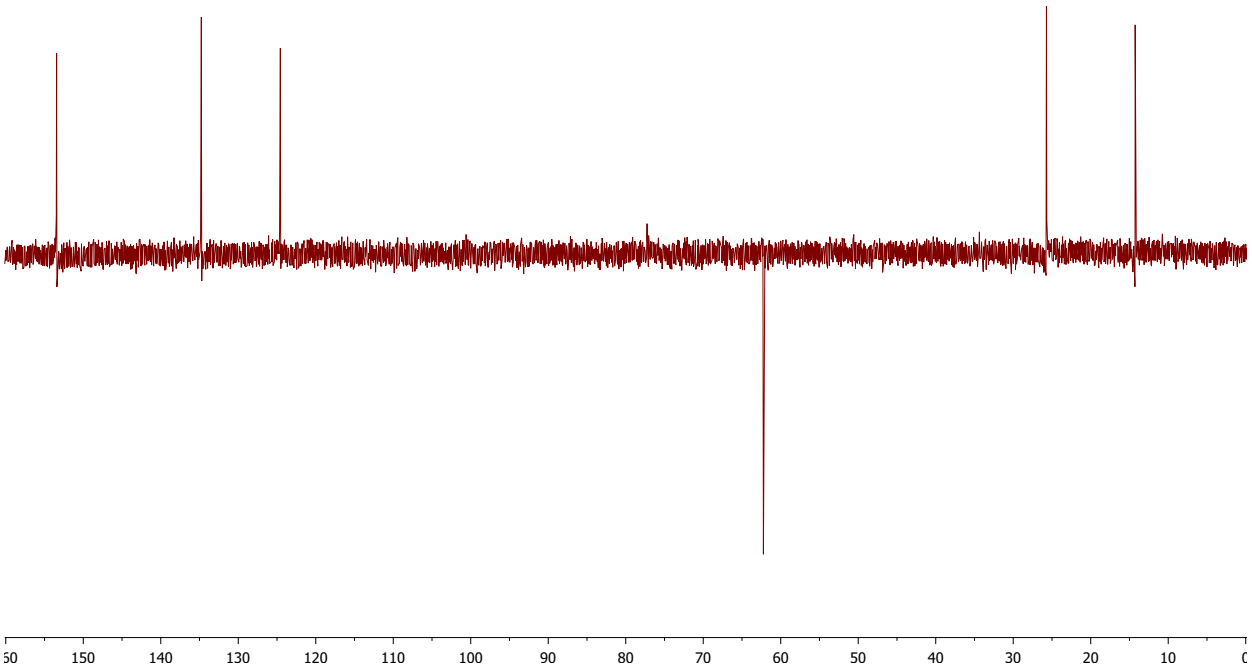

Figure 6.38: DEPT135 of **23** (101 MHz, $CDCl_3$).

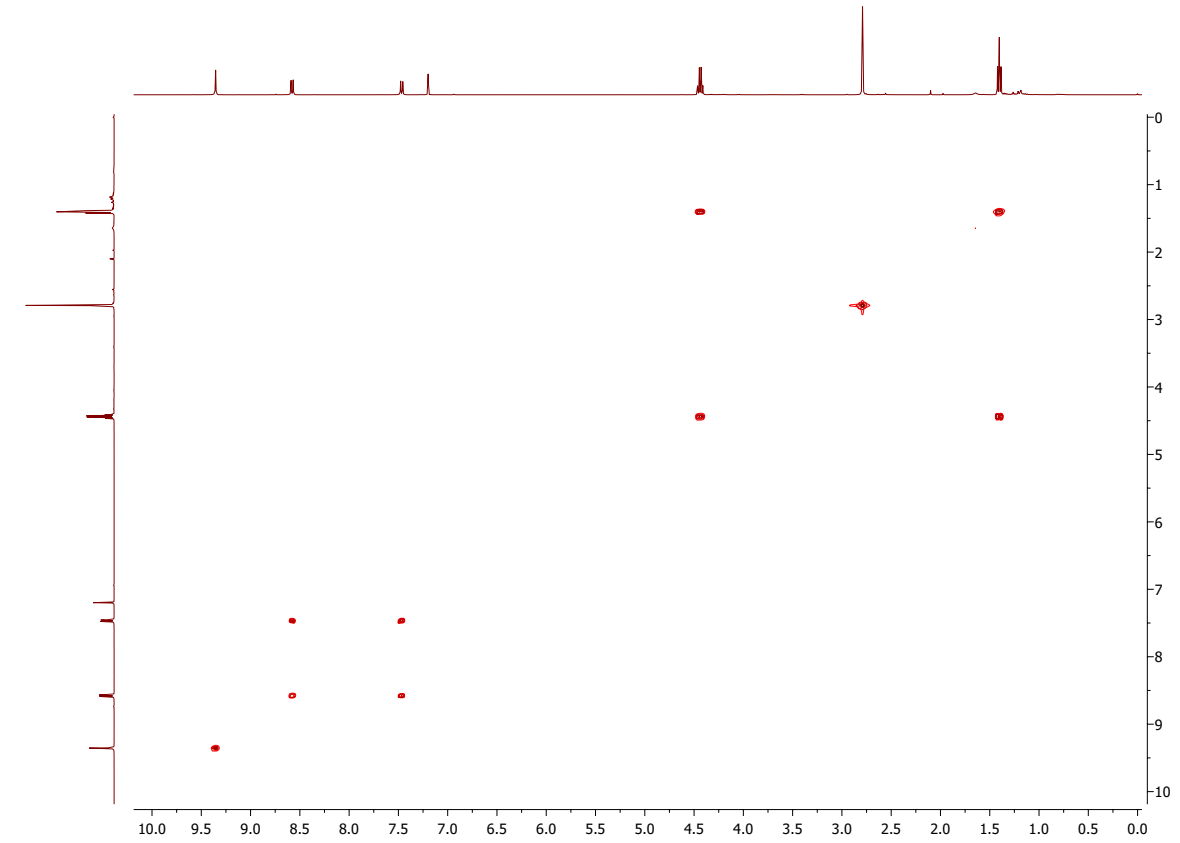

Figure 6.39: COSY of **23** (400 MHz, $CDCl_3$).

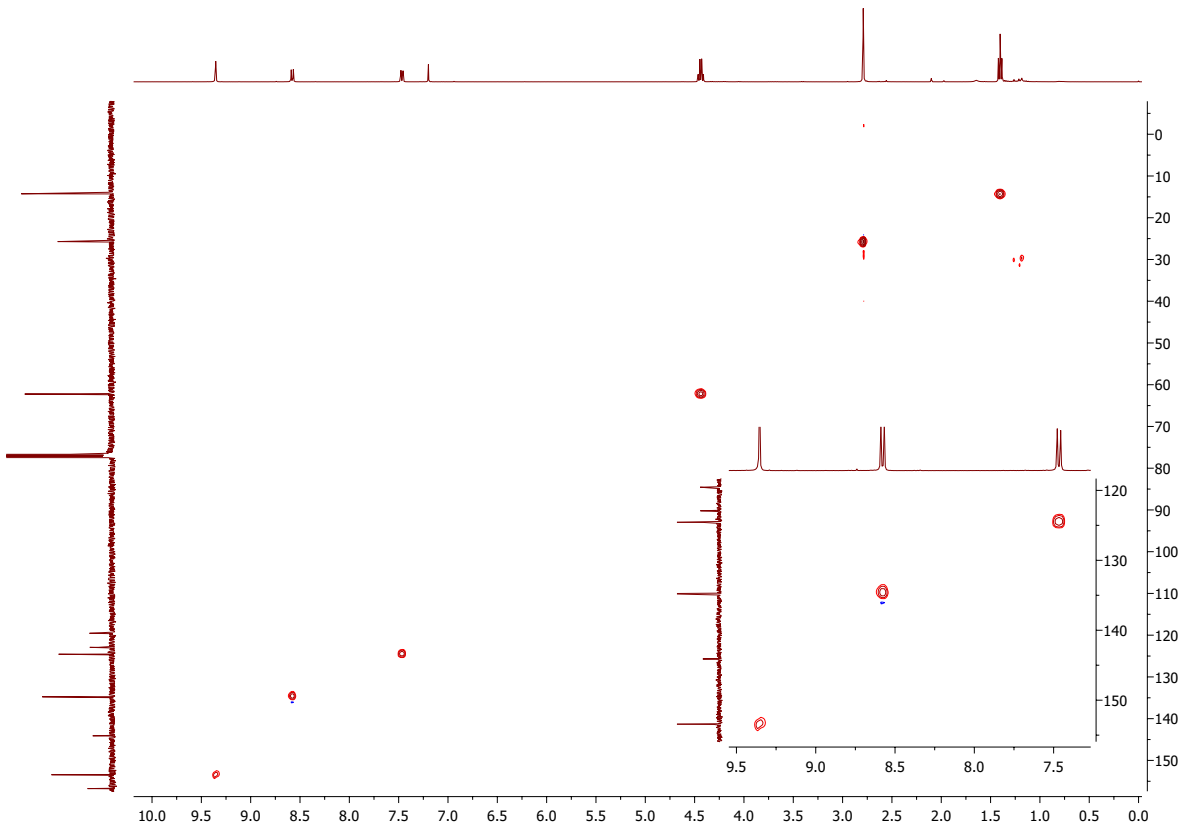

Figure 6.40: HSQC of **23** (400 MHz, $CDCl_3$).

6.13 Diethyl 3-quinolinylphosphonate (34)

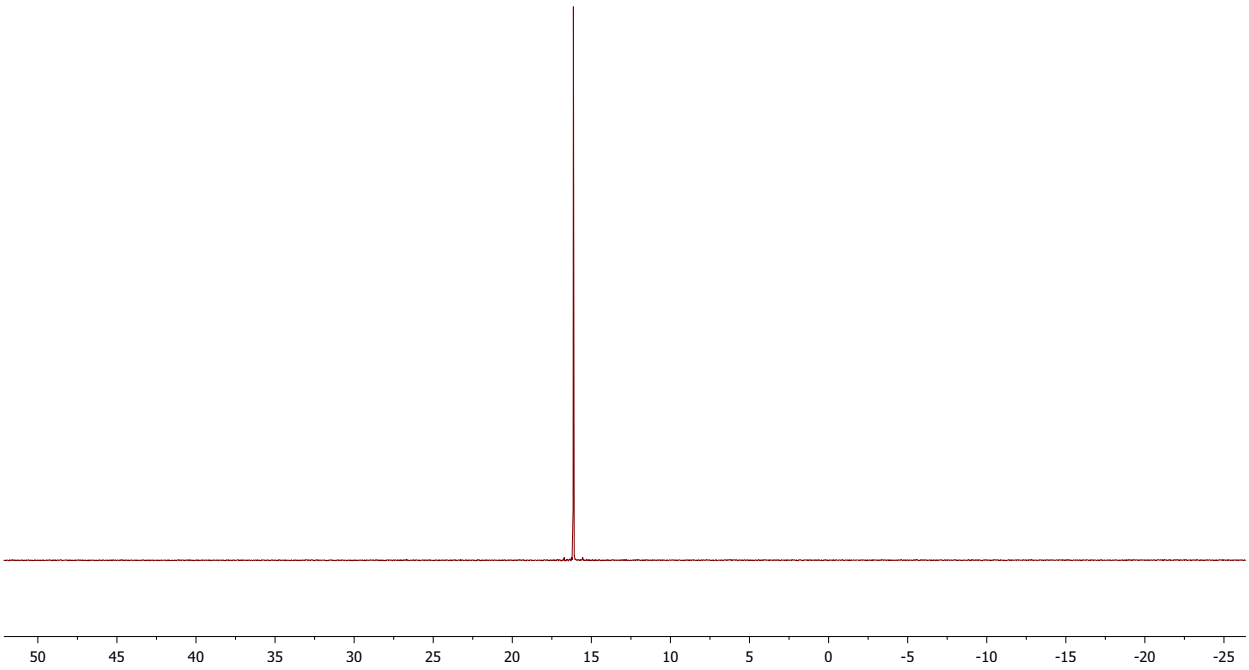

Figure 6.41: ^{31}P NMR (decoupled) of **34** (162 MHz, $CDCl_3$).

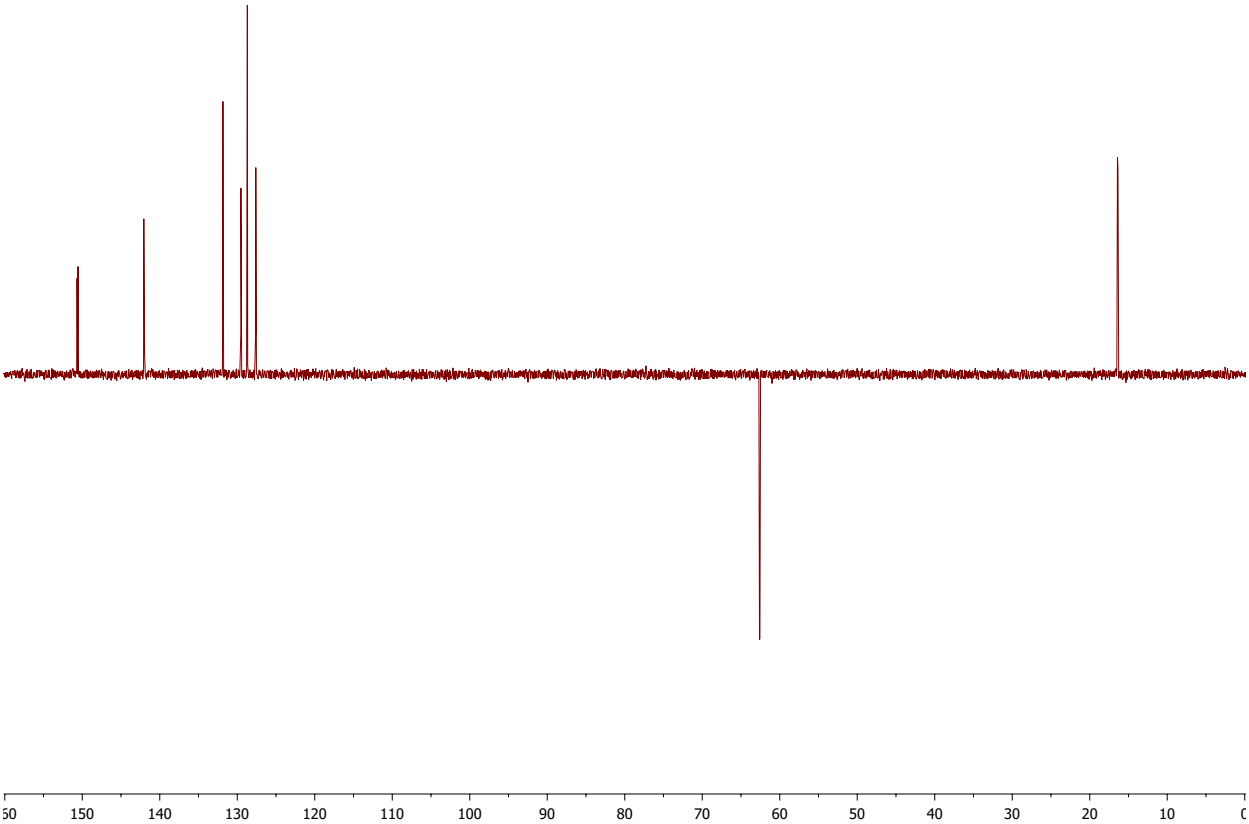

Figure 6.42: DEPT135 of **34** (101 MHz, $CDCl_3$).

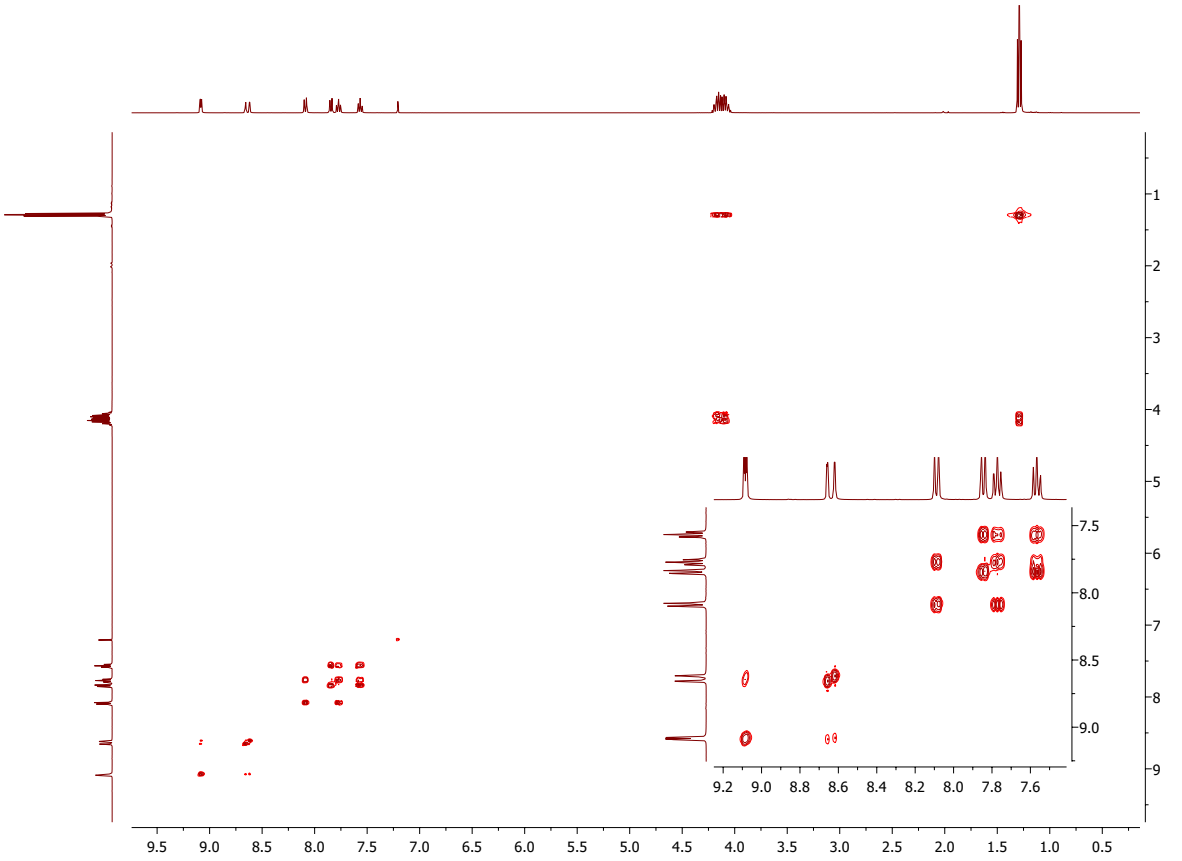

Figure 6.43: COSY of **34** (400 MHz, $CDCl_3$).

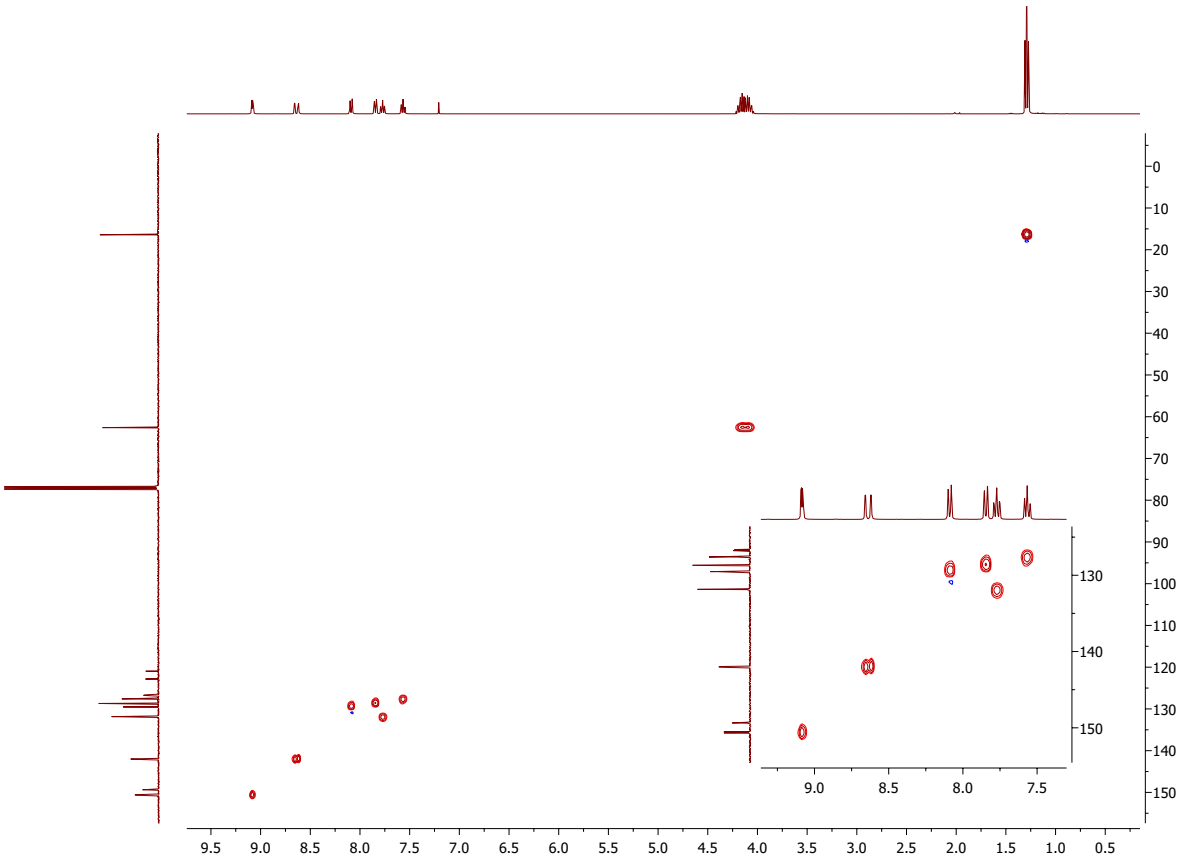

Figure 6.44: HSQC of **34** (400 MHz, $CDCl_3$).

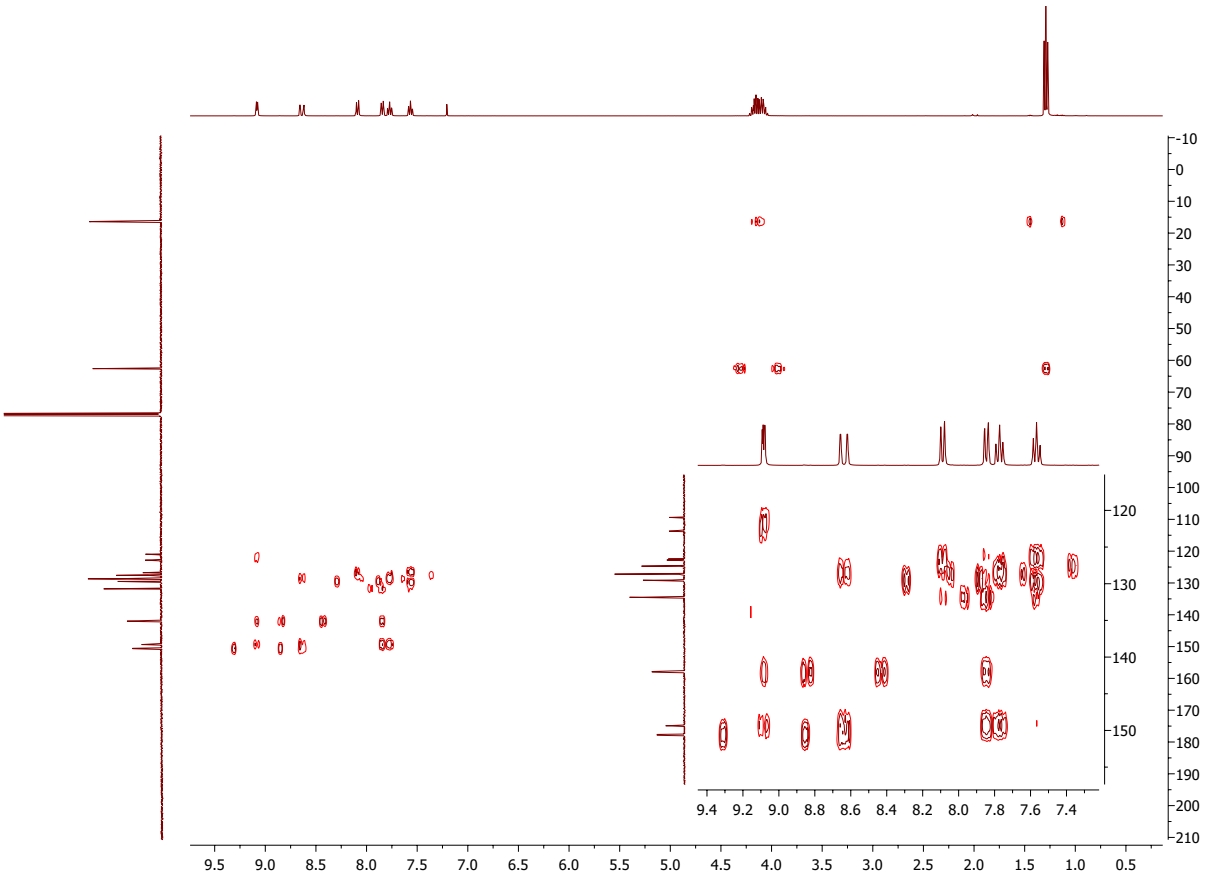

Figure 6.45: HMBC of **34** (400 MHz, $CDCl_3$).

6.14 Diethyl 6-methoxy-3-quinolinylphosphonate (48)

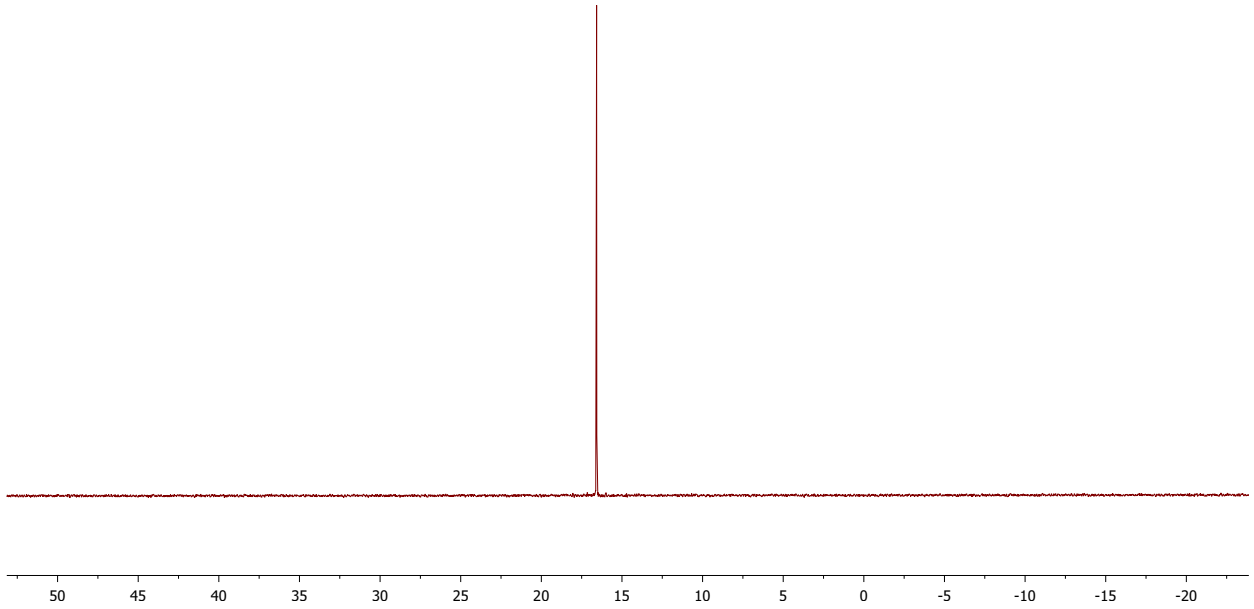

Figure 6.46: ^{31}P NMR (decoupled) of **48** (162 MHz, $CDCl_3$).

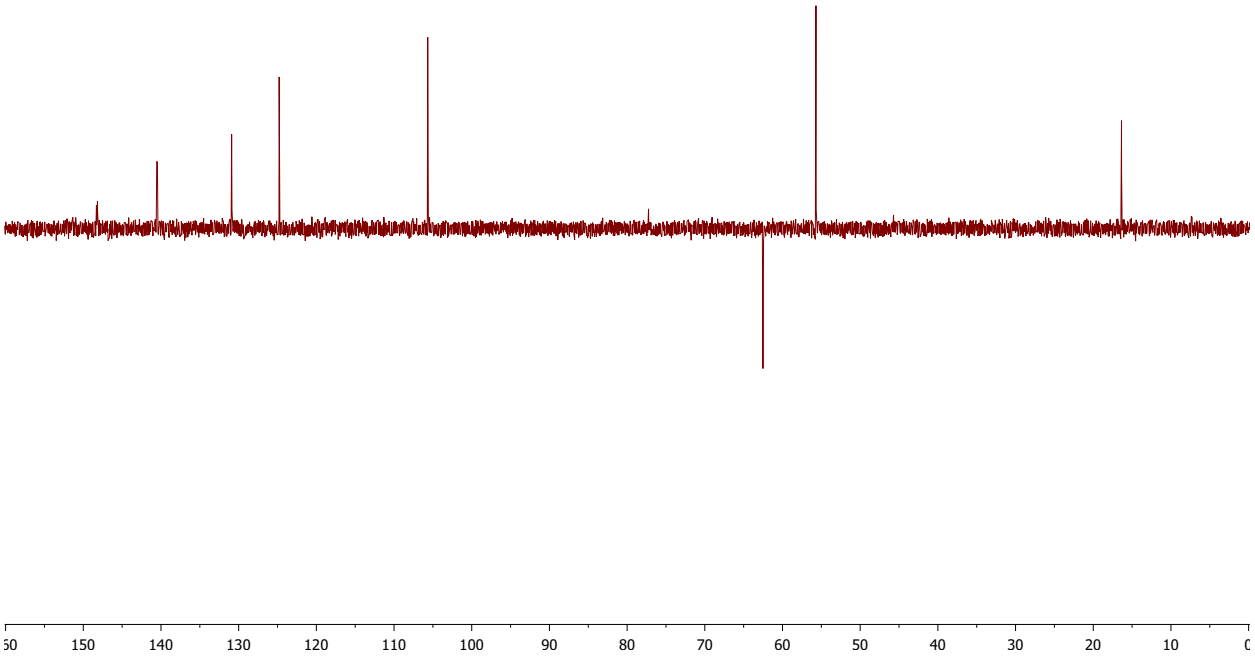

Figure 6.47: DEPT135 of **48** (101 MHz, $CDCl_3$).

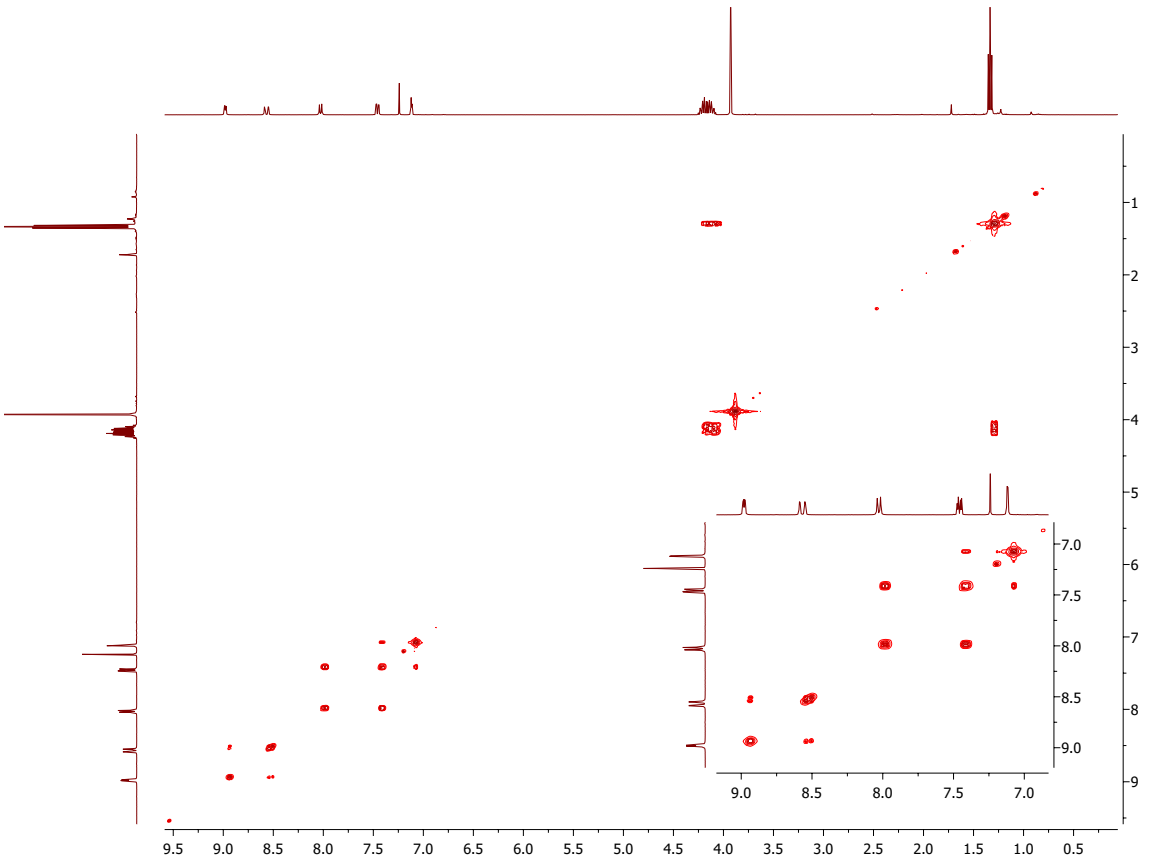

Figure 6.48: COSY of **48** (400 MHz, $CDCl_3$).

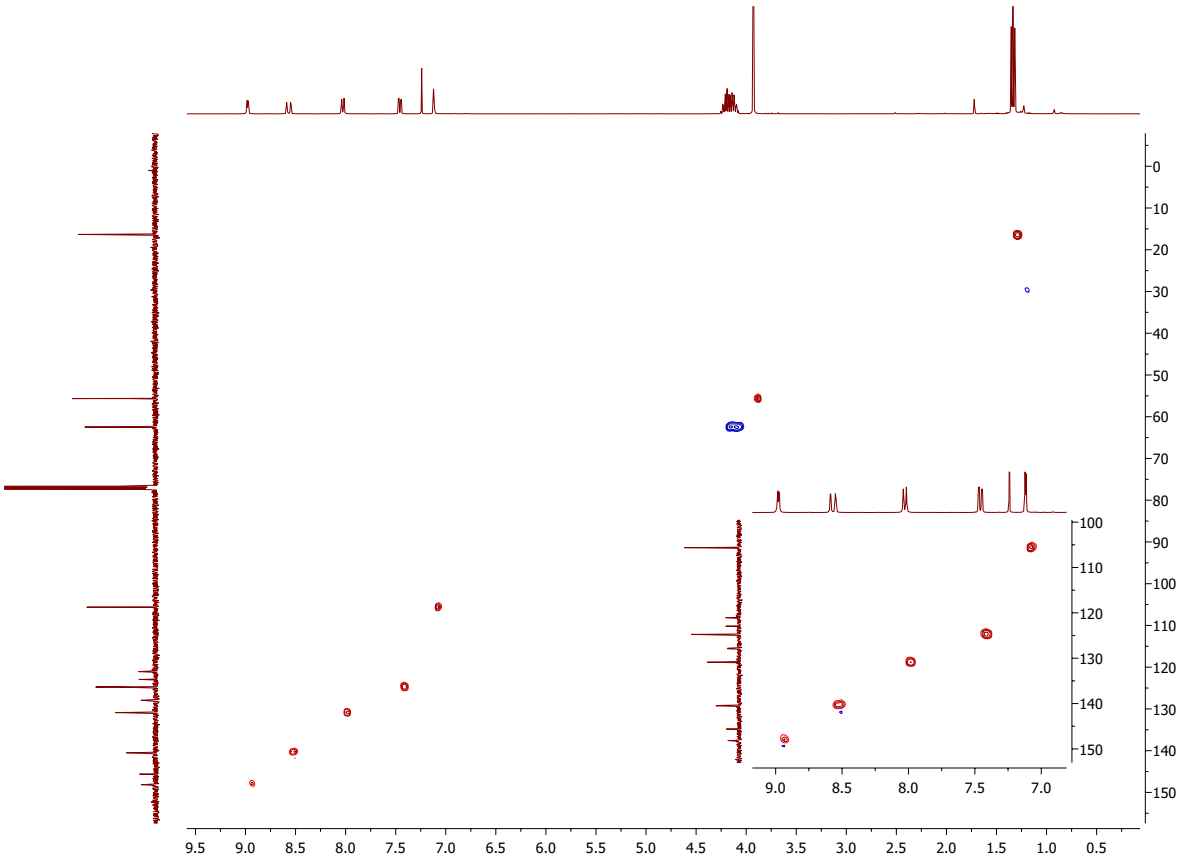

Figure 6.49: HSQC of **48** (400 MHz, $CDCl_3$).

6.15 Diethyl 6-benzyloxy-3-quinolinylphosphonate (49)

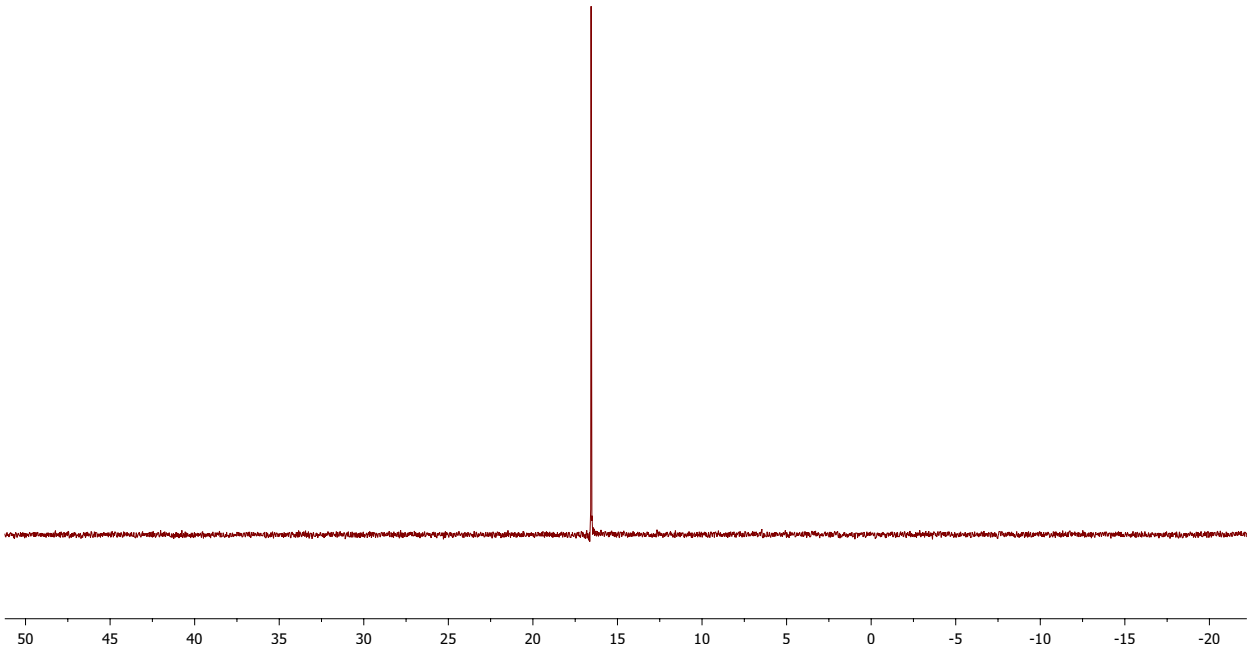

Figure 6.50: ^{31}P NMR (decoupled) of **49** (162 MHz, $CDCl_3$).

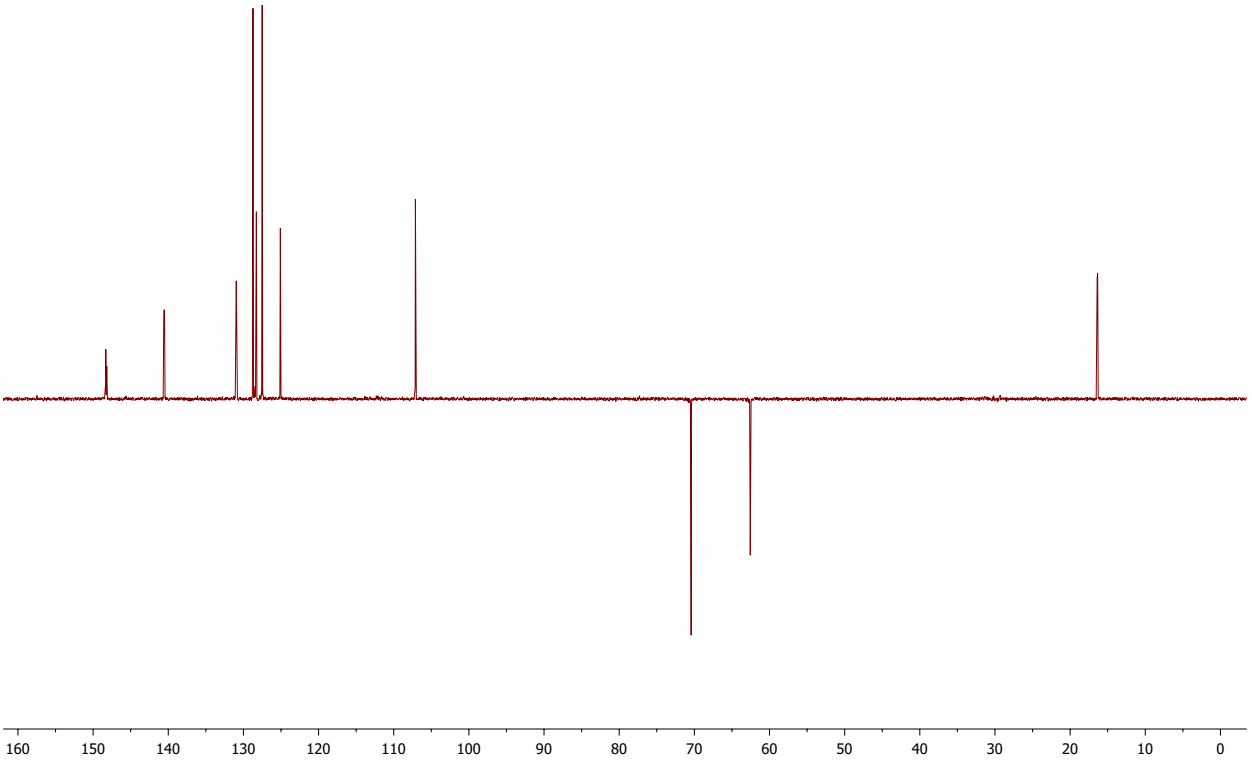

Figure 6.51: DEPT135 of **49** (101 MHz, $CDCl_3$).

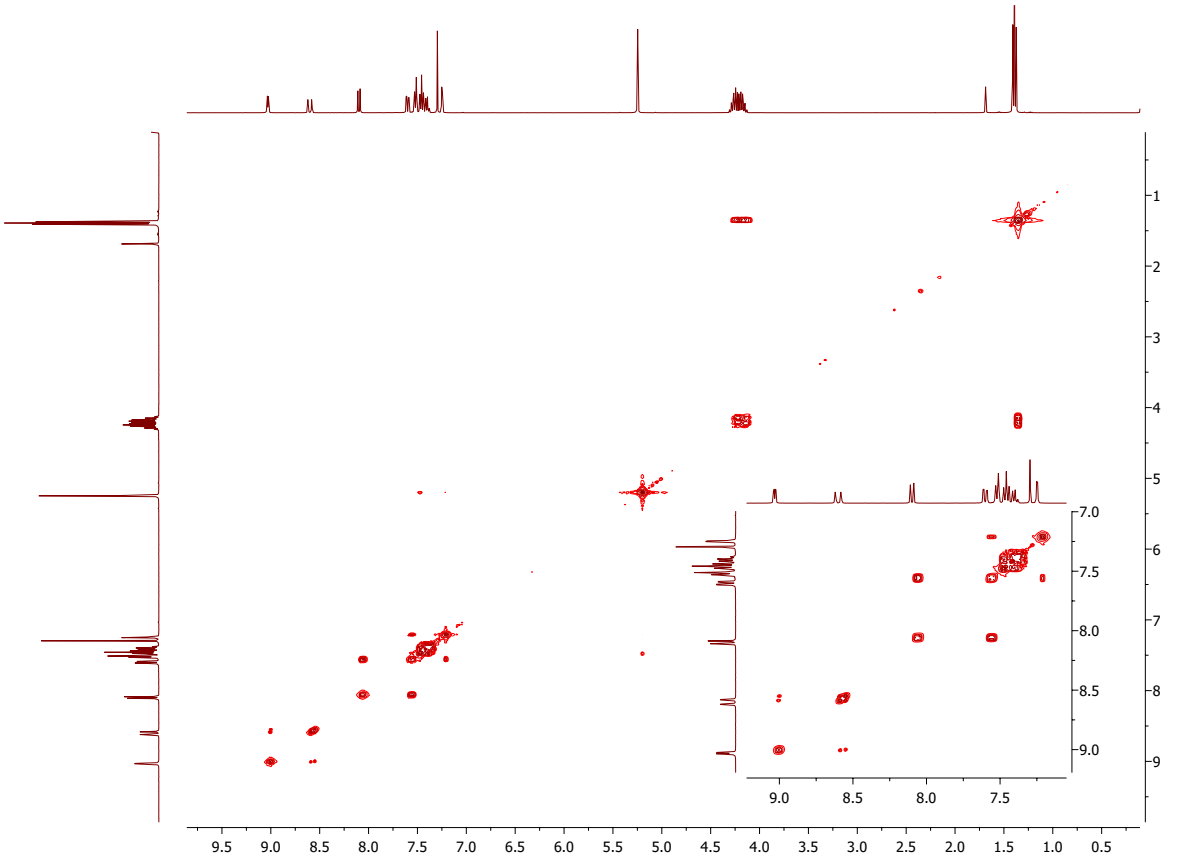

Figure 6.52: COSY of **49** (400 MHz, $CDCl_3$).

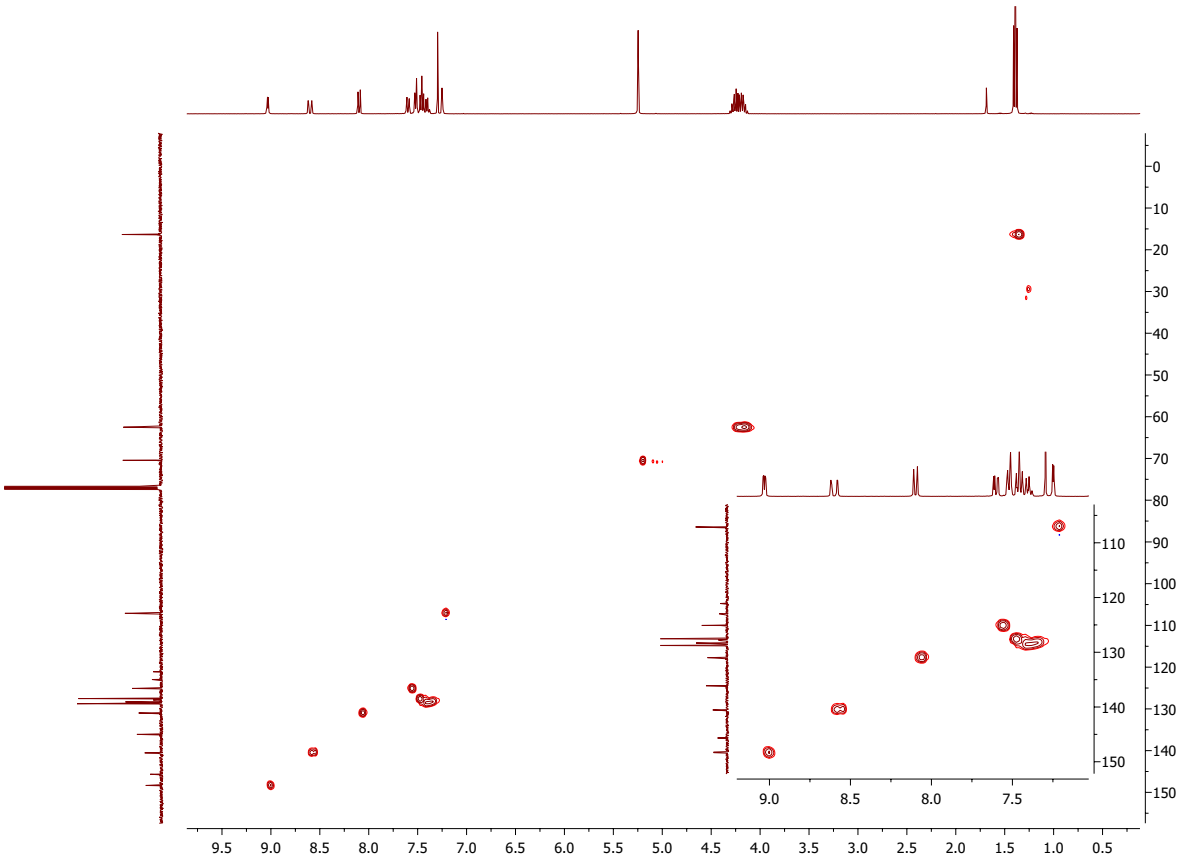

Figure 6.53: HSQC of **49** (400 MHz, $CDCl_3$).

6.16 Diethyl 6-bromo-3-quinolinylphosphonate (50)

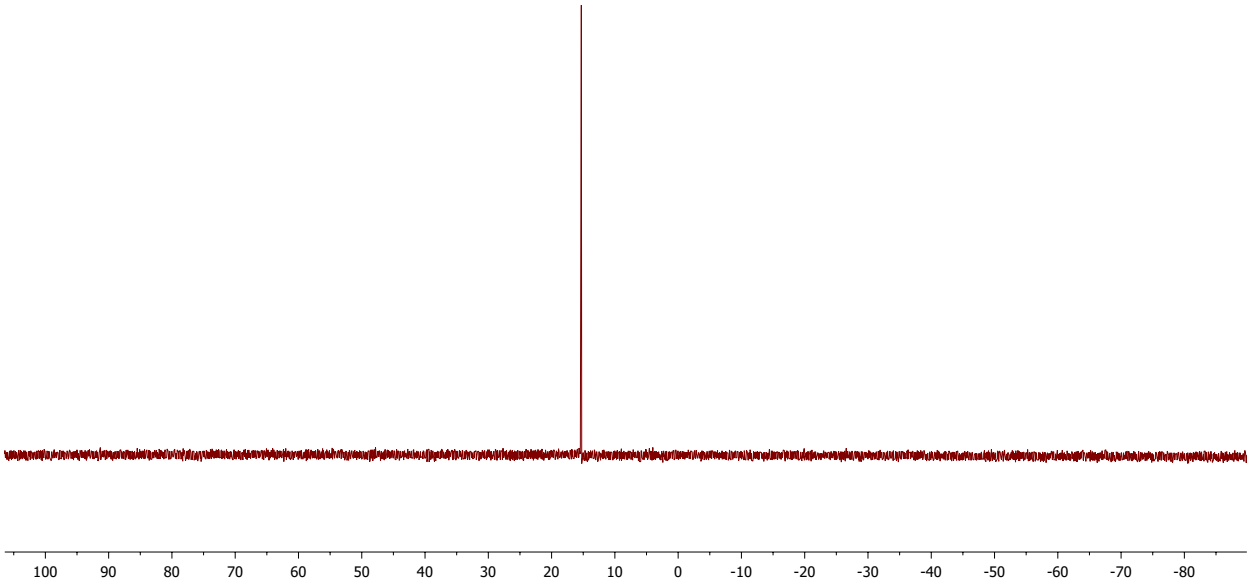

Figure 6.54: ^{31}P NMR (decoupled) of **50** (162 MHz, $CDCl_3$).

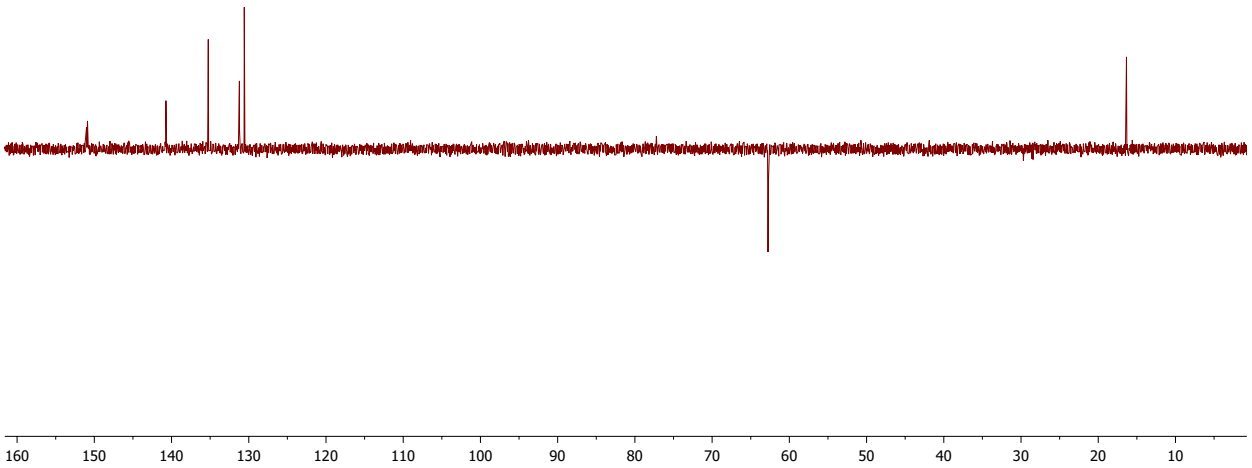

Figure 6.55: DEPT135 of **50** (101 MHz, $CDCl_3$).

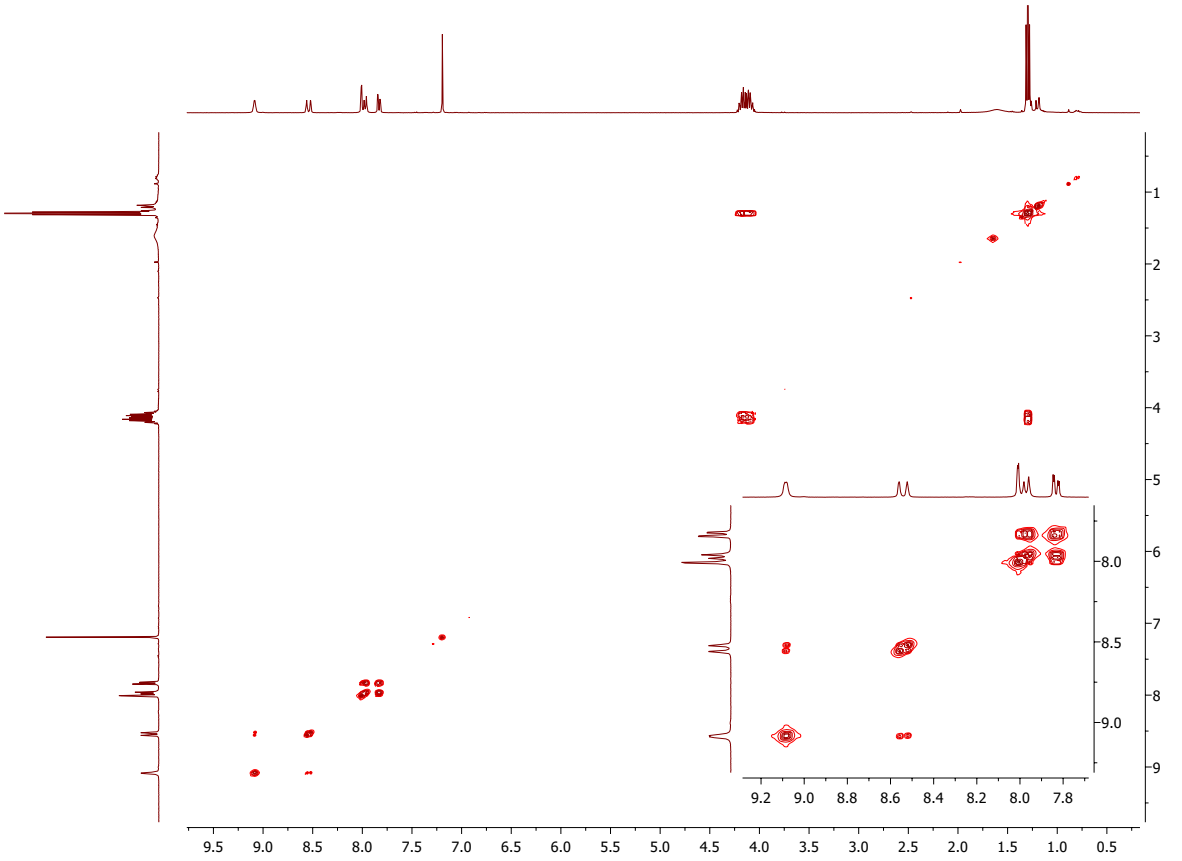

Figure 6.56: COSY of **50** (400 MHz, $CDCl_3$).

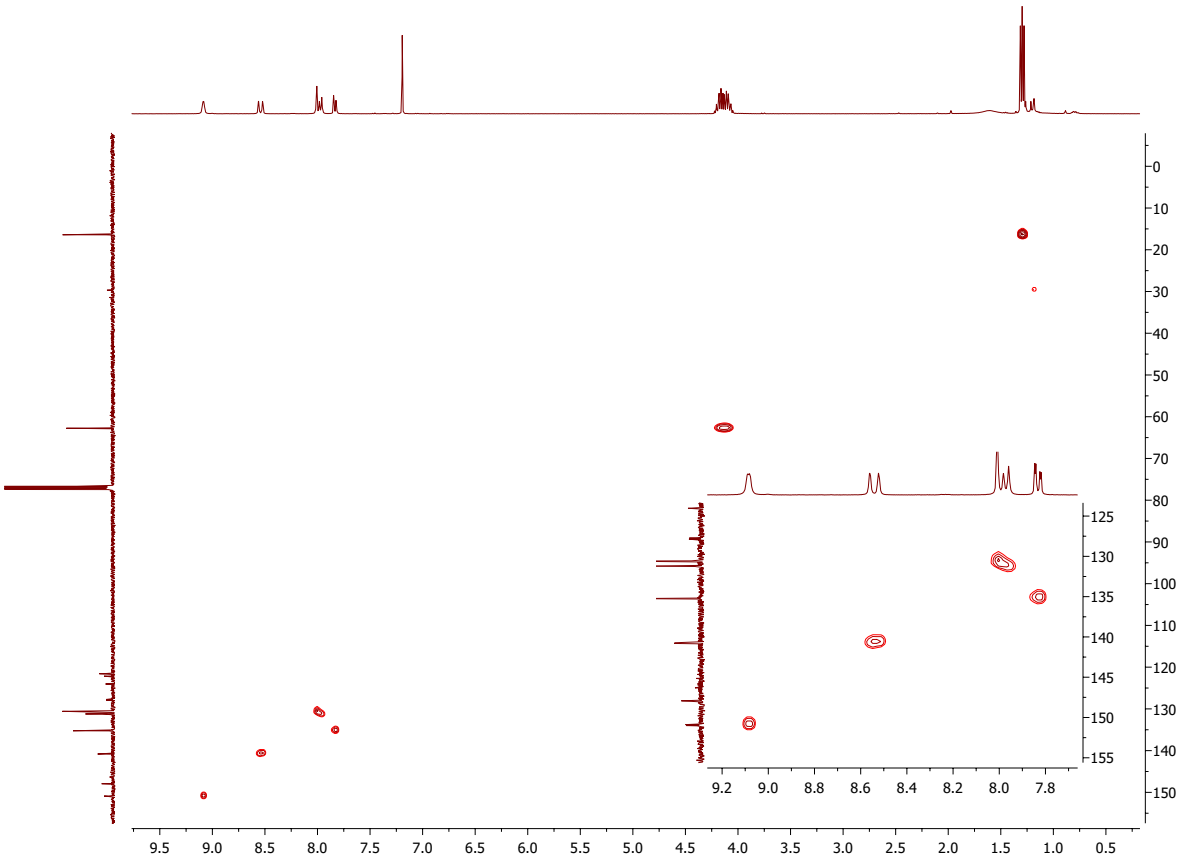

Figure 6.57: HSQC of **50** (400 MHz, $CDCl_3$).

6.17 Diethyl 6,7-difluoro-3-quinolinylphosphonate (51)

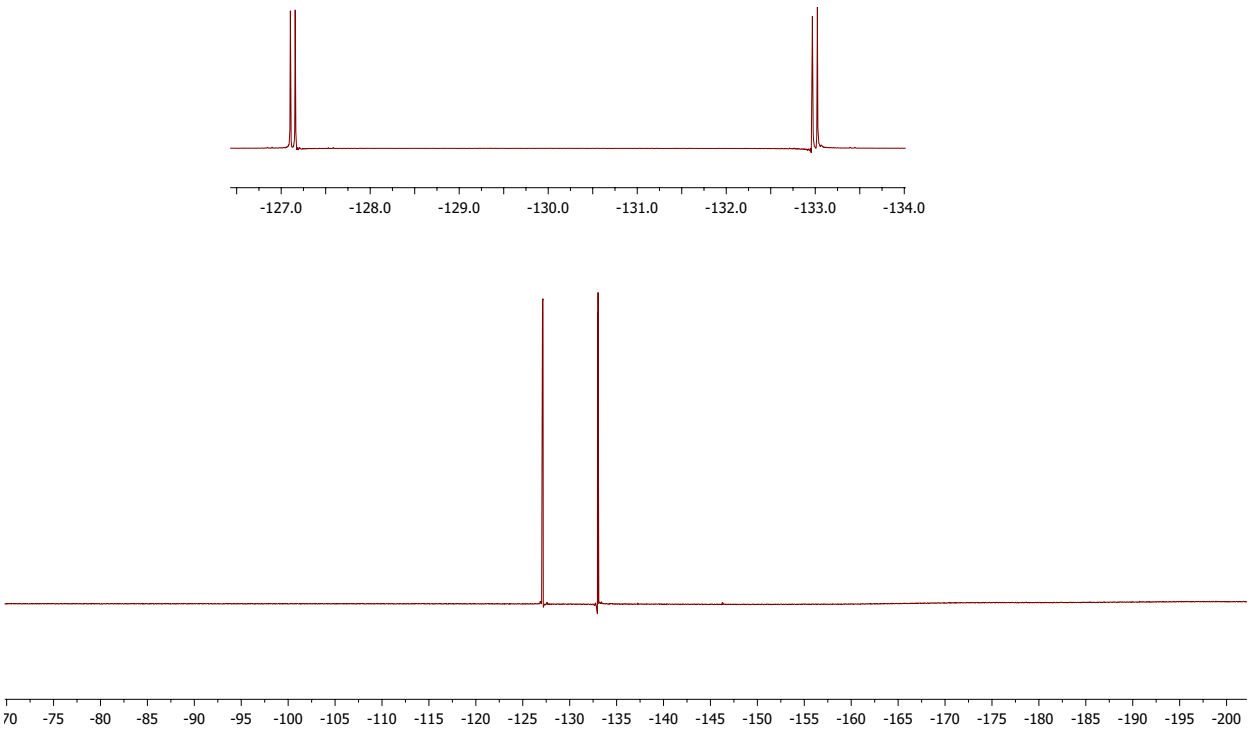

Figure 6.58: ^{19}F NMR (decoupled) of **51** (377 MHz, $CDCl_3$).

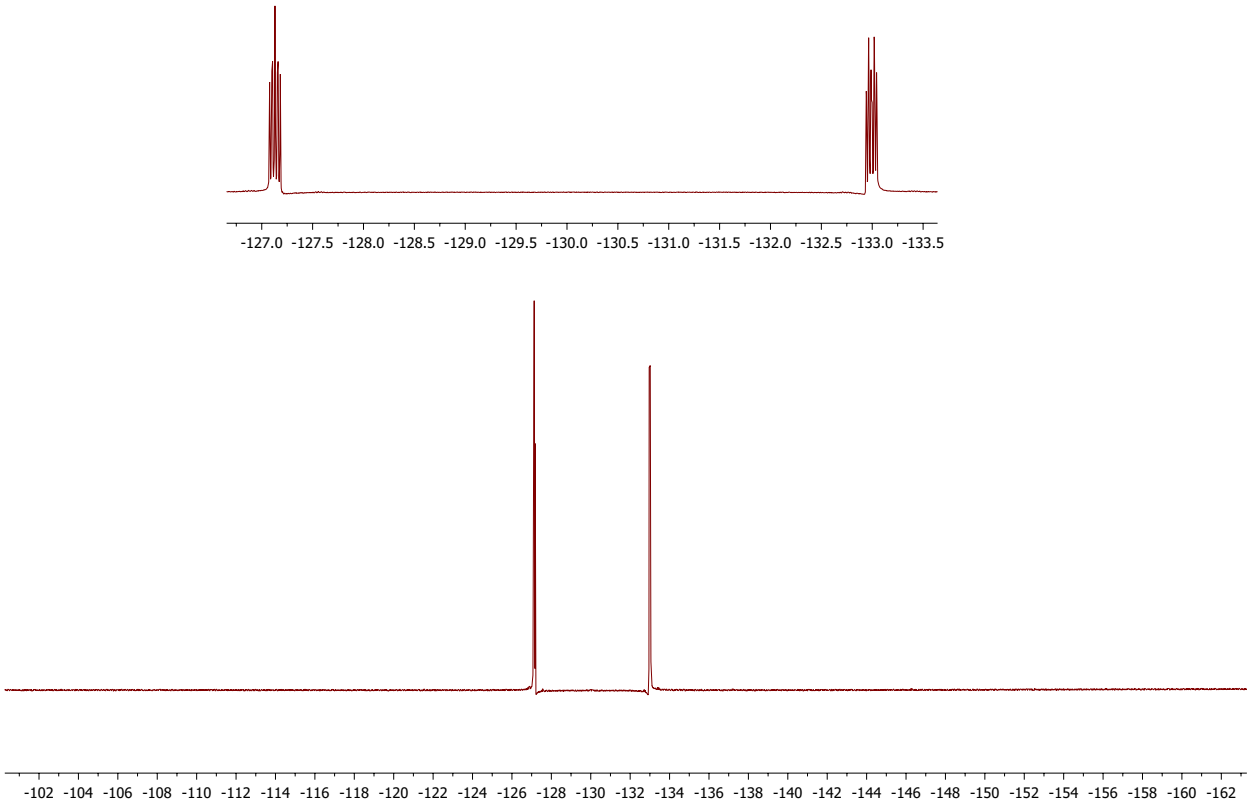

Figure 6.59: ^{19}F NMR (coupled) of **51** (377 MHz, $CDCl_3$).

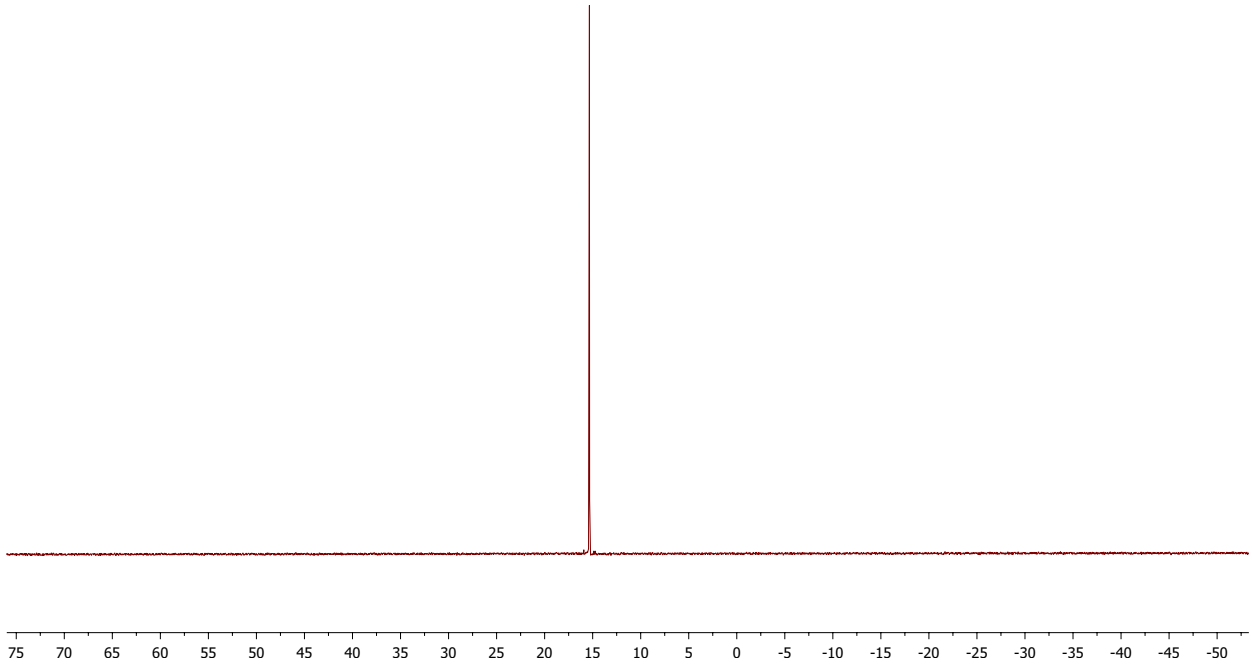

Figure 6.60: ^{31}P NMR (decoupled) of **51** (162 MHz, $CDCl_3$).

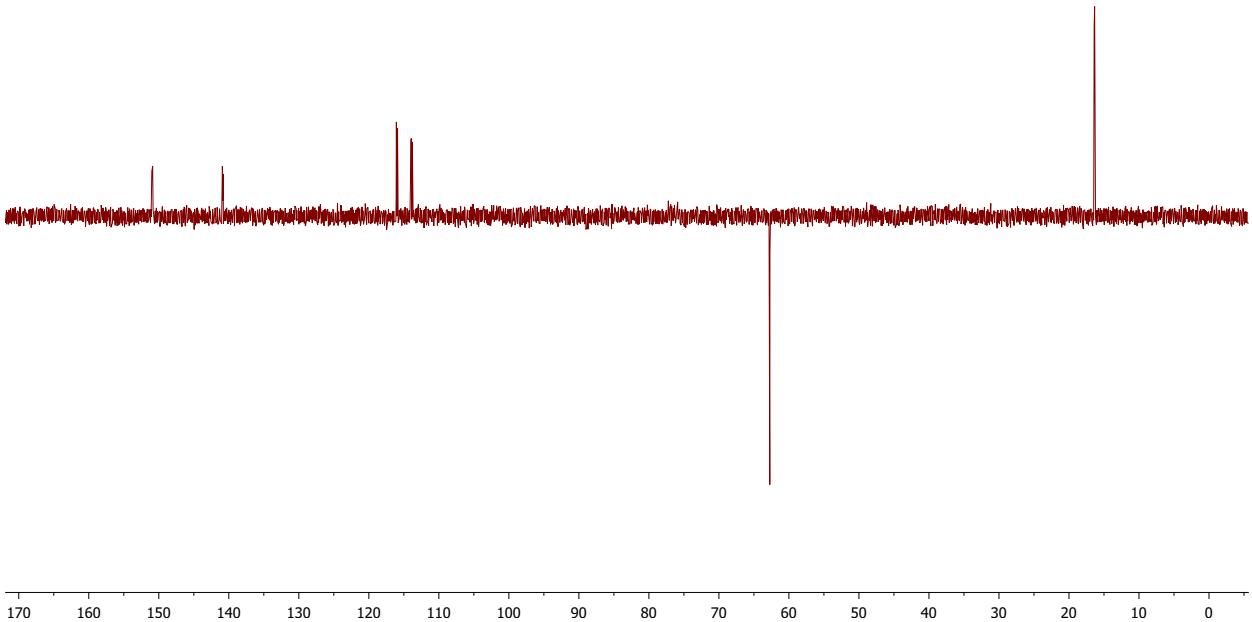

Figure 6.61: DEPT135 of **51** (101 MHz, $CDCl_3$).

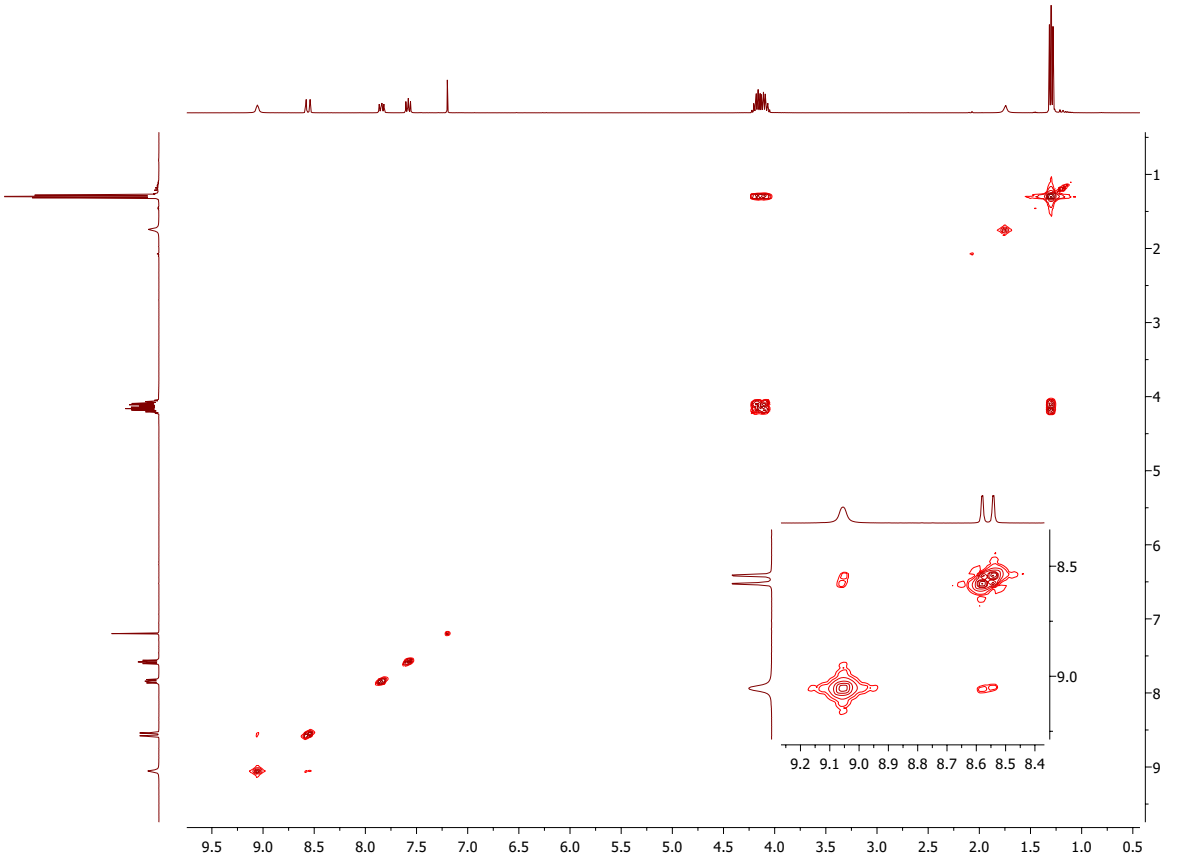

Figure 6.62: COSY of **51** (400 MHz, $CDCl_3$).

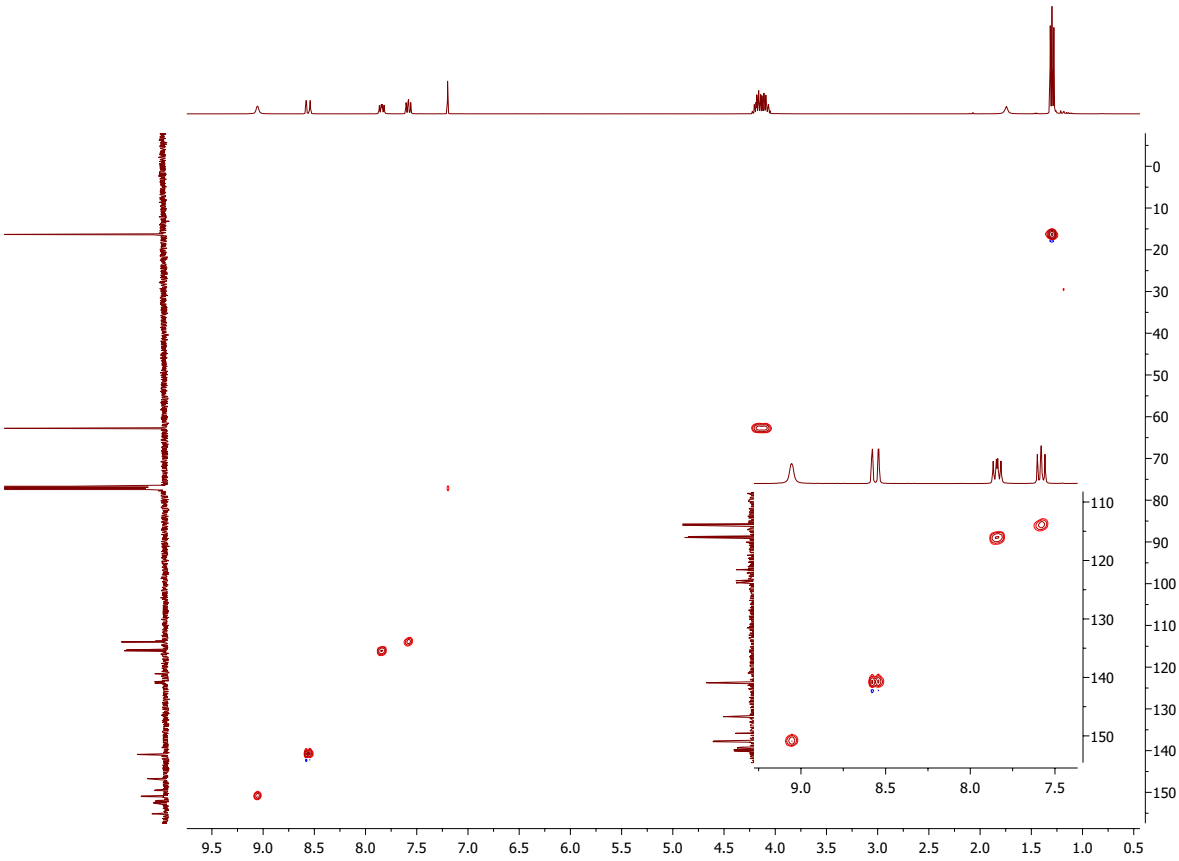

Figure 6.63: HSQC of **51** (400 MHz, $CDCl_3$).

6.18 Diethyl 7-bromo-3-quinolinylphosphonate (52)

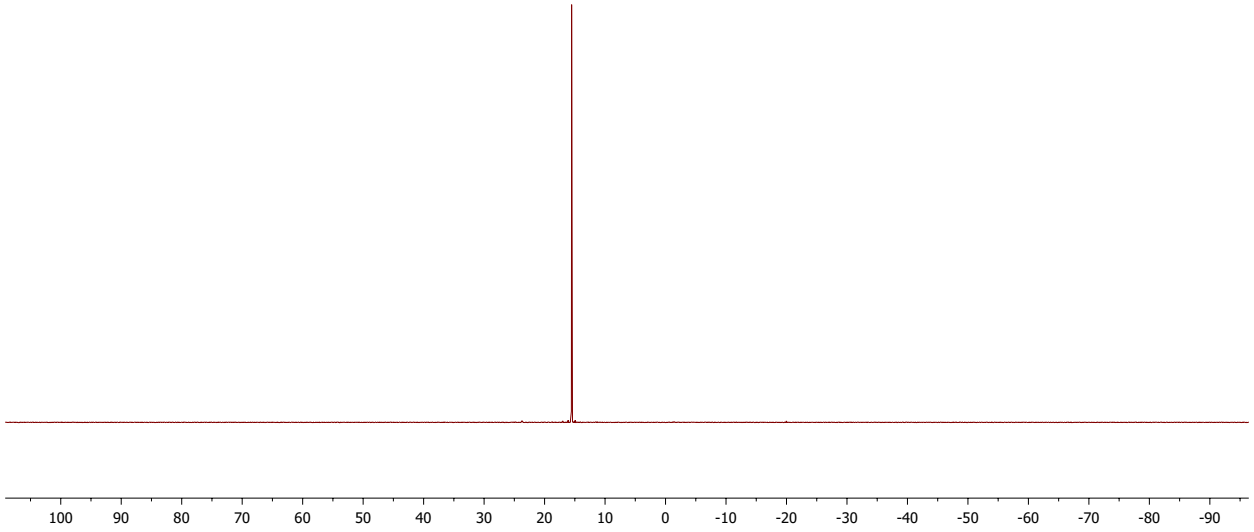

Figure 6.64: ^{31}P NMR (decoupled) of **52** (162 MHz, $CDCl_3$).

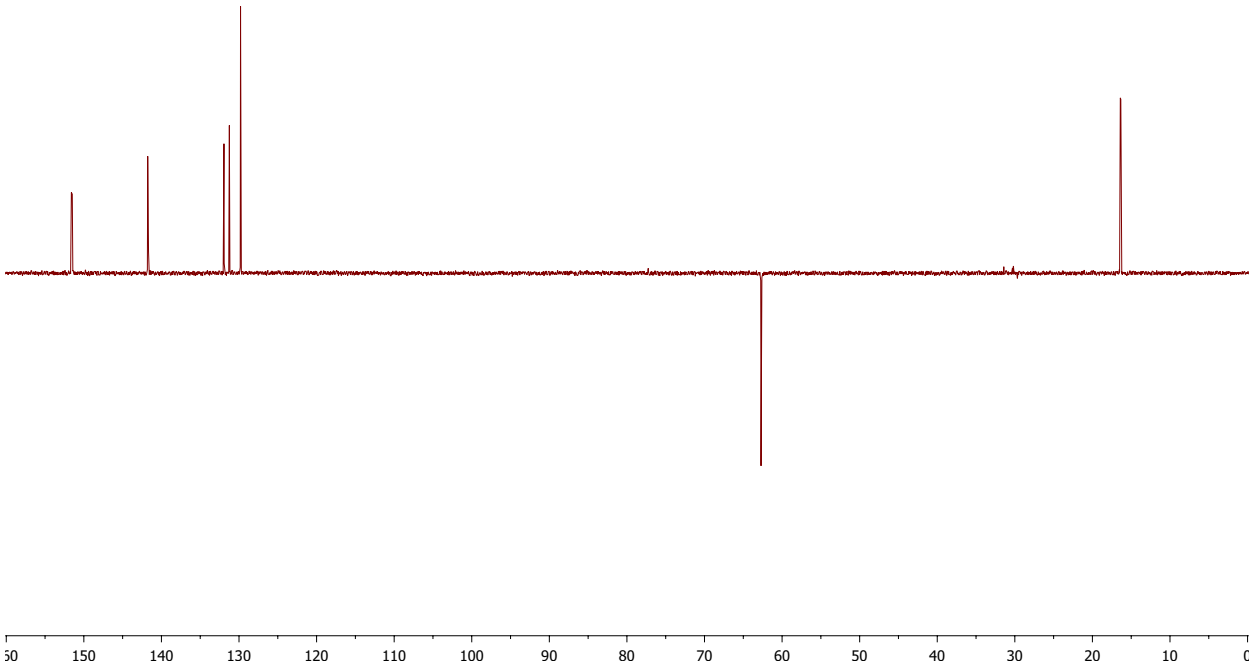

Figure 6.65: DEPT135 of **52** (101 MHz, $CDCl_3$).

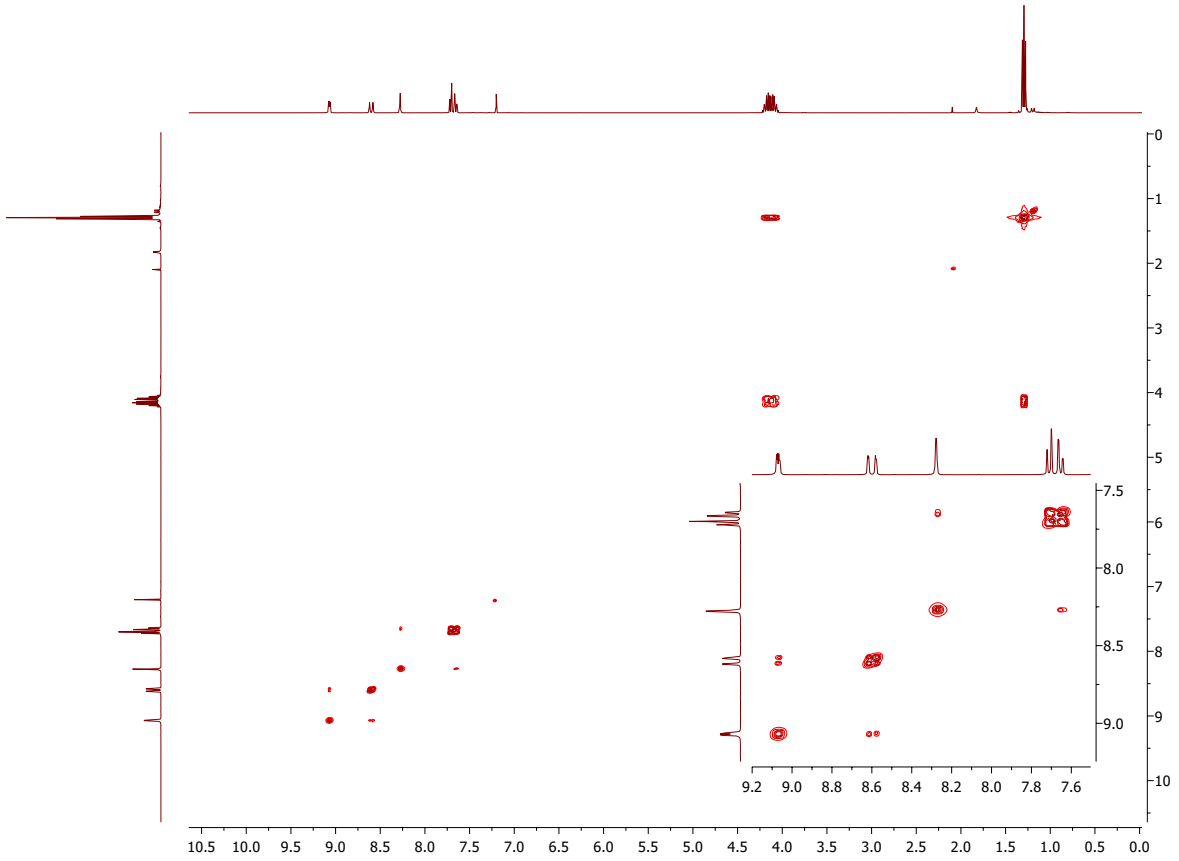

Figure 6.66: COSY of **52** (400 MHz, $CDCl_3$).

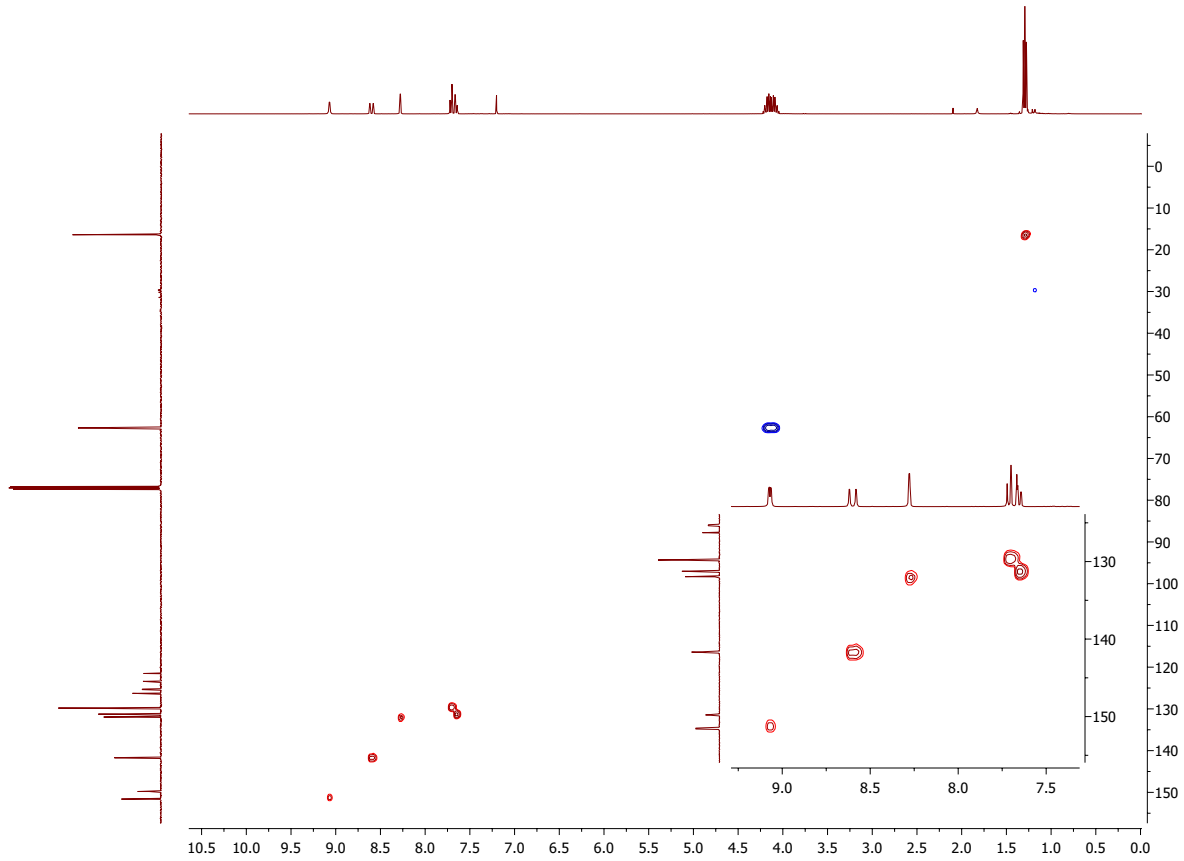

Figure 6.67: HSQC of **52** (400 MHz, $CDCl_3$).

6.19 Diethyl 6-nitro-3-quinolinylphosphonate (53)

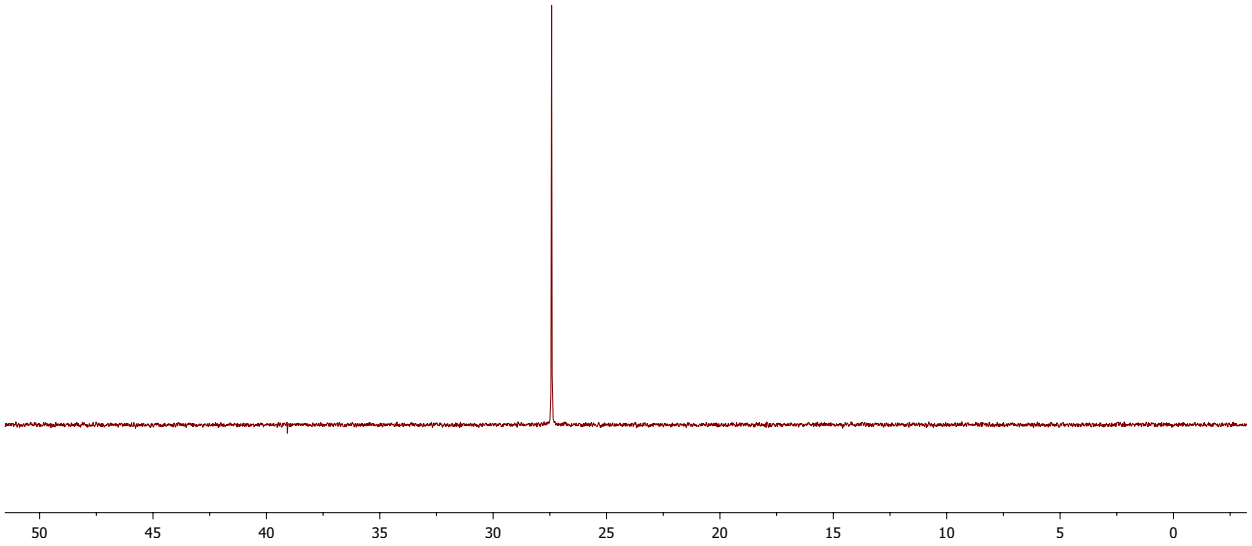

Figure 6.68: ^{31}P NMR (decoupled) of **53** (162 MHz, $CDCl_3$).

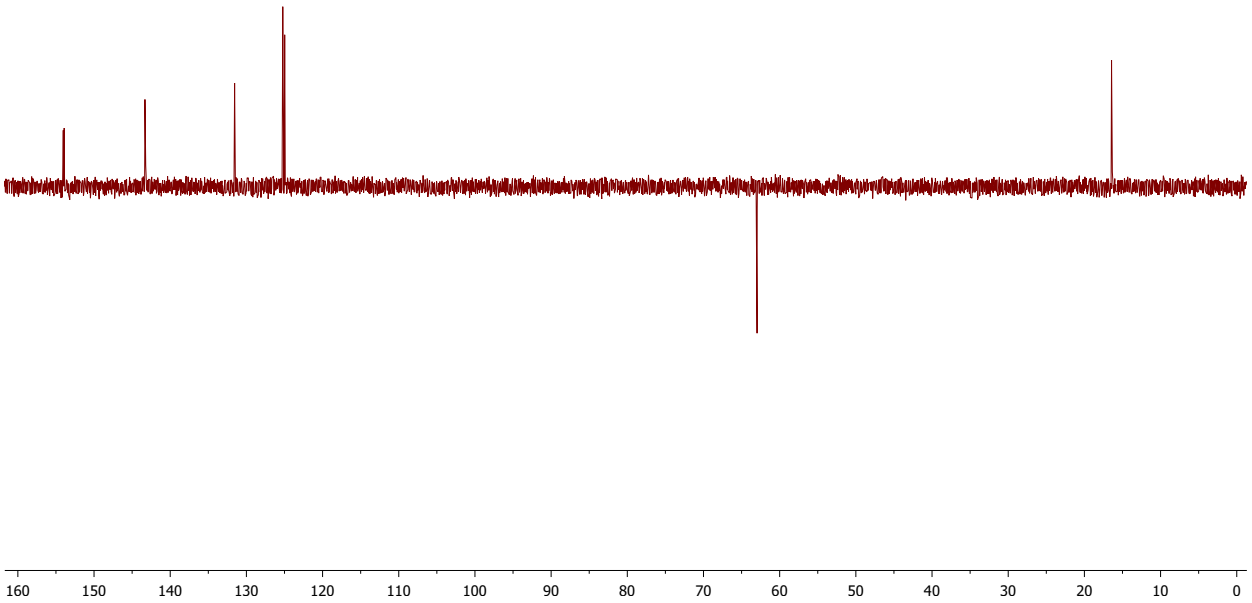

Figure 6.69: DEPT135 of **53** (101 MHz, $CDCl_3$).

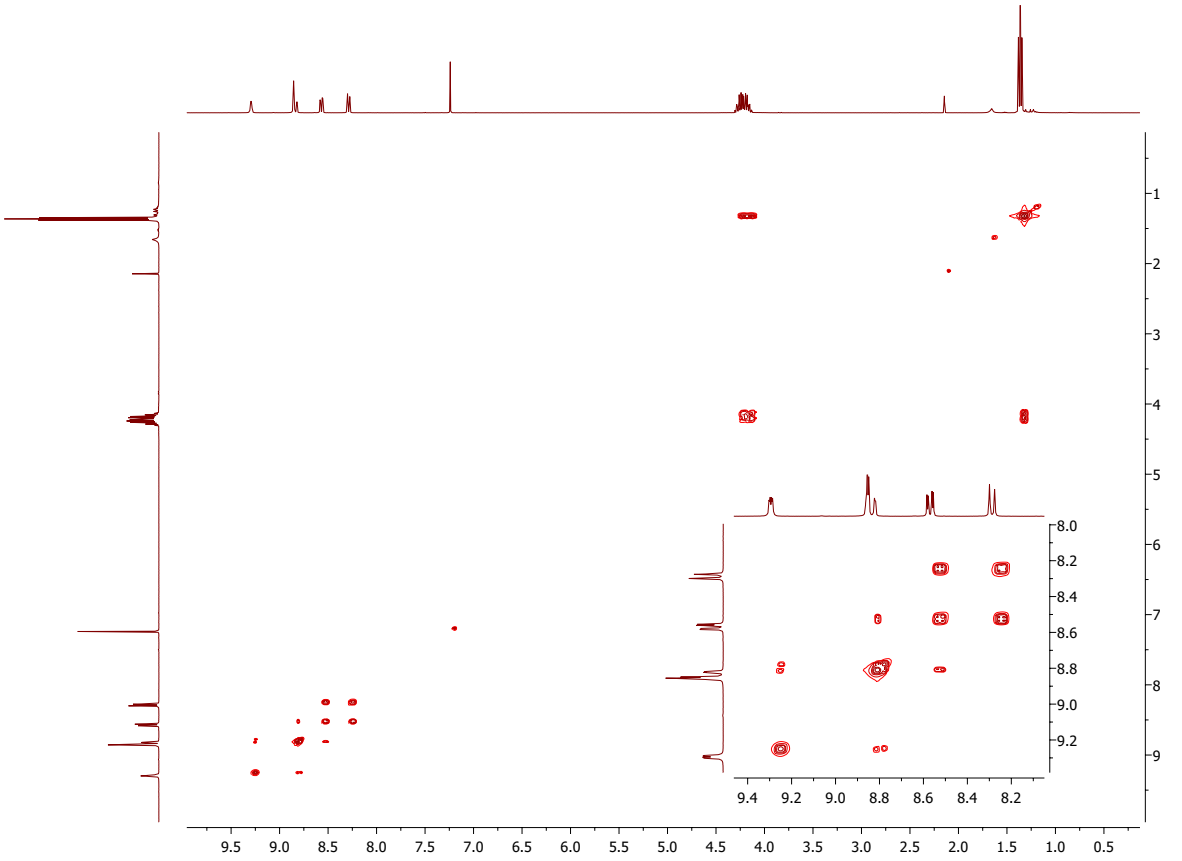

Figure 6.70: COSY of **53** (400 MHz, $CDCl_3$).

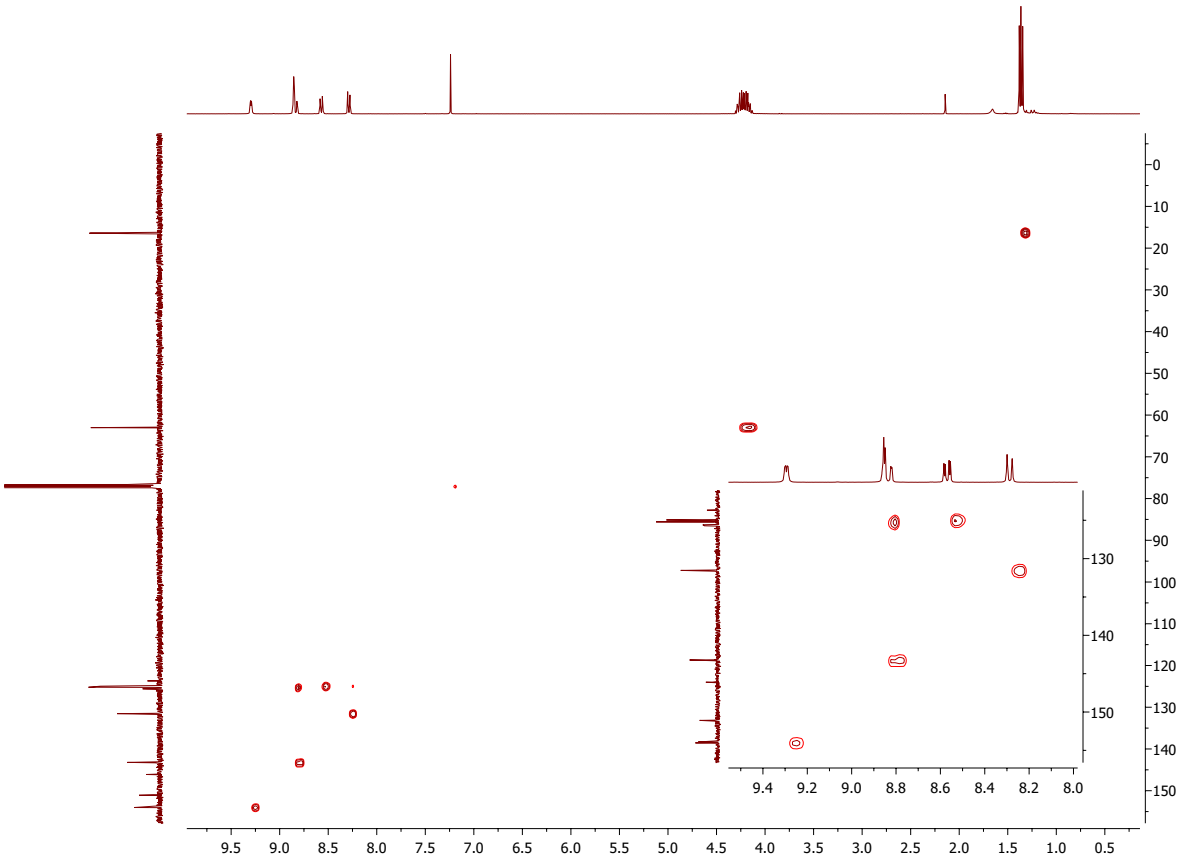

Figure 6.71: HSQC of **53** (400 MHz, $CDCl_3$).

6.20 Diethyl 4-chloro-3-quinolinylphosphonate (54)

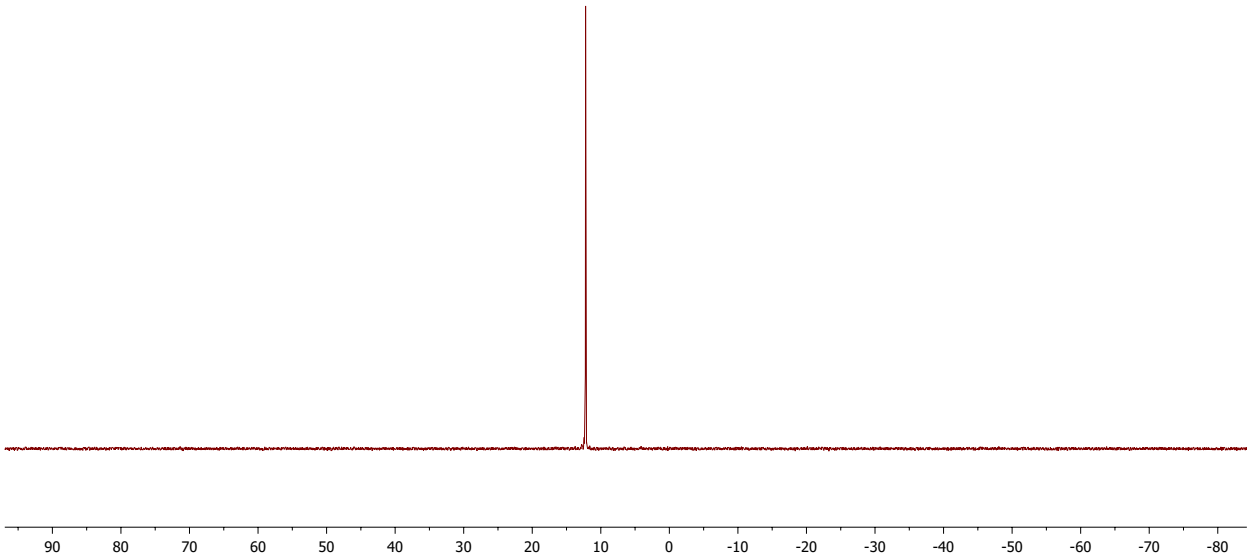

Figure 6.72: ^{31}P NMR (decoupled) of **54** (162 MHz, $CDCl_3$).

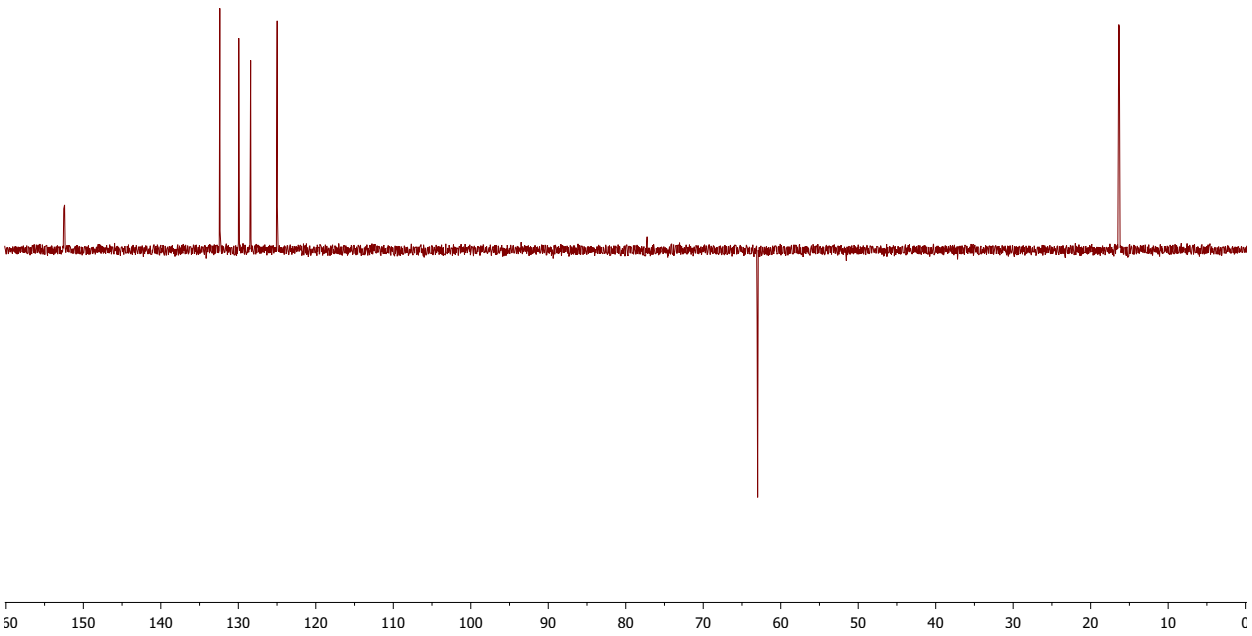

Figure 6.73: DEPT135 of **54** (101 MHz, $CDCl_3$).

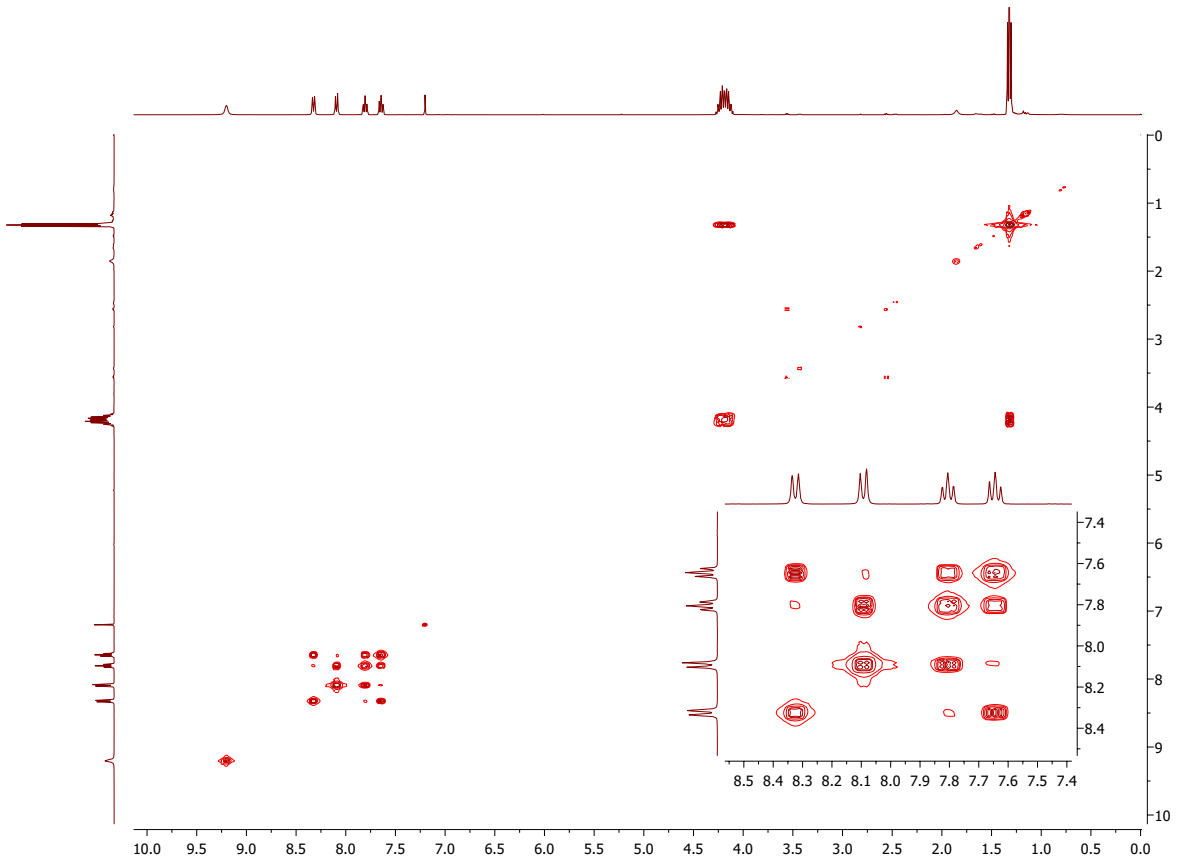

Figure 6.74: COSY of **54** (400 MHz, $CDCl_3$).

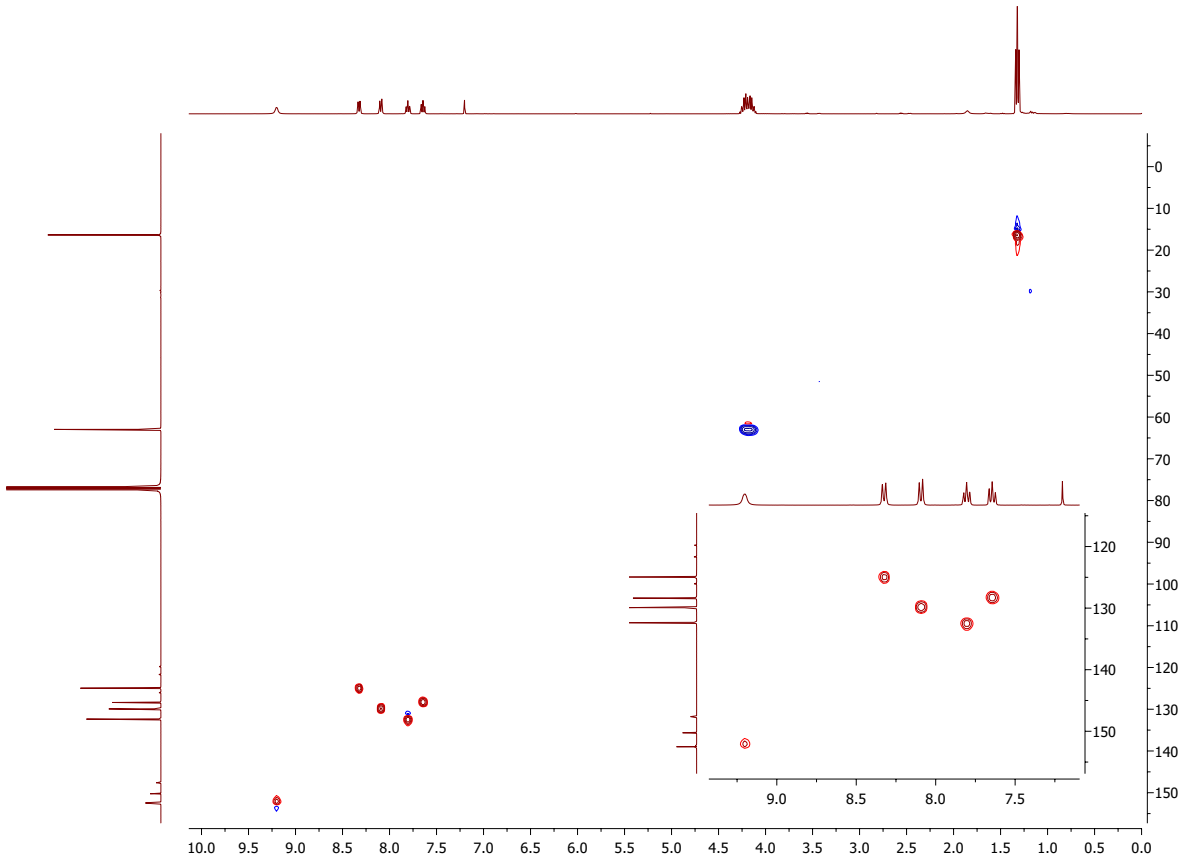

Figure 6.75: HSQC of **54** (400 MHz, $CDCl_3$).

6.21 Single crystal X-ray diffraction data

6.21.1 3-chloro-5,6-difluoroindole (46)

Crystal data

Empirical formula	$C_8H_4ClF_2N$
Formula weight	187.57
Color, shape	Colorless, block
Crystal size (mm^3)	0.74 x 0.55 x 0.42
Crystal system, space group	Monoclinic, P $2_1/n$
a, b, c (Å)	8.7638(6), 9.7059(6), 8.9119(6)
α, β, γ (°)	90, 106.8170(10), 90
Volume ($Å^3$)	725.63(8)
Z	1
Temperature (K)	105
ρ_{calc} (g/cm^3)	1.717
μ (mm^{-1})	0.493
F(000)	376
Radiation	Mo Kα (λ= 0.71073)

Data collection

Absorption correction	Multi-scan, SADABS (Bruker, 2016)
Index ranges	$-15 \leq h \leq 15$, $-17 \leq k \leq 17$, $-15 \leq l \leq 15$
T_{min}, T_{max}	0.859, 1.000
Θ_{max} (°)	38.6
Measured reflections	28239
Independent reflections	4096
Observed [I>=2σ(I)] reflections	3516
R_{int}, R_{sigma}	0.0344, 0.0213

Refinement

Reflections/parameters/restraints	4096/112/0
$R[F^2 > 2\sigma F^2]$	0.0315
$wR(F^2)$	0.0818
S (goodness of fit)	1.069
$\Delta\rho_{max}$, $\Delta\rho_{min}$ ($e\ Å^{-3}$)	0.61, -0.40
H-atom treatment	Mixed

6.21.2 Diethyl 6-bromo-3-quinolinylphosphonate (50)

Crystal data

Empirical formula	$C_{13}H_{15}BrNO_3P$
Formula weight	344.14
Color, shape	Colorless, plate
Crystal size (mm^3)	0.5 x 0.5 x 0.07
Crystal system, space group	Triclinic, P-1
a, b, c (Å)	5.937(3), 7.636(3), 17.042(8)
α, β, γ (°)	82.370(10), 82.555(11), 85.894(11)
Volume ($Å^3$)	758.1(6)
Z	2
Temperature (K)	298
ρ_{calc} (g/cm^3)	1.508
μ (mm^{-1})	2.819
F(000)	348
Radiation	Mo Kα (λ= 0.71073)

Data collection

Absorption correction	Multi-scan, SADABS-2016/2 (Bruker, 2016/2)
Index ranges	$-7 \leq h \leq 7$, $-9 \leq k \leq 9$, $-21 \leq l \leq 21$
T_{min}, T_{max}	0.3955, 0.7454
Θ_{max} (°)	26.5
Measured reflections	18417
Independent reflections	3137
Observed [I>=2σ(I)] reflections	2052
R_{int}, R_{sigma}	0.0754, 0.0527

Refinement

Reflections/parameters/restraints	3137/175/0
$R[F^2 > 2\sigma F^2]$	0.0527
$wR(F^2)$	0.1275
S (goodness of fit)	1.025
$\Delta\rho_{max}$, $\Delta\rho_{min}$ (e $Å^{-3}$)	0.43, -0.45
H-atom treatment	Constrained

6.21.3 Diethyl 6,7-difluoro-3-quinolinylphosphonate (51)

Crystal data

Empirical formula	$C_{13}H_{14}F_2NO_3P$
Formula weight	301.23
Color, shape	Clear colorless, plate
Crystal size (mm^3)	0.477 x 0.174 x 0.067
Crystal system, space group	Triclinic, P-1
a, b, c (Å)	7.9611(10), 8.7295(11), 11.3713(14)
α, β, γ (°)	73.566(3), 72.584(3), 88.300(4)
Volume ($Å^3$)	721.92(16)
Z	2
Temperature (K)	298
ρ_{calc} (g/cm^3)	1.3857
μ (mm^{-1})	0.218
F(000)	312.4126
Radiation	Mo Kα (λ= 0.71073)

Data collection

Absorption correction	Multi-scan, SADABS-2016/2 (Bruker, 2016/2)
Index ranges	$-9 \leq h \leq 9$, $-10 \leq k \leq 10$, $-13 \leq l \leq 13$
T_{min}, T_{max}	0.4910, 0.7451
Θ_{max} (°)	24.9
Measured reflections	7866
Independent reflections	2507
Observed [I>=2σ(I)] reflections	1777
R_{int}, R_{sigma}	0.1602, 0.1033

Refinement

Reflections/parameters/restraints	2507/182/0
$R[F^2 > 2\sigma F^2]$	0.0705
$wR(F^2)$	0.1813
S (goodness of fit)	1.0565
$\Delta\rho_{max}$, $\Delta\rho_{min}$ ($e\ Å^{-3}$)	0.60, -0.43
H-atom treatment	Constrained

Bibliography

[1] Hanne Therese Bonge, Benjamin Pintea, and Tore Hansen. "Highly efficient formation of halodiazoacetates and their use in stereoselective synthesis of halocyclopropanes". In: *Org. Biomol. Chem.* 6 (20 2008), pp. 3670–3672. DOI: 10.1039/B814374A.

[2] Hanne Therese Bonge and Tore Hansen. "Intermolecular C-H and Si-H Insertion Reactions with Halodiazoacetates". In: *Synthesis* 2009.01 (2009), pp. 91–96. DOI: 10.1055/s-0028-1083272.

[3] Magnus Mortén, Martin Hennum, and Tore Bonge-Hansen. "Synthesis of quinoline-3-carboxylates by a Rh(II)-catalyzed cyclopropanation-ring expansion reaction of indoles with halodiazoacetates". In: *Beilstein Journal of Organic Chemistry* 11 (2015), pp. 1944–1949.

[4] Christian Schnaars and Tore Hansen. "Halodiazophosphonates, a New Class of Diazo Compounds for the Diastereoselective Intermolecular Rh(II) Catalyzed Cyclopropanation". In: *Organic Letters* 14.11 (June 2012), pp. 2794–2797. DOI: 10.1021/ol3010276.

[5] Christian Schnaars, Martin Hennum, and Tore Bonge-Hansen. "Nucleophilic Halogenations of Diazo Compounds, a Complementary Principle for the Synthesis of Halodiazo Compounds: Experimental and Theoretical Studies". In: *The Journal of Organic Chemistry* 78.15 (2013), pp. 7488–7497. DOI: 10.1021/jo401050c.

[6] Åsmund Kaupang and Tore Bonge-Hansen. "α-Bromodiazoacetamides –a new class of diazo compounds for catalyst-free, ambient temperature intramolecular C–H insertion reactions". In: *Beilstein Journal of Organic Chemistry* 9 (2013), pp. 1407–1413. DOI: 10.3762/bjoc.9.157.

[7] Magnus Mortén. "α-Halodiazoacetater: en studie av stabilitet og reaktivitet". PhD thesis. University of Oslo, 2015.

[8] Ned D Heindel and Stephen A Fine. "Alcoholysis of 4-chloroquinolines to 4(1H)-quinolones". In: *Journal of Organic Chemistry* 35.3 (1970), pp. 796–798. DOI: 10.1021/jo00828a057.

[9] *Norsk helseinformatikk - Antibiotika*. 2018. URL: http://nhi.no/pasienthandboka/sykdommer/infeksjoner/antibiotika-1761.

[10] *Discovery and development of Penicillin*. 2018. URL: https://www.acs.org/content/acs/en/education/whatischemistry/landmarks/flemingpenicillin.html.

[11] *Center for Disease Control and Prevention - Antibiotic/antimicrobial resistance*. 2018. URL: http://www.cdc.gov/drugresistance/.

[12] *Folkehelseinstituttet - Om tuberkulose*. 2018. URL: http://www.fhi.no/nettpub/smittevernveilederen/sykdommer-a-a/tuberkulose/#om-tuberkulose.

[13] *WHO - Antibiotic resistance*. 2018. URL: http://www.who.int/mediacentre/factsheets/antibiotic-resistance/en/.

[14] *CDC - About antimicrobial resistance*. 2018. URL: https://www.cdc.gov/drugresistance/about.html.

[15] Julian Davies and Dorothy Davies. "Origins and Evolution of Antibiotic Resistance". In: *Microbiology and Molecular Biology Reviews* 74.3 (September 2010), pp. 417–433.

[16] A. P. Magiorakos et al. "Multidrug-resistant, extensively drug-resistant and pandrug-resistant bacteria: an international expert proposal for interim standard definitions for acquired resistance". In: *Clinical Microbiology and Infection* 18.3 (), pp. 268–281. DOI: 10.1111/j.1469-0691.2011.03570.x.

[17] Matthew E. Falagas, Patra K. Koletsi, and Ioannis A. Bliziotis. "The diversity of definitions of multidrug-resistant (MDR) and pandrug-resistant (PDR) Acinetobacter baumannii and Pseudomonas aeruginosa". In: *Journal of Medical Microbiology* 55.12 (2006), pp. 1619–1629.

[18] Martin Exner et al. "Antibiotic resistance: What is so special about multidrug-resistant Gram-negative bacteria?" In: *GMS Hygiene and Infection Control* 12 (2017). DOI: 10.3205/dgkh000290.

[19] *WHO - List of bacteria for which new antibiotics are urgently needed*. 2018. URL: http://www.who.int/mediacentre/news/releases/2017/bacteria-antibiotics-needed/en/.

[20] *WHO - Antimicrobial resistance: global report on surveillance 2014*. 2018. URL: http://www.who.int/drugresistance/documents/surveillancereport/en/.

[21] *European Center for Disease Prevention and Control - Antimicrobial resistance and healthcare-associated infections programme*. 2018. URL: http://ecdc.europa.eu/en/healthtopics/antimicrobial-resistance-and-consumption/antimicrobial-resistance-healthcare-associated-infections-programme/Pages/ARHAI.aspx.

[22] John A Joule and Keith Mills. *Heterocyclic Chemistry*. 5th. Wiley-Blackwell, 2010.

[23] Jain S Sharma PC Jain A. "Fluoroquinolone antibacterials: a review on chemistry, microbiology and therapeutic prospects". In: *Acta Poloniae Pharmaceutica - Drug Researc* 66.6 (2009), pp. 587–604.

[24] Lester A. Mitscher. "Bacterial topoisomerase inhibitors: Quinolone and Pyridone". In: *Chemical Reviews* 105.2 (2005), pp. 559–592. DOI: 10.1021/cr030101q.

[25] Valentina Uivarosi. "Metal Complexes of Quinolone Antibiotics and Their Applications: An Update". In: *Molecules* 18.9 (2013), p. 11153.

[26] George Y. Lesher et al. "1,8-Naphthyridine Derivatives. A New Class of Chemotherapeutic Agents". In: *Journal of Medicinal and Pharmaceutical Chemistry* 5.5 (1962), pp. 1063–1065. DOI: 10.1021/jm01240a021.

[27] Frank Temilolu Idowu aand Schweizer. "Ubiquitous Nature of Fluoroquinolones: The Oscillation between Antibacterial and Anticancer Activities". In: *Antibiotics* 6.4 (2017).

[28] A. M. Emmerson and A. M. Jones. "The quinolones: decades of development and use". In: *Journal of Antimicrobial Chemotherapy* 51.suppl 1 (2003), pp. 13–20. DOI: 10.1093/jac/dkg208.

[29] Katie J. Aldred, Robert J. Kerns, and Neil Osheroff. "Mechanism of Quinolone Action and Resistance". In: *Biochemistry* 53.10 (2014), pp. 1565–1574. DOI: 10.1021/bi5000564.

[30] Mark Farrington, Morris J. Brown, and Pankaj Sharma. "Chapter 13 - Antibacterial drugs A2 - Bennett, Peter N." In: *Clinical Pharmacology (Eleventh Edition)*. Oxford: Churchill Livingstone, 2012, pp. 173–190. DOI: https://doi.org/10.1016/B978-0-7020-4084-9.00052-5.

[31] Dana E. King, Robb Malone, and Sandra H. Lilley.
"New Classification and Update on the Quinolone Antibiotics".
In: *American Family Physician* 61.9 (2000), p. 2741.

[32] J.F Acar and F.W Goldstein. "Trends in Bacterial Resistance to Fluoroquinolones".
In: *Clinical Infectious Diseases* 24.1 (1997), pp. 67–73.

[33] Joaquim Ruiz. "Mechanisms of resistance to quinolones: target alterations, decreased accumulation and DNA gyrase protection".
In: *Journal of Antimicrobial Chemotherapy* 51.5 (2003), pp. 1109–1117.
DOI: 10.1093/jac/dkg222.

[34] A. C. Gentry and N. Osheroff.
"DNA Topoisomerases: Type II A2 - Lennarz, William J". In:
Encyclopedia of Biological Chemistry. Academic Press, 2013, pp. 163–168.
DOI: http://dx.doi.org/10.1016/B978-0-12-378630-2.00246-2.

[35] Virginia E. Anderson et al.
"Quinolones inhibit DNA religation mediated by Staphylococcus aureus topoisomerase IV. Changes in drug mechanism across evolutionary boundaries."
In: *J. Biol. Chem.* 274.50 (1999), pp. 35927–35932. DOI: 10.1074/jbc.274.50.35927.

[36] Rosaleen J. Anderson et al. "Quinolone Antibacterial Agents". In: *Antibacterial Agents*. John Wiley & Sons, Ltd, 2012, pp. 35–61. DOI: 10.1002/9781118325421.ch2.

[37] Faye M Barnard and Anthony Maxwell.
"Interaction between DNA Gyrase and Quinolones: Effects of Alanine Mutations at GyrA Subunit Residues Ser(83) and Asp(87)".
In: *Antimicrobial Agents and Chemotherapy* 45.7 (2001), pp. 1994–2000.
DOI: 10.1128/AAC.45.7.1994-2000.2001.

[38] Peter M. Hawkey. "Mechanisms of quinolone action and microbial response".
In: *Journal of Antimicrobial Chemotherapy* 51.suppl 1 (2003), pp. 29–35.

[39] Ivan Laponogov et al. "Structural insight into the quinolone-DNA cleavage complex of type IIA topoisomerases". In: *Nat Struct Mol Biol* 16.6 (2009), pp. 667–669.
DOI: 10.1038/nsmb.1604.

[40] Katie J. Aldred et al. "Topoisomerase IV-quinolone interactions are mediated through a water-metal ion bridge: mechanistic basis of quinolone resistance".
In: *Nucleic Acids Research* 41.8 (2013), pp. 4628–4639.

[41] Ivan Laponogov et al.
"Structural Basis of Gate-DNA Breakage and Resealing by Type II Topoisomerases".
In: *PLoS ONE* 5.6 (2010), pp. 1–8. DOI: 10.1371/journal.pone.0011338.

[42] Benjamin D. Bax et al.
"Type IIA topoisomerase inhibition by a new class of antibacterial agents".
In: *Nature* 466.7309 (2010), pp. 935–940. DOI: 10.1038/nature09197.

[43] Alexandre Wohlkonig et al. "Structural basis of quinolone inhibition of type IIA topoisomerases and target-mediated resistance".
In: *Nat Struct Mol Biol* 17.99 (2010), pp. 1152–1153. DOI: 10.1038/nsmb.1892.

[44] Katie J. Aldred et al. "Role of the Water-Metal Ion Bridge in Mediating Interactions between Quinolones and Escherichia coli Topoisomerase IV."
In: *Biochemistry* 53.34 (2014), pp. 5558–5567. DOI: 10.1021/bi500682e.

[45] Katie J Aldred et al. "Drug Interactions with Bacillus anthracis Topoisomerase IV: Biochemical Basis for Quinolone Action and Resistance".
In: *Biochemistry* 51.1 (2012), pp. 370–381. DOI: 10.1021/bi2013905.

[46] Katie J. Aldred et al. "Bacillus anthracis GrlAV96A Topoisomerase IV, a Quinolone Resistance Mutation That Does Not Affect the Water-Metal Ion Bridge".
In: *Antimicrobial Agents and Chemotherapy* 58.12 (Dec. 2014), pp. 7182–7187.

[47] Lance R. Peterson. “Quinolone Molecular Structure-Activity Relationships: What We Have Learned about Improving Antimicrobial Activity”.
In: *Clinical Infectious Diseases* 33.Supplement 3 (2001), S180–S186.

[48] John M. Domagala. “Structure-activity and structure-side-effect relationships for the quinolone antibacterials”.
In: *Journal of Antimicrobial Chemotherapy* 33.4 (1994), pp. 685–706.

[49] Belsis Llorente, Fabrice Leclerc, and Robert Cedergren. “Using SAR and QSAR analysis to model the activity and structure of the quinolone—DNA complex”.
In: *Bioorganic & Medicinal Chemistry* 4.1 (1996), pp. 61 –71.
DOI: http://dx.doi.org/10.1016/0968-0896(96)83749-7.

[50] Yuan-Qiang Hu et al. “4-Quinolone hybrids and their antibacterial activities”.
In: *European Journal of Medicinal Chemistry* 141 (2017), pp. 335–345.
DOI: https://doi.org/10.1016/j.ejmech.2017.09.050.

[51] S. Jubie et al. “Design, synthesis, and docking studies of novel ofloxacin analogues as antimicrobial agents”. In: *Medicinal Chemistry Research* 21.7 (2012), pp. 1403–1410.
DOI: 10.1007/s00044-011-9655-8.

[52] Rama Kant et al. “Design, synthesis and biological evaluation of ciprofloxacin tethered bis-1,2,3-triazole conjugates as potent antibacterial agents”.
In: *European Journal of Medicinal Chemistry* 124 (2016), pp. 218–228.
DOI: https://doi.org/10.1016/j.ejmech.2016.08.031.

[53] Ling Zhang et al.
“Design and biological evaluation of novel quinolone-based metronidazole derivatives as potent Cu2+ mediated DNA-targeting antibacterial agents”.
In: *Bioorganic & Medicinal Chemistry Letters* 25.17 (2015), pp. 3699–3705.
DOI: https://doi.org/10.1016/j.bmcl.2015.06.041.

[54] Sheng-Feng Cui, Dinesh Addla, and Cheng-He Zhou.
“Novel 3-Aminothiazolquinolones: Design, Synthesis, Bioactive Evaluation, SARs, and Preliminary Antibacterial Mechanism”.
In: *Journal of Medicinal Chemistry* 59.10 (2016), pp. 4488–4510.
DOI: 10.1021/acs.jmedchem.5b01678.

[55] Yu Cheng et al. “Multi-targeting exploration of new 2-aminothiazolyl quinolones: Synthesis, antimicrobial evaluation, interaction with DNA, combination with topoisomerase IV and penetrability into cells”.
In: *European Journal of Medicinal Chemistry* 124 (2016), pp. 935–945.
DOI: https://doi.org/10.1016/j.ejmech.2016.10.011.

[56] Jason A. Wiles et al. “Isothiazoloquinolones containing functionalized aromatic hydrocarbons at the 7-position: Synthesis and in vitro activity of a series of potent antibacterial agents with diminished cytotoxicity in human cells”.
In: *Bioorganic & Medicinal Chemistry Letters* 16.5 (2006), pp. 1272–1276.
DOI: https://doi.org/10.1016/j.bmcl.2005.11.065.

[57] Ha Young Kim et al.
“Exploration of the Activity of 7-Pyrrolidino-8-methoxyisothiazoloquinolones against Methicillin-Resistant Staphylococcus aureus (MRSA)”.
In: *Journal of Medicinal Chemistry* 54.9 (2011), pp. 3268–3282.
DOI: 10.1021/jm101604v.

[58] Masahiro FUJITA et al. “Imidazo- and Triazoloquinolones as Antibacterial Agents. Synthesis and Structure-Activity Relationships”.
In: *CHEMICAL & PHARMACEUTICAL BULLETIN* 43.12 (1995), pp. 2123–2132.
DOI: 10.1248/cpb.43.2123.

[59] Michael R. Barbachyn and John E. Macor.
"Chapter 17 - Recent Advances in the Discovery of Hybrid Antibacterial Agents". In: *Annual Reports in Medicinal Chemistry*. Vol. 43. Academic Press, 2008, pp. 281–290. DOI: https://doi.org/10.1016/S0065-7743(08)00017-1.

[60] Mikhail F. Gordeev et al. "Novel oxazolidinone–quinolone hybrid antimicrobials". In: *Bioorganic & Medicinal Chemistry Letters* 13.23 (2003), pp. 4213–4216. DOI: 10.1016/j.bmcl.2003.07.021.

[61] Mamun-Ur Rashid et al.
"Ecological impact of MCB3837 on the normal human microbiota". In: *International Journal of Antimicrobial Agents* 44.2 (2014), pp. 125–130. DOI: https://doi.org/10.1016/j.ijantimicag.2014.03.016.

[62] Mamun-Ur Rashid et al.
"In vitro activity of MCB3681 against Clostridium difficile strains". In: *Anaerobe* 28 (2014), pp. 216–219. DOI: 10.1016/j.anaerobe.2014.07.001.

[63] Micheal A. Pfaller, Arthur L. Barry, and Peter C. Fuchs.
"RO 23–9424, a new cephalosporin 3'-quinolone: in-vitro antimicrobial activity and tentative disc diffusion interpretive criteria". In: *Journal of Antimicrobial Chemotherapy* 31.1 (1993), pp. 81–88.

[64] Tomislav Karoli et al. "Structure aided design of chimeric antibiotics". In: *Bioorganic & Medicinal Chemistry Letters* 22.7 (2012), pp. 2428–2433. DOI: 10.1016/j.bmcl.2012.02.019.

[65] Richard L. Jarvest et al.
"Nanomolar Inhibitors of Staphylococcus aureus Methionyl tRNA Synthetase with Potent Antibacterial Activity against Gram-Positive Pathogens". In: *Journal of Medicinal Chemistry* 45.10 (May 2002), pp. 1959–1962. DOI: 10.1021/jm025502x.

[66] Alka Madaan et al.
"1,8-Naphthyridine Derivatives: A Review of Multiple Biological Activities". In: *Archiv der Pharmazie* 348.12 (2015), pp. 837–860. DOI: 10.1002/ardp.201500237.

[67] Abeer Ahmed and Mohsen Daneshtalab.
"Nonclassical Biologoical Activities of Quinolone Derivatives". In: *Journal of Pharmacy and Pharmaceutical Sciences* 15.1 (2012), pp. 52–72.

[68] Jonathan A Abbas and Robert K Stuart. "Vosaroxin: a novel antineoplastic quinolone". In: *Expert Opinion on Investigational Drugs* 21.8 (2012), pp. 1223–1233. DOI: 10.1517/13543784.2012.699038.

[69] Xue-Dong Jia et al.
"Synthesis and in vitro antitumor activity of novel naphthyridinone derivatives". In: *Chinese Chemical Letters* 28.2 (2017), pp. 235–239. DOI: 10.1016/j.cclet.2016.07.024.

[70] Johnny Y. Nagasawa et al. "6-Benzylamino 4-oxo-1,4-dihydro-1,8-naphthyridines and 4-oxo-1,4-dihydroquinolines as HIV integrase inhibitors". In: *Bioorganic & Medicinal Chemistry Letters* 21.2 (2011), pp. 760–763. DOI: https://doi.org/10.1016/j.bmcl.2010.11.108.

[71] Murugesan Dinakaran et al.
"Antitubercular activities of novel benzothiazolo naphthyridone carboxylic acid derivatives endowed with high activity toward multi-drug resistant tuberculosis". In: *Biomedicine & Pharmacotherapy* 63.1 (2009), pp. 11–18. DOI: https://doi.org/10.1016/j.biopha.2007.10.009.

[72] Dharmarajan Sriram et al. "Antimycobacterial Activities of Novel 1-(Cyclopropyl/tert-butyl/4-fluorophenyl)-1,4-dihydro- 6-nitro-4-oxo-7-(substituted

secondary amino)-1,8-naphthyridine-3-carboxylic Acid".
In: *Journal of Medicinal Chemistry* 50.24 (2007), pp. 6232–6239.
DOI: 10.1021/jm700999n.

[73] Lian-Shun Feng et al. "Synthesis and in vitro antimycobacterial activity of 8-OCH3 ciprofloxacin methylene and ethylene isatin derivatives".
In: *European Journal of Medicinal Chemistry* 46.1 (2011), pp. 341–348.
DOI: 10.1016/j.ejmech.2010.11.023.

[74] Amy Sarah Ginsburg, Jacques H Grosset, and William R Bishai. "Fluoroquinolones, tuberculosis, and resistance".
In: *The Lancet Infectious Diseases* 3.7 (2003), pp. 432–442.
DOI: https://doi.org/10.1016/S1473-3099(03)00671-6.

[75] *Vosaroxin Clinical Trials*. 2018.
URL: https://www.sunesis.com/clinical_trials.php.

[76] *Study of Vosaroxin or Placebo in Combination With Cytarabine in Patients With First Relapsed or Refractory AML (VALOR)*. 2018. URL: https://clinicaltrials.gov/ct2/show/results/NCT01191801?term=vosaroxin\&rank=7.

[77] *QINPREZO™ (vosaroxin)*. 2018. URL: https://www.sunesis.com/qinprezo.php.

[78] Christopher A. Lipinski. "Chapter 27. Bioisosterism in Drug Design". In: ed. by Denis M. Bailey. Vol. 21. Annual Reports in Medicinal Chemistry. Academic Press, 1986, pp. 283 –291.
DOI: https://doi.org/10.1016/S0065-7743(08)61137-9.

[79] K.R Mahadik S.S Kadam and K.G Bothara. *Principles of Medicinal Chemistry*. 18th ed. Vol. 2. Nirali Prakashan, 17th edition. Chap. 19 - Drug Design.

[80] Lidia Lima and Eliezer Barreiro. "Bioisosterism: A Useful Strategy for Molecular Modification and Drug Design".
In: 12 (Feb. 2005), pp. 23–49.

[81] "Gould-Jacobs Reaction". In: *Comprehensive Organic Name Reactions and Reagents*. American Cancer Society, 2010. Chap. 276, pp. 1252–1255.
DOI: 10.1002/9780470638859.conrr276.

[82] Arthur A. Santilli, Anthony C. Scotese, and John A. Yurchenco. "Synthesis and antibacterial evaluation of 1,2,3,4-tetrahydro-4-oxo-1,8-naphthyridine-3-carboxylic acid esters, carbonitriles, and carboxamides".
In: *Journal of Medicinal Chemistry* 18.10 (1975), pp. 1038–1041.
DOI: 10.1021/jm00244a021.

[83] Yoshiyuki Takase Jun-ichi Matsumoto and Yoshiro Nishimura. *Novel naphthyridine derivatives, intermediates thereof, processes for preparation thereof, and use thereof*. Patent. Patent: US4352803A. 1979.

[84] *Novel naphtyridine derivatives and pharmaceutical compositions containing them*. Patent. Patent: EP0009425 (A1). 1980.

[85] DANIEL T.W. CHU and PRABHAVATHI B. FERNANDES. "Recent Developments in the Field of Quinolone Antibacterial Agents".
In: *Advances in Drug Research*. Vol. 21. Advances in Drug Research. Academic Press, 1991, pp. 39 –144.
DOI: https://doi.org/10.1016/B978-0-12-013321-5.50007-2.

[86] 2016. URL: http://www.chemdrug.com/article/8/3284/16419155.html.

[87] Theodor Curtius. "Ueber die Einwirkung von salpetriger Säure auf salzsauren Glycocolläther".
In: *Berichte der deutschen chemischen Gesellschaft* 16.2 (1883), pp. 2230–2231.
DOI: 10.1002/cber.188301602136.

[88] H. V. Pechmann. "Ueber Diazomethan".
In: *Berichte der deutschen chemischen Gesellschaft* 27.2 (1894), pp. 1888–1891.
DOI: 10.1002/cber.189402702141.

[89] Steven D Burke and Paul A Grieco.
"Intramolecular Reactions of Diazocarbonyl Compounds. Organic Reactions." In:
vol. 26. 2. John Wiley & Sons, Ltd, 2005, pp. 361–475.

[90] Vinod K. Singh, Arpita DattaGupta, and G. Sekar.
"Catalytic Enantioselective Cyclopropanation of Olefins Using Carbenoid Chemistry".
In: *Synthesis* 1997.02 (1997), pp. 137–149. DOI: 10.1055/s-1997-1172.

[91] Maurice. Brookhart and William B. Studabaker.
"Cyclopropanes from reactions of transition metal carbene complexes with olefins".
In: *Chemical Reviews* 87.2 (1987), pp. 411–432. DOI: 10.1021/cr00078a008.

[92] Michael P. Doyle et al. "Catalytic Carbene Insertion into C–H Bonds".
In: *Chemical Reviews* 110.2 (2010), pp. 704–724. DOI: 10.1021/cr900239n.

[93] Shou-Fei Zhu and Qi-Lin Zhou. "Transition-Metal-Catalyzed Enantioselective Heteroatom–Hydrogen Bond Insertion Reactions".
In: *Accounts of Chemical Research* 45.8 (2012), pp. 1365–1377.
DOI: 10.1021/ar300051u.

[94] Albert Padwa. "Catalytic Decomposition of Diazo Compounds as a Method for Generating Carbonyl-Ylide Dipoles".
In: *Helvetica Chimica Acta* 88.6 (2005), pp. 1357–1374.
DOI: 10.1002/hlca.200590109.

[95] Albert Padwa, Bo Cheng, and Yan Zou. "Natural Product Synthesis via the Rhodium Carbenoid-Mediated Cyclization of α-Diazo Carbonyl Compounds".
In: *Australian Journal of Chemistry* 67.3 (2014), pp. 343–353.

[96] Alan Ford et al. "Modern Organic Synthesis with α-Diazocarbonyl Compounds".
In: *Chemical Reviews* 115.18 (2015), pp. 9981–10080.
DOI: 10.1021/acs.chemrev.5b00121.

[97] H Boersch. "Die Konstitution der Diazofettsäuren. I". In: *Mh. Chem* 65 (1935), p. 331.

[98] Klaus Clusius and Ursula Lüthi.
"Reaktionen mit 15N. XXIV. Zur Bildungsweise und Struktur des Diazoessigesters".
In: *Helvetica Chimica Acta* 40.2 (1957), pp. 445–456.
DOI: 10.1002/hlca.19570400224.

[99] M Regitz and G Maas. *Diazo Compounds – Properties and Synthesis*. 1986.
DOI: 10.1016/B978-0-12-585840-3.50018-0.

[100] "Diazomethane MAK Value Documentation, 1999". In:
The MAK-Collection for Occupational Health and Safety.
Wiley-VCH Verlag GmbH & Co. KGaA, 2002.
DOI: 10.1002/3527600418.mb33488e0013.

[101] R.S. & Liebman Hosmane. "Paradigms and Paradoxes: Diazomethane and Ethyl Diazoacetate: The Role of Substituent Effects on Stability".
In: *Structural Chemistry* 13.5-6 (2002), pp. 501–503. DOI: 10.1023/A:1020573723147.

[102] Thorsten Bug et al. "How Nucleophilic Are Diazo Compounds?"
In: *Chemistry – A European Journal* 9.17 (2003), pp. 4068–4076.
DOI: 10.1002/chem.200304913.

[103] Amos B. Smith and R.Karl Dieter.
"The acid promoted decomposition of α-diazo ketones".
In: *Tetrahedron* 37.14 (1981), pp. 2407 –2439.
DOI: https://doi.org/10.1016/S0040-4020(01)88898-0.

[104] W. J. Albery and M. H. Davies.
"Decomposition of ethyl diazoacetate in H2O + D2O mixtures".
In: *Trans. Faraday Soc.* 65 (1969), pp. 1066–1073. DOI: 10.1039/TF9696501066.

[105] John D. Roberts, Warren Watanabe, and Robert E. McMahon. "The Kinetics and Mechanism of the Reaction of Diphenyldiazomethane and Benzoic Acid in Ethanol1".
In: *Journal of the American Chemical Society* 73.2 (1951), pp. 760–765.
DOI: 10.1021/ja01146a078.

[106] R.A. More O'Ferrall. "The Reactions of Aliphatic Diazocompounds with Acids". In: vol. 5. Advances in Physical Organic Chemistry. 1967, pp. 331 –399.
DOI: https://doi.org/10.1016/S0065-3160(08)60313-5.

[107] H. Staudinger and Alice Gaule. "Vergleich der Stickstoff-Abspaltung bei verschiedenen aliphatischen Diazoverbindungen".
In: *Berichte der deutschen chemischen Gesellschaft* 49.2 (1916), pp. 1897–1918.
DOI: 10.1002/cber.19160490245.

[108] W. Jugelt and L. Berseck. "Über Aryl-aroyl-diazomethane; Kinetik und Mechanismus der säurekatalytischen Hydrolyse p-substituierter Phenyl-benzoyl-diazomethane".
In: *Zeitschrift für Chemie* 6.11 (1966), pp. 420–421. DOI: 10.1002/zfch.19660061108.

[109] W. Jugelt and D. Schmidt. "Kinetik und mechanismus der säurekatalysierten hydrolyse von 2-diazo-acenaphthenon-(1)". In: *Tetrahedron Letters* 8.11 (1967), pp. 985 –989.
DOI: 10.1016/S0040-4039(00)90621-X.

[110] W. Jugelt and L. Berseck.
"Struktur und reaktivität aliphatischer diazoverbindungen, IV. Mitteilung kinetik und mechanismus der säurekatalysierten hydrolyse von aroyl-diazoäthanen".
In: *Tetrahedron Letters* 9.22 (1968), pp. 2659 –2664.
DOI: https://doi.org/10.1016/S0040-4039(00)89667-7.

[111] W. Jugelt and D. Schmidt. "Protonierungsgeschwindigkeitskonstanten und salzeffekte in der säurekatalysierten hydrolyse einiger aliphatischer diazoverbindungen".
In: *Tetrahedron* 24.1 (1968), pp. 59 –64.
DOI: https://doi.org/10.1016/0040-4020(68)89008-8.

[112] W. Jugelt and K. Drahn. "Struktur und reaktivität aliphatischer diazoverbindungen—XIII: Untersuchungen zum mechanismus der säurekatalysierten hydrolyse von α-diazo-phosphonsäureestern und α-diazo-phosphinoxiden".
In: *Tetrahedron* 25.23 (1969), pp. 5585 –5594.
DOI: https://doi.org/10.1016/S0040-4020(01)83064-7.

[113] Didier Bourissou et al. "Stable Carbenes".
In: *Chemical Reviews* 100.1 (2000), pp. 39–92. DOI: 10.1021/cr940472u.

[114] Eric V Anslyn and Dennis A Dougherty. *Modern Physical Organic Chemistry*. 2006. Chap. 1.

[115] W. von E. Doering and Wm. A. Henderson.
"The Electron-seeking Demands of Dichlorocarbene in its Addition to Olefins".
In: *Journal of the American Chemical Society* 80.19 (1958), pp. 5274–5277.
DOI: 10.1021/ja01552a065.

[116] Jack Hine and Stanton J. Ehrenson.
"The Effect of Structure on the Relative Stability of Dihalomethylenes1".
In: *Journal of the American Chemical Society* 80.4 (1958), pp. 824–830.
DOI: 10.1021/ja01537a018.

[117] Philip S. Skell and Albert Y. Garner. "Reactions of Bivalent Carbon Compounds. Reactivities in Olefin-Dibromocarbene Reactions".
In: *Journal of the American Chemical Society* 78.20 (1956), pp. 5430–5433.
DOI: 10.1021/ja01601a073.

[118] Roald Hoffmann, Geoffrey D. Zeiss, and George W. Van Dine.
"The electronic structure of methylenes".
In: *Journal of the American Chemical Society* 90.6 (1968), pp. 1485–1499.
DOI: 10.1021/ja01008a017.

[119] Min Zhang et al.
"Evolution of Structure and Reactivity in a Series of Iconic Carbenes".
In: *The Journal of Organic Chemistry* 77.2 (2012), pp. 843–850.
DOI: 10.1021/jo2023558.

[120] Robert A. Moss. "Carbenic selectivity in cyclopropanation reactions".
In: *Accounts of Chemical Research* 13.2 (1980), pp. 58–64. DOI: 10.1021/ar50146a005.

[121] Robert A. Moss. ""Carbon Dichloride": Dihalocarbenes Sixty Years After Hine".
In: *The Journal of Organic Chemistry* 75.17 (2010), pp. 5773–5783.
DOI: 10.1021/jo100390p.

[122] Robert A. Moss and Karsten Krogh-Jespersen.
"Carbenic philicity and the 'intrinsic reactivity index'".
In: *Tetrahedron Letters* 54.32 (2013), pp. 4303 –4305.
DOI: https://doi.org/10.1016/j.tetlet.2013.06.007.

[123] R. Huisgen. "Kinetics and Mechanism of 1,3-Dipolar Cycloadditions".
In: *Angewandte Chemie International Edition in English* 2.11 (1963), pp. 633–645.
DOI: 10.1002/anie.196306331.

[124] E. Buchner and Th. Curtius.
"Synthese von Ketonsäureäthern aus Aldehyden und Diazoessigäther".
In: *Berichte der deutschen chemischen Gesellschaft* 18.2 (1885), pp. 2371–2377.
DOI: 10.1002/cber.188501802118.

[125] Fritz Schlotterbeck. "Umwandlung von Aldehyden in Ketone durch Diazomethan. (Erwiderung an Hrn. H. Meyer)".
In: *Berichte der deutschen chemischen Gesellschaft* 40.2 (1907), pp. 1826–1827.
DOI: 10.1002/cber.19070400285.

[126] Zerong Wang. "Büchner-Curtius-Schlotterbeck Reaction". In:
Comprehensive Organic Name Reactions and Reagents. John Wiley & Sons, Inc., 2010.
DOI: 10.1002/9780470638859.conrr124.

[127] G. W. Cowell and A. Ledwith. "Developments in the chemistry of diazo-alkanes".
In: *Q. Rev. Chem. Soc.* 24 (1970), pp. 119–167. DOI: 10.1039/QR9702400119.

[128] Nuno R. Candeias, Roberta Paterna, and Pedro M. P. Gois.
"Homologation Reaction of Ketones with Diazo Compounds".
In: *Chemical Reviews* 116.5 (2016), pp. 2937–2981.
DOI: 10.1021/acs.chemrev.5b00381.

[129] Takuya Hashimoto, Yuki Naganawa, and Keiji Maruoka.
"Stereoselective Construction of Seven-Membered Rings with an All-Carbon Quaternary Center by Direct Tiffeneau–Demjanov-type Ring Expansion".
In: *Journal of the American Chemical Society* 131.18 (2009), pp. 6614–6617.
DOI: 10.1021/ja900941k.

[130] F. Arndt and B. Eistert. "Ein Verfahren zur Überführung von Carbonsäuren in ihre höheren Homologen bzw. deren Derivate". In: *Berichte der deutschen chemischen Gesellschaft (A and B Series)* 68.1 (1935), pp. 200–208.
DOI: 10.1002/cber.19350680142.

[131] Peter Yates. "The Copper-catalyzed Decomposition of Diazoketones1".
In: *Journal of the American Chemical Society* 74.21 (1952), pp. 5376–5381.
DOI: 10.1021/ja01141a047.

[132] Albert Padwa et al. “Ligand effects on dirhodium(II) carbene reactivities. Highly effective switching between competitive carbenoid transformations”. In: *Journal of the American Chemical Society* 115.19 (1993), pp. 8669–8680. DOI: 10.1021/ja00072a021.

[133] Huw M. L. Davies et al. “Effect of carbenoid structure on the reactivity of rhodium-stabilized carbenoids”. In: *Tetrahedron Letters* 39.25 (1998), pp. 4417–4420. DOI: https://doi.org/10.1016/S0040-4039(98)00836-3.

[134] Huw M. L. Davies and Rohan E. J. Beckwith. “Catalytic Enantioselective C–H Activation by Means of Metal–Carbenoid-Induced C–H Insertion”. In: *Chemical Reviews* 103.8 (2003), pp. 2861–2904. DOI: 10.1021/cr0200217.

[135] Huw M. L. Davies and Walji A. M. *Modern Rhodium-Catalyzed Organic Reactions*. Wiley-VCH Verlag GmbH & Co. KGaA, 2005, pp. 301–340.

[136] Huw M. L. Davies and Øystein Loe. “Intermolecular C-H Insertions of Donor/Acceptor-Substituted Rhodium Carbenoids: A Practical Solution for Catalytic Enantioselective C-H Activation”. In: *Synthesis* 2004.16 (2004), pp. 2595–2608. DOI: 10.1055/s-2004-834876.

[137] Huw M. L. Davies and Justin R. Denton. “Application of donor/acceptor-carbenoids to the synthesis of natural products”. In: *Chem. Soc. Rev.* 38 (11 2009), pp. 3061–3071. DOI: 10.1039/B901170F.

[138] Michael P. Doyle and David C. Forbes. “Recent Advances in Asymmetric Catalytic Metal Carbene Transformations”. In: *Chemical Reviews* 98.2 (1998), pp. 911–936. DOI: 10.1021/cr940066a.

[139] Biswajit Saha, Tatsuya Uchida, and Tsutomu Katsuki. “Asymmetric intramolecular cyclopropanation of diazo compounds with metallosalen complexes as catalyst: structural tuning of salen ligand”. In: *Tetrahedron: Asymmetry* 14.7 (2003), pp. 823 –836. DOI: 10.1016/S0957-4166(03)00167-8.

[140] Robert Paulissen et al. “Transition metal catalysed reactions of diazocompounds - II insertion in the hydroxylic bond”. In: *Tetrahedron Letters* 14.24 (1973), pp. 2233 –2236. DOI: https://doi.org/10.1016/S0040-4039(01)87603-6.

[141] Christine G. Espino et al. “Expanding the Scope of C–H Amination through Catalyst Design”. In: *Journal of the American Chemical Society* 126.47 (2004), pp. 15378–15379. DOI: 10.1021/ja0446294.

[142] Jørn Hansen and Huw M L Davies. “High Symmetry Dirhodium(II) Paddlewheel Complexes as Chiral Catalysts”. In: *Coordination chemistry reviews* 252.5-7 (2008), pp. 545–555. DOI: 10.1016/j.ccr.2007.08.019.

[143] Stephen T Liddle. *Molecular Metal-Metal Bonds: Compounds, Synthesis, Properties*. John Wiley & Sons, Ltd, 2015, pp. 285–312.

[144] Huw M. L. Davies et al. “Asymmetric Cyclopropanations by Rhodium(II) N-(Arylsulfonyl)prolinate Catalyzed Decomposition of Vinyldiazomethanes in the Presence of Alkenes. Practical Enantioselective Synthesis of the Four Stereoisomers of 2-Phenylcyclopropan-1-amino Acid”. In: *Journal of the American Chemical Society* 118.29 (1996), pp. 6897–6907. DOI: 10.1021/ja9604931. eprint: https://doi.org/10.1021/ja960493.

[145] Geoffrey G. Cox et al. “Chemoselectivity of rhodium carbenoids. A comparison of the selectivity for O-H insertion reactions or carbonyl ylide formation versus aliphatic and

aromatic C-H insertion and cyclopropanation".
In: *Tetrahedron* 49.23 (1993), pp. 5109 –5126. DOI: 10.1016/S0040-4020(01)81876-7.
[146] Jiapian Huang, Yi Yang, and Zhiyuan Chen.
"Rhodium(II)-Catalyzed Regioselective Carbenoid Insertion Reaction of Simple Indoles with N-Sulfonyltriazoles: A Rapid Access to Tryptamine Vinylogues".
In: *Advanced Synthesis & Catalysis* 358.2 (2016), pp. 201–206.
DOI: 10.1002/adsc.201500792.
[147] Alexandre F. Trindade et al.
"Fine Tuning of Dirhodium(II) Complexes: Exploring the Axial Modification".
In: *ACS Catalysis* 2.3 (2012), pp. 370–383. DOI: 10.1021/cs200597a.
[148] Alexandre F. Trindade et al. "Axial Coordination of NHC Ligands on Dirhodium(II) Complexes: Generation of a New Family of Catalysts".
In: *The Journal of Organic Chemistry* 73.11 (2008), pp. 4076–4086.
DOI: 10.1021/jo800087n.
[149] Hélène Lebel et al. "Stereoselective Cyclopropanation Reactions".
In: *Chemical Reviews* 103.4 (2003), pp. 977–1050. DOI: 10.1021/cr010007e.
[150] Hans-Ulrich Reissig and Reinhold Zimmer. "Donor–Acceptor-Substituted Cyclopropane Derivatives and Their Application in Organic Synthesis".
In: *Chemical Reviews* 103.4 (2003), pp. 1151–1196. DOI: 10.1021/cr010016n.
[151] Henry N. C. Wong et al.
"Use of cyclopropanes and their derivatives in organic synthesis".
In: *Chemical Reviews* 89.1 (1989), pp. 165–198. DOI: 10.1021/cr00091a005.
[152] Albert Demonceau et al. "Transition-metal-catalysed reactions of diazoesters. Insertion into C-H bonds of paraffins by carbenoids".
In: *J. Chem. Soc., Chem. Commun.* (14 1981), pp. 688–689.
DOI: 10.1039/C39810000688.
[153] Catherine N. Slattery, Alan Ford, and Anita R. Maguire.
"Catalytic asymmetric C–H insertion reactions of α-diazocarbonyl compounds".
In: *Tetrahedron* 66.34 (2010), pp. 6681 –6705.
DOI: https://doi.org/10.1016/j.tet.2010.05.073.
[154] J. V. Santiago and A. H. L. Machado.
"Enantioselective carbenoid insertion into C(sp3)–H bonds".
In: *Beilstein Journal of Organic Chemistry* 12 (2016), pp. 882–902.
[155] Tomoya Miura, Qiang Zhao, and Masahiro Murakami. "Selective Functionalization of Aromatic C(sp2)–H Bonds in the Presence of Benzylic C(sp3)–H Bonds by Electron-Deficient Carbenoids Generated from 4-Acyl-1-Sulfonyl-1,2,3-Triazoles".
In: *Angewandte Chemie International Edition* 56.52 (2017), pp. 16645–16649.
DOI: 10.1002/anie.201709384.
[156] Jianxian Gong et al. "Total Synthesis of (±) Maoecrystal V".
In: *Journal of the American Chemical Society* 132.47 (2010), pp. 16745–16746.
DOI: 10.1021/ja108907x.
[157] Thomas N. Salzmann et al. "A stereocontrolled synthesis of (+)-thienamycin".
In: *Journal of the American Chemical Society* 102.19 (1980), pp. 6161–6163.
DOI: 10.1021/ja00539a040.
[158] Albert. Padwa and Susan F. Hornbuckle. "Ylide formation from the reaction of carbenes and carbenoids with heteroatom lone pairs".
In: *Chemical Reviews* 91.3 (1991), pp. 263–309. DOI: 10.1021/cr00003a001.
[159] Albert Padwa. "Domino reactions of rhodium(ii) carbenoids for alkaloid synthesis".
In: *Chem. Soc. Rev.* 38 (11 2009), pp. 3072–3081. DOI: 10.1039/B816701J.

[160] Christopher J. Moody and Roger J. Taylor. "Rhodium carbenoid mediated cyclisations. Synthesis and rearrangement of cyclic sulphonium ylides". In: *Tetrahedron Letters* 29.46 (1988), pp. 6005 –6008. DOI: 10.1016/S0040-4039(00)82252-2.

[161] F. Gerhart, U. Schöllkopf, and H. Schumacher. "Joddiazoessigsäure-äthylester und seine Zersetzung zu Äthoxycarbonyl-jodcarben". In: *Angewandte Chemie* 79.1 (1967), p. 50. DOI: 10.1002/ange.19670790106.

[162] U. Schöllkopf and M. Reetz. "Zur stabilität von brom- und jod-diazoessigsäureäthylester und zum verhalten von brom- und jod-äthoxycarbonylcarben". In: *Tetrahedron Letters* 10.20 (1969), pp. 1541 –1544. DOI: 10.1016/S0040-4039(01)87939-9.

[163] Ulrich Schöllkopf et al. "Halogen-diazoessigsäureäthylester aus Quecksilber-bis-diazoessigsäureäthylester". In: *Justus Liebigs Annalen der Chemie* 716.1 (1968), pp. 204–206. ISSN: 1099-069. DOI: 10.1002/jlac.19687160129.

[164] Ulrich Schöllkopf and Norbert Rieber. "C-Alkylierung von Silber-diazoessigsäure-äthylester und Silberdiazoketonen mit SN1-aktiven Halogeniden". In: *Chemische Berichte* 102.2 (1969), pp. 488–493. DOI: 10.1002/cber.19691020216.

[165] Magnus Mortén, Martin Hennum, and Tore Bonge-Hansen. "On the cause of low thermal stability of ethyl halodiazoacetates". In: *Beilstein Journal of Organic Chemistry* 12 (2016), pp. 1590–1597. DOI: 10.3762/bjoc.12.155.

[166] Christopher S. Neumann, Danica Galonić Fujimori, and Christopher T. Walsh. "Halogenation Strategies In Natural Product Biosynthesis". In: *Chemistry & Biology* 15.2 (2008), pp. 99 –109. DOI: 10.1016/j.chembiol.2008.01.006.

[167] Gordon W. Gribble. "Natural Organohalogens: A New Frontier for Medicinal Agents?" In: *Journal of Chemical Education* 81.10 (2004), p. 1441. DOI: 10.1021/ed081p1441.

[168] Tao Ye and M. Anthony McKervey. "Organic Synthesis with .alpha.-Diazo Carbonyl Compounds". In: *Chemical Reviews* 94.4 (1994), pp. 1091–1160. DOI: 10.1021/cr00028a010.

[169] Maura Marinozzi, Fabrizio Pertusati, and Michaela Serpi. "λ5-Phosphorus-Containing α-Diazo Compounds: A Valuable Tool for Accessing Phosphorus-Functionalized Molecules". In: *Chemical Reviews* 116.22 (2016), pp. 13991–14055. DOI: 10.1021/acs.chemrev.6b00373.

[170] William S. Wadsworth and William D. Emmons. "The Utility of Phosphonate Carbanions in Olefin Synthesis". In: *Journal of the American Chemical Society* 83.7 (1961), pp. 1733–1738. DOI: 10.1021/ja01468a042.

[171] Leopold Horner, Hellmut Hoffmann, and Hans G. Wippel. "Phosphororganische Verbindungen, XII. Phosphinoxyde als Olefinierungsreagenzien". In: *Chemische Berichte* 91.1 (1958), pp. 61–63. DOI: 10.1002/cber.19580910113.

[172] Leopold Horner et al. "Phosphororganische Verbindungen, XX. Phosphinoxyde als Olefinierungsreagenzien". In: *Chemische Berichte* 92.10 (1959), pp. 2499–2505. DOI: 10.1002/cber.19590921017.

[173] Dietmar Seyferth, Robert S. Marmor, and Peter Hilbert.
"Reactions of dimethylphosphono-substituted diazoalkanes. (MeO)2P(O)CR transfer to olefins and 1,3-dipolar additions of (MeO)2P(O)C(N2)R".
In: *The Journal of Organic Chemistry* 36.10 (1971), pp. 1379–1386.
DOI: 10.1021/jo00809a014.

[174] Susumu Ohira.
"Methanolysis of Dimethyl (1-Diazo-2-oxopropyl) Phosphonate: Generation of Dimethyl (Diazomethyl) Phosphonate and Reaction with Carbonyl Compounds".
In: *Synthetic Communications* 19.3-4 (1989), pp. 561–564.
DOI: 10.1080/00397918908050700.

[175] Gerald J. Roth et al.
"Further Improvements of the Synthesis of Alkynes from Aldehydes".
In: *Synthesis* 2004.01 (2004), pp. 59–62. DOI: 10.1055/s-2003-44346.

[176] Spencer C. Peck, Jiangtao Gao, and Wilfred A. van der Donk. "Chapter Six - Discovery and Biosynthesis of Phosphonate and Phosphinate Natural Products".
In: *Natural Product Biosynthesis by Microorganisms and Plants, Part B*. Vol. 516. Methods in Enzymology. Academic Press, 2012, pp. 101 –123.
DOI: 10.1016/B978-0-12-394291-3.00029-0.

[177] Thomas S. Elliott et al.
"The use of phosphate bioisosteres in medicinal chemistry and chemical biology".
In: *Med. Chem. Commun.* 3 (7 2012), pp. 735–751. DOI: 10.1039/C2MD20079A.

[178] A. Michael Downey and Christopher W. Cairo. "Synthesis of [small alpha]-brominated phosphonates and their application as phosphate bioisosteres".
In: *Med. Chem. Commun.* 5 (11 2014), pp. 1619–1633. DOI: 10.1039/C4MD00255E.

[179] Manfred Regitz, Bernd Weber, and Udo Eckstein.
"Investigations on Diazo Compounds and Azides, XXXII. - Substitution Reactions at the Diazo Carbon of Diazomethylphosphoryl Compounds".
In: *Liebigs Annalen der Chemie* 1979.7 (1979), pp. 1002–1019.
DOI: 10.1002/jlac.197919790711.

[180] Emil Fischer and Albert Steche. "1) Verwandlung der Indole in Hydrochinoline)".
In: *Justus Liebigs Annalen der Chemie* 242.3 (1887), pp. 348–366.
DOI: 10.1002/jlac.18872420309.

[181] Gaetano Magnanini. "Ueber die Verwandlung der Indole in Chinolinderivate".
In: *Berichte der deutschen chemischen Gesellschaft* 20.2 (1887), pp. 2608–2614.
DOI: 10.1002/cber.188702002102.

[182] C.W. Rees and C.E. Smithen.
"The Reactions of Heterocyclic Compounds with Carbenes". In: vol. 3.
Advances in Heterocyclic Chemistry. Academic Press, 1964, pp. 57 –78.
DOI: 10.1016/S0065-2725(08)60541-3.

[183] Hans Wynberg. "The Reimer-Tiemann Reaction."
In: *Chemical Reviews* 60.2 (1960), pp. 169–184. DOI: 10.1021/cr60204a003.

[184] *Ethyl diazoacetate*. 2018. URL: https://www.sigmaaldrich.com/catalog/product/aldrich/e22201?lang=en&region=NO.

[185] Vladimir Levchenko. "Design and Synthesis of Novel Rh(II)-containing Polymer Catalysts. Organometallic Gold(III) Catalysis in Organic Synthesis".
PhD thesis. University of Oslo, 2016.

[186] Yan Cai et al. "Iron-Catalyzed C-H Fuctionalization of Indoles".
In: *Advanced Synthesis & Catalysis* 353.16 (), pp. 2939–2944.
DOI: 10.1002/adsc.201100334.

[187] Geoff Rayner-Canham and Tina Overton. *Descriptive Inorganic Chemistry*. 6th ed. W H Freeman, 2012-13.

[188] Shu-Bin Zhao and Suning Wang. "Luminescence and reactivity of 7-azaindole derivatives and complexes". In: *Chem. Soc. Rev.* 39 (8 2010), pp. 3142–3156. DOI: 10.1039/C001897J.

[189] Suning Wang. "Luminescence and electroluminescence of Al(III), B(III), Be(II) and Zn(II) complexes with nitrogen donors". In: *Coordination Chemistry Reviews* 215.1 (2001), pp. 79 –98. DOI: 10.1016/S0010-8545(00)00403-3.

[190] F. Albert Cotton, Dennis G. Lay, and Michelle Millar. "Preparation and structure of a quadruply bonded dimolybdenum compound containing the 7-azaindolyl ligand". In: *Inorganic Chemistry* 17.1 (Jan. 1978), pp. 186–188. DOI: 10.1021/ic50179a035.

[191] Pascal Dufour et al. "Crystal structures of 7-azaindole, an unusual hydrogen-bonded tetramer, and of two of its methylmercury(II) complexes". In: *Canadian Journal of Chemistry* 68.1 (1990), pp. 193–201. DOI: 10.1139/v90-025.

[192] Deacon Glen B. et al. "Synthesis and Structures of cisoidand transoidBis(1,2-dimethoxyethane)bis(η2-pyrazolato)lanthanoid(II) Complexes". In: *European Journal of Inorganic Chemistry* 5 (1999), pp. 751–761. DOI: 10.1002/(SICI)1099-0682(199905)1999:5<751::AID-EJIC751>3.0.CO;2-5.

[193] F. Albert. Cotton and Timothy R. Felthouse. "Molecular and chain structures of four tetrakis(.mu.-propionato)-dirhodium(II) complexes with axial nitrogen-donor ligands". In: *Inorganic Chemistry* 20.2 (1981), pp. 600–608. DOI: 10.1021/ic50216a053.

[194] Dmitry Pogozhev, Stephane A. Baudron, and Mir Wais Hosseini. "From insertion of rhodium acetate paddlewheels into functionalized 7-azaindole hydrogen-bonded dimers to infinite architectures". In: *Dalton Transactions* 40.28 (2011), pp. 7403–7411. DOI: 10.1039/C1DT10359H.

[195] Michael C. Pirrung, Hao Liu, and Andrew T. Morehead. "Rhodium Chemzymes:thin space Michaelis–Menten Kinetics in Dirhodium(II) Carboxylate-Catalyzed Carbenoid Reactions". In: *Journal of the American Chemical Society* 124.6 (2002), pp. 1014–1023. DOI: 10.1021/ja011599l.

[196] Dennis Gillingham and Na Fei. "Catalytic X-H insertion reactions based on carbenoids". In: *Chem. Soc. Rev.* 42 (12 2013), pp. 4918–4931. DOI: 10.1039/C3CS35496B.

[197] Magnus Mortén. "α-Halodiazoacetater: en studie av stabilitet og reaktivitet". PhD thesis. University of Oslo, 2015.

[198] C. W. Rees and C. E. Smithen. "181. The mechanism of heterocyclic ring expansions. Part I. The reaction of 2,3-dimethylindole with dichlorocarbene". In: *J. Chem. Soc.* (1964), pp. 928–937. DOI: 10.1039/JR9640000928.

[199] M. Ruz. "ZINC: Properties and Determination A2 - Caballero, Benjamin". In: Academic Press, 2003, pp. 6267–6272. DOI: 10.1016/B0-12-227055-X/01308-0.

[200] William S. Sheldrick. "Preparation and Structure of Zinc(II) Complexes of Purine and 7-Azaindole". In: *Zeitschrift für Naturforschung B* 37.5 (1982), pp. 653–656. DOI: 10.1515/znb-1982-0521.

[201] N.J. Thumar, Q.H. Wei, and W.H. Hu. "Chapter Two - Recent Advances in Asymmetric Metal-Catalyzed Carbene Transfer from Diazo Compounds Toward Molecular Complexity". In: vol. 66. Advances in Organometallic Chemistry. 2016, pp. 33 –91. DOI: 10.1016/bs.adomc.2016.08.002.

[202] Minmin Yang et al. “A New Route To Hindered Tertiary Amines”. In: *The Journal of Organic Chemistry* 66.20 (2001), pp. 6729–6733. DOI: 10.1021/jo010583a.

[203] Richard T. Buck; Christopher J. Moody; Adrian G. Pepper. “N-H Insertion reactions of rhodium carbenoids. Part 4. New chiral dirhodium(II) carboxylate catalysts”. In: *Archive for Organic Chemistry* 2002 (8). DOI: 10.3998/ark.5550190.0003.803.

[204] *pka table*. 2018. URL: http://www.d-bernier.fr/pKa.php.

[205] Ulrich Wietelmann and Richard J. Bauer. “Lithium and Lithium Compounds”. In: *Ullmann’s Encyclopedia of Industrial Chemistry*. American Cancer Society, 2000. DOI: 10.1002/14356007.a15_393.

[206] Christian A. Kuttruff, Hendrik Zipse, and Dirk Trauner. “Concise Total Syntheses of Variecolortidesfour-per-em-spaceA and B through an Unusual Hetero-Diels–Alder Reaction”. In: *Angewandte Chemie International Edition* 50.6 (), pp. 1402–1405. DOI: 10.1002/anie.201006154.

[207] Jaya Prakash Das and Sujit Roy. “Catalytic Hunsdiecker Reaction of α,β-Unsaturated Carboxylic Acids:thin space How Efficient Is the Catalyst?” In: *The Journal of Organic Chemistry* 67.22 (2002), pp. 7861–7864. DOI: 10.1021/jo025868h.

[208] Liang Wang et al. “Enantioselective α-Chlorination of Aldehydes with Recyclable Fluorous (S)-Pyrrolidine-Thiourea Bifunctional Organocatalyst”. In: *Synlett* 2010.03 (2010), pp. 433–436. DOI: 10.1055/s-0029-1219198.

[209] Nis Halland et al. “Direct Organocatalytic Asymmetric α-Chlorination of Aldehydes”. In: *Journal of the American Chemical Society* 126.15 (2004), pp. 4790–4791. DOI: 10.1021/ja049231m.

[210] Pelkey Erin T. “Metalation of Indole”. In: *ChemInform* 42.43 (2011). DOI: 10.1002/chin.201143236.

[211] Jörg Pietruszka and Andreas Witt. “Synthesis of the Bestmann-Ohira Reagent”. In: *Synthesis* 2006.24 (2006), pp. 4266–4268. DOI: 10.1055/s-2006-950307.

[212] Marc Presset et al. “Diazo-Transfer Reactions to 1,3-Dicarbonyl Compounds with Tosyl Azide”. In: *Synthesis* 16 (2011), pp. 2549–2552. DOI: 10.1055/s-0030-1260107.

[213] Hideo Tomioka, Naoki Toriyama, and Yasuji Izawa. “Nucleophilic cleavage reactions of cyclic and acyclic .alpha.-diazo-.beta.-ketophosphoryl compounds”. In: *The Journal of Organic Chemistry* 42.3 (1977), pp. 552–554. DOI: 10.1021/jo00423a035.

[214] Heinrich Heydt et al. “p-Toluenesulfonyl Azide”. In: *Encyclopedia of Reagents for Organic Synthesis*. American Cancer Society, 2008.

[215] Julian R. Kuttner and Gerhard Hilt. “Synthesis of Acyclic Polycarbonyl Compounds via Ozonolysis of Cyclohexa-1,4-dienes”. In: *Synthesis* 47.08 (2015), pp. 1170–1180. DOI: 10.1055/s-0034-1380148.

[216] Christian Scnaars. “Development of Novel Methodology for the in situ Preparation of Halodiazo Compounds and Investigation of Reactivities of α-Onium Diazo Compounds”. PhD thesis. University of Oslo, 2014. URL: https://www.duo.uio.no/bitstream/handle/10852/39925/dravhandling-schnaars-DUO.pdf?sequence=1.

[217] Indrajit Ghosh, Rizwan S. Shaikh, and Burkhard König. “Sensitization-Initiated Electron Transfer for Photoredox Catalysis”.

In: *Angewandte Chemie International Edition* 56.29 (), pp. 8544–8549. DOI: 10.1002/anie.201703004.

[218] Mavallur Varalakshmi, Doddaga Srinivasulu, and Venkata S. Kotakadi. "Nano-BF3.SiO2 Catalyst-Promoted Michaelis-Arbuzov Reaction: Solvent-Free Synthesis and Antimicrobial Evaluation". In: *Phosphorus, Sulfur, and Silicon and the Related Elements* 190.9 (2015), pp. 1518–1524. DOI: 10.1080/10426507.2014.996643.

[219] Marcin Kalek, Martina Jezowska, and Jacek Stawinski. "Preparation of Arylphosphonates by Palladium(0)-Catalyzed Cross-Coupling in the Presence of Acetate Additives: Synthetic and Mechanistic Studies". In: *Advanced Synthesis & Catalysis* 351.18 (), pp. 3207–3216. DOI: 10.1002/adsc.200900590.

[220] Palacios Francisco, Aparicio Domitila, and Vicario Javier. "Synthesis of Quinolinylphosphane Oxides and -phosphonates from N-Arylimines Derived from Phosphane Oxides and Phosphonates". In: *European Journal of Organic Chemistry* 2002.24 (2002), pp. 4131–4136. DOI: 10.1002/1099-0690(200212)2002:24<4131::AID-EJOC4131>3.0.CO;2-W.

[221] Yuzhen; Zhang Li; Bai Xu Zhu Yue; Liao. *Phenanthroline phosphonic acid derivative and preparation method therefor and application thereof*. Patent: WO2015154716 (A1). 2015. URL: https://worldwide.espacenet.com/publicationDetails/biblio?CC=WO&NR=2015154716A1&KC=A1&FT=D&ND=3&date=20151015&DB=EPODOC&locale=en_EP#.

[222] Marcelo Zaldini Hernandes et al. "Halogen Atoms in the Modern Medicinal Chemistry: Hints for the Drug Design". In: 11 (Mar. 2010), pp. 303–14.

[223] Henry F. Russell et al. "5-SUBSTITUTED INDOLES via SODIUM INDOLINE-2-SULFONATE. A REEXAMINATION". In: *Organic Preparations and Procedures International* 17.6 (1985), pp. 391–399. DOI: 10.1080/00304948509355525.

[224] William G. Kofron and Leona M. Baclawski. "A convenient method for estimation of alkyllithium concentrations". In: *The Journal of Organic Chemistry* 41.10 (1976), pp. 1879–1880. DOI: 10.1021/jo00872a047.

[225] Scott C. Virgil. "N-Bromosuccinimide". In: *Encyclopedia of Reagents for Organic Synthesis*. John Wiley & Sons, Ltd, 2001. ISBN: 9780470842898. DOI: 10.1002/047084289X.rb318.

[226] N. A. Gol'dberg and G. P. Balabanov. "Preparation and properties of azides of aromatic sulfonic acids." In: *Zh. Org. Khim.* 1.9 (1965), pp. 1604–6.

[227] Jérôme Waser et al. "Hydrazines and Azides via the Metal-Catalyzed Hydrohydrazination and Hydroazidation of Olefins". In: *Journal of the American Chemical Society* 128.35 (2006), pp. 11693–11712. DOI: 10.1021/ja062355+.

[228] Chikara Kaneko and Sachiko Yamada. "The Isomerization of 1aH-Oxazirino [2, 3-alpha;] quinoline 1a-carbonitrile and Its Substituted Derivatives to the Corresponding 3-Hydoxyquinoline Derivatives". In: *CHEMICAL & PHARMACEUTICAL BULLETIN* 15.5 (1967), pp. 663–669. DOI: 10.1248/cpb.15.663.

[229] Herbert E. Johnson. *Process for preparing aminoindole compounds*. Patent. 1965.

[230] Masayuki; Tanaka Keigo; Inoue Satoshi; Tsukada Itaru; Haneda Toru; Ueda Norihiro; Abe Shinya; Sagane Koji Nakamoto Kazutaka; Matsukura. *Novel antifungal agent comprising heterocyclic compound*. Patent.

Patent: WO2005033079A1. 2005.
URL: https://patents.google.com/patent/WO2005033079A1/en.
[231] Hideo; Mitani Toru; Nakashita Mitsuo Nakagome Takenari; Agui. *Alkyl 1-alkyl-4-oxo-1,8-naphthyridine-3-carboxylates and alkyl 1-alkyl-4-quinolone-3-carboxylates*. Patent number: DE2103805. 1971.
[232] Gerald R. Lappin. "Cyclization of 2-Aminopyridine Derivatives. I. Substituted Ethyl 2-Pyridylaminomethylenemalonates1,2".
In: *Journal of the American Chemical Society* 70.10 (1948), pp. 3348–3350.
DOI: 10.1021/ja01190a038.
[233] Mikhail D. Kosobokov, Igor D. Titanyuk, and Irina P. Beletskaya. "An expedient synthesis of diethyl diazomethylphosphonate".
In: *Mendeleev Communications* 21.3 (2011), pp. 142 –143.
DOI: https://doi.org/10.1016/j.mencom.2011.04.009.
[234] P. Tavs and F. Korte. "Zur herstellung aromatischer phosponsäureester aus arylhalogeniden und trialkylphosphiten". In: *Tetrahedron* 23.12 (1967), pp. 4677 –4679.
DOI: 10.1016/S0040-4020(01)92565-7.